EPA-650/2-74-093

OCTOBER 1974

Environmental Protection Technology Series

FINE PARTICLE SCRUBBER PERFORMANCE TESTS

Office of Research and Development
U.S. Environmental Protection Agency
Washington, DC 20460

EPA-650/2-74-093

FINE PARTICLE SCRUBBER PERFORMANCE TESTS

by

S. Calvert, N. C. Jhaveri, S. Yung

A. P. T., Inc.
P. O. Box 71
Riverside, California 92502

Contract No. 68-02-0285
ROAP No. 21ADJ-037
Program Element No. 1AB012

EPA Project Officer: L. E. Sparks

Control Systems Laboratory
National Environmental Research Center
Research Triangle Park, North Carolina 27711

Prepared for

OFFICE OF RESEARCH AND DEVELOPMENT
U.S. ENVIRONMENTAL PROTECTION AGENCY
WASHINGTON, D.C. 20460

October 1974

This report has been reviewed by the Environmental Protection Agency and approved for publication. Approval does not signify that the contents necessarily reflect the views and policies of the Agency, nor does mention of trade names or commercial products constitute endorsement or recommendation for use.

PREFACE

This report, "Fine Particle Scrubber Performance Tests", is the final report submitted to the Control Systems Laboratory for E.P.A. Contract No. 68-02-0285.

Scrubber performance data relating fine particle penetration to particle size and operating parameters are needed to validate and/or develop engineering design methods so that performance can be predicted with more confidence. Careful measurements of particle size and concentration into and out of the scrubber were completed for 7 types of scrubbers on various pollution sources. Useful mathematical models were validated for all but one of the scrubbers. Recommendations for future work are given.

Dr. Leslie E. Sparks of the Control Systems Laboratory, National Environmental Research Center, Environmental Protection Agency, was the Project Officer for this program.

Dr. Seymour Calvert of A.P.T., Inc. was the Project Director.

Eight industrial organizations permitted tests to be performed at their facilities and assisted the program in many ways.

CONTENTS

FIGURES

FIGURES

FIGURES

FIGURES

FIGURES

TABLES

TABLES

TABLES

INTRODUCTION

The need for more reliable data on the fine particle collection efficiency of air pollution control scrubbers has become increasingly apparent as control requirements have grown more demanding. Major efforts, such as the Wet Scrubber System Study (Calvert et al., 1972), to augment our ability to design better scrubbers and to predict their performance have illuminated this need. Design methods, including mathematical models, have been developed from basic theory plus whatever good data were available but to a large extent they were untested. Thus, one could not either predict performance for present scrubber designs and operating conditions or extrapolate into better combinations of design and performance with a reasonable degree of confidence.

It is very difficult to compare scrubber performances in different situations without knowing efficiency as a function of particle size, commonly called: "grade efficiency." Even on an empirical basis, there have been so few carefully and properly done performance tests that the capabilities of existing systems were not known. Collection effiency in terms of overall particle mass was rarely tested because of a predominant concern for only the outlet particulate loading or emission rate. The few data which had been published were generally unsatisfactory for use because of inadequate methodology, undefined parameters, insufficient quantity, and similar inadequacies.

The program reported here was initiated in response to the need for additional reliable performance data on fine

particle scrubbers. The objectives were as follows:

1. Obtain data on fine particle collection efficiency as a function of particle size for scrubbers operating on representative industrial emission sources. Fine particles are those smaller than several microns in diameter. Record pertinent data on scrubber design and operating conditions.
2. Reconcile the performance data with existing mathematical models, such as those presented in the "Scrubber Handbook" by Calvert, et al. (1972). Where necessary and to the extent possible, develop better models and/or design approaches.
3. Obtain data on scrubber system costs for investment, operation, and maintenance.
4. Compile the available information on scrubber operating characteristics and problems (including entrainment), maintenance requirements, corrosion and erosion experience, and similar items regarding system behavior.

SUMMARY, CONCLUSIONS AND RECOMMENDATIONS

SUMMARY

A summary of the performance test program is given in tabular form below:

Test #	Source	Scrubber	Approximate Cut Diameter
1	Metal Melting	Hybrid	-
2	Urea Prilling Tower	Valve Tray (Koch Flexitray)	1.2 μmA
3	KCl dryer	Vaned Centrifugal (Ducon)	1.2 μmA
4	Coal fired utility boiler	Mobile Bed (T.C.A.)	0.4 μmA
5	Coal fired utility boiler	Venturi (Chemico)	0.7 μmA
6	NaCl dryer	Wetted fiber	0.8 μmA
7	NaCl dryer	Impingement Plate (Sly Impinjet)	1.0 μmA
8	Foundry Cupola	Venturi Rod	0.3 μmA

NOTE: Cut diameter is for 50% penetration.

Test No. 1 was started and had to be postponed due to operating problems. Upon returning to the plant to resume the test it was found that the scrubber system had been drastically modified and it was then decided to abandon the test. The remaining tests were all completed despite the necessity to interrupt tests No. 2, 3, 4, and 5 because of plant shut-downs.

The experimental and computational methods were modified as the program proceeded and experience led to the evolution of better tools. Initially the focus of interest was in the particle size range from a few tenths to several microns diameter; or essentially what could be measured by means of a cascade impactor. Later in the program there developed a further concern for smaller particles, ranging down to 0.01 micron diameter. It then became necessary to employ

some additional technique for particle size measurement. A diffusion battery system was chosen for this purpose. The evolution of a useful and convenient diffusion battery apparatus is still in progress.

All scrubber performance tests present problems in coping with entrained liquid in the outlet and many tests also involve a high loading of large particles in the inlet gas. Both situations necessitate the use of a pre-cutting device to remove the heavy liquid or solid loading from the sample gas before it reaches the cascade impactor. Several approaches were tried before a satisfactory pre-cutter was designed and proven in practice.

In general, there are a variety of problems depending on the specific case and causing the test method possibilities to be less than ideal. Most tests require the exercise of judgement in deciding on the best compromise which will yield valid data for the purpose at hand.

Analysis of the data for the computation of particle penetration as a function of particle size was satisfactorily accomplished by means of a graphical technique. A digital computation approach proved to be useful for some cases but not for all. Consequently, both methods were used where possible and checked against one another. The combined effect of errors in experimental measurements on computational procedures causes the uncertainty of penetration determinations to be $\pm 10\%$ or more at a given diameter. Fortunately, the dependence of penetration on particle diameter is so great that it usually overshadows the effect of errors and one can obtain meaningful results for, say, the particle size at 50% penetration.

Comparison of the experimental results with mathematical models (or design equations) was successful in six out of seven cases. The results of this comparison may be summarized as follows:

1. Valve tray on urea prill tower - A sieve plate model compared well with the data after accounting for particle growth due to water vapor condensation.
2. Vaned centrifugal on KCl dryer - A gas atomized spray model gave predictions which agreed with the data if reasonable allowance is made for growth due to condensation.
3. Mobile bed on coal-fired boiler - No satisfactory model is available and attempts to find a reasonable mechanism to account for the high efficiency were not successful. Particle growth due to condensation caused by H_2SO_4 adsorption is a probable contributor to the performance.
4. Venturi on coal-fired boiler - The model for a venturi in terms of particle cut diameter correlated with pressure drop agrees well with the experimental results.
5. Wetted fiber on NaCl dryer - The model for collection on fibers yields a good prediction after allowing for reasonable growth due to condensation.
6. Impingement plate on NaCl dryer - A model based on impingement from round jets gives good agreement with the data after allowing for particle growth due to condensation.
7. Venturi rod on cupola - The venturi model gives a good prediction for particles larger than about

1.0 micron aerodynamic diameter but does not account for low penetration for the sub-micron particles. Brownian diffusion can explain the high efficiency for particles smaller than a few tenths micron aerodynamic diameter.

Cooperating Organizations

The names of the organizations who cooperated in this program are not given because of the agreement to report the results without identification of the source. We are appreciative of their help in allowing the tests to be made and in providing facilities, assistance, and information.

CONCLUSIONS

The program achieved the principle objective of obtaining reliable performance data for the validation of mathematical models for scrubber design. Scrubbers of several types on a variety of sources, including two very large power plant boilers, were studied and the results add very significantly to our engineering ability. It is possible to predict performance for fine particle collection with much more confidence than one could prior to these evaluations.

A recently developed relationship between particle cut (50% efficiency) diameter and scrubber pressure drop has been tested with the data of this program. In all except one case, the new correlation gives very good results and is shown to be a very powerful and convenient design method.

The experimental methods for measuring fine particle collection efficiency remain more difficult and less accurate than one would like, despite improvements evolved

by our organization and other investigators. The time required to take the data also contributes to the cost of the study because the longer the test period, the higher the probability that the plant will break down and abort the test. In several cases, the scrubber system reliability is a problem while the intrinsic capability of the scrubber (when operating) is satisfactory.

Data on capital investment, operating costs and maintenance were generally not available in complete or reliable form. Operating problems related mostly to those caused by entrainment, solids deposition, and scaling. Plugging, corrosion, fan unbalancing, and similar problems stem from the aforementioned causes.

RECOMMENDATIONS

Recommendations stemming from the present study include items in the nature of methods whose use appears warranted, additional tests which should be made, experimental methods to be improved, model development required and additional research needed in related areas. For brevity, these are listed below:

A. Recommended methods

1. Particle penetration predictions for scrubbers other than mobile beds can be made with reasonable confidence by means of the cut diameter - pressure drop correlation.
2. Measurement of fine particle penetration in the inertial impaction regime can be done with useful accuracy by means of cascade impactors.

B. Additional scrubber tests needed
   1. Mobile bed scrubbers on a variety of sources with and without condensation effects
   2. Pre-formed spray scrubbers
   3. Venturi scrubbers at high pressure drop, on non-wettable particles, and on large gas flows
   4. Plate type scrubbers on systems without condensation effects and with non-wettable particles
   5. Impingement and entrainment type scrubbers
   6. Systems with wet fans

C. Experimental method improvement
   1. Better impactor catch weighing
   2. More convenient and reliable diffusion battery system
   3. Instantaneous particle size and concentration analysis
   4. Aerosol dilution system for use with particle counters and diffusion batteries
   5. Particle density measurement
   6. Opacity measurement for saturated gas streams.

D. Model development needed
   1. Performance model for mobile bed
   2. Reliable particle growth prediction for soluble materials in near-saturated gas

E. Additional related research
   1. Particle growth by condensation on soluble materials at relative humidity of 100% and less
   2. Effect of adsorbed gases on particle growth (e.g., H_2SO_4 on fly ash)
   3. Particle collection efficiency in well controlled mobile bed experiments.

METHOD

The method of approach to the program objectives involved a number of experimental determinations to obtain collection efficiency data, the aquisition of information on system characteristics and behavior, and computations which utilized the performance data and mathematical models. Over the course of the program the methods and apparatus used were generally improved and were modified to suit each specific test situation but the main features were similar and will be described here.

The most important experimental measurements were those regarding particle size and concentration. In the beginning of the program the size range of primary interest was from a few tenths to a few microns diameter, which is within the measurement range of a cascade impactor. Later the size range was extended downward by an order of magnitude and it was necessary to use a diffusion battery in addition to the cascade impactor. The apparatus and methods used are outlined below.

1. Gas velocity distribution and parameters had to be measured at the inlet and outlet of the scrubber in order to define the following:
   a. Conditions for isokinetic sampling.
   b. Particle concentration per unit volume of dry gas, which is a consistent basis for comparing inlet with outlet in the computation of efficiency.
   c. Gas flow rate.
   d. Amount of liquid entrainment in the outlet.

The necessary gas parameters were measured as shown in Table 1-1 below:

Table 1-1- GAS MEASUREMENTS

Parameter	Method
Velocity and Flow rate	A type "S" pitot tube was calibrated in the stack with a standard pitot tube and then used to make a multipoint traverse.
Temperature	A thermocouple or a dial thermometer was used for traversing.
Pressure	A water or mercury manometer measured pressure by means of a static pressure tube inserted in the duct.
Humidity	Wet and dry bulb temperature measurements were made on a flowing sample withdrawn from the stack. Outlets are generally saturated and require some heating in order to use this technique. Condensate and adsorption by a drying tube in a modified E.P.A. sampling train were also measured and used for confirmation.
Gas density	Depending on the test, dry gas density was measured by means of a pycnometer technique or computed from process conditions. Humid gas density (to be used in pitot tube computations) was calculated from dry gas density and humidity.
Liquid Entrainment	The quantity of liquid entrainment in the outlet was measured from the liquid collected in the pre-cutter used upstream of the cascade impactor in some runs and by means of a dye-treated paper technique for drop size determination in some.

2. Particle sampling and size analysis data in all tests were taken by means of cascade impactors. The early tests were made with a sampling probe from the stack to an externally mounted cascade impactor. Later tests were all made with the impactor in the stack in order to minimize probe losses. The three types of cascade impactors which were used are:

   a. An Andersen "viable" sampler for about 30ℓ/min (1 CFM) of sample was used ex-stack. It was calibrated by means of polystyrene latex particles and a Climet particle counter. A glass fiber paper filter was used after the impactor.

   b. A Brink cascade impactor for about 6ℓ/min was used for both in- and ex-stack measurements. It was also followed by a glass fiber paper filter to collect particles smaller than the last stage cut size. This impactor was calibrated as the Andersen was.

   c. An University of Washington (Pilat) Mark III Cascade Impactor for about 30ℓ/min was used for in-stack sampling. It contains a filter holder after the last impaction stage. The manufacturer's calibration was used for this impactor.

All of the impactors were operated with inlet nozzles appropriately sized to give isokinetic sampling. In the later tests a pre-cutter was used to remove either the heavy particle loading from inlet samples or the entrained liquid from outlet samples. A cyclone separator with about a 3 μmA cut diameter was first used but a round jet impactor with about an 8 μmA cut diameter was found to have better characteristics and was adopted for use for both

inlet and outlet sampling. The impactors were either given time to reach the duct gas temperature or were heated to prevent moisture deposition.

Several types of particle collection substrates were used with the impactors. Generally a pre-weighed, greased aluminum foil substrate was used. In some cases a glass fiber paper substrate was used. Silicone vacuum grease was either wiped on the foils or applied as a solution in an organic solvent.

Impactor substrates and filters were weighed with an analytical balance to the nearest tenth milligram (10^{-4} g). Tare weights were taken after drying in an oven and desiccator. Sample weights were taken both before and after drying.

Sample Bias

It is important to note that the program objective is to investigate scrubber performance on fine particles and, consequently, it is not necessary that the methods used be accurate for large particles. This makes the sampling simpler in the following ways:

a. Isokinetic conditions are not important for fine particles. For example, the error caused by sampling 4 μmA particles at a velocity 50% higher or lower than the gas stream velocity would only be about 2 or 3% of the concentration.

b. The fine particles will be well distributed in the gas stream, except in cases where streams with different particle concentrations have not had time to mix, so single point sampling is generally sufficient. To illustrate, we may note that the Stokes stopping distance of a 3 μmA particle with an initial velocity of 15 m/sec (50 ft/sec) is about 0.04 cm (0.016") and for a 1 μmA diameter particle it is one ninth of that. Since the stopping distance is the maximum a particle can be displaced

from a gas stream line by going around a right-angle turn, it is obvious that fine particle distribution in the gas stream will be negligibly affected by flow direction changes.

c. The effect of a pre-cutter on the size resolution of a cascade impactor is not significant in the size range of interest, so long as the pre-cutter has a cut diameter larger than several microns.

Particle size distributions were plotted on log-probability paper and described in terms of the approximate mass median aerodynamic diameter and geometric standard deviation which were obtained from the best straight line through the data. Collection efficiency was computed by means of a technique which utilizes a plot of the cumulative particle mass concentration versus particle aerodynamic diameter. We use the symbol "μmA" for aerodynamic diameter, which is equal to particle diameter (d_p) in μm (microns) times the square root of the particle density (ρ_p) in g/cm^3 times the square root of the Cunningham slip correction factor (C'). This computation is described in detail later in this report.

Comparison of the particle collection performance with the prediction of mathematical models is described in the separate chapters on the individual performance tests. Other data and information specific to each test are also presented in the appropriate chapters.

COMPUTATION AND MODELING METHODS

The computation of penetration as a function of particle size has been done in our previous reports by means of a method which involved some graphical steps. Curve fitting to the data points and the measurement of curve slopes were done "by eye" and involved subjective judgement. In an effort to standardize the method we developed a completely defined computational procedure and it is presented in the following section. By using the same mathematical procedure, different individuals should arrive at the same answer.

Overall penetration is defined as:

$$\overline{Pt} = \frac{1}{W_t} \int_0^W Pt_i \, dW \qquad (2\text{-}1)$$

where W_t is the total particle mass and Pt_i is the penetration for particle diameter, d_{pi}, and it is given by:

$$Pt_i = \frac{f\,(d_{pi})_{outlet}}{f\,(d_{pi})_{inlet}} = \frac{\left[\frac{dW}{d(d_{pi})}\right]_{outlet}}{\left[\frac{dW}{d(d_{pi})}\right]_{inlet}} \qquad (2\text{-}2)$$

where $\left[\frac{dW}{d(d_{pi})}\right]$ is the slope of the cumulative mass versus particle diameter curve at d_{pi} and equals $f\,(d_{pi})$.

In order to calculate this quantity, we must fit the cumulative mass data with a mathematical function.

Several mathematical functions, e.g., hyperbolic tangent function, exponential function, Rosin-Rammler distribution function and polynomial function, etc., have been tried. None of these functions gives a satisfactory fit for the whole range of particle size. They fit the data very well in the upper range of particle size. However, valuable information were lost in the small particle size range since

these functions all have the tendency to smooth the data points.

In order to overcome these difficulties, several alternative approaches have been tested. One of these is to fit only the lower range with a curve instead of the whole range. This is acceptable because we are only interested in the ability of the scrubber to control small particle emissions.

Among these functions, only the high degree polynomial function follows the data points closely. Therefore, it was used to compute the scrubber collection efficiencies. A method of least squares technique, which is presented in appendix A of this chapter, was used to fit the function to the experimental data.

COMMENTS ON CURVE FITTING BY POLYNOMIAL

The estimation of parameters by least squares causes a smoothing of a given set of data and eliminates, to some degree, errors in observation, measurements, recording, transmission and conversion, as well as other types of random error which may have been introduced in data. Systematic errors or bias errors will not be eliminated by the least square technique.

Figure 2-1 compares the polynomial fit with actual data. Curve A is a 3rd degree polynomial fit for the first five data points. Curve B is a 4th degree polynomial fit for the first 6 points and curve C is a 3rd degree polynomial fit for the first 6 points. From this figure, it clearly shows that curves A and B fit the experimental data almost exactly at the lower end of the curve and oscillate at the upper end. Curve C tends to smooth the data points. Since we are only interested in small particles, 3rd degree polynomial fit for the first 5 points is accurate enough for us to calculate the slope of the curve and particle penetration.

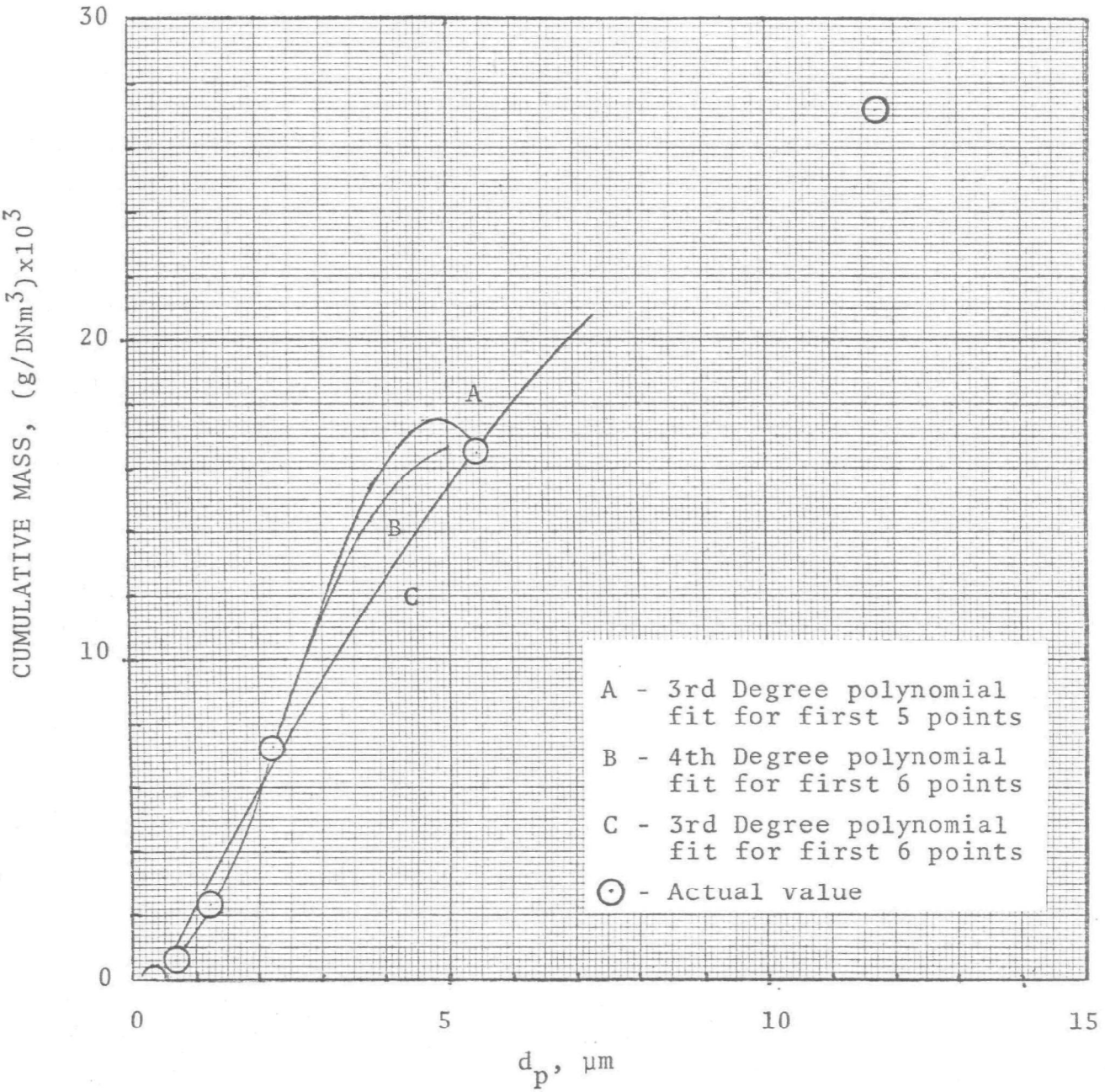

Figure 2-1 - Comparison of actual data and values calculated from polynomial.

CUT DIAMETER METHOD

Difficulty of separation

The "cut diameter" method, first described in the "Scrubber Handbook" (Calvert et al. 1972) and further discussed by Calvert et al. (1974), can be used as a convenient method for particle collection efficiency prediction. This method is based on the idea that the most significant single parameter to define both the difficulty of separating particles from gas and the performance of a scrubber is the particle diameter for which collection efficiency is 0.5 (50%).

For inertial impaction, the most common particle separation process in presently used scrubbers, aerodynamic diameter defines the particle properties of importance.

$$d_{pa} = d_p (\rho_p C')^{1/2}, \text{ common units} = \mu m(g/cm^3)^{1/2} \equiv \mu mA \quad (2\text{-}3)$$

When other separation mechanisms are important, other particle properties may be more significant but this will occur generally when "d_p" is less than a micron.

When a range of sizes is involved, the overall collection efficiency will depend on the amount of each size present and on the efficiency of collection for that size. We can take these into account if the difficulty of separation is defined as the aerodynamic diameter at which collection efficiency (or penetration) must be 50%, in order that the necessary overall efficiency for the entire size distribution be attained. This particle size is the required "separation cut diameter", "d_{RC}" and it is related to the required overall penetration, Pt, and the size distribution parameters.

The number and weight size distribution data for most industrial particulate emissions follow the log probability law. Hence, the two well established parameters of the log-normal law adequately describe the size distributions of

particulate matter. They are the geometric mean weight diameter "d_{pg}" and the geometric standard deviation "σ_g".

Penetration for many types of inertial collection equipment can be expressed as a function of constants "A_a" and "B":

$$Pt = \exp\ (-A_a\ d_{pa}{}^{B}) \qquad (2\text{-}4)$$

One may use the simplifying assumption that this relationship can be based on actual diameter, d_p. This will not introduce much error and it will conservatively utilize too low an efficiency for particles smaller than a micron or so. Thus:

$$Pt = \exp\ (-Ad_p{}^{B}) \qquad (2\text{-}5)$$

Packed towers, centrifugal scrubbers, and sieve plate columns follow the above relationship. For the packed tower and sieve plate column "B" has a value of 2. For centrifugal scrubbers "B" is about 0.67. Venturi scrubbers also follow the above relationship and B ≃ 2 when the throat impaction parameter is between 1 and 10.

The overall (integrated) penetration, $\bar{P}t$, of any device on a dust of any type of size distribution will be:

$$\bar{P}t = \int_0^W \left(\frac{dw}{w}\right) Pt \qquad (2\text{-}6)$$

The right-hand side of the above equation is the integral of the product of each weight fraction of dust times the penetration on that fraction. If equation (2-6) is solved for a log-normal size distribution and collection as given by equation (2-5), the resulting equation can be solved to yield Figures 2-2 and 2-3.

Figure 2-2 is a plot of "$\bar{P}t$" vs.$(d_{p50}/d_{pg})^B$ with "B ln (σ_g)" as a parameter. For a required "Pt" one can find the

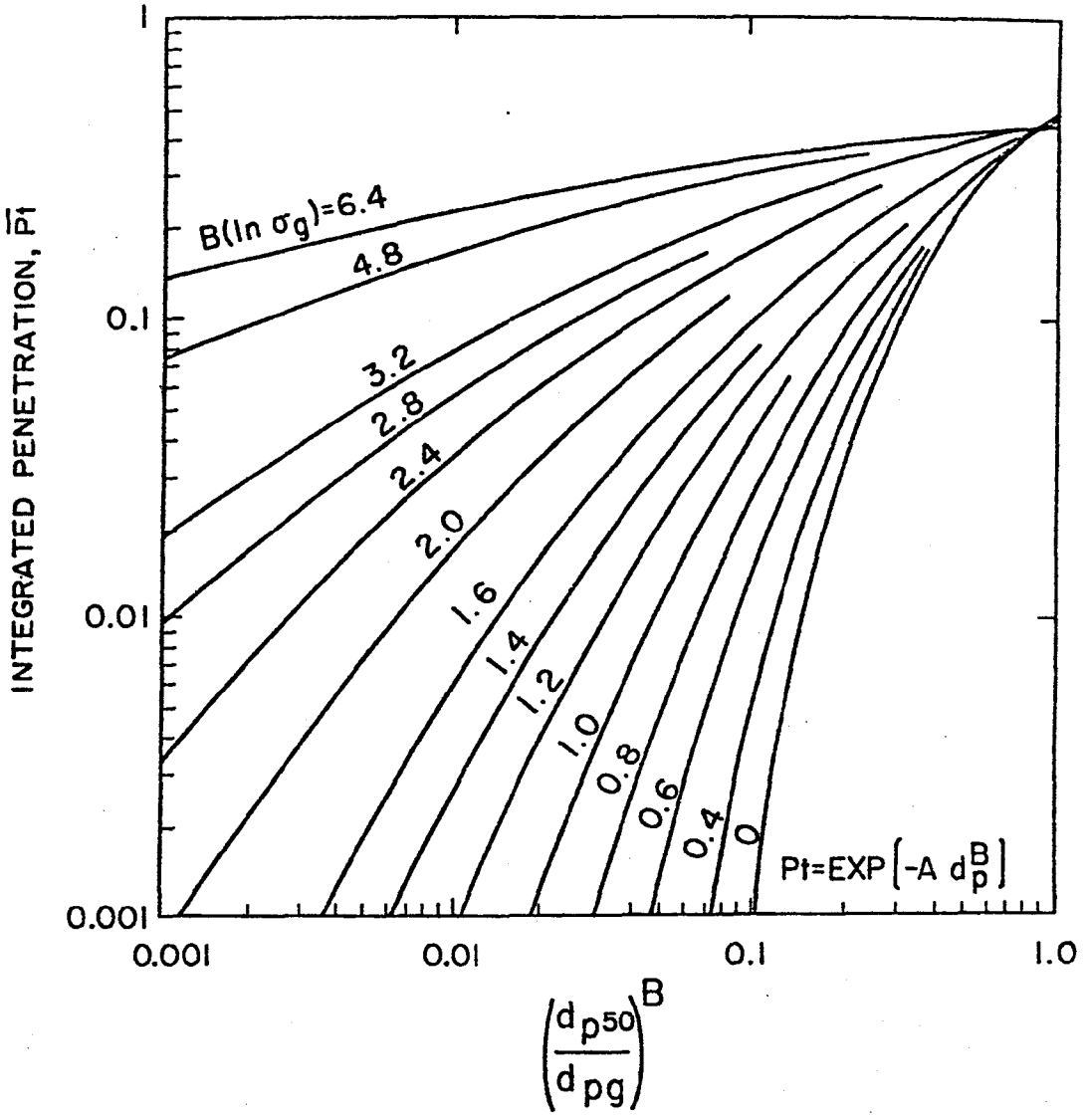

Figure 2-2. Integrated (overall) penetration as a function of cut diameter, particle parameters and collector characteristic.

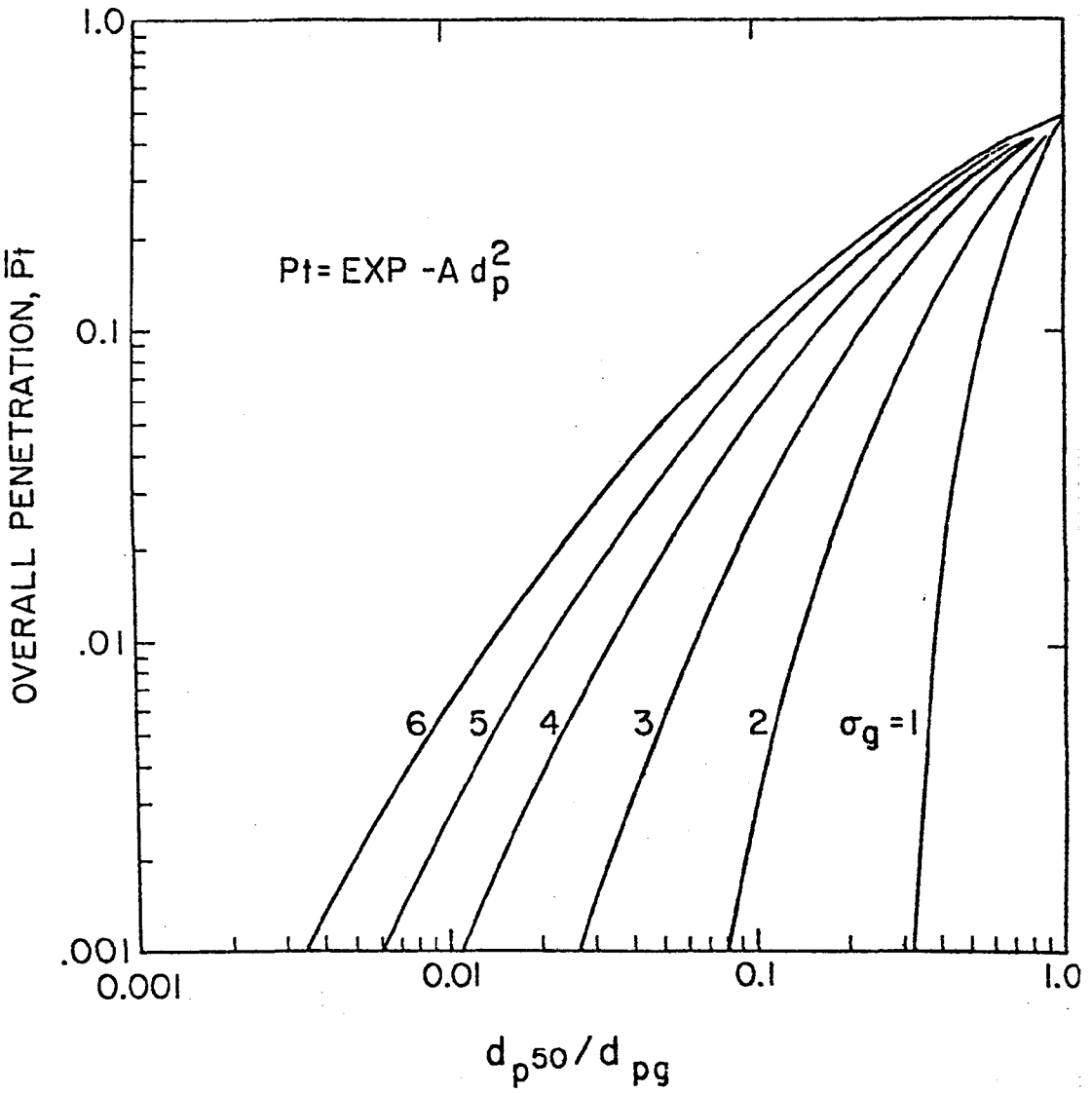

Figure 2-3. Overall penetration as a function of cut diameter and particle parameters for common scrubber characteristic, B = 2.

value of d_{RC} when "d_{pg}", "σ_g", and "B" are given. For convenience, Figure 2-3 is presented as a plot of "Pt" vs. (d_{p50}/d_{pg}) with σ_g as the parameter when B = 2.

To illustrate the use of the separation cut diameter, assume that 2% penetration is needed for dust with d_{pg} = 10 μm, ρ_p = 3g/cm^3 and σ_g = 3. If a scrubber such as a packed bed, sieve plate, or venturi is to be used, Figure 2-3 shows the cut diameter, d_{p50}, must be 0.09 x (d_{pg}) = 0.9 μm. The corresponding aerodynamic diameter is d_{RC} = 1.7 μm (g/cm^3)$^{1/2}$ = 1.7 μmA. Of course if the scrubber is capable of a smaller cut diameter, that is good; so "d_{RC}" is the maximum cut diameter acceptable. Some scrubbers, such as venturis, are only approximately fitted by relating penetration to exp (d_p^2) and more accurate plots can be prepared by using more representative performance equations. To avoid confusion these will not be given here, although they are presented in the "Scrubber Handbook".

Scrubber Performance

Collection efficiencies have been reported in the form of "grade efficiency" curves, which are plots of particle collection efficiency versus particle diameter for "typical" scrubbers. Unfortunately, there can be great variation in performance, depending on operating conditions and scrubber geometry so that one would need a grade efficiency curve for each important set of parameters.

The cut diameter approach proves to be a much more compact way to characterize scrubber performance. Performance graphs for a number of the important types of scrubbers are presented by Calvert et al. (1974). Capability is defined by "performance cut diameter", "d_{PC}", which is the aerodynamic particle diameter at which the scrubber gives 50% collection efficiency.

Once a scrubber type, size, and operating conditions are chosen by matching the "separation" and "performance" cut diameters, (i.e., $d_{RC} = d_{PC}$) a more accurate efficiency-diameter relationship can be developed and a more accurate computation of overall penetration can be made. The reason this step is necessary is that the relationship between overall penetration and separation cut diameter is shown in Figures 2-2 and 2-3 is only correct for packed beds and similar devices and is an approximation for others.

SCRUBBER ENERGY

The energy required for particle scrubbing is mainly a function of the gas pressure drop, except for pre-formed sprays and mechanically aided scrubbers. Previously we have been shown that there is an empirical relationship between particle penetration and power input to the scrubber for a given scrubber and a specific particle size distribution (Lapple and Kamack (1955) and Semerau (1960)). However, this "power law" did not provide a way to predict performance vs. power input for any size dust, without first determining the relationship experimentally.

A new relationship between "d_{PC}" and scrubber pressure drop (S. Calvert, 1974) is presented here. Figure 2-4 is a plot of performance cut diameter, d_{PC}, versus gas pressure drop for sieve plates, venturi (and similar), impingement plates, and packed columns. Predictions were made by means of design methods given in the "Scrubber Handbook"

1. Sieve plate penetration and pressure drop predictions for one plate are plotted as lines 1a and 1b for perforation diameters of 0.5 cm and 0.3 cm, respectively, and F=0.4. Cut diameters for other froth densities (F) can be computed from

the relationship that they are inversely proportional to "F". Cut diameters for two and three plates in series would be 84% and 80% of those for one plate at any given pressure drop. Note that these predictions are for wettable particles and that both froth density and pressure drop are dependent on plate design and operation.

2. Venturi penetration and pressure drop data are given for f = 0.25 and f = 0.5 in lines 2a and 2b, respectively. The predictions are for a liquid to gas ratio, $Q_L/Q_G \sim 1\ \ell/m^3$, corresponding to about the minimum pressure drop for a given penetration. Data recently obtained by A.P.T. for a large coal-fired power plant scrubber fit a value of f = 0.5.

3. Impingement plate data used for line #3 were predicted for one plate. Cut diameters for 2 and 3 plates in series are 88% and 83% of those shown in line #3.

4. Packed column performance as shown by line #4 is representative of columns from 1 to 3 meters high and packing of 2.5 cm nominal diameter.

To estimate the penetration for particle diameters other than the cut size, under a given set of operating conditions, one can use the approximation of equation (2-5) with B = 2.0. Alternatively, one could use more precise data or predictions for a given scrubber. Figure 2-5 is a plot of the ratio of particle aerodynamic diameter to cut diameter versus penetration for that size particle (d_{pa}), on log-probability paper. One line is for equation (2-5) and the other is based on data for a venturi scrubber.

Performance Limit for Inertial Impaction

The limit of what one can expect of a scrubber utilizing inertial impaction is clearly indicated by Figure 2-4. If a

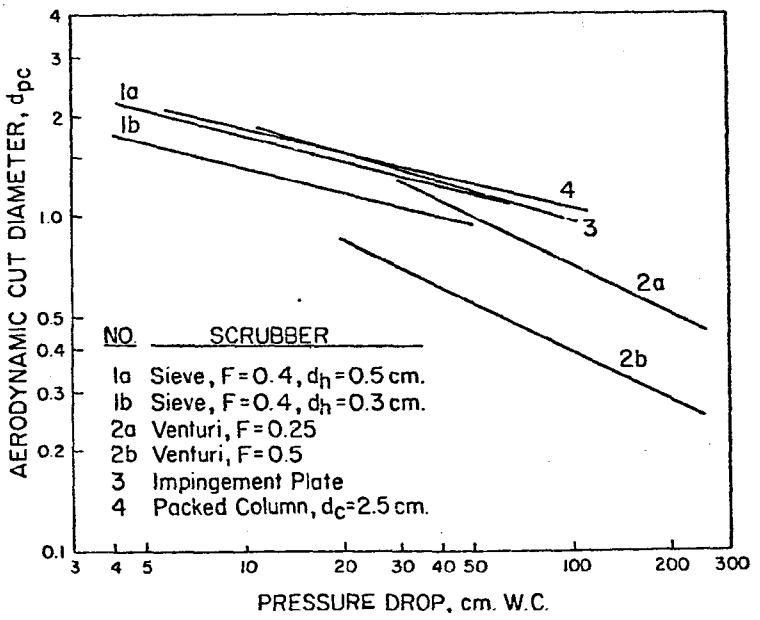

Figure 2-4. Representative cut diameter as a function of pressure drop for several scrubber types.

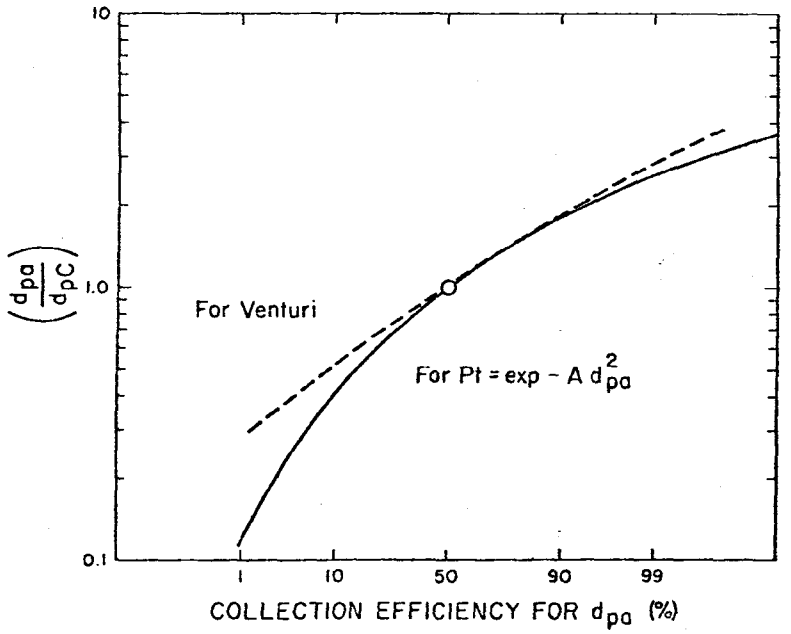

Figure 2-5. Ratio of particle diameter to cut diameter as a function of collection efficiency.

cut diameter of 1.0 μmA, or smaller is required, the necessary pressure drop is in the medium to high energy range. High efficiency on particles smaller than 0.5 μmA diameter would require extremely high pressure drop if inertial impaction were the only mechanism active.

High efficiency scrubbing of sub-micron particles at moderate pressure drop is possible, but it required either the application of some particle separation force which is not dependent on gas velocity or the growth of particles so that they can be collected easily. Particle separation phenomena which offer promise and have been proven to some extent are the "flux forces" due to diffusiophoresis, thermophoresis, and electrophoresis. Brownian diffusion is also useful when particles are smaller than about 0.1 μm diameter.

Particle growth can be accomplished through:

1. Coagulation (agglomeration)
2. Chemical reaction
3. Condensation on particles
4. Ultrasonic vibrations
5. Electrostatic attraction

Diffusional Collection

Particle collection by Brownian diffusion can be described by relationships for mass transfer and it is possible to outline the magnitude of efficiency which can be attained with typical scrubbers. The general relationship which describes particle deposition in any control device in which turbulent mixing eliminates any concentration gradient normal to the flow outside the boundary layer and in which the deposition velocity is constant is:

$$Pt = \exp - \left(\frac{u_{PD} A_d}{Q_G} \right) \qquad (2\text{-}7)$$

where, u_{PD} = particle deposition velocity

A_d = total outside surface area of drops in scrubber

Q_G= gas volumetric flow rate.

The particle deposition velocity for Brownian diffusion, u_{BD}, can be estimated from penetration theory as:

$$u_{BD} = 1.13 \left(\frac{D_p}{\theta}\right)^{1/2} \qquad (2\text{-}8)$$

For packed columns the penetration time, θ, can be taken as the time required for the gas to travel one packing diameter. For plate scrubbers which involve bubbles rising through liquid, the penetration time for a circulating bubble is about that for the bubble to rise one diameter, as shown by Taheri and Calvert (1968). For spray scrubbers the penetration time is that for the gas to travel one drop diameter.

Predictions of particle penetration due to Brownian diffusion only were made by means of equations (2-7) and (2-8) for a typical sieve plate and packed columns. A prediction for a venturi scrubber was made by means of "Scrubber Handbook" equation (5.2.6-17), for gas phase controlled mass transfer.

The results are plotted on Figure 2-6 as collection efficiency vs. particle diameter. It can be seen that high efficiency collection of 0.01 μm diameter particles is readily attainable with a three plate scrubber, typical of a moderately effective device for mass transfer. Collection efficiency for particles a few tenths micron diameter is poor, as is well known.

Particle separation by flux force mechanisms is not amenable to such simple treatment as Brownian diffusion because of the variation of deposition velocity with heat and mass transfer rates within the scrubber.

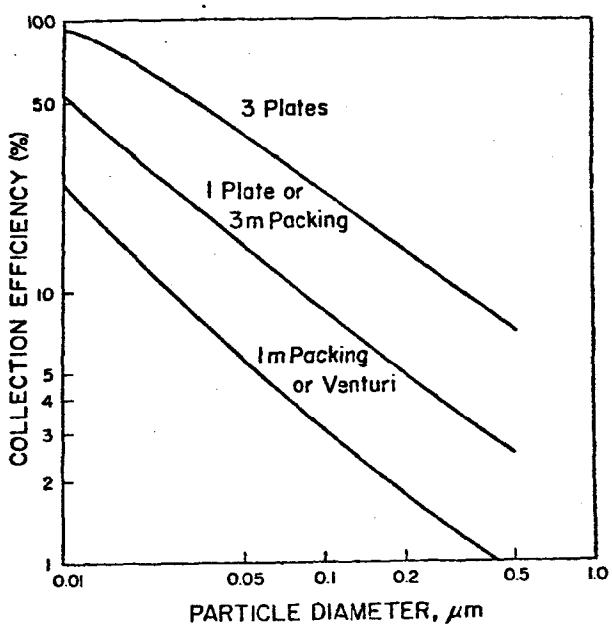

Figure 2-6. Predicted particle collection by diffusion in plates, packing, and venturi scrubbers.

APPENDIX 2-A
CURVE FITTING TECHNIQUE

CURVE FITTING TECHNIQUE

The principle of least squares is employed to derive information about the functional relation between particle diameter and cumulative mass, assuming such a relation exists, from a set of data pairs (d_{pi}, W_i) $(i = o, n)$.

The technique is to fit a function of the form

$$F(d_p) = a_o f_o (d_{pi}) + a_j f_j (d_{pi}) +----+ a_m f_m (d_{pi}) \quad (2\text{-A-}1)$$

to a set of data pairs.

Where $f_j (d_{pi})$ are some arbitrary functions and a_o, a_j ---- a_m are independent parameters to be determined. These parameters may either be linear or non-linear. In the present study, we only considered linear parameters.

The difference between the approximating function value, $F(d_{pi})$, and the corresponding data value, W_i, is called residual, r_i, and is defined by the relation

$$r_i = F(d_{pi}) - W_i \qquad (i = o, n) \qquad (2\text{-A-}2)$$

The function that best approximates the given set of data in a least-squares sense is that the function produces the minimum value of the sum Q of the squared residuals

$$Q = \sum_i [F(d_{pi}) - W_i]^2$$

$$= \sum_i [a_o f_o (d_{pi}) + a_1 f_1 (d_{pi}) +---+ a_m f_m (d_{pi}) - W_i]^2 \qquad (2\text{-A-}3)$$

A minimum is obtained when m + 1 partials of Q (a_o, --- a_m) with respect to parameters a_j (j = o, m), simultaneously vanish, i.e., when

$$\frac{\partial Q}{\partial a_j} \equiv 2 \sum_i [F(d_{pi}) - W_i] \frac{\partial F(d_{pi})}{\partial a_j} = 0$$

$$\text{or} \equiv 2 \sum_i [a_o f_o (d_{pi}) + a_1 f_1 (d_{pi}) + \text{---} + a_m f(d_{pi}) - W_i]$$

$$f_j (d_{pi}) = 0, j = 0, \text{---} m$$

(2-A-4)

In matrix form, this becomes

$$\begin{bmatrix} \Sigma [f_o(d_{pi})]^2 & \Sigma f_o(d_{pi}) f_1(d_{pi}) & \Sigma f_o(d_{pi}) f_m(d_{pi}) \\ \Sigma f_1(d_{pi}) f_o(d_{pi}) & \Sigma [f_1(d_{pi})]^2 & \Sigma f_1(d_{pi}) f_m(d_{pi}) \\ \Sigma f_m(d_{pi}) f_o(d_{pi}) & \Sigma f_m(d_{pi}) f_1(d_{pi}) & \Sigma [f_m(d_{pi})]^2 \end{bmatrix} \begin{bmatrix} a_o \\ a_1 \\ a_m \end{bmatrix}$$

$$= \begin{bmatrix} \Sigma f_o(d_{pi}) W_i \\ \Sigma f_o(d_{pi}) W_i \\ \Sigma f_1(d_{pi}) W_i \\ \Sigma f_m(d_{pi}) W_i \end{bmatrix} \qquad (2\text{-A-5})$$

The solution (a_o, a_1 ---, a_m) of equation (2-A-5) can be computed by inverting the matrix of coefficients in that equation, and multiplying the right-hand column matrix by this inverse matrix.

In the case of curve fitting by polynomial,

$$f_j\ (d_{pi}) = (d_{pi})^j, \quad j = 0, 1, \text{---}\ m$$

and the coefficient matrix is

$$\begin{bmatrix} n+1 & \Sigma\, d_{pi} & \text{----} & \Sigma\, (d_{pi})^m \\ \Sigma\, d_{pi} & \Sigma\, (d_{pi})^2 & \text{----} & \Sigma\, (d_{pi})^{m+1} \\ \text{----------} & \text{----------} & \text{----------} & \text{----------} \\ \Sigma\, (d_{pi})^m & \Sigma\, (d_{pi})^{m+1} & \text{---} & \Sigma\, (d_{pi})^{2m} \end{bmatrix}$$

Once the functional relationship between particle diameter and cumulative mass is obtained, the calculation of penetration is straightforward.

VALVE TRAY ON UREA PRILLING TOWER
(Koch Flexitray)

SOURCE AND SCRUBBER

An 85 Am^3/min (3,000 ACFM) valve tray (Multi-Venturi Flexitray) scrubber for urea prilling tower exhaust was chosen for the second performance test. The scrubber, which was designed and built by Koch Engineering Company utilizes two trays in series. The bottom tray contains 27 openings and the top tray contains 70 openings. Each of the openings is surmounted by a spider cage holding a floating cap, or "valve" (Figure 3-1). In addition, each tray is equipped with downcomers and weir flow baffles that control the scrubbing liquid as it flows across the tray and then to the tray below.

The scrubber was a pilot plant installed to determine its effectiveness in scrubbing particles from the urea prill tower exhaust gas which was brought down to ground level from the tower top, about 46 m (150 ft) above ground. The gas enters the bottom of the scrubber and flows upward through the trays. At low gas velocities, the lightweight caps (located in every other row) rise first, whereas the heavy weight caps (in the alternate rows) remain in the closed position. All the caps are fully opened as the vapor flow attains the design conditions.

The liquid flows across the tray deck and is kept in a constant froth by the gas which flows from the caps. There is always a head of froth maintained by the weir. After passing through the trays the gas passes through a mist eliminator. The scrubbed gas then flows from the top of the scrubber to the induced draft fan and a short stack.

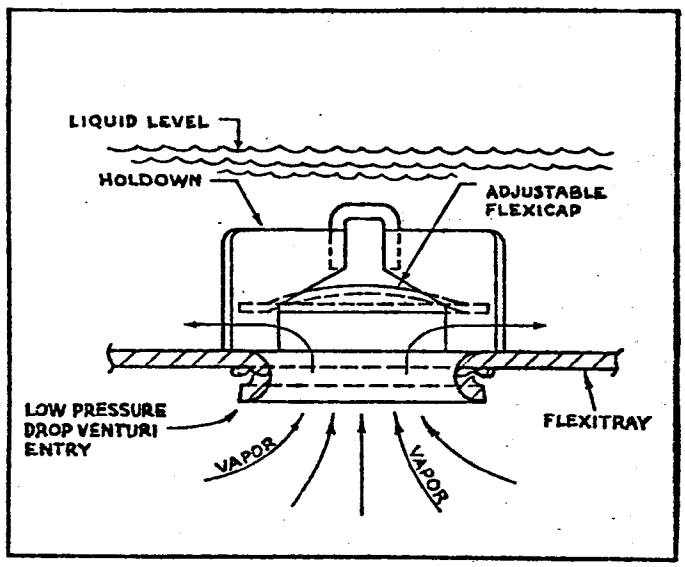

Figure 3-1 - Assembly of a scrubbing element on the Flexi Tray

Because this scrubber was a pilot plant, there were no data available on operating problems, maintenance, economics, etc.

TEST METHOD

The performance of the scrubber was determined by analyzing the particle size distribution and mass loading of the inlet and outlet gas samples. As in all of the performance tests, each sample was taken at one point in the duct. A modified E.P.A. sampling train equipped with a cascade impactor was used for particle size sampling. Two types of impactors,an Andersen Sampler and University of Washington Mark III Cascade Impactor (or Pilat), were used for this purpose.

An in-stack cyclone pre-cutter was attached to the sampling probe. The cyclone collects particles larger than about 3 μmA diameter and leaves the fine particles to be collected by the cascade impactor/back-up filter assembly.

The effect of condensation on particle size was studied during this performance test. Therefore, in some of the test runs the impactor was kept in-stack and allowed to heat up to stack temperature before sampling. In other runs the impactor was ex-stack and with electric heating tape wrapped around the outside jacket of the impactor. The temperature of the impactor was controlled by a variac on the heating circuit. Details on each run's impactor location were listed in Table 3-1.

Scrubber inlet and outlet gas temperatures were measured by mercury filled glass bulb thermometers. Gas temperature at the sampling location was measured during each test run. The inlet and outlet stack pressures were measured with a

Table 3-1. IMPACTOR LOCATION

RUN NO.	IMPACTOR LOCATION
1a, 2a, 3a, 4a	in-stack
1b, 2b, 3b, 4b	ex-stack
5, 6, 7	in-stack
8	ex-stack (heated probe)
9, 10	ex-stack (heated probe)
Inlet of 11, 12, 13, 14	ex-stack (heated probe)
Outlet of 11, 12, 13, 14	ex-stack (heated probe)

U-tube manometer. Barometric pressures were determined before each run from an aneroid barometer. The stack gas humidities were determined by dry and wet bulb thermometer. Gas flow rate was measured by means of a calibrated S-type pitot tube traverse.

IMPACTOR CALIBRATION

Since different types of cascade impactors were used in a simultaneous inlet and outlet sampling, the agreement between these impactors was determined before making any interpretation of the data. Four sets of samples from the scrubber inlet gas stream were taken simultaneously with an in-stack U. W. impactor and an ex-stack Andersen Sampler. These sets were taken to compare and calibrate the stage cut diameters, d_{p50}, between the U. W. and Andersen impactors. Test results were listed in Tables 3-A-1 through 3-A-4 and were plotted in Figures 3-B-1 and 3-B-2.

A discrepancy was found (see Figures 3-B-1 and 3-B-2) in the measurement of particle size distribution between the Andersen and the U. W. impactors. For consistency, the Andersen Sampler was calibrated against the U. W. impactor, which was assumed to be correctly calibrated. The calibrated cut diameter, d_{p50}, for each stage of the Andersen Sampler was taken to be the diameter, based on the U. W., corresponding to the mass fraction undersize measured by the Andersen. For example, Figure 3-B-1 shows that the cut diameter for stage 7 of the Andersen was 0.36 μmA according to the manufacturer's calibration, but 24% undersize would correspond to a cut diameter of about 0.58 μmA based on the U. W. data and calibration. Table 3-2 shows the calibrations for the last 4 stages of the Andersen Sampler as given by the manufacturer and as calibrated against the U. W.

Table 3-2. ANDERSEN SAMPLER CALIBRATIONS AT 0.028 m^3/min (1 CFM)

Stage No.	Stage Cut Diameter, μmA	
	Manufacturer	Field Calibration
4	1.75	2.0
5	0.9	1.5
6	0.54	1.0
7	0.36	0.6

SAMPLING RESULTS

Wet and Dry Particle Size

The scrubber outlet samples were taken either in the duct after the exhaust fan or between the scrubber exit and the exhaust fan. It was found that particulate matter coming out of the scrubber was in the form of urea-water drops, because crystals and liquid drops were observed on the last two collection plates of the Andersen Sampler. Therefore, the particle size measured will be that of a "grown" particle and will not correspond directly with the inlet size data for dry particles. The actual dry particle size would be smaller and the curve of cumulative mass vs. "d_{pa}" should shift to the left as indicated by the dotted curve on Figure 3-2.

In order to determine the nature of the grown particles measured in the exit, some samples were taken in such a way as to avoid evaporation of the urea-water drops. Runs 5 and 6 (see Tables 3-A-5 and 3-A-6) were done with an in-stack U. W. impactor to sample the outlet gas stream between the scrubber exit and the exhaust fan. Liquid drops on the collection plates of the U. W. were observed when this sampling technique was used. Each of the impactor collection plates was

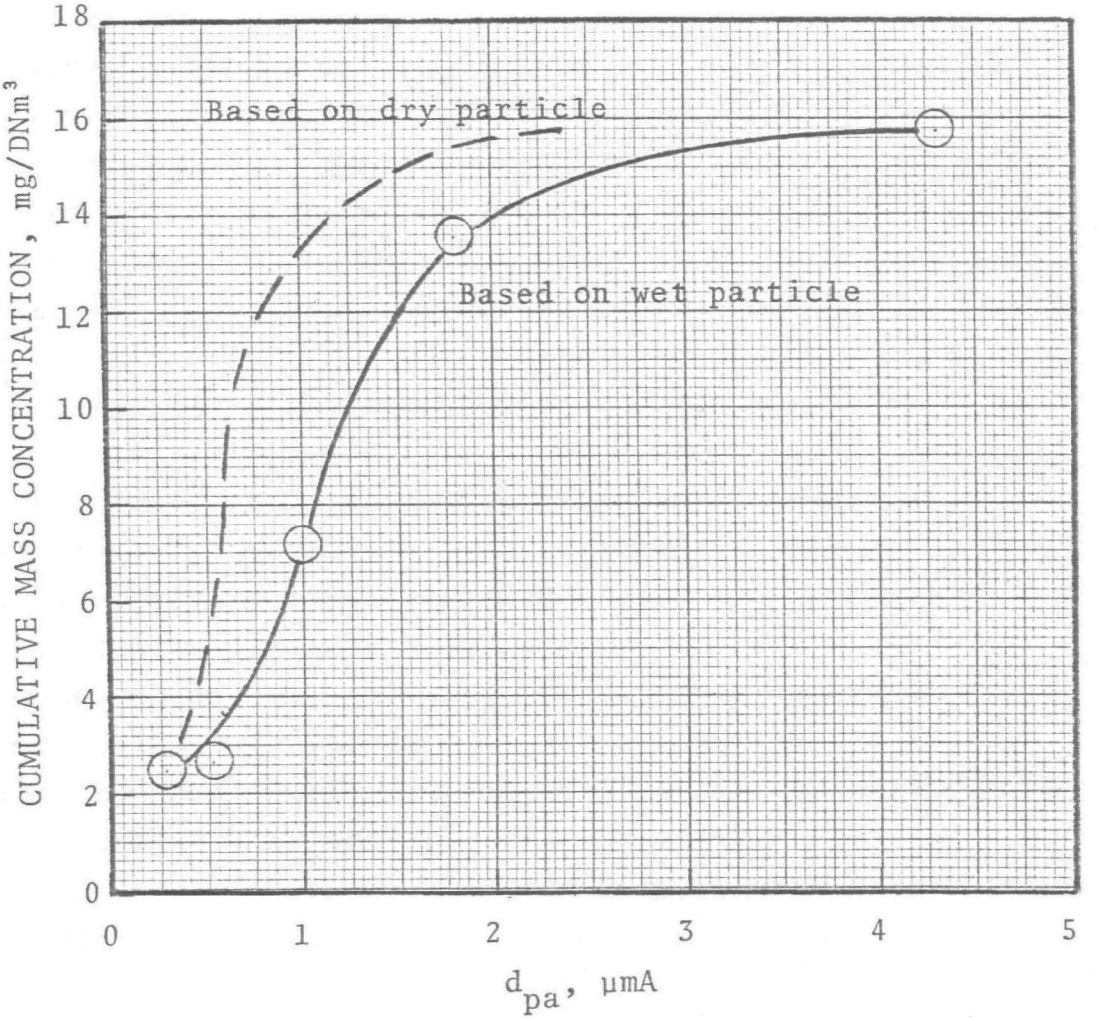

Figure 3-2 - Cumulative mass concentration distribution for Run #6.

weighed before and after putting it in a silica gel filled desiccator. Particle sizes "d_{pa}" and drop sizes "d_d" are derived from either of the following alternative assumptions.

Alternative 1 - The water collected on the cascade impactor collection plates is in the form of water drops when passing through the cascade impactor jets. The urea caught on the plates is in the form of dry urea particles when passing through the cascade impactor jets.

Alternative 2 - The material caught on the impactor plates is in the form of drops of urea-water solution.

It was proven in test Runs 7 and 8 (see Tables 3-A-7 and 3-A-8) that Alternative 2 is more valid than Alternative 1. Test No. 7 is an outlet test run with an in-stack U. W. Run 8 was taken with an ex-stack U. W. attached to a heated sampling probe. The heated sampling probe was used to evaporate water in the sample gas before it reached the U. W., so that dry particles were measured by the impactor. Figure 3-B-3 shows that the results from both of these tests correlate very closely when the Run 7 data are converted to the dry basis, assuming alternative 2 is correct. Therefore, equivalent dry particle size may be calculated from the urea-water drop size for the outlet sampling test with an in-stack U. W.

Once the dry particle and wet particle size relationship was found, the prediction of particle growth based on dry particle size was possible. Figure 3-3 is a curve showing the dry and wet particle size relation for this particle composition.

Scrubber Operating Condition and Particle Data

Six simultaneous scrubber inlet and outlet samples were taken to determine scrubber performance related to the particle

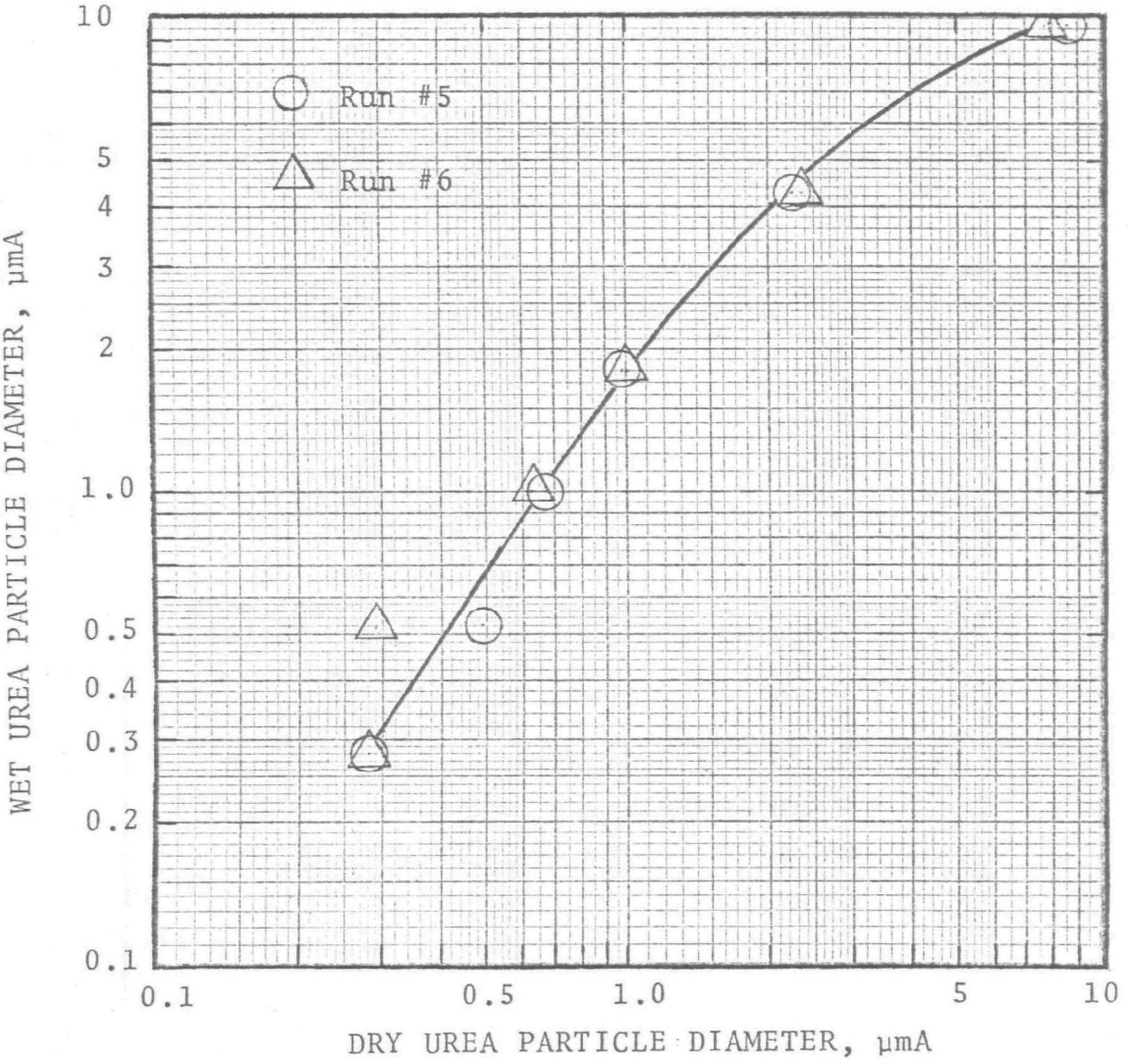

Figure 3-3 - Urea-Water solution drop diameter versus Original Dry urea particle diameter.

size. These test runs were grouped into two data sets corresponding to different urea prill tower operating conditions. Runs 9 and 10 were in set "A", Runs 11 through 14 were in set "B". The prill tower operating conditions were shown in the following tabulation. Buckets are the devices used for atomizing the urea into liquid drops which are then solidified into prills.

Urea Prill Tower Operating Conditions

Data Set	Type of Urea Prill Bucket	Urea Prill Temp. °C
A	"Old"	88
B	Tuttle	71

The scrubber operating conditions during these tests were as follows:

1. Gas parameters were shown in the tabulation below

Gas Parameters	Inlet	Outlet
Temperature	27°C	17°C
Pressure, cm W.C.	-15.0	-35.0
A m^3/min	86	85
ACFM	3,100	3,000
DN m^3/min @ °C	78.6	78.6
DSCFM @ 70°C	2,990	2,990
Vol. % H_2O vapor	1.5	2.0

2. Pressure drop data (in cm W.C.)

Run No.	Bottom Tray	Top Tray	Demister
9	14.2	5.6	0.76
10	12.2	7.4	0.76
11	11.2	5.8	0.76
12	10.7	5.8	0.76
13	10.7	5.8	0.76
14	5.3	6.1	—

3. Scrubber liquor flow rate (in m^3/min)

Run No.	Inlet	Outlet
9	0.047 (12.5 GPM)	0.047 (12.5 GPM)
10	0.047 (12.5 GPM)	0.047 (12.5 GPM)
11	0.06 (16 GPM)	0.06 (16 GPM)
12	0.06 (16 GPM)	0.06 (16 GPM)
13	0.06 (16 GPM)	0.06 (16 GPM)
14	0.049 (13 GPM)	0.049 (13 GPM)

4. Entrainment was not measured in this performance test.

The particle concentration and size data which were obtained in this performance test are presented in Tables 3-A-9 through 3-A-14. Figures 3-B-4, 3-B-5 and 3-B-6 are log-probability plots of inlet and outlet particle size distributions for data sets A and B. There are some variations between set A and B in particle sizes. This is mainly due to different

urea buckets. The mass median diameter and geometric standard deviation for these sampling runs are listed in the following tabulation:

Run No.	Inlet		Outlet	
	d_{p50}, μmA	σ_g	d_{p50}, μmA	σ_g
9	0.82	1.7	1.2	2.2
10	0.82	1.7	1.2	2.2
11	1.1	1.5	0.9	1.9
12	1.1	1.5	0.9	1.9
13	1.1	1.5	0.9	1.9
14	1.1	1.5	0.9	1.9

Cumulative mass concentration was plotted against aerodynamic particle size to yield Figures 3-4 through 3-9.

PARTICLE PENETRATION

The ability of a scrubber to control particulate emissions is interpreted in terms of "grade efficiency" curves, which are plots of particle collection efficiency, or particle penetration versus particle diameter. The penetration can be described as the ratio of the outlet cumulative mass distribution slope to the inlet cumulative mass distribution slope, as given in equation (2-2). The slopes, $dM/d(d_{pi})$, are determined by graphical procedures on Figures 3-4 and 3-9 for the scrubber inlet/outlet samples. The particle collection efficiencies obtained by this method were plotted in Figures 3-10 and 3-11. It should be noted that the penetration for particles smaller than 1.0 μmA in Figure 3-10 is highly dependent on the shape of the cumulative mass distribution in Figures 3-4 and 3-5.

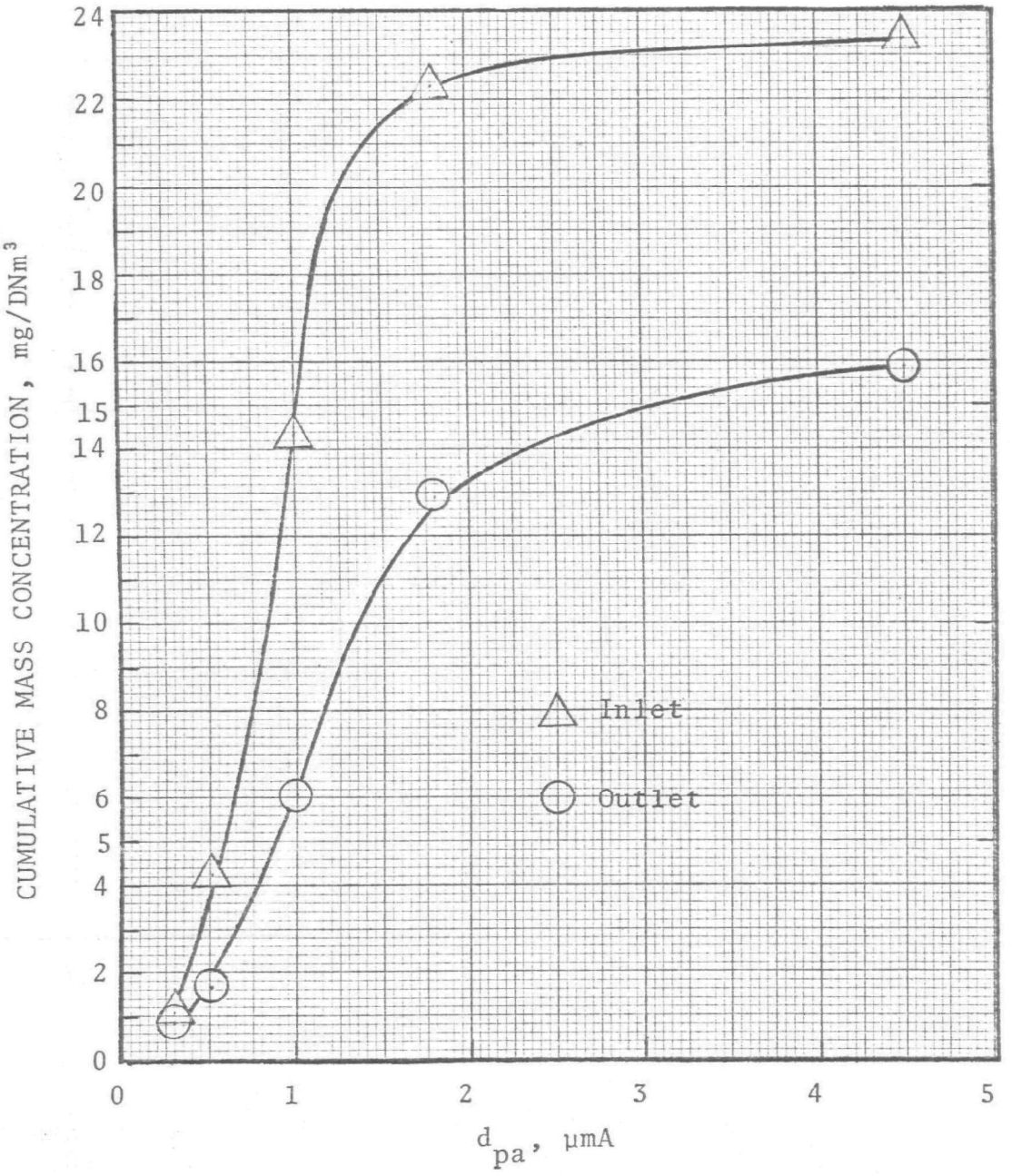

Figure 3-4 - Cumulative mass versus aerodynamic particle size for Run #9.

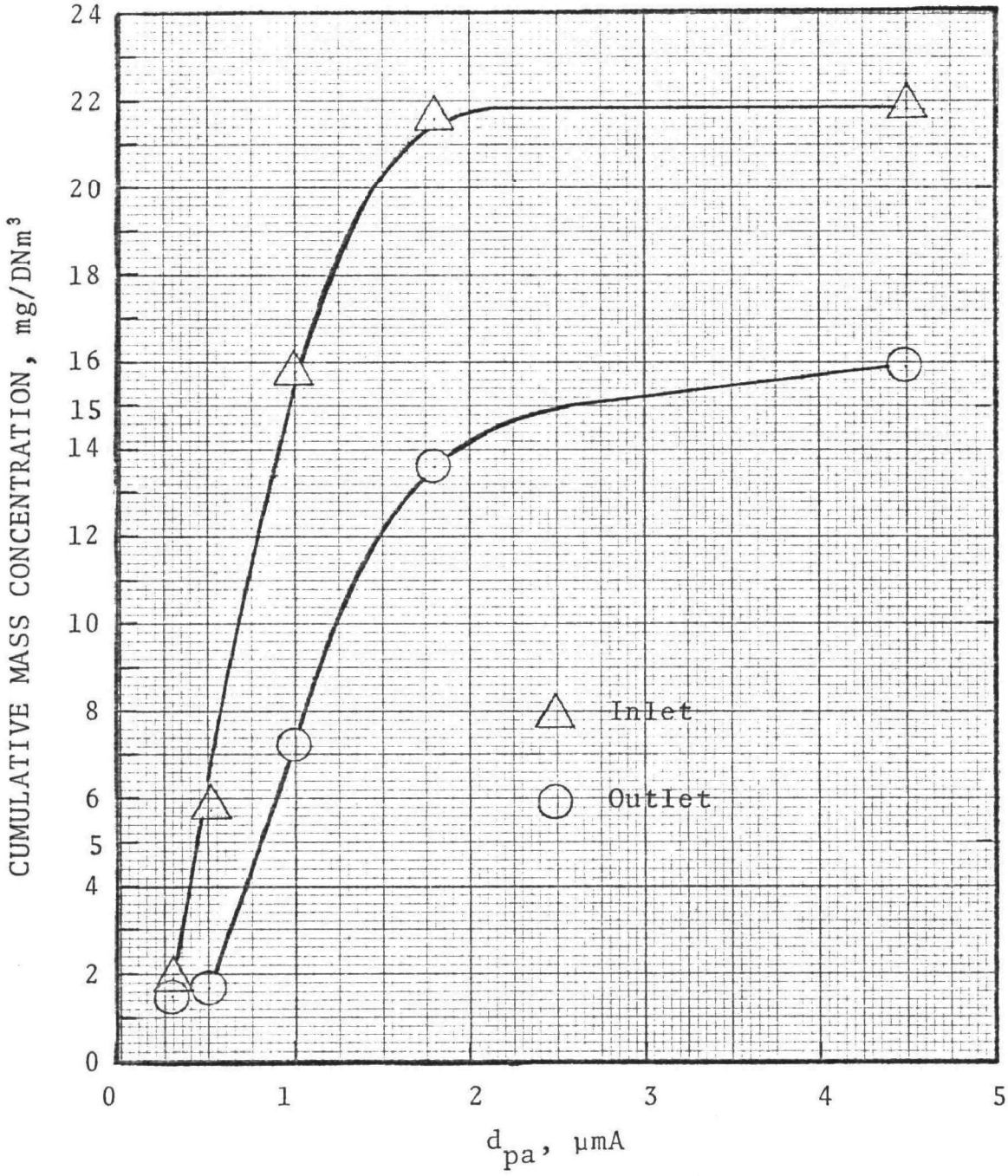

Figure 3-5 - *Cumulative mass versus aerodynamic* particle diameter for Run #10.

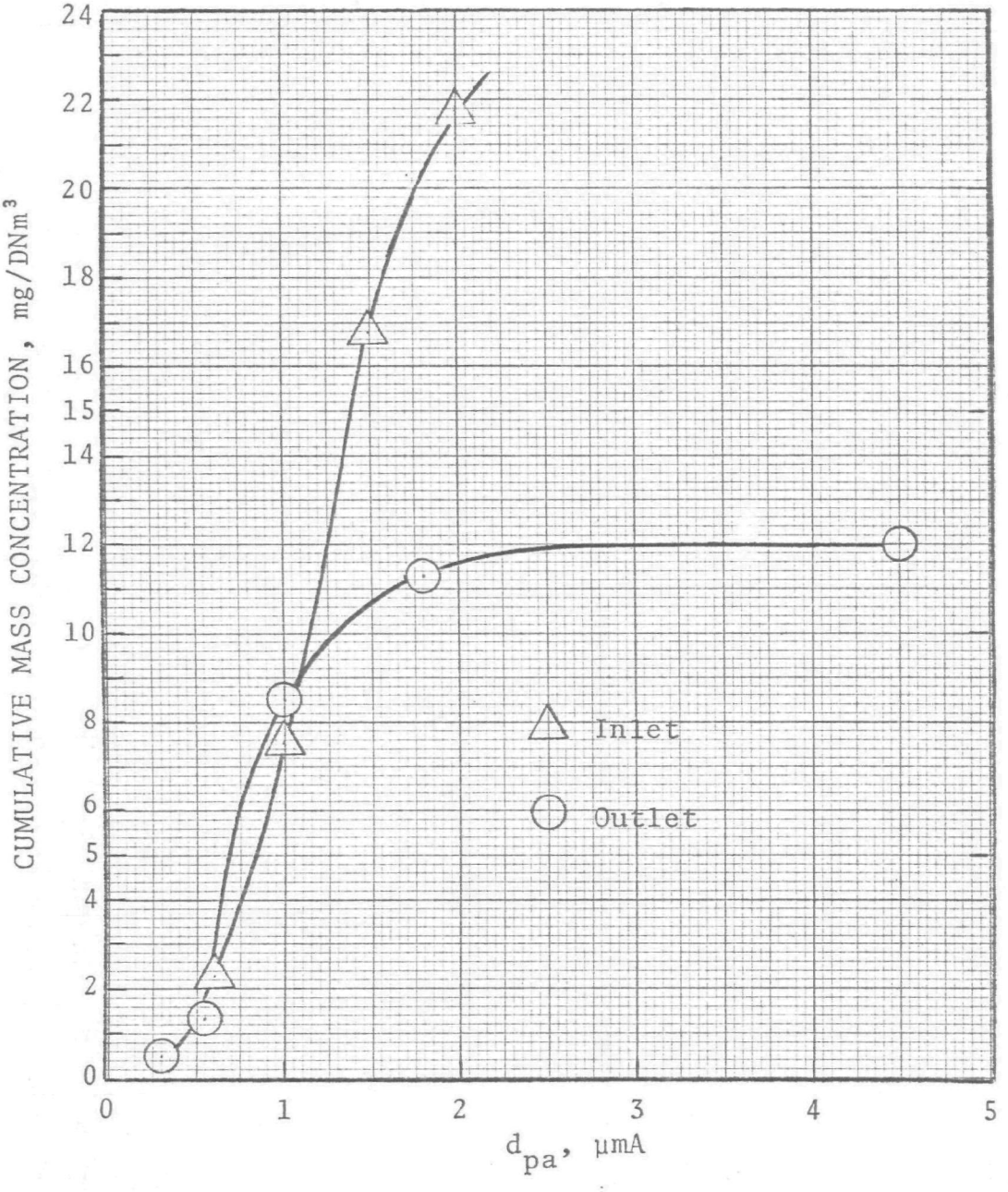

Figure 3-6 - Cumulative mass versus aerodynamic particle diameter for Run #11.

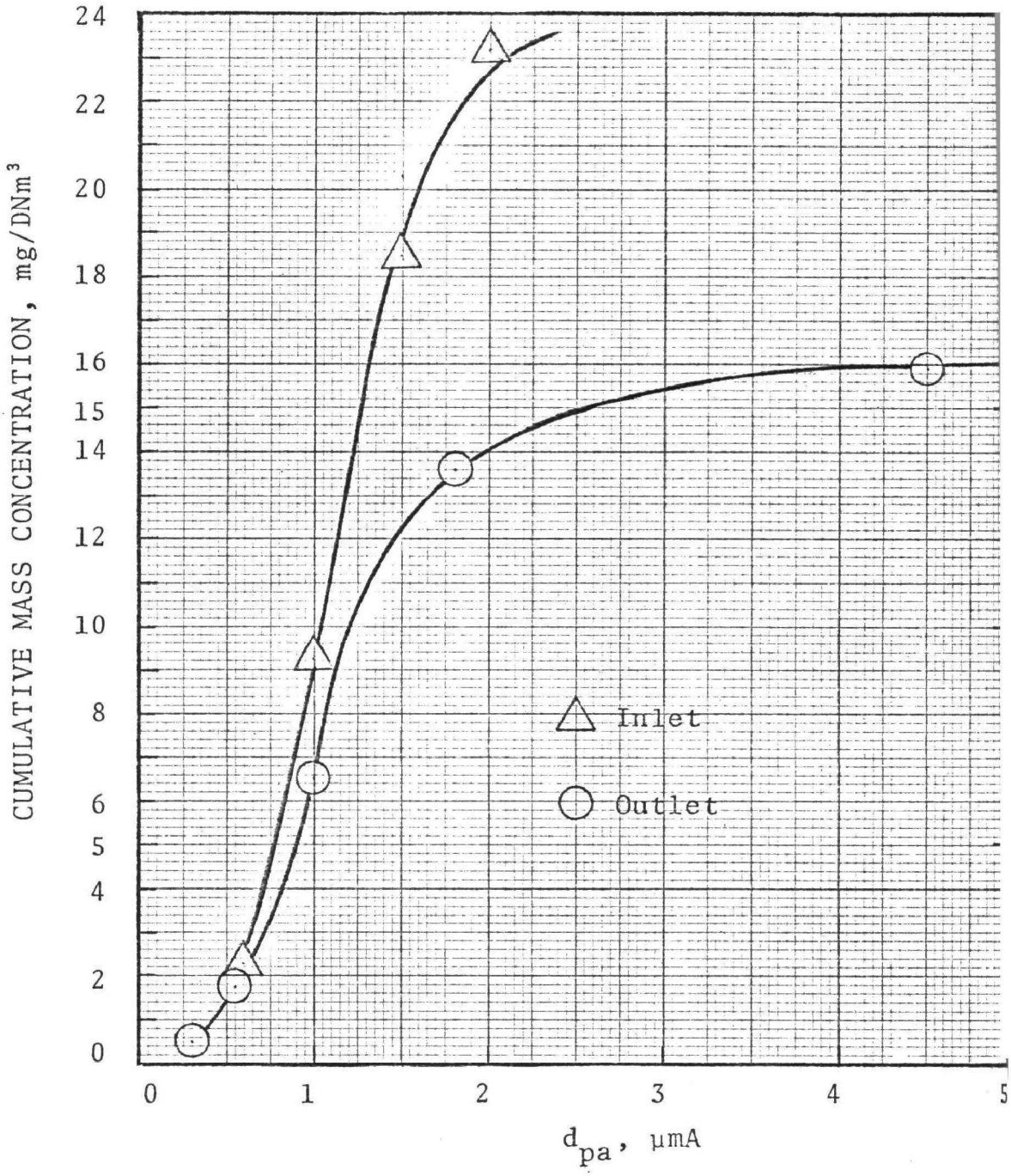

Figure 3-7 - Cumulative mass versus aerodynamic particle diameter for Run #12.

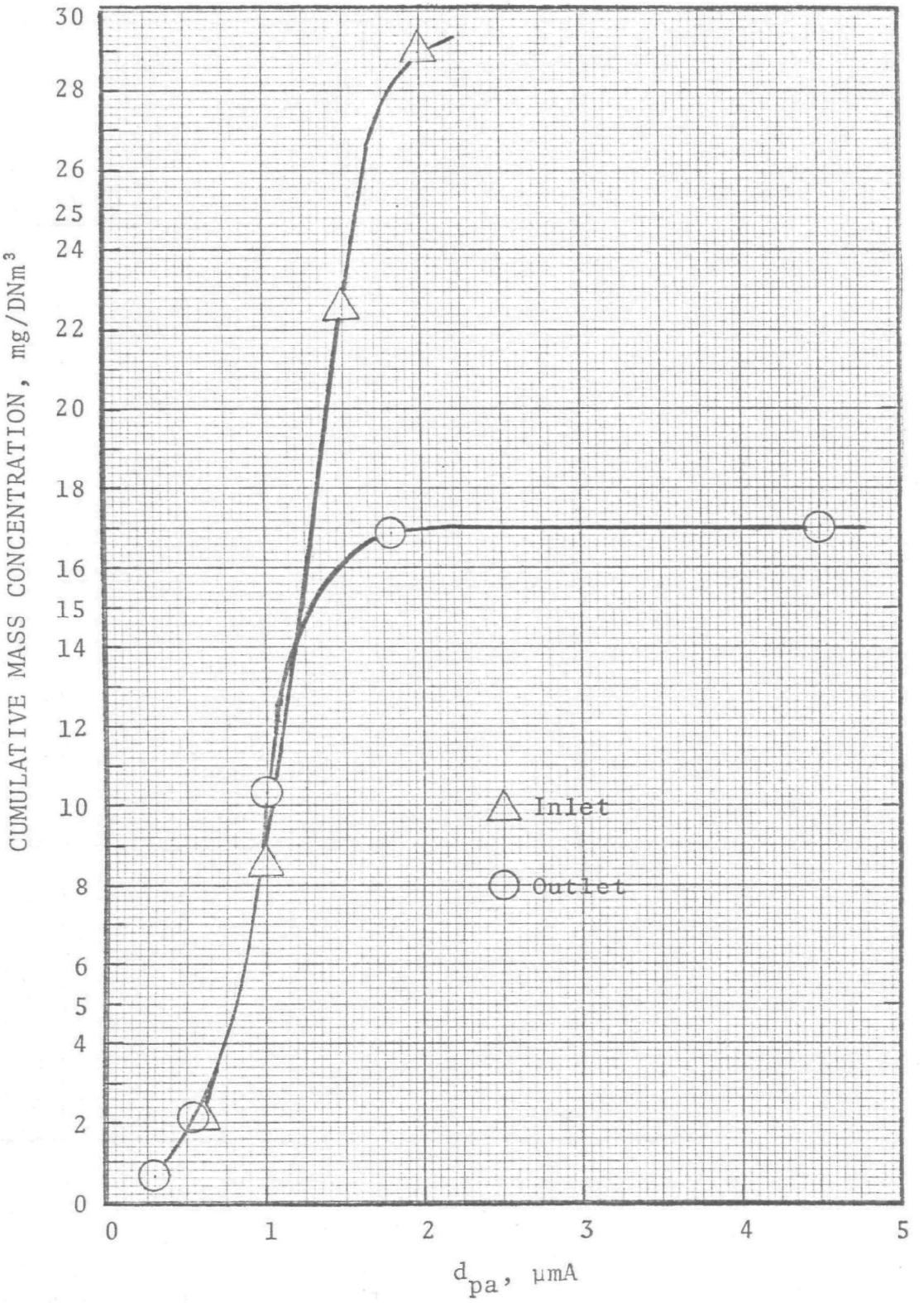

Figure 3-8 - Cumulative mass versus aerodynamic particle diameter

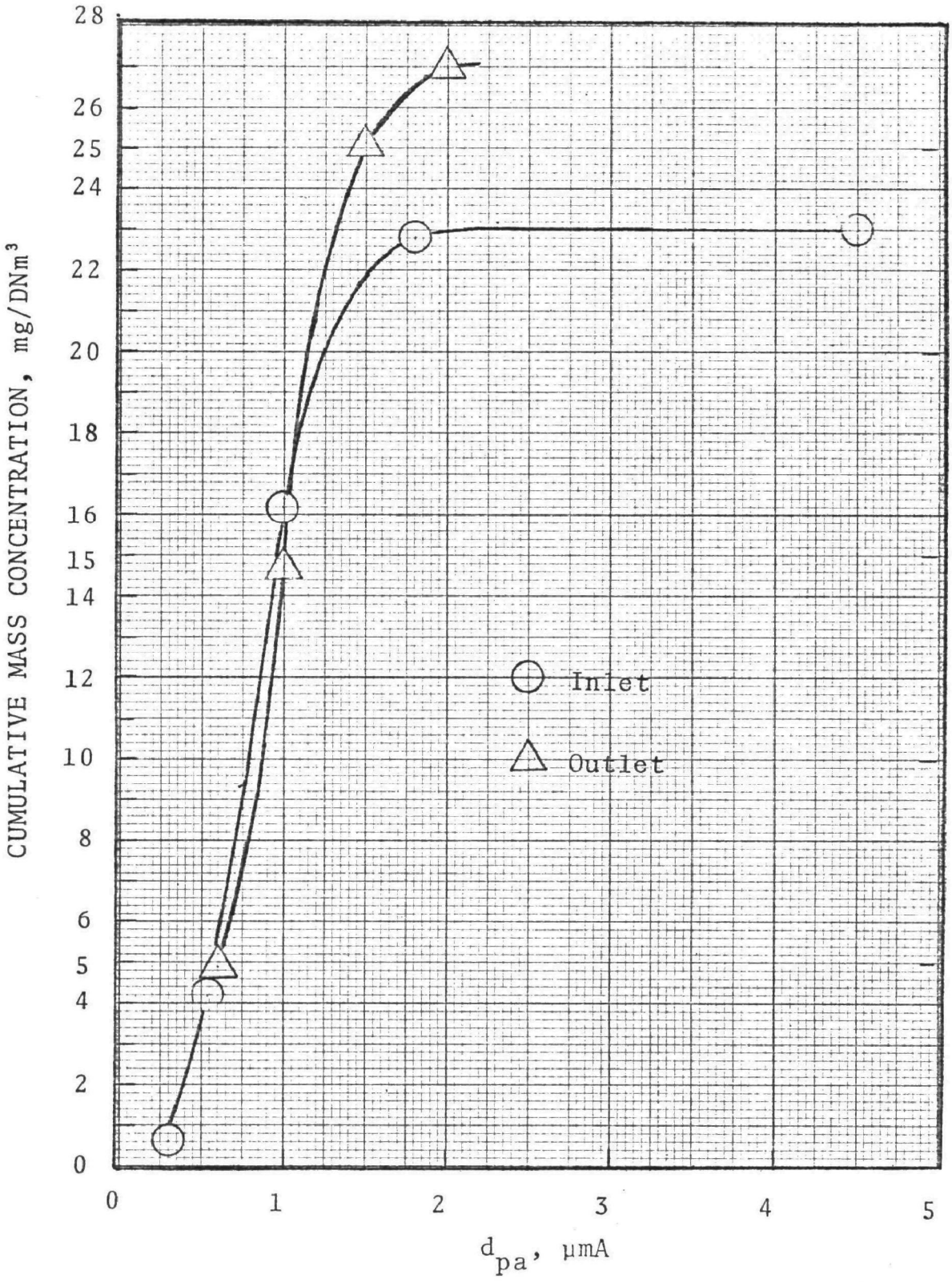

Figure 3-9 - Cumulative mass versus aerodynamic particle diameter for Run #14.

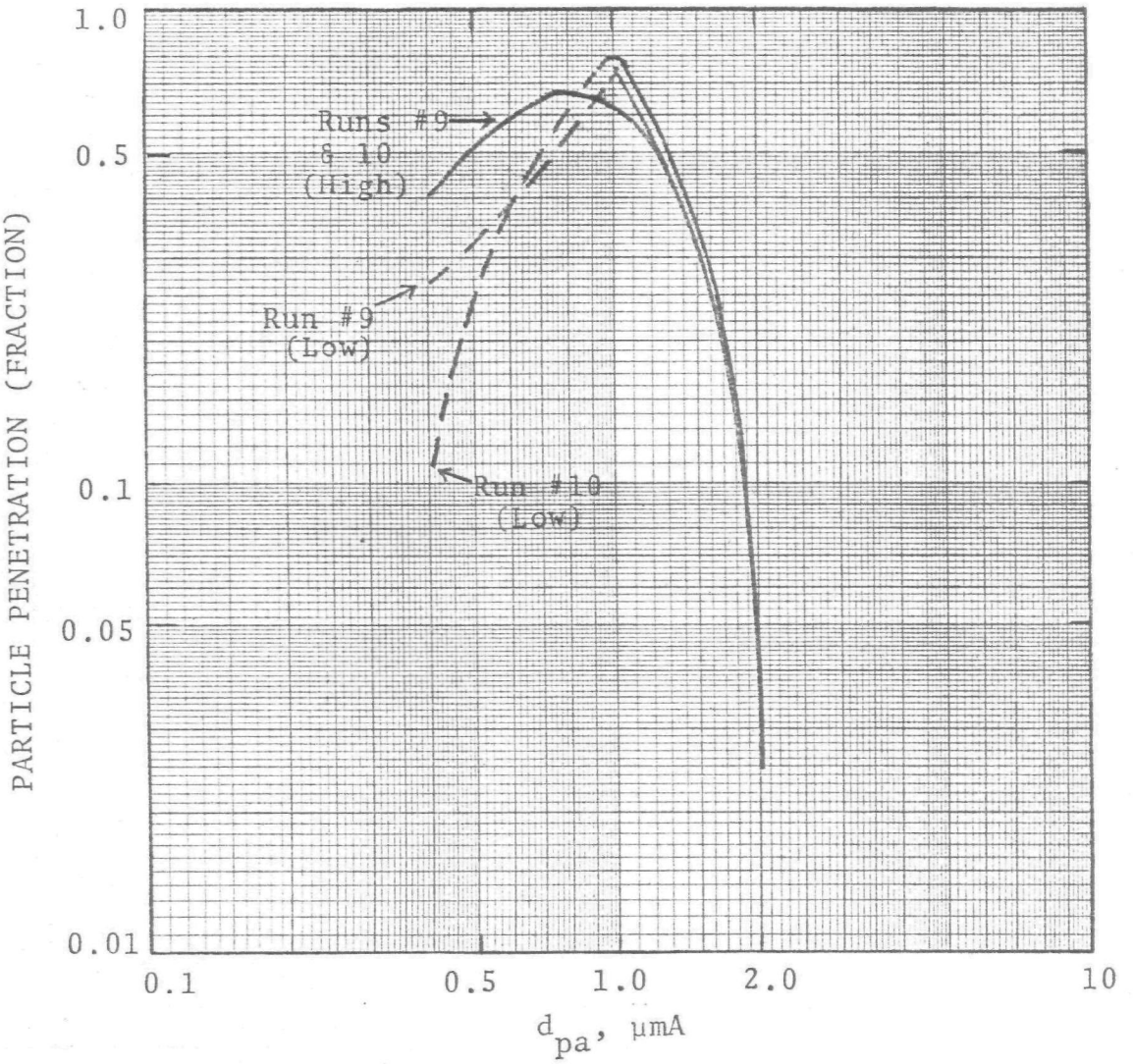

Figure 3-10 - Fractional penetration curves for data set "A".

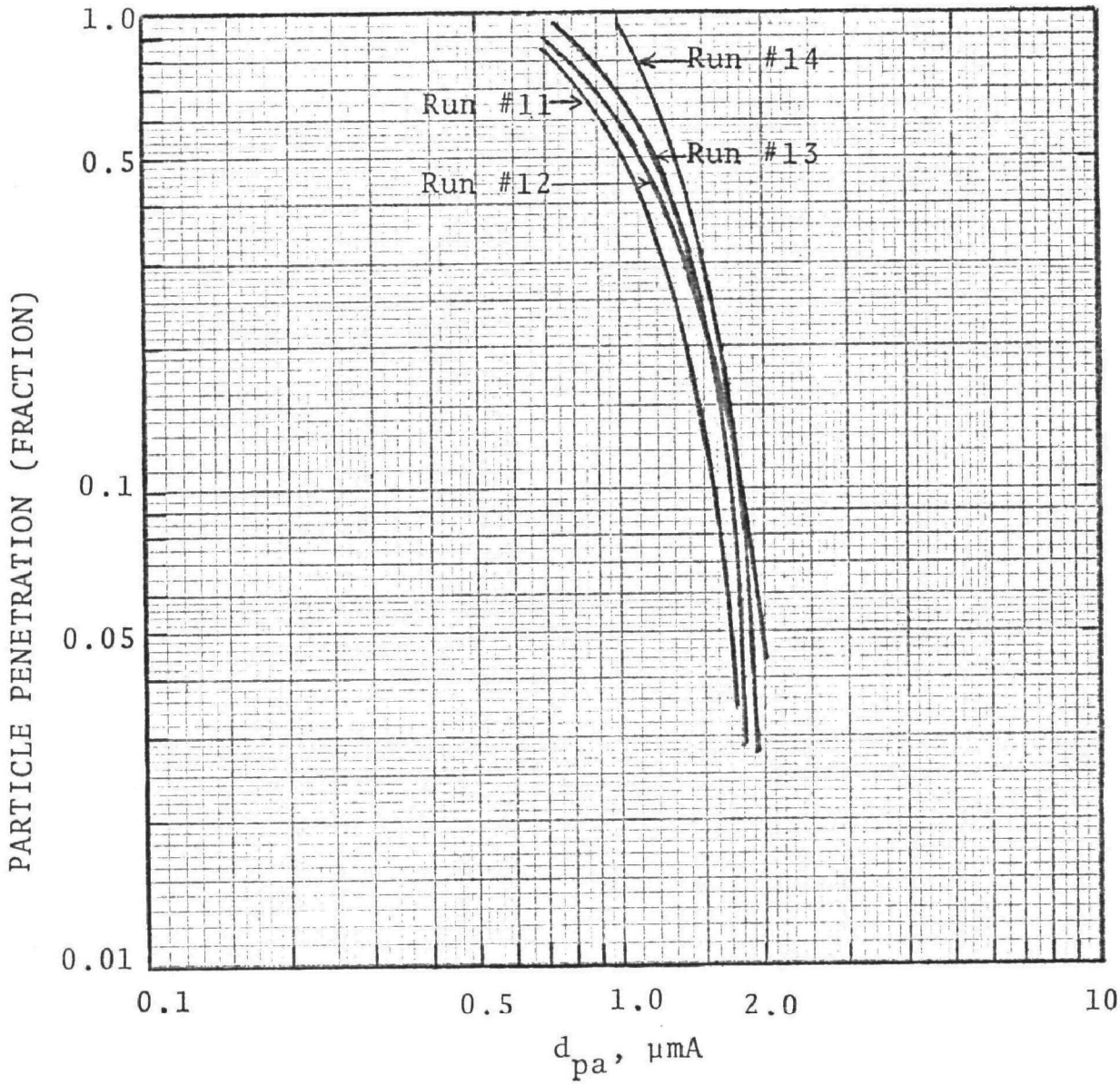

Figure 3-11 - Fractional penetration curves for data set "B".

Lines for high and low computations based on different distribution curve shapes are shown in Figure 3-10 for Runs 9 and 10.

MATHEMATICAL MODEL

No specific performance model was available for a valve tray so it was necessary to determine whether something suitable could be adapted from the available design methods. It was hypothesized that the gas jet emerging from the slot between the valve cap and the tray orifice might give collection comparable to the round gas jets which emerge from a sieve plate and that the dependence on foam density might also be comparable. The fractional collection efficiency, E_p, for particle collection by inertial impaction in a sieve plate column is given in the "Scrubber Handbook" (S. Calvert et al., 1972) as

$$E_p = 1 - \exp\left[-40\ F^2\ K_p\right] \qquad (3\text{-}1)$$

"Scrubber Handbook" (S.H.B.) Eq. 4.6.4-1 and Eq. 4.6.4-3

where foam density is in the range of $0.38 < F < 0.65$ and "K_p" is the inertial parameter given by:

$$K_p = \frac{d_{pa}^2\ u_h}{9\ \mu_G\ d_h} \qquad (3\text{-}2)$$

(S.H.B. Eq. 4.6.2-4)

For extensive discussion on these equations, refer to the Section 4.6.3 of the "Scrubber Handbook". These equations are based on sieve plate performance data. The following data were used to calculate the predicted performance.

Top Tray

70 scrubbing elements on the tray

$F = 0.33$

u_h = 2,000 cm/sec = gas velocity in the slot between the valve cap and the tray

Top Tray (continued)

ρ = 1.34 g/cm^3 = urea particle density

d_h = 0.7 cm = the width of the slot

Bottom Tray

27 scrubbing elements on the tray

F = 0.4

u_h = 5,200 cm/sec

ρ_p = 1.34 g/cm^3

d_h = 0.7 cm

It was assumed that no particle growth occurred during the particle collection in the bottom tray, and that all particle growth happened between the top and bottom trays. Figure 3-3 was used to obtain the particle diameter for the calculation of the top tray penetration.

The results of the calculations were plotted in Figures 3-12 and 3-13 for data sets A and B, respectively. Actual penetration obtained by going through the graphical procedures were also plotted on those figures as a comparison.

It appears that the experimental values are slightly higher than those calculated from the S.H.B. equations (4.6.4-1) and (4.6.4-3) and the agreement is quite good.

CONCLUSIONS

Uncertainties in some of the particle size measurements for submicron diameters are sufficiently large so that the computed penetration for particles of about 0.5 μmA diameter can vary over a range of 25% or more. A large factor is the unreliability of the cascade impactor manufacturer's calibration. The cross-calibration of the two impactor types used in this test provides for consistency between the two, but did not verify the calibration of the U. W. impactor. In later work this was done.

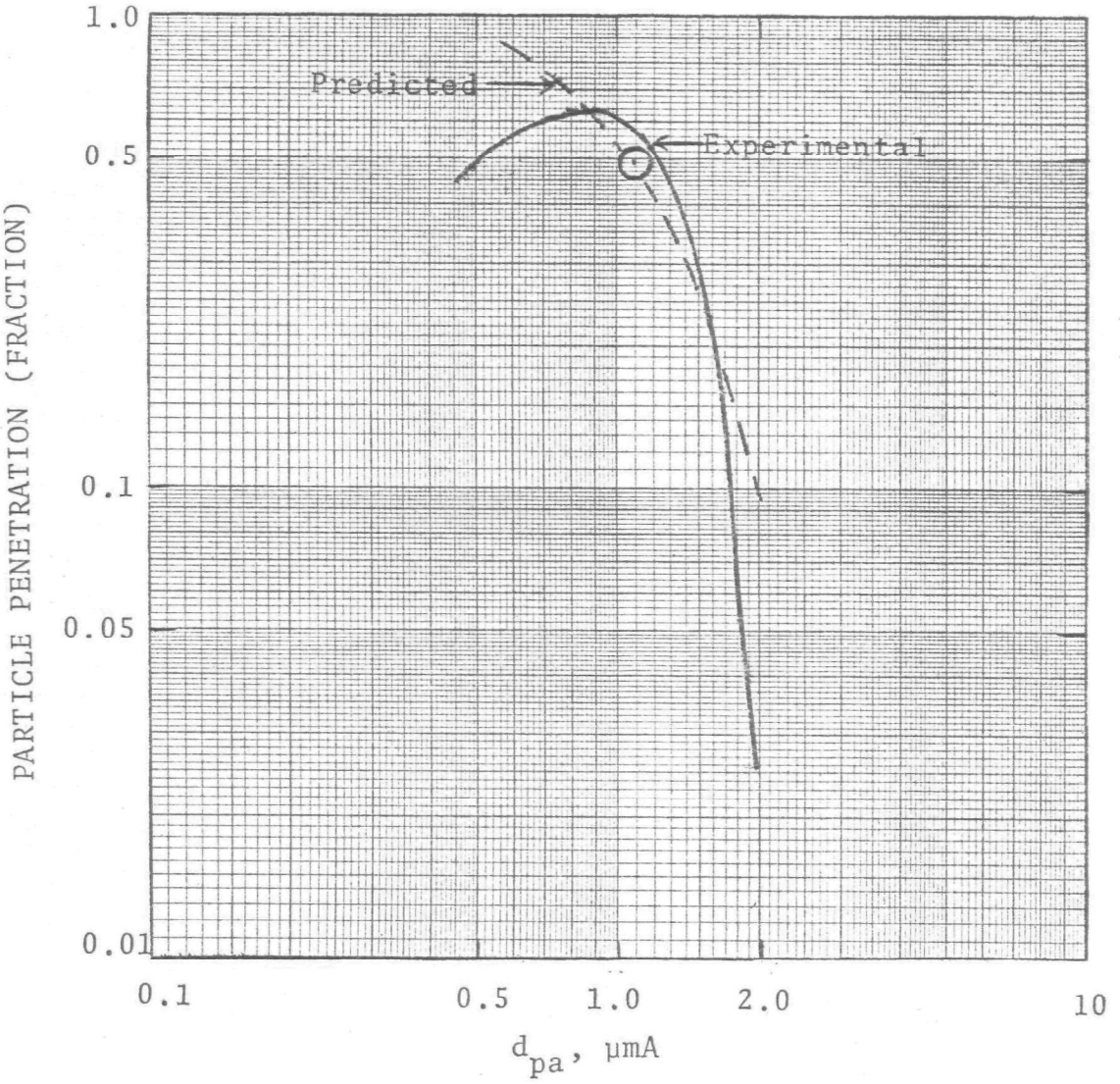

Figure 3-12 - Predicted and experimental penetrations for data set "A".

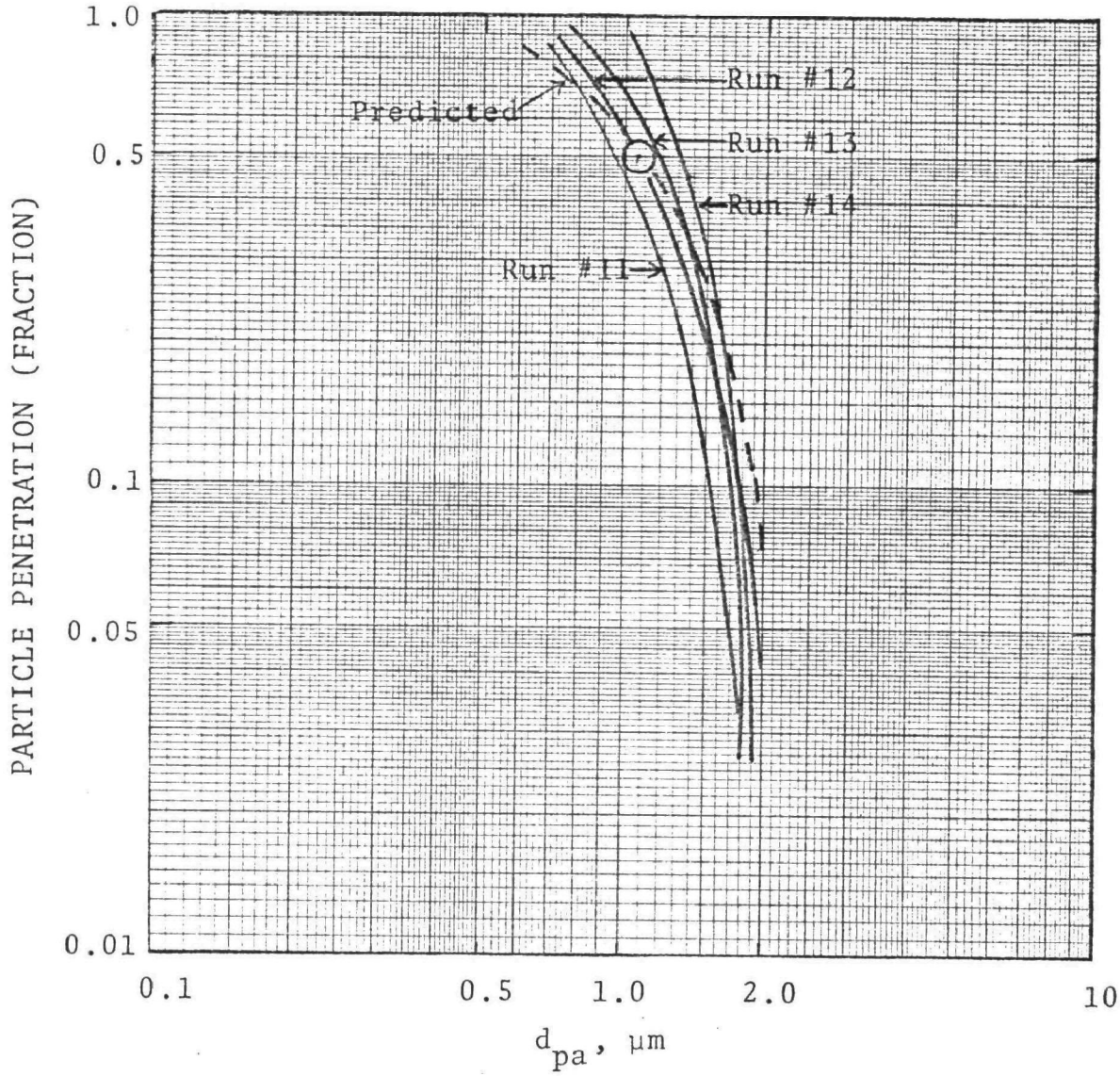

Figure 3-13 - Predicted and experimental penetrations for data set "B".

As demonstrated by this work, the S.H.B. equations (4.6.4-1) and (4.6.4-3) may be used to predict the performance of a 85 Am^3/min (3,000 ACFM) two stage valve tray scrubber. It is also noted that particle growth within the scrubber significantly increases particle collection efficiency. Since the foam density, F, was approximated, an even better fit of the experimental data can be obtained by varying the value of "F" to be used in the S.H.B. equation (4.6.4-1).

APPENDIX 3-A
PARTICLE SIZE DATA

TABLE 3-A-1 PARTICLE DATA FOR RUN #1

Impactor Stage No.	U. W. Mark III		Andersen	
	W_{cum} (mg)	$d_{p_{50}}$ (μmA)	W_{cum} (mg)	$d_{p_{50}}$ (μmA) (Mfg.cal.)
0			21.7	9.6
1	22.6	22	21.3	6.0
2	22.0	9.7	20.7	4.0
3	22.0	4.5	20.4	2.78
4	22.0	1.8	20.1	1.75
5	21.0	1.0	19.9	0.9
6	13.5	0.52	18.1	0.54
7	4.0	0.28	12.9	0.36
Filter	1.0		5.4	
Sample Volume (DNm^3)	0.939		0.875	

TABLE 3-A-2 PARTICLE DATA FOR RUN #2

Impactor Stage No.	U. W. Mark III		Andersen	
	W_{cum} (mg)	$d_{p_{50}}$ (μmA)	W_{cum} (mg)	$d_{p_{50}}$ (μmA) (Mfg.cal.)
0				
1	14.2	22	14.7	6.0
2	13.7	9.7	14.6	4.0
3	13.7	4.5	14.5	2.78
4	13.7	1.8	14.3	1.75
5	13.6	1.0	14.3	0.9
6	9.3	0.52	12.4	0.54
7	3.0	0.28	8.4	0.36
Filter	1.2		3.2	
Sample Volume (DNm^3)	0.640		0.626	

TABLE 3-A-3 PARTICLE DATA FOR RUN #3

Impactor Stage No.	U. W. Mark III		Andersen	
	W_{cum} (mg)	d_{p50} (μmA)	W_{cum} (mg)	d_{p50} (μmA) (Mfg.cal.)
0			18.5	
1	16.3	22	18.1	
2	15.8	9.7	17.8	4.0
3	15.7	4.5	17.4	2.78
4	15.6	1.8	16.9	1.75
5	13.0	1.0	16.5	0.9
6	4.3	0.52	12.8	0.54
7	0.5	0.28	5.2	0.36
Filter	0.3		1.2	
Sample Volume (DNm^3)	0.526		0.519	

TABLE 3-A-4 PARTICLE DATA FOR RUN #4

Impactor Stage No.	U. W. Mark III		Andersen	
	W_{cum} (mg)	d_{p50} (μmA)	W_{cum} (mg)	d_{p50} (μmA) (Mfg.cal.)
0			12.3	
1	13.4	22	12.1	6.0
2	13.1	9.7	12.0	4.0
3	13.0	4.5	11.9	2.78
4	12.9	1.8	11.9	1.75
5	10.5	1.0	11.9	0.9
6	2.4	0.52	8.0	0.54
7	0.5	0.28	2.8	0.36
Filter	0.2		0.7	
Sample Volume (DNm^3)	0.436		0.426	

TABLE 3-A-5 PARTICLE DATA FOR RUN #5

Impactor Stage No.	Stage Initial Weight g	Stage Final Weight		Stage Cut Size	
		wet g	dry g	wet µmA	dry µmA
1	0.1102	0.1107	0.1107	22	
2	0.1509	0.1514	0.1512	9.7	8.57
3	0.1503	0.1509	0.1507	4.3	2.25
4	0.1512	0.1677	0.1534	1.8	0.98
5	0.1563	0.1973	0.1613	1.0	0.67
6	0.1565	0.1715	0.1597	0.52	0.49
7	0.1507	0.1516	0.1513	0.28	0.28
Filter	0.1386	0.1392	0.1392		
Sample Volume (DNm^3)	0.735				

TABLE 3-A-6 PARTICLE DATA FOR RUN #6

Impactor Stage No.	Stage Initial Weight g	Stage Final Weight		Stage Cut Size	
		wet g	dry g	wet µmA	dry µmA
1	0.1117	0.1119	0.1115	22	
2	0.1561	0.1563	0.1562	9.7	7.76
3	0.1575	0.1577	0.1576	4.3	2.35
4	0.1538	0.1644	0.1552	1.8	1.0
5	0.1545	0.1852	0.1584	1.0	0.62
6	0.1569	0.1769	0.1603	0.52	0.285
7	0.1540	0.1552	0.1541	0.28	0.28
Filter	0.1336	0.1345	0.1345		
Sample Volume (DNm^3)	0.612				

TABLE 3-A-7 PARTICLE DATA FOR RUN #7

Impactor Stage No.	Stage Initial Weight g	Stage Final Weight		Stage Cut Size	
		wet g	dry g	wet µmA	dry µmA
1	0.0810	0.0811	0.0812	22	
2	0.1583	0.1583	0.1584	9.7	
3	0.1620	0.1522	0.1621	4.5	3.1
4	0.1612	0.1848	0.1673	1.8	0.82
5	0.1611	0.2117	0.1643	1.0	0.67
6	0.1652	0.1753	0.1674	0.52	0.25
7	0.1591	0.1698	0.1594	0.28	0.28
Filter	0.1363	0.1471	0.1370		
Sample Volume (DNm^3)	0.55				

TABLE 3-A-8 PARTICLE DATA FOR RUN #8

Impactor Stage No.	Stage Initial Weight g	Stage Final Weight		Stage Cut Size	
		wet g	dry g	wet µmA	dry µmA
1	0.0789	0.0799	0.0799	22	22
2	0.1679	0.1680	0.1679	9.7	9.7
3	0.1633	0.1634	0.1633	4.5	4.5
4	0.1650	0.1653	0.1651	1.8	1.8
5	0.1654	0.1691	0.1687	1.0	1.0
6	0.1740	0.1812	0.1800	0.52	0.52
7	0.1634	0.1656	0.1652	0.28	0.28
Filter	0.1479	0.1434	0.1632		
Sample Volume (DNm^3)	0.50				

TABLE 3-A-9 INLET AND OUTLET SAMPLE PARTICLE DATA FOR SIMULTANEOUS RUN #9

Impactor Stage Number	Inlet		Outlet	
	W_{cum} (mg)	d_{pc} (μmA)	W_{cum} (mg)	d_{pc} (μmA)
0				
1	22.6	22	12.8	22
2	22.0	9.7	12.3	9.7
3	22.0	4.5	12.0	4.5
4	22.0	1.8	11.6	1.8
5	21.0	1.0	9.4	1.0
6	13.5	0.52	4.4	0.52
7	4.0	0.28	1.2	0.28
Filter	1.0		0.6	
Sample Volume (DNm^3)	0.94		0.73	
Type of Impactor	U.W.		U.W.	

TABLE 3-A-10 INLET AND OUTLET SAMPLE PARTICLE DATA FOR SIMULTANEOUS RUN #10

Impactor Stage Number	Inlet		Outlet	
	W_{cum} (mg)	d_{pc} (μmA)	W_{cum} (mg)	d_{pc} (μmA)
0				
1	14.2	22	10.1	22
2	13.7	9.7	9.9	9.7
3	13.7	4.5	9.8	4.5
4	13.7	1.8	9.7	1.8
5	13.6	1.0	8.3	1.0
6	9.3	0.52	4.4	0.52
7	3.0	0.28	1.0	0.28
Filter	1.2		0.9	
Sample Volume (DNm^3)	0.63		0.61	
Type of Impactor	U.W.		U.W.	

TABLE 3-A-11 INLET AND OUTLET SAMPLE PARTICLE DATA FOR SIMULTANEOUS RUN #11

Impactor Stage Number	Inlet		Outlet	
	W_{cum} (mg)	d_{pc} (μmA)	W_{cum} (mg)	d_{pc} (μmA)
0	16.5			
1	15.8		9.1	22
2	15.6		8.4	9.7
3	15.1		7.7	4.5
4	14.8	2.0	7.2	1.8
5	14.2	1.5	6.8	1.0
6	10.9	1.0	5.1	0.52
7	4.9	0.6	0.8	0.28
Filter	1.5		0.3	
Sample Volume (DNm^3)	0.65		0.60	
Type of Impactor	Andersen		U.W.	

TABLE 3-A-12 INLET AND OUTLET SAMPLE PARTICLE DATA FOR SIMULTANEOUS RUN #12

Impactor Stage Number	Inlet		Outlet	
	W_{cum} (mg)	d_{pc} (μmA)	W_{cum} (mg)	d_{pc} (μmA)
0	16.3			
1	15.8		6.8	22
2	15.8		6.6	9.7
3	15.8		6.5	4.5
4	15.6	2.0	6.5	1.8
5	15.3	1.5	6.5	1.0
6	12.2	1.0	4.1	0.52
7	6.1	0.6	1.1	0.28
Filter	1.8		0.3	
Sample Volume (DNm^3)	0.66		0.63	
Type of Impactor	Andersen		U.W.	

TABLE 3-A-13 INLET AND OUTLET SAMPLE PARTICLE DATA FOR SIMULTANEOUS RUN #13

Impactor Stage Number	Inlet		Outlet	
	W_{cum} (mg)	d_{pc} (μmA)	W_{cum} (mg)	d_{pc} (μmA)
0	19.6			
1	19.1			22
2	19.1		10.9	9.7
3	19.1		10.9	4.5
4	19.1	2.0	10.9	1.8
5	19.1	1.5	10.8	1.0
6	14.9	1.0	6.6	0.52
7	5.6	0.6	1.4	0.28
Filter	1.4		0.4	
Sample Volume (DNm^3)	0.66		0.64	
Type of Impactor	Andersen		U.W.	

TABLE 3-A-14 INLET AND OUTLET SAMPLE PARTICLE DATA FOR SIMULTANEOUS RUN #14

Impactor Stage Number	Inlet		Outlet	
	W_{cum} (mg)	d_{pc} (μmA)	W_{cum} (mg)	d_{pc} (μmA)
0	14.8			
1	14.8		12.5	22
2	14.8		11.5	9.7
3	14.7		11.5	4.5
4	14.4	2.0	11.5	1.8
5	14.3	1.5	11.4	1.0
6	13.3	1.0	8.1	0.52
7	7.8	0.6	2.1	0.28
Filter	2.6		0.3	
Sample Volume (DNm^3)	0.53		0.50	
Type of Impactor	Andersen		U.W.	

APPENDIX 3-B
PARTICLE SIZE DISTRIBUTION PLOTS

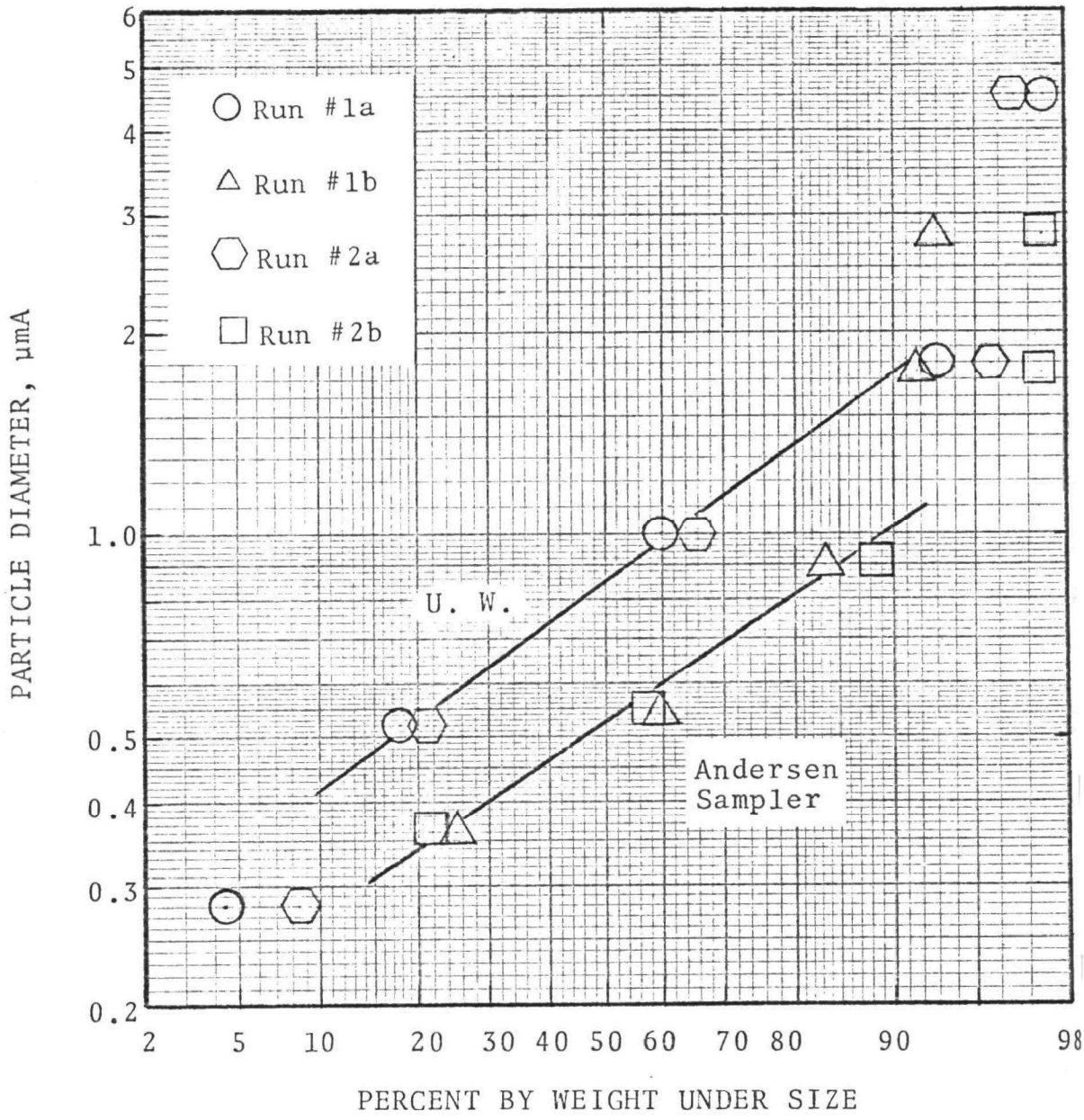

Figure 3-B-1 - Particle size distribution measured by the U.W. and Andersen Cascade Impactors.

NOTE: The numbering system used here is that "a" denotes size measured by U. W. and "b" size measured by Andersen in a simultaneous run (designated by number)

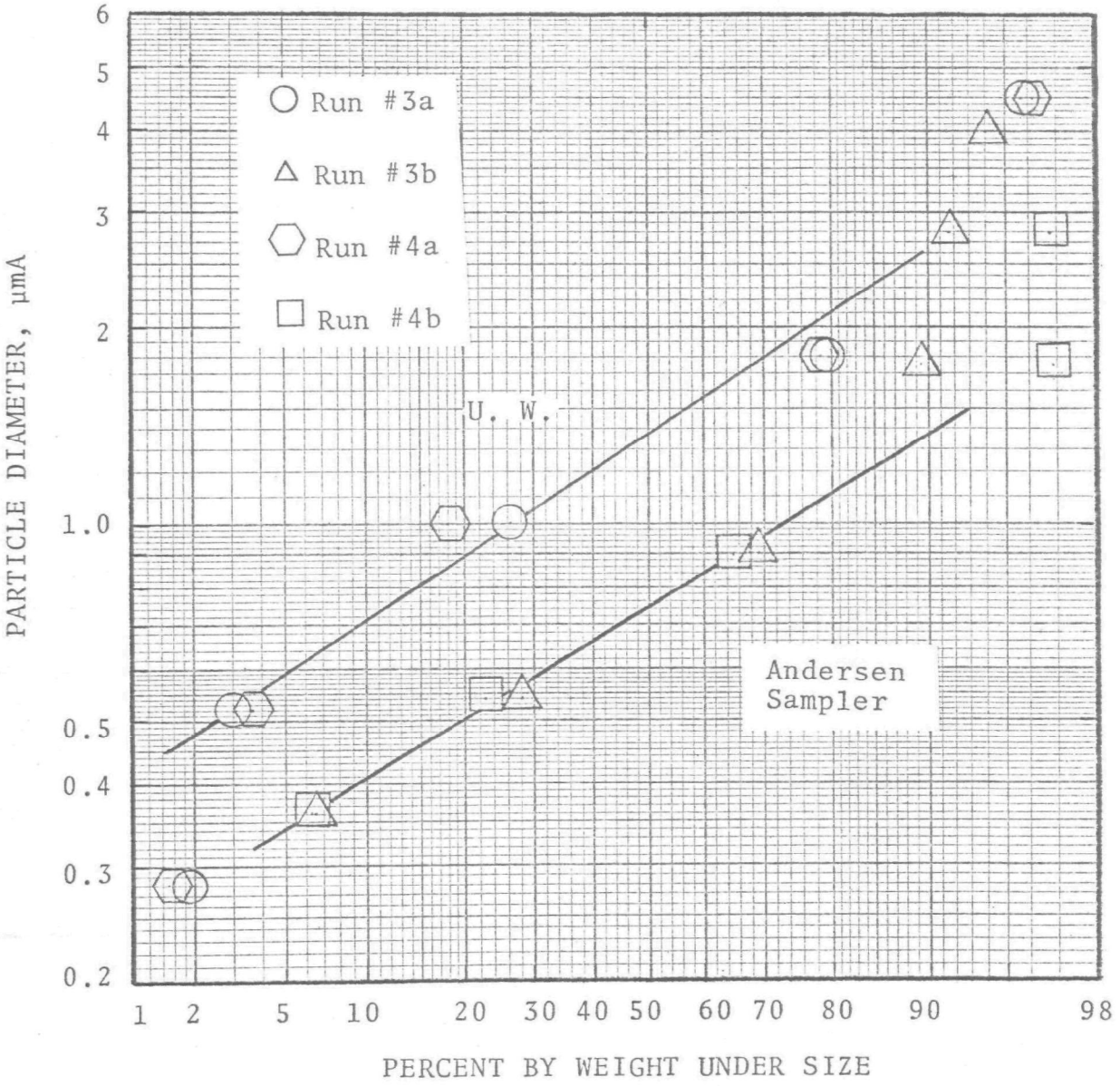

Figure 3-B-2 - Particle size distribution, measured by the U. W. and Andersen cascade impactors.

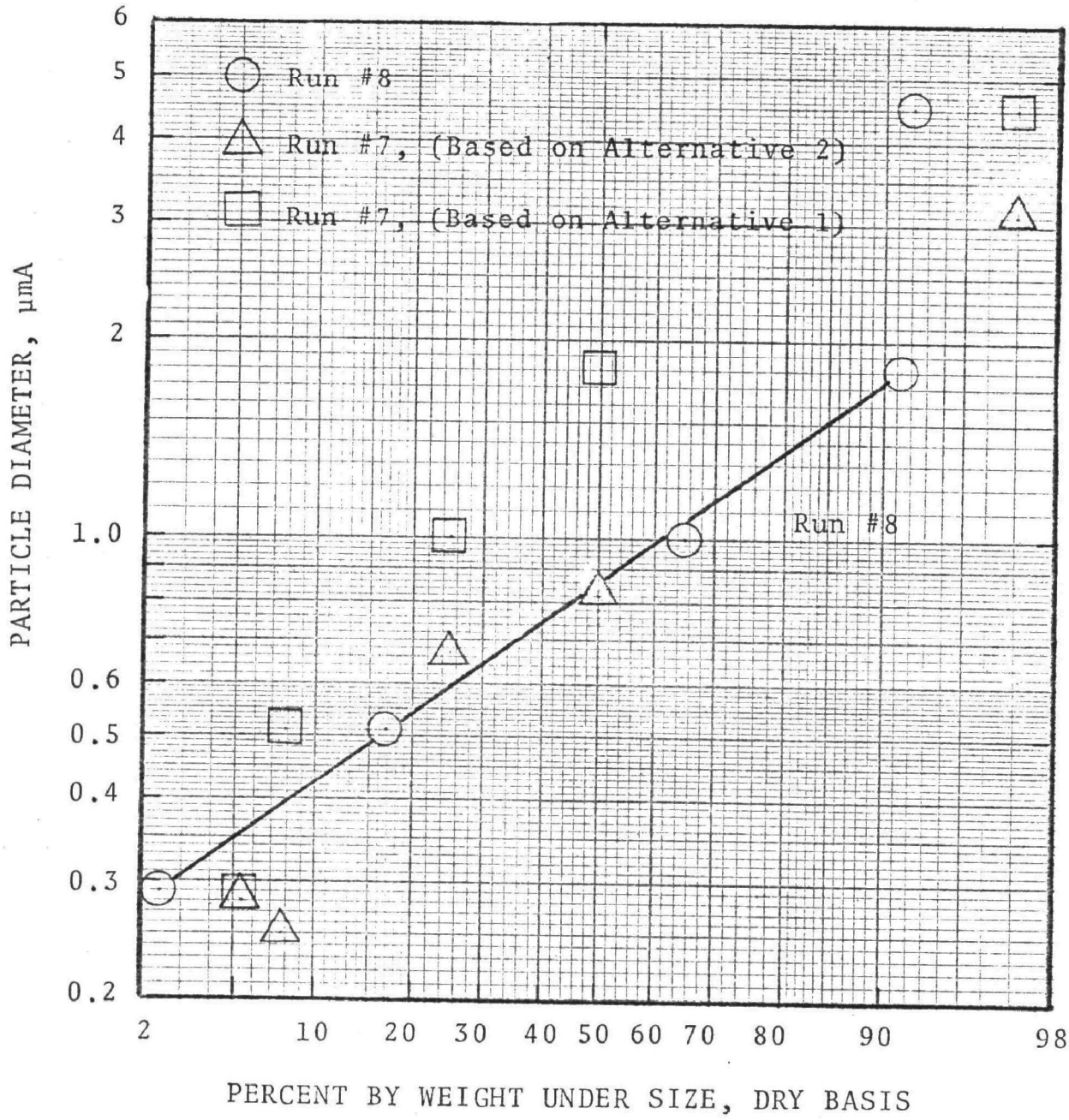

Figure 3-B-3 - Dry particle size distribution obtained with in-stack and ex-stack U. W. cascade impactor.

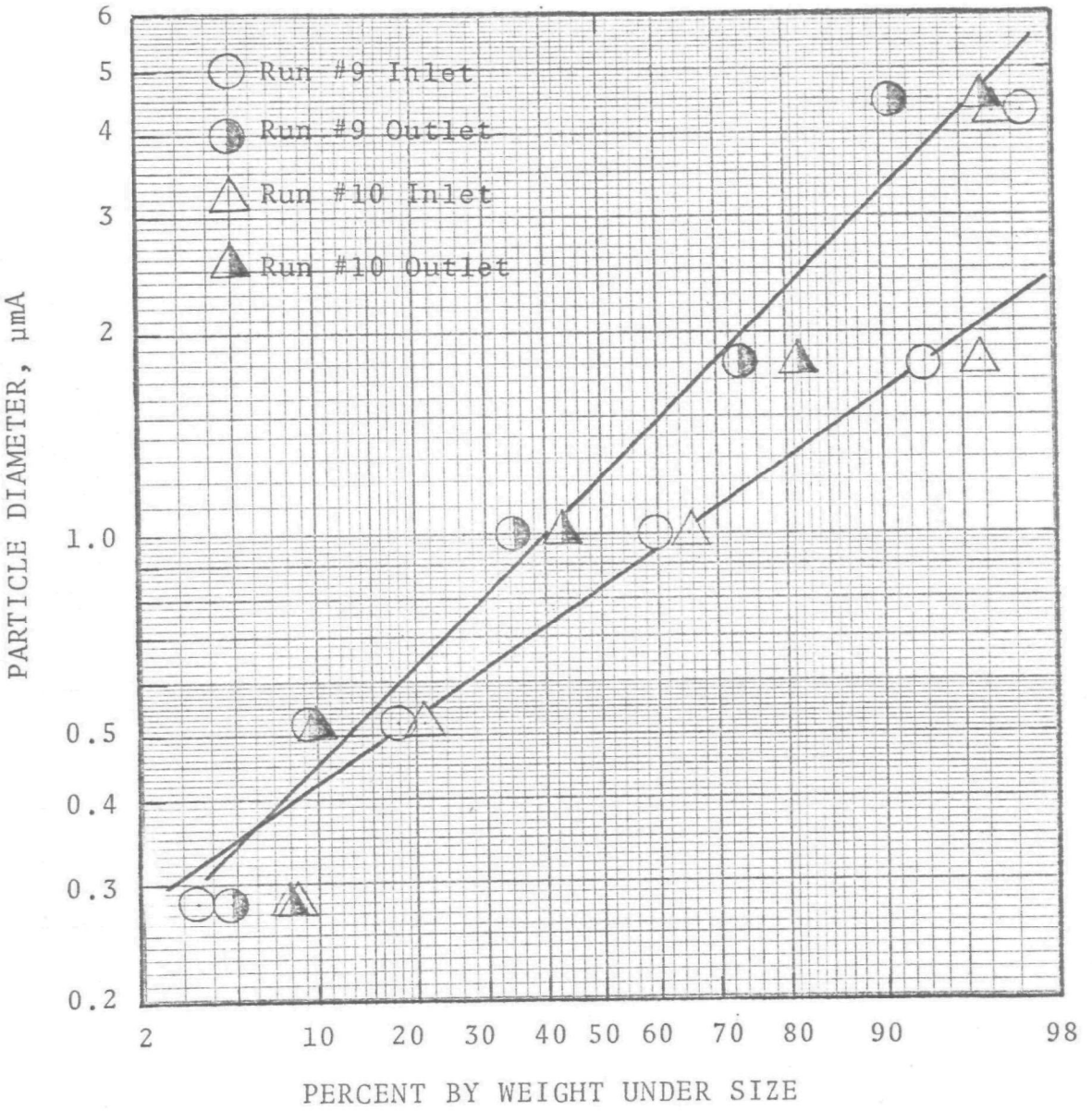

Figure 3-B-4 - Particle size distribution for data set A.

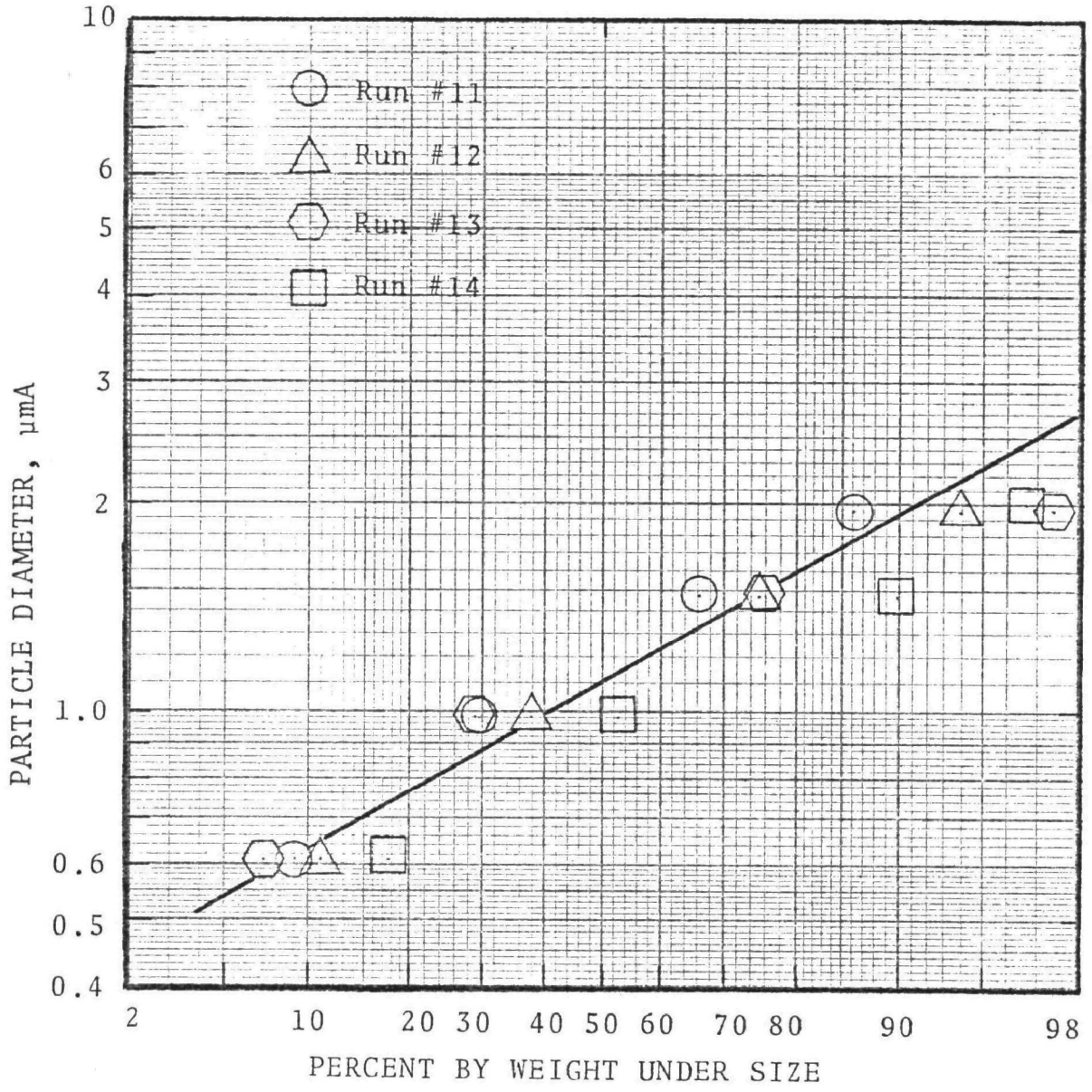

Figure 3-B-5 - Inlet particle size distribution (data set B).

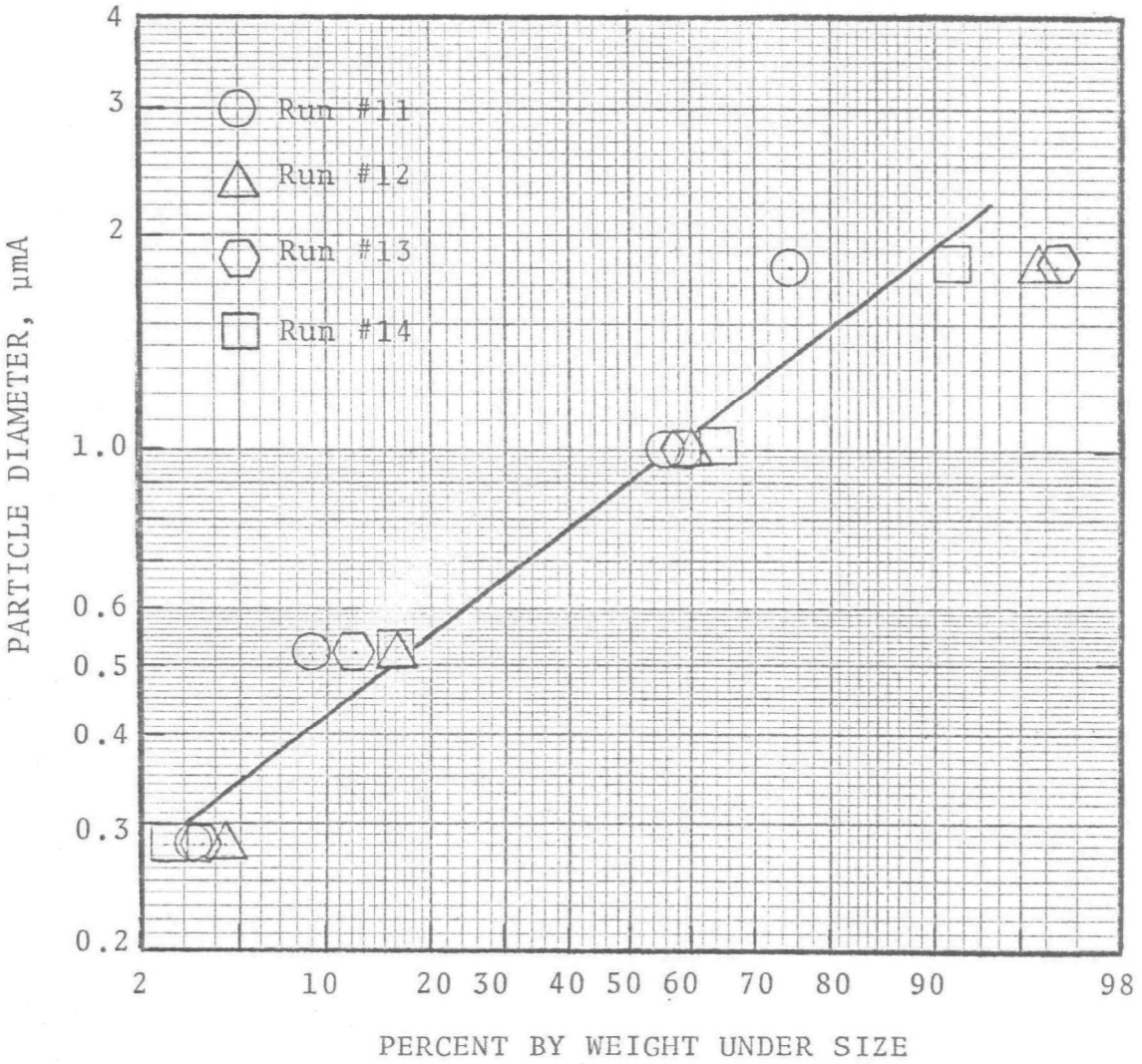

Figure 3-B-6 - Outlet particle size distribution (data set B)

VANED CENTRIFUGAL ON POTASH DRYER
(Ducon Multivane Scrubber)

SOURCE AND SCRUBBER

A Ducon Multivane scrubber was selected for the third scrubber performance test. This scrubber is designed to clean the exhaust gas from a rotary drier which removes the moisture from 22,680 Kg/hour (25 TPH) of potassium chloride crystals. The rotary drier is gas-fired with oil as a standby fuel for periods of natural gas shortage.

The scrubber is The Ducon Company's Multivane Scrubber Size-84 Type-L Model II (Figure 4-1). The scrubber outlet duct is 106.68 cm in diameter and inlet is a 60.96 cm by 91.44 cm rectangular duct. The scrubber pressure drop varies from 6.5 to 8.0 cm W.C. (or 2.7" to 3.3" H_2O). The scrubber liquor flow rate is 0.12 m^3/min (32 GPM) as measured by an orifice meter on the inlet line of the scrubber liquor circuit. Liquid is introduced through spray nozzles located between the wash and eliminator turning vanes inside the scrubber.

TEST METHOD

In this performance test, three types of impactors (Andersen Sampler, University of Washington Mark III and Brink) were used for particle measurements. Greased aluminum foil substrates were used on each of the collection plates of the Andersen and U. W. Mark III impactors and filter papers were used on the Brink collection plates. Substrates for the impactor plates were cut out of thick aluminum foil. A 20% solution of silicone vacuum grease in benzene was prepared. Five drops of this solution were placed on the substrates with an eye dropper. It was then evenly spread

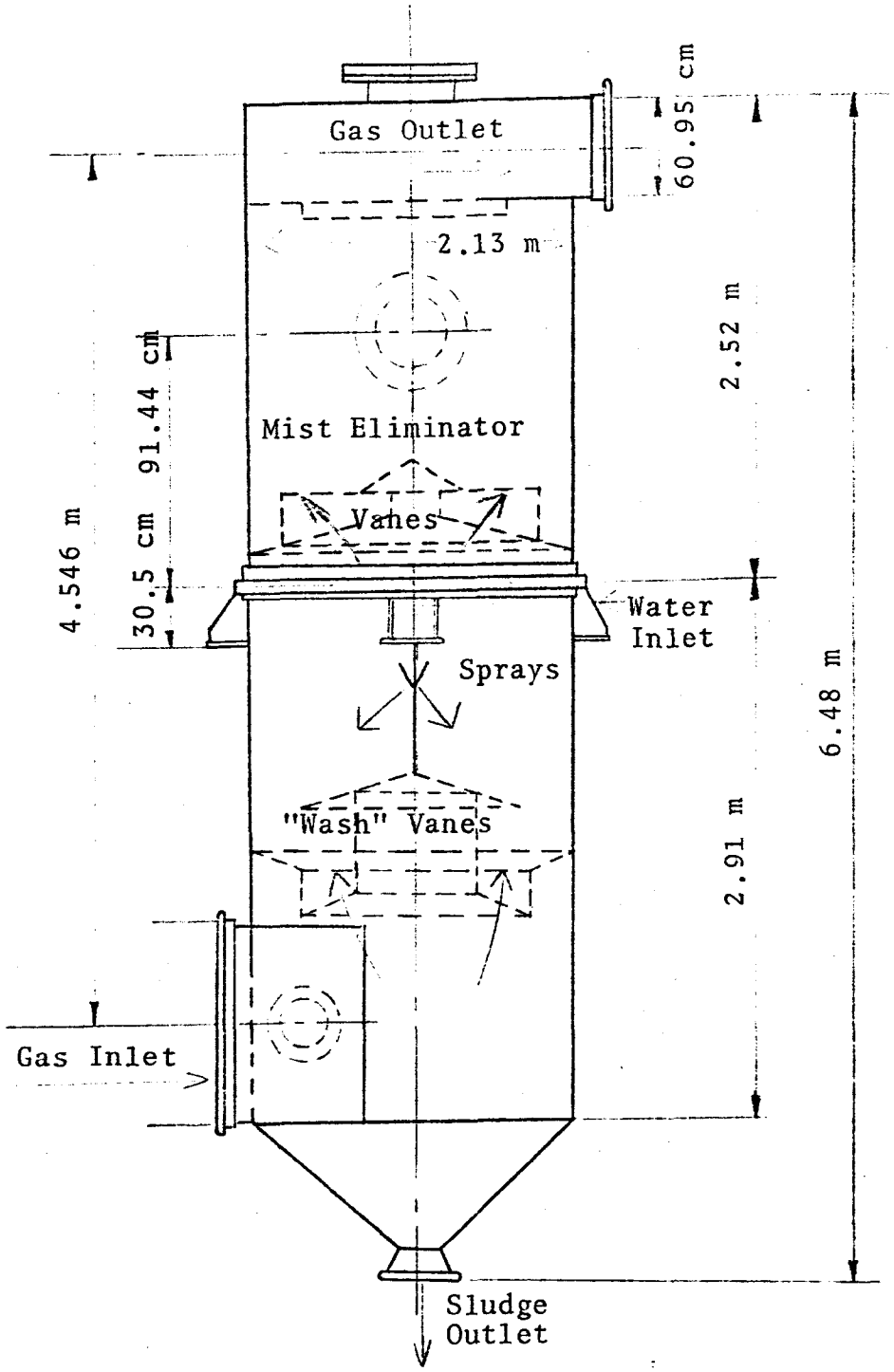

Figure 4-1 - Ducon Multivane scrubber.

out on the substrates with a policeman, taking care that it did not spread to the bottom of the substrates. These were then placed in aluminum foil storage cups and heated in an oven for two hours at 200°C. Then they were cooled and stored in a desiccator for about 10 hours. Prior to each run, the substrates and filter were removed from the desiccator, weighed with the storage cups and loaded in the impactor.

Both sampling probes in the inlet and outlet ducts were kept at one position during the entire sampling period. The location of the impactor was chosen such that the gas velocity at that location is close to the average gas velocity in the duct. The sample flow rate was also fixed during runs.

In most of the test runs, the impactor was kept in-stack, however, in some test runs, the impactor was ex-stack. Whenever this occurred, the impactor was put in a heated box. In some runs, the entrainment was heavy, therefore an in-line miniature glass cyclone was used to prevent entrained liquid drops from entering the impactor. Details on each run's impactor operating condition are listed in Table 4-1.

Sample flow rates were measured with the usual EPA Method 5 instruments so as to obtain isokinetic (or near isokinetic) sampling. Scrubber inlet and outlet gas temperatures were measured by mercury filled glass bulb thermometers. Gas temperature at the sampling location was measured during each test run. Stack pressures were measured with a U-tube manometer. Barometric pressures were determined before each run from an aneroid barometer. Stack gas humidities were determined by EPA method 4 and by dry and wet bulb thermometer. Gas volumetric flow rate was calculated from velocity traverse data obtained by means of a calibrated S-type pitot tube.

A total of 23 impactor test runs and 4 filter runs were performed. Among those 7 impactor runs were purged due to

Table 4-1. IMPACTOR OPERATING CONDITIONS

Run No.	Sampling Location	IMPACTOR					Remark
		Type	Location	Stage Lining	Heated	Precutter Used	
1	Outlet	Andersen	ex-stack	Greased Aluminum	Yes	No	
2	Outlet	Andersen	ex-stack	"	Yes	No	Test Void (broken probe)
3	Outlet	Andersen	ex-stack	"	Yes	No	
4	Outlet	Andersen	ex-stack	"	Yes	No	
5	Outlet	Andersen	ex-stack	"	Yes	No	
6	Inlet	Andersen	ex-stack	"	Yes	No	Test purged (nozzle broken)
7	Inlet	Andersen	ex-stack	"	Yes	No	Test void
8	Inlet	Andersen	ex-stack	"	Yes	No	
9	Inlet	Andersen	ex-stack	"	Yes	No	
10	Inlet	Andersen	ex-stack	"	Yes	No	Test purged
11	Inlet	Andersen	ex-stack	"	Yes	No	
12	Inlet	Andersen	ex-stack	"	Yes	No	
13	Inlet	U. of W.	in-stack	"	No	Yes	Test difficulty
14	Inlet	U. of W.	in-stack	"	No	Yes	Dryer shut-down
15	Inlet	U. of W.	in-stack	"	No	Yes	
16	Inlet	U. of W.	in-stack	"	No	Yes	
17	Inlet	U. of W.	in-stack	"	No	Yes	
18	Outlet	U. of W.	in-stack	"	No	No	
19	Outlet	U. of W.	in-stack	"	No	No	
20	Inlet	U. of W.	in-stack	"	No	Yes	Test aborted
21	Inlet	U. of W.	in-stack	"	No	Yes	
22	Outlet	U. of W.	in-stack	"	No	No	
23a*	Outlet	Brink	in-stack	Filter	No	No	
23b*	Inlet	U. of W.	in-stack	Greased Aluminum	No	Yes	

*NOTE: This is a simultaneous inlet and outlet test run.

various operating difficulties and plant shut-down problems. All filter runs were conducted in-stack.

RESULTS

Scrubber Operating Conditions

There was an interruption of the test program by a plant shutdown. The scrubber operating conditions during the test period were as follows:

1. Gas flow rates were different before and after the interruption. Gas parameters are listed in the tabulation below:

Gas Parameters (Before Interruption)

Gas Parameters	Inlet	Outlet
Temperature	196°C (385°F)	78°C (172°F)
Pressure	2.3 cm W.C.	
A m^3/min	623	504
ACFM	22,000	17,800
DNm^3/min @ 0°C	323	322
DSCFM @ 70°F	11,200	12,100
Vol. % H_2O Vapor	19	19

Gas Parameters (After Interruption)

Gas Parameters	Inlet	Outlet
Temperature	204°C (400°F)	77°C (170°F)
Pressure	1.8 cm W.C.	
A m^3/min	464.5	339.8
ACFM	16,400	12,000
DNm^3/min @ 0°C	255	220
DSCFM @ 70°F	9,000	8,280
Vol. % H_2O Vapor	18.0	18.0

2. Pressure drop across the scrubber is 8.0 cm W.G.
3. Liquid flow rate and parameters are as follows:

Liquid Parameter

LIQUID PARAMETERS	INLET	OUTLET
Temperature	52°C (125°F)	
m^3/min	0.12	0.12
GPM	32	32
L/G	1.5	
Specific gravity	1.07	1.07
Suspensed solid	-	-
Dissolved solid	-	-
Treatment	-	-

Particle Data

The particle concentration and size data which were obtained in this performance test are tabulated in Appendix 4-A. Runs #17, 18, 21, 22, 23a and 23b were taken when the drier and scrubber run at normal operating conditions. Among these runs, only runs #23a and 23b were simultaneous runs. Figures 4-B-1 and 4-B-2 are log-probability plots of inlet and outlet particle size distribution for these test runs respectively. The "actual" mass median diameter, geometric standard deviation, and aerodynamic mass median diameter for the outlet samples are listed in the following table.

RUN NO.	18	22	23a
d_{p50}, μm	1.4	2.9	0.7
σ_g	4.3	3.9	4.1
d_{pg}, μmA	2.1	4.1	1.1

Cumulative mass concentration was plotted against particle diameter to yield Figures 4-2 through 4-4.

The rest of the test data were not plotted here because the primary objectives of those runs were to test the equipment set-up and to determine adequate sampling time.

Particle Penetration

Particle penetration was computed by the general method described in a previous section of this report. As the first step in this computation it was necessary to plot cumulative particle mass versus particle diameter. Figures 4-2, 4-3, and 4-4 are such plots for three sets of inlet and outlet runs. Because the cyclone pre-cutter was used on the inlet runs, the impactor stage weight gains were less than they would have been without the pre-cutter. Consequently, the true particle size distribution must be determined by compensating the impactor data for the effect of the pre-cutter. This compensation was performed on the basis of the approximations that the cyclone cut diameter was about 2.0 μmA and that cyclone penetration varies exponentially with $(-d_{pa}^2)$.

The dashed curves on Figures 4-2 through 4-4 are fit by eye with the compensated data points for the inlet samples. Particle penetrations were computed from the ratio of slopes of the outlet and inlet cumulative distributions, based on the curves fit by eye. The penetration results are plotted in Figure 4-5 for the three pairs of runs, in terms of actual diameter (density = 2.0) rather than aerodynamic diameter. The data for run no. 21 show too much scatter to be useful for more than a general confirmation of the other runs.

MATHEMATICAL MODEL

Preliminary computations showed that the particle collection efficiency given by this scrubber could not be

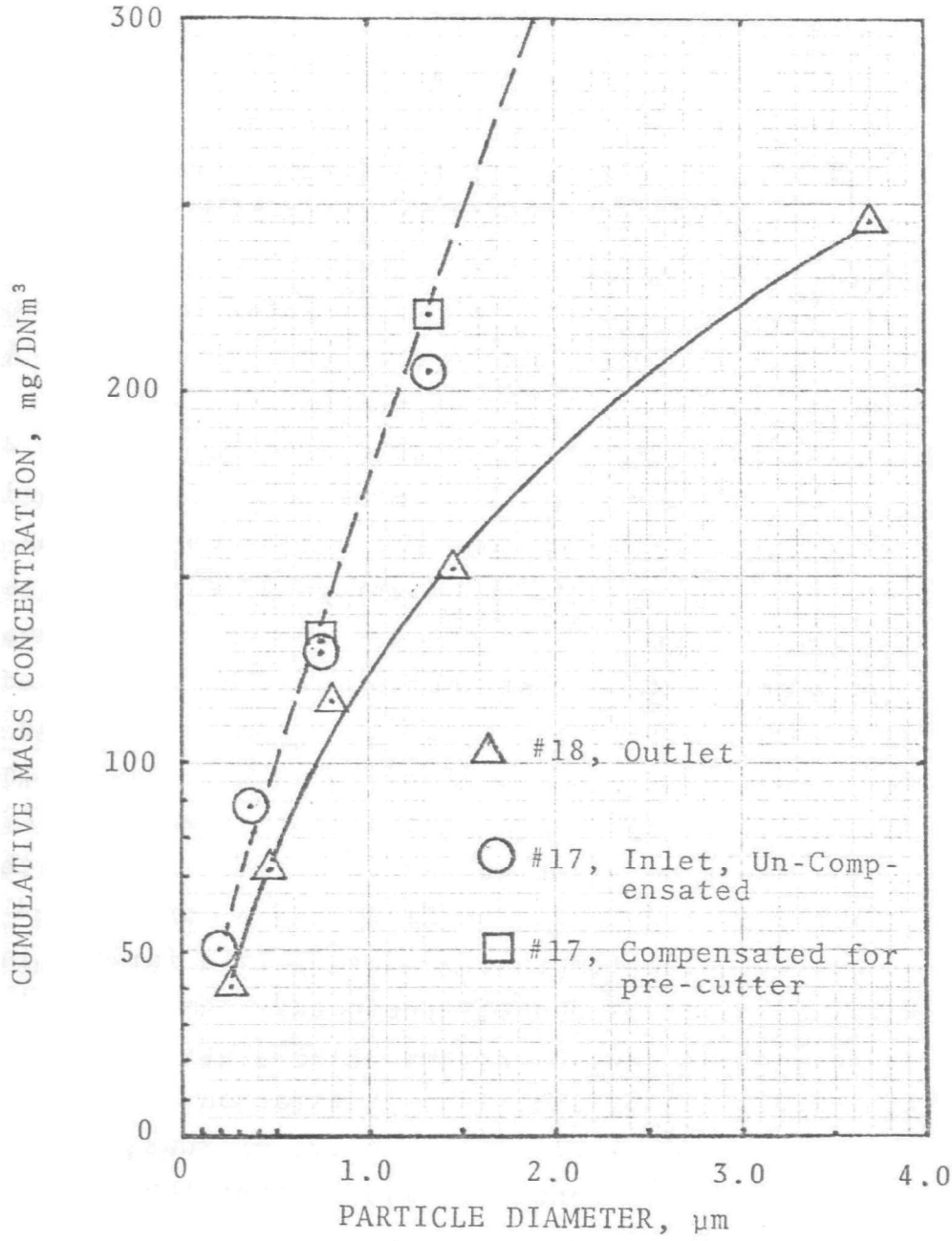

Figure 4-2 - Cumulative mass versus particle diameter.

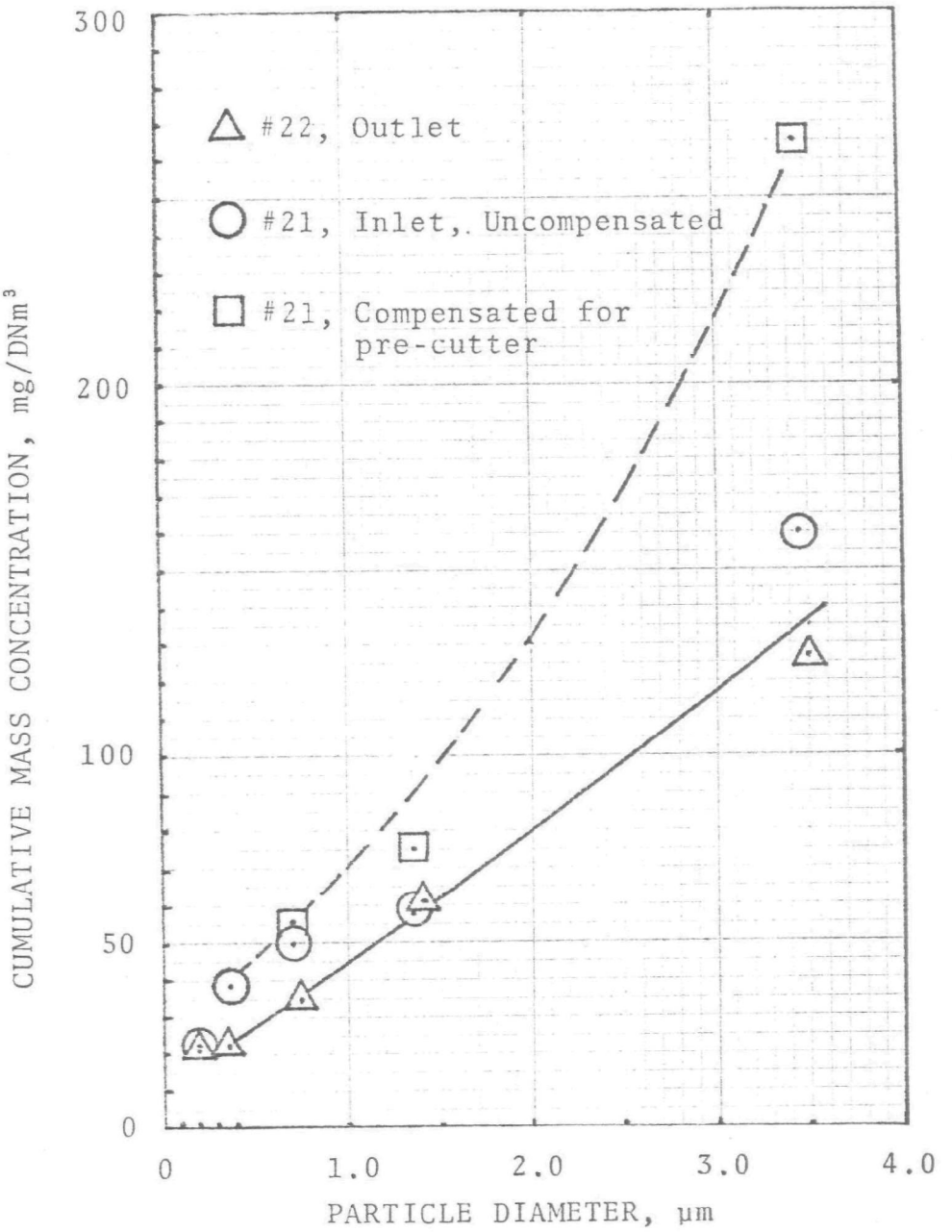

Figure 4-3 - Cumulative mass versus particle diameter.

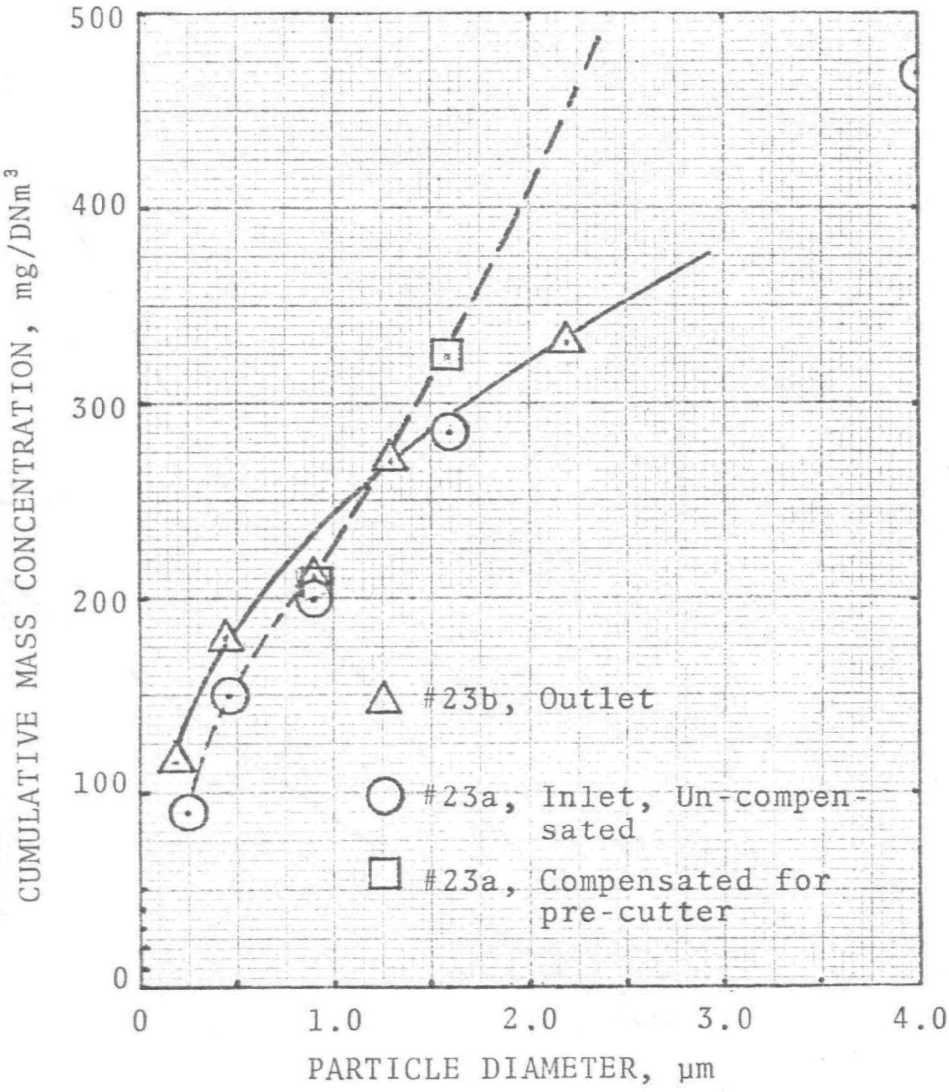

Figure 4-4 - Cumulative mass versus particle diameter.

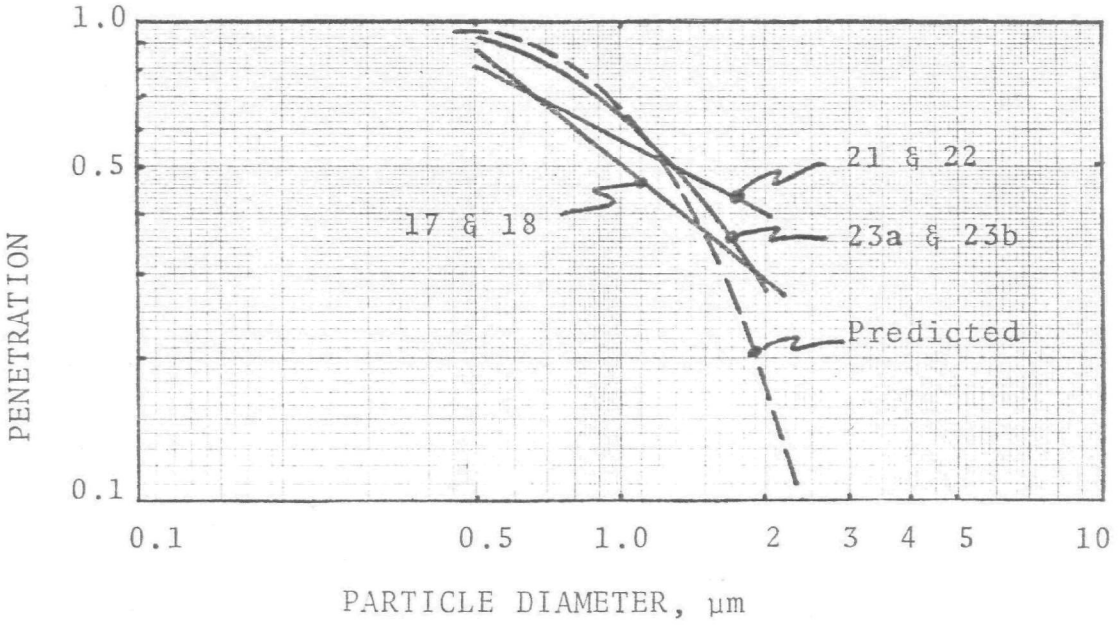

Figure 4-5 - Experimental and predicted penetrations.

accounted for simply by centrifugal deposition caused by the vanes in the scrubber. Prediction of collection efficiency based on the assumption that the scrubber mechanism was a counter-flow spray tower were also too low to fit the data.

We then decided to test the hypothesis that water sprayed on top of the vanes tends to collect on the vanes and be atomized and reentrained by the upward spiraling gas flow. This mechanism would involve the recirculation of water at some unknown rate and would provide particle collection through impaction on the water drops as in a co-current, gas atomized spray scrubber. Our approach to the computation of collection efficiency based on this mechanism is given below.

Particle penetration for a gas-atomized scrubber can be estimated by means of the cut diameter - pressure drop method (Calvert, 1974). Figure 4-6 is a plot of cut diameter versus scrubber pressure drop for several scrubber types and conditions. Figure 4-7 is a plot of the ratio of particle diameter to cut diameter versus collection efficiency. As can be seen on Figure 4-6, the cut diameter for a gas-atomized (venturi) scrubber at 7.6 cm W.C. pressure drop ranges from 2.5 μmA at f = 0.25 to 1.3 μmA at f = 0.5. These diameters correspond to 1.7 μm and 0.85 μm actual diameter for a particle density of 2.0 g/cm^3.

Figure 4-5 indicates that the cut diameter was about 1.2 μm (or about 1.8 μmA). This corresponds to a value of f = 0.4, which is typical for wettable particles. Penetrations for other particle diameters were computed for an aerodynamic performance cut diameter, d_{PC}, = 1.8 μmA, utilizing Figure 4-7.

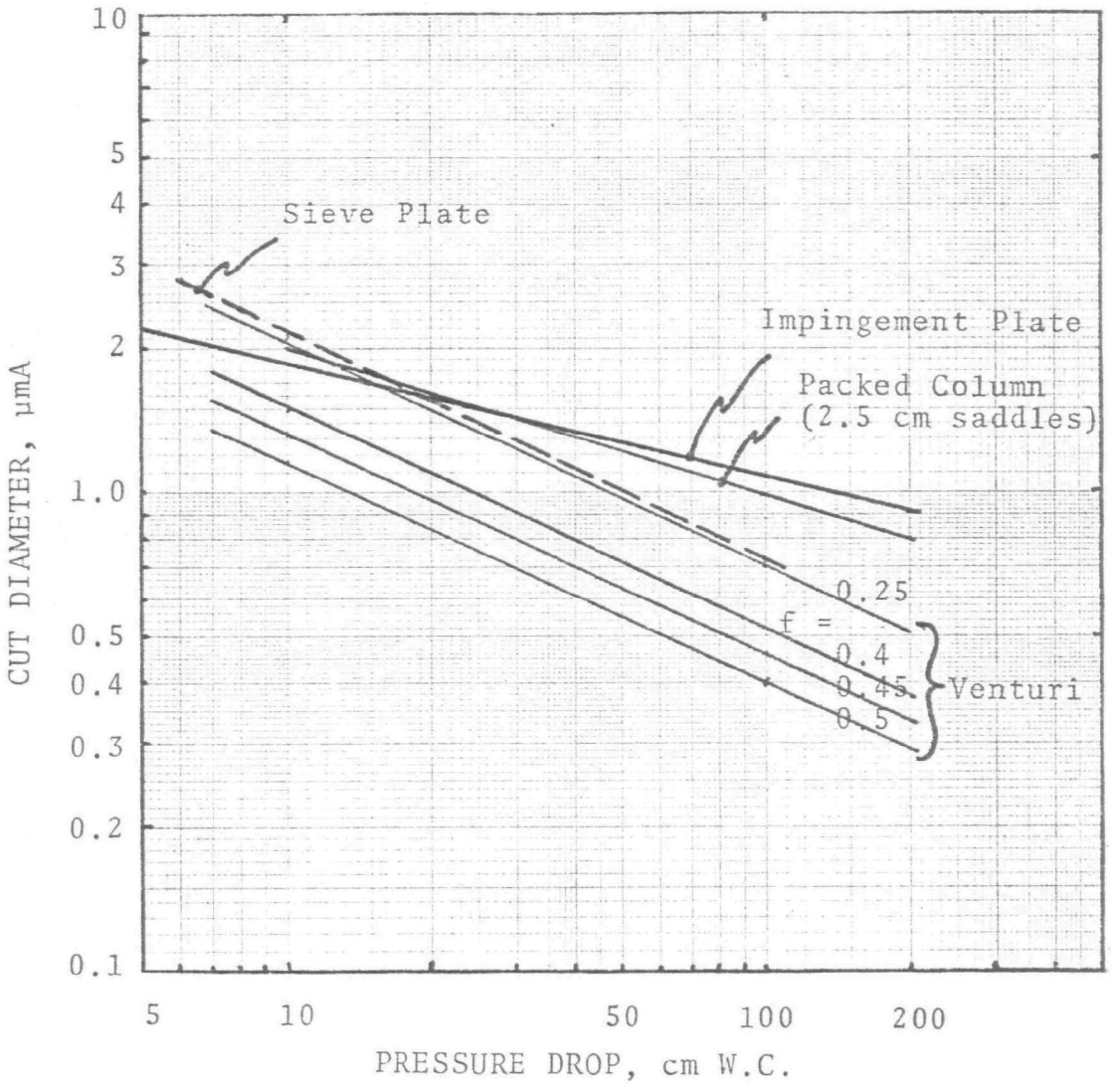

Figure 4-6 - Cut diameter - pressure drop correlations. (Calvert, 1974)

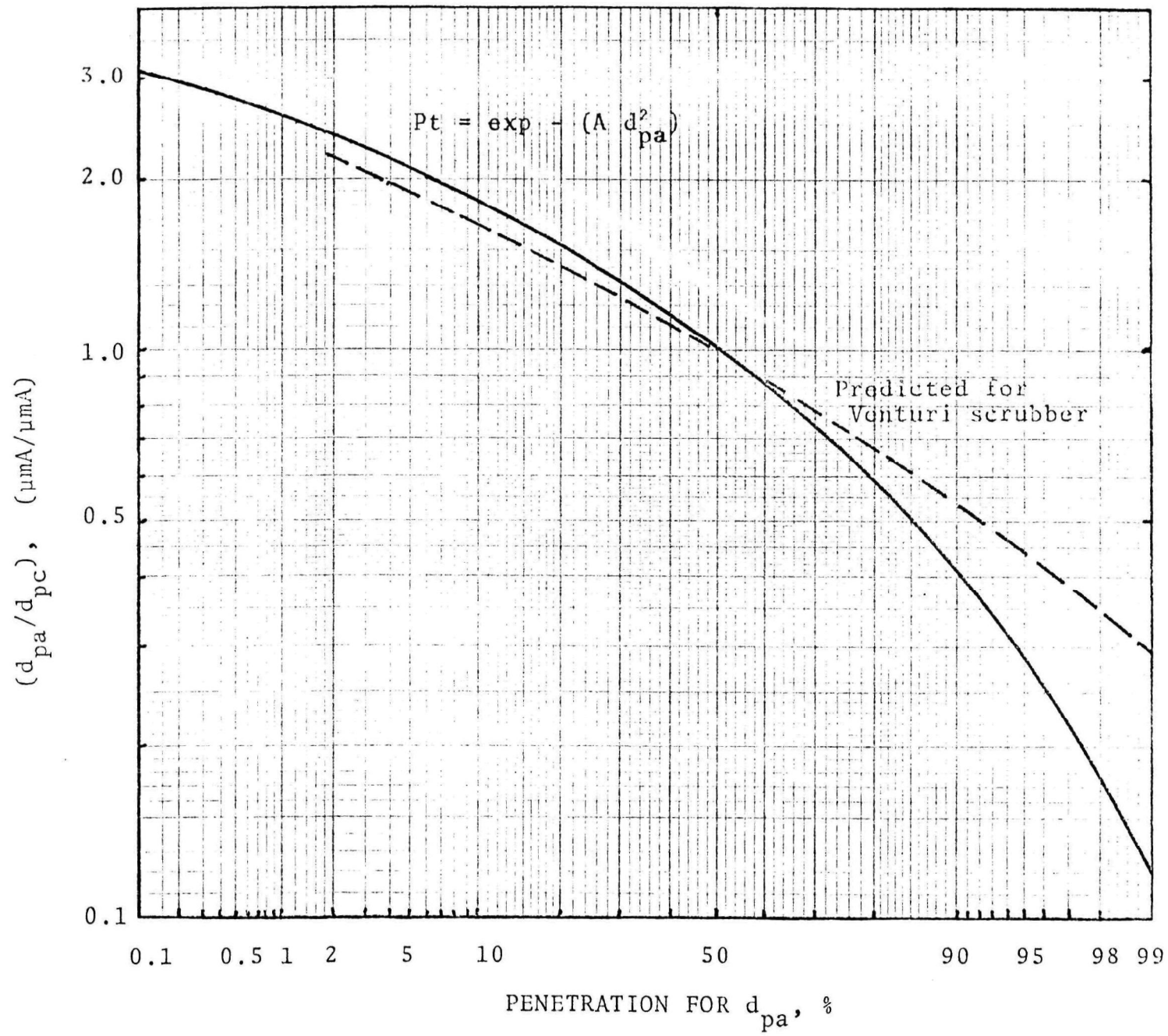

Figure 4-7 - Predicted particle diameter - penetration relationship for inertial impaction (Calvert, 1974).

CONCLUSIONS

The general operation of this scrubber was not hampered by any substantial problems although entrainment separation was not very effective. Particle collection efficiency was what would be expected for a low pressure drop scrubber and would have to be increased to meet recent air pollution regulations.

The unit mechanism responsible for particle collection in this scrubber appears to be collection on drops, rather than in curved conduits. Penetration can be accounted for by means of a gas-atomized spray model.

The cyclone pre-cutter which was used on the inlet samples had too low a cut diameter and it substantially reduced the impactor stage catches. Consequently, it is not possible to compute penetrations for particles larger than about 1.5 μm diameter with much accuracy. The experience of this test showed the advantage of using a pre-cutter with a cut diameter greater than 5.0 μmA.

A P P E N D I X 4-A
PARTICLE DATA

RUN #1 (Outlet)

Impactor Stage No.	W_{cum} (mg)	d_{pc} * (μm)
Precutter		
0		
1		
2		4.7
3	33.6	3.3
4	33.6	2.1
5	26.5	1.1
6	17.2	0.65
7	10.6	0.43
Filter	7.7	
Sample Volume (DNm^3)	0.460	
Type of Impactor	Andersen	

RUN #3 (Outlet)

Impactor Stage No.	W_{cum} (mg)	d_{pc} (μm)
Precutter		
0	88.4	11
1	88.0	7.0
2	87.4	4.7
3	85.3	3.3
4	83.1	2.1
5	68.6	1.1
6	49.4	0.65
7	30.2	0.43
Filter	21.7	
Sample Volume (DNm^3)	0.868	
Type of Impactor	Andersen	

*NOTE: Particle diameters were computed from the aerodynamic cut sizes based on a particle density of 2.0 g/cm^3 and the appropriate C'.

RUN #4 (Outlet)

Impactor Stage No.	W_{cum} (mg)	d_{pc} (μm)
Precutter		
0	98.2	11
1	97.3	7.0
2	96.8	4.7
3	96.1	3.3
4	92.5	2.1
5	76	1.1
6	49.7	0.65
7	35.2	0.43
Filter	27.2	
Sample Volume (DNm^3)	1.020	
Type of Impactor	Andersen	

RUN #5 (Outlet)

Impactor Stage No.	W_{cum} (mg)	d_{pc} (μm)
Precutter		
0	69.1	11.0
1	68.9	7.0
2	68.8	4.7
3	67.5	3.3
4	63.9	2.1
5	52	1.1
6	36.5	0.65
7	25.7	0.43
Filter	20	
Sample Volume (DNm^3)	0.481	
Type of Impactor	Andersen	

RUN #8 (Inlet)

Impactor Stage No.	W_{cum} (mg)	d_{pc} (μm)
Precutter		
0		
1	22.2	10.2
2	15.5	6.1
3	11.2	3.7
4	5.5	2.2
5	2.8	1.1
6	1.8	0.65
7		
Filter	1.4	
Sample Volume (DNm^3)	0.0144	
Type of Impactor	Andersen	

RUN #9 (Inlet)

Impactor Stage No.	W_{cum} (mg)	d_{pc} (μm)
Precutter		
0	22.8	12.4
1	17.8	7.9
2	11.3	5.3
3	9.8	3.7
4	6.5	2.4
5	3.4	1.3
6		
7		
Filter	1.3	
Sample Volume (DNm^3)	0.0141	
Type of Impactor	Andersen	

RUN #11 (Inlet)

Impactor Stage No.	W_{cum} (mg)	d_{pc} (μm)
Precutter		
0	77.8	11
1	75.7	7.0
2	74.5	4.7
3	72.7	3.3
4	10.8	2.1
5	6.8	1.1
6	4	0.65
7	3.4	0.43
Filter	3.0	
Sample Volume (DNm^3)	0.0568	
Type of Impactor	Andersen	

RUN #12 (Inlet)

Impactor Stage No.	W_{cum} (mg)	d_{pc} (μm)
Precutter		
0	20.4	11
1	20.0	7.0
2	18.4	4.7
3	17.0	3.3
4	14.7	2.1
5	10.3	1.1
6	6.1	0.65
7	4.6	0.43
Filter	3.9	
Sample Volume (DNm^3)	0.033	
Type of Impactor	Andersen	

RUN #15 (Inlet)

Impactor Stage No.	W_{cum} (mg)	d_{pc} (μm)
Precutter	2949.3	
0		
1	200.6	16.5
2	188.2	7.23
3	187.5	3.35
4	125.4	1.32
5	51.9	0.73
6	35.8	0.37
7	27.5	0.2
Filter	15.5	
Sample Volume (DNm^3)	0.595	
Type of Impactor	U. W. Mark III	

RUN #16 (Inlet)

Impactor Stage No.	W_{cum} (mg)	d_{pc} (μm)
Precutter	1503.8	
0		
1	78.9	16.5
2	76.2	7.23
3	74.6	3.35
4	47.3	1.32
5	18.9	0.73
6	13.3	0.37
7	12.4	0.2
Filter	3.4	
Sample Volume (DNm^3)	0.42	
Type of Impactor	U.W. Mark III	

RUN #17 (Inlet

Impactor Stage No.	W_{cum} (mg)	d_{pc} (μm)
Precutter	2669.4	
0		
1	84.6	16.5
2	79.9	7.23
3	78.7	3.35
4	61.3	1.32
5	36.5	0.73
6	23.2	0.37
7	15.7	0.2
Filter	9.2	
Sample Volume (DNm^3)	0.179	
Type of Impactor	U. W. Mark III	

RUN #18 (Outlet)

Impactor Stage No.	W_{cum} (mg)	d_{pc} (μm)
Precutter		
0		
1	117.7	18.1
2	112.7	7.85
3	105.7	3.67
4	82.1	1.45
5	51.1	0.80
6	39.4	0.41
7	24.2	0.22
Filter	12.7	
Sample Volume (DNm^3)	0.336	
Type of Impactor	U. W. Mark III	

RUN #19 (Outlet)

Impactor Stage No.	W_{cum} (mg)	d_{pc} (μm)
Precutter		
0		
1	133.3	17.67
2	119.5	7.65
3	104.3	3.58
4	75.6	1.42
5	44.1	0.78
6	29.4	0.397
7	21.1	0.21
Filter	11.8	
Sample Volume (DNm^3)	0.343	
Type of Impactor	U. W. Mark III	

RUN #21 (Inlet)

Impactor Stage No.	W_{cum} (mg)	d_{pc} (μm)
Precutter	3225.1	
0		
1	136.8	16.8
2	104.3	7.36
3	99.5	3.44
4	59.1	1.35
5	21.2	0.73
6	17.8	0.37
7	13.9	0.2
Filter	8.7	
Sample Volume (DNm^3)	0.368	
Type of Impactor	U. W. Mark III	

RUN #22 (Outlet)

Impactor Stage No.	W_{cum} (mg)	d_{pc} (μm)
Precutter		
0		
1	65.6	17.1
2	60.9	7.5
3	53.4	3.47
4	35.6	1.38
5	17	0.756
6	9.6	0.387
7	6.5	0.208
Filter	6.0	
Sample Volume (DNm^3)	0.280	
Type of Impactor	U. W. Mark III	

RUN #23a (Outlet)

Impactor Stage No.	W_{cum} (mg)	d_{pc} (μm)
Precutter		
0		
1	17.5	2.21
2	13.3	1.29
3	10.8	0.87
4	8.4	0.45
5	7.2	0.188
6		
7		
Filter	4.7	
Sample Volume (DNm^3)	0.04	
Type of Impactor	Brink	

RUN #23b (Inlet)

Impactor Stage No.	W_{cum} (mg)	d_{pc} (μm)
Precutter	2388.8	
0		
1	148.8	19.90
2	145.3	8.72
3	141.3	4.03
4	99.1	1.61
5	60.4	0.90
6	42.2	0.46
7	31.7	0.253
Filter	18.8	
Sample Volume (DNm^3)	0.211	
Type of Impactor	U. W. Mark III	

APPENDIX 4-B
PARTICLE SIZE DISTRIBUTION PLOTS

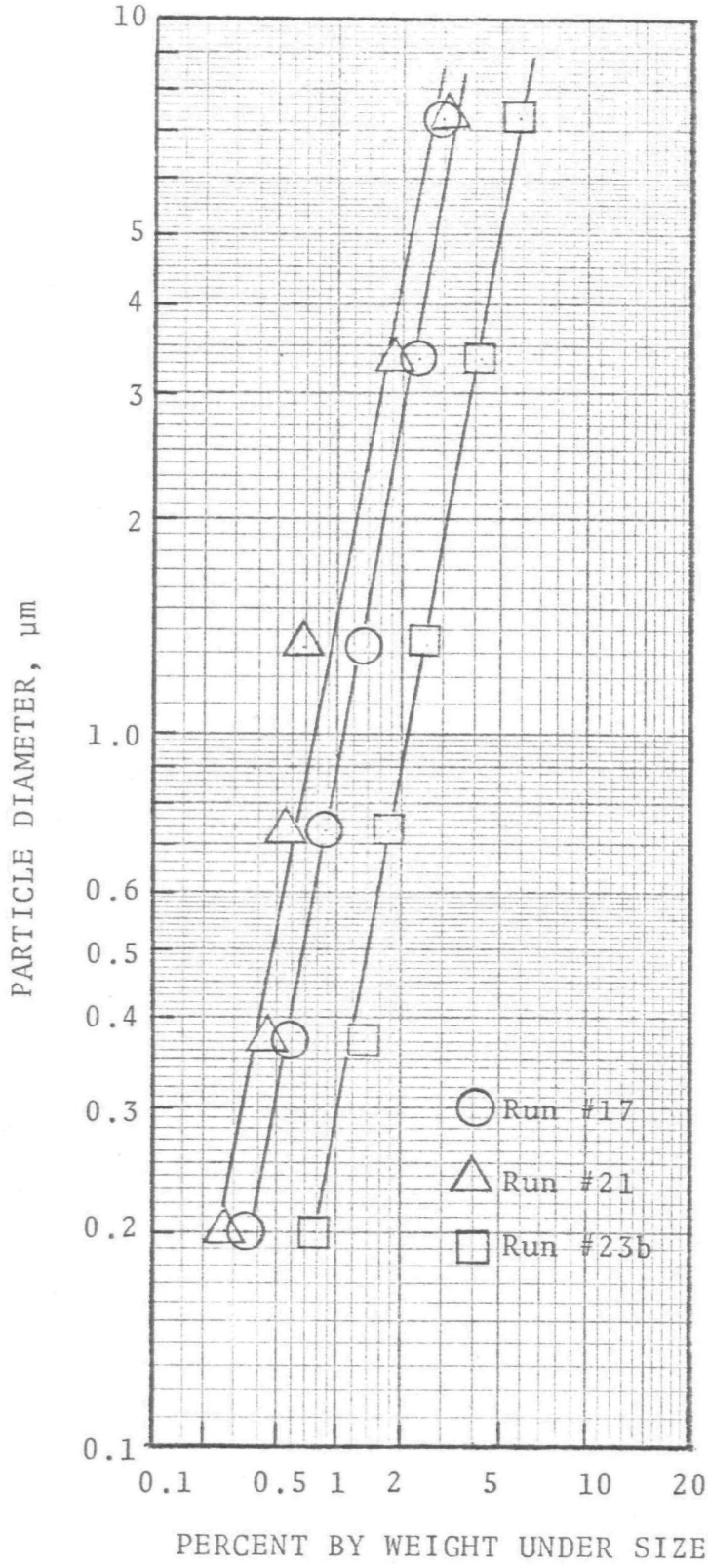

Figure 4-B-1 - Inlet particle size distribution.

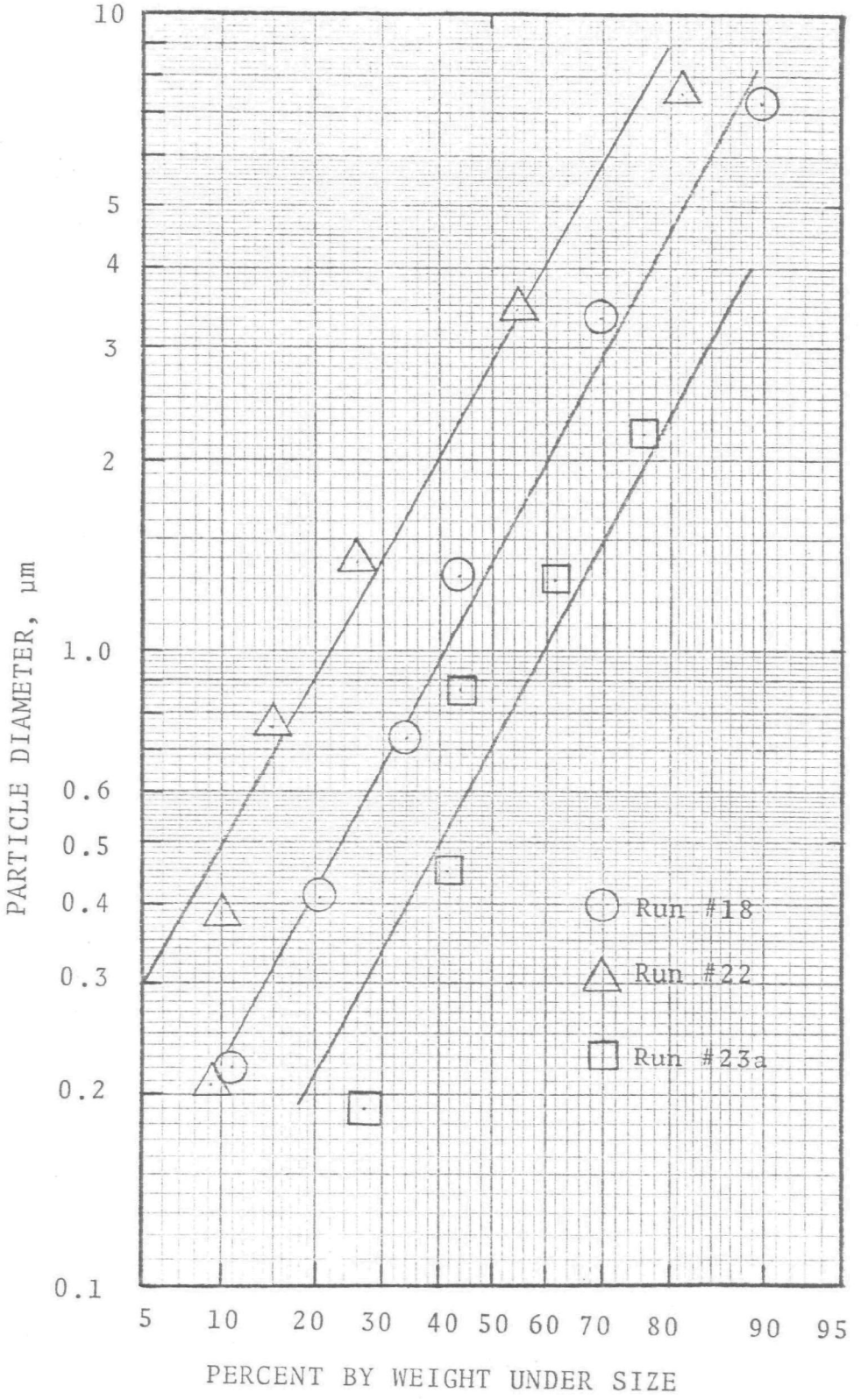

Figure 4-B-2 - Outlet particle size distribution.

MOBILE BED ON COAL-FIRED BOILER
(T.C.A. Scrubber)

SOURCE AND SCRUBBER

A model 6,700 TCA (Turbulent Contact Absorber) scrubber designed by UOP, Air Correction Division, was the subject of the fourth performance test. This type of scrubber utilizes mobile (fluidized) beds of 3.8 cm (1.5") diameter polypropylene spheres as the three contacting stages. (See Figure 5-1). The scrubber is equipped with a chevron mist eliminator made of fiberglass reinforced plastic.

This system was installed to clean the exhaust gas from an electrostatic precipitator used to control the particulate emission from a 165 M.W. utility steam boiler. The boiler is a Babcock & Wilcox Radiant Boiler (Built in 1961) with a steam capacity of 517,560 kg/hr at design pressure of 1.51×10^6 kg/m^2 and steam temperature of 540.6°C. An analysis of the coal burned in the boiler is given in Table 5-A-1.

The boiler flue gas passes from the boiler to the electrostatic precipitator, through 2 fans in parallel, and then to a presaturator spray inside the scrubber body. The gas is cooled in the presaturator from about 143.0°C (290°F) to about 57.0°C (135°F). From the presaturator stage the gas passes through three parallel scrubber compartments, each of which has a series of 3 stages of fluidized balls. The compartments divide the gas stream in the proportions of 20%-60%-20%.

After the scrubber, the gas passes through a chevron type entrainment separator and then to a reheater. Pressure drop through the scrubber is about 30.0 cm W.C. (12"), 5.0 cm (2") through the entrainment separator, and 9.4 cm

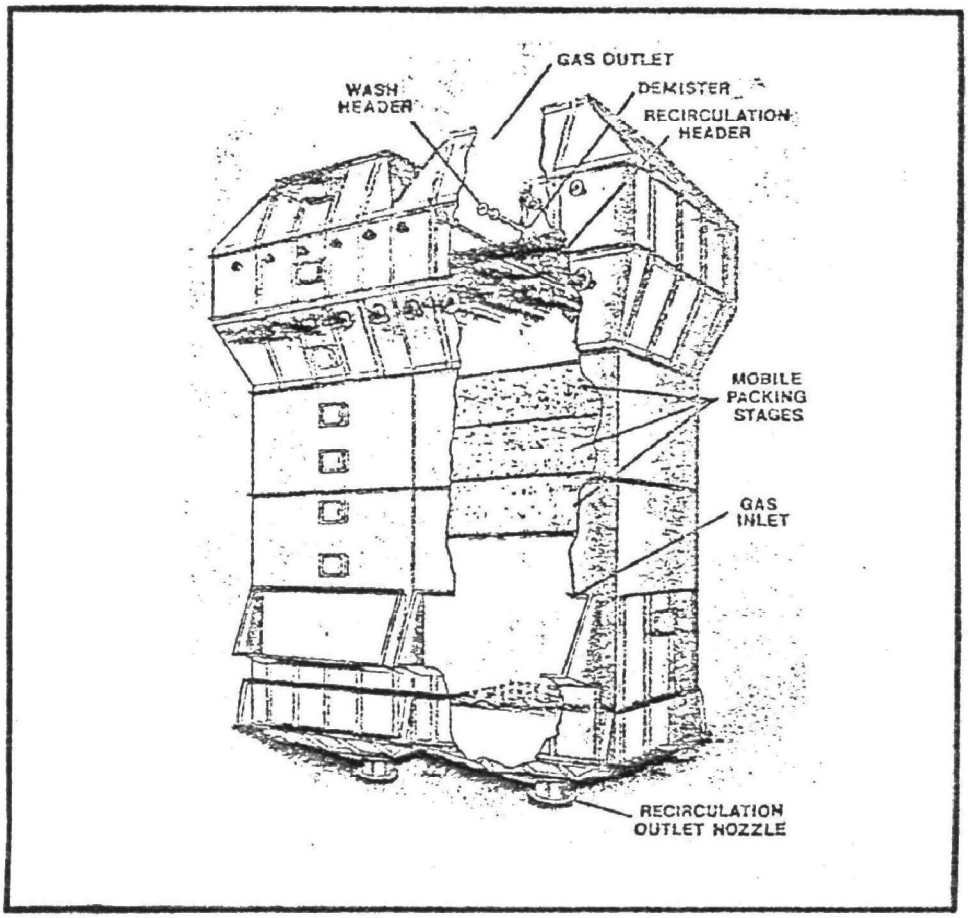

Figure 5-1- Mobile Bed Scrubber.

(3.7") through the reheater. The gas is reheated to about 85.0°C (185°F) in order to provide buoyancy and to prevent condensation in the stack.

The scrubber has four parallel inlet ducts (two into each fan) and three parallel outlet ducts. The inlet ducts are all 3.37 m x 1.03 m (132.5"x40.5") rectangles and the center outlet duct is 4.58 m x 2.29 m (15'x7.5'). Figure 5-2 shows these ducts and their sampling point locations. The inlet duct west of center and the center outlet duct were used for sampling.

Test Method

The most essential part of the performance test was the determination of particle size distribution and concentration (loading) in the inlet and outlet of the scrubber. A modified E.P.A. Method 5 train with an in-stack University of Washington (or Pilat) cascade impactor was used for particle measurements. Gas flow rate was determined by means of type "S" pitot tube traverses along with the necessary temperature and pressure measurements. Sample flows were measured with the usual E.P.A. train instruments so as to obtain isokinetic sampling.

Two series of tests were made; one during July, 1973 and the second from September 10 through September 14, 1973. Plant problems caused an eventual shut-down and abortion of the first series of tests. The second series of tests consisted of three inlet and three outlet samples, which were taken at different times (i.e., not simultaneous inlet-outlet pairs). While not ideal, the taking of separate inlet and outlet samples appeared acceptable in view of steady plant operation and the fairly consistent data which were obtained, based on preliminary computations.

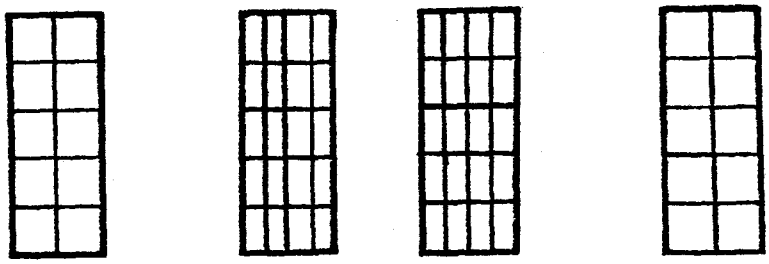

FOUR INLET DUCTS

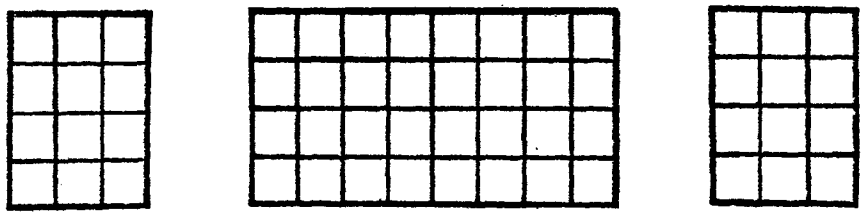

THREE OUTLET DUCTS

(NOTE: Grids show sampling areas)

Figure 5-2 - Duct arrangements.

The inlet sampling point was located upstream of the fan and the pre-saturator. The impactor was kept at one position during the entire sampling period. Because the particle concentration was so low (due to the electrostatic precipitator upstream) it was not necessary to use a pre-cutter ahead of the U. W. impactor. Outlet samples had to be taken after the reheater because of sample port location, so it was not possible to make any measurements of liquid entrainment and it was not necessary to heat the impactor.

Possible sample bias due to particle inertia effects (segregation) was not very significant in this test for two reasons. First, any errors in the sampling of large particles will not affect penetration for the fine particles. Second, the particles entering the scrubber have been pre-cleaned by the electrostatic precipitator and thus are fairly small, except for the large particles reentrained during rapping.

Operating Conditions

The scrubber operating conditions during the test period were as follows:

1. Gas flow rate computed as 4 times the rate measured in one duct was 18,000 A m^3/min (630,000 ACFM) at about 143.0°C (290°F), 61.5 cm Hg (24.2"Hg) pressure and 5% H_2O vapor. The flow rate computed as 1.67 times the 10,000 A m^3/min (360,000 ACFM) measured at the center scrubber compartment outlet was 17,000 A m^3/min (600,000 ACFM) at about 85°C (185°F), 64 cm Hg (25.2"Hg), and 18% H_2O vapor. Data provided by the power plant personnel from previous tests were 545,000 ACFM at 272°F (at 150 MW load) and 640,000 ACFM (at 165 MW). These

are in good agreement with the data from this test. Gas flow rate through the scrubber is 9,000 DN m^3/min @ 0°C, 76.0 cm Hg (or 340,000 DSCFM @ 70°F, 14.7 psia).

2. Slurry flow rate to the scrubber was reported by the power plant as approximately 113.0 m^3/min (30,000 GPM). Makeup water is introduced into the pre-saturator at a rate of 1.44 m^3/min (380 GPM). The total pre-saturator spray rate was around 6.8 m^3/min (1,800 GPM).
3. Gas velocity in the scrubber is usually maintained at 2.8 m/sec (9.2 ft/sec) ±20% in order to keep the balls fluidized.
4. Entrainment could not be measured but is known to be excessive because it causes plugging of the gas pre-heater.

PARTICLE DATA

The data obtained on particle concentration and size are presented in Tables 5-A-2 and 5-A-3. Size distributions for these runs are shown in Figures 5-B-1 and 5-B-2, log-probability plots of the inlet and outlet data. As shown on the plots, the inlet particles have a mass median diameter, d_{pg}, of about 3.0 µmA and a geometric standard deviation, σ_g, of about 2.5. The outlet particles have $d_{pg} \simeq 0.5$ µmA and $\sigma_g \simeq 6.0$.

Cumulative mass concentration was plotted against aerodynamic size to yield Figures 5-3 and 5-4. The solid curves are for the third degree polynomials fit by the least squares method. The dashed lines are the curves fitted by eye. The polynomial fit for the outlet samples is obviously unrealistic above 2 µmA particle diameter, especially if one plots all of

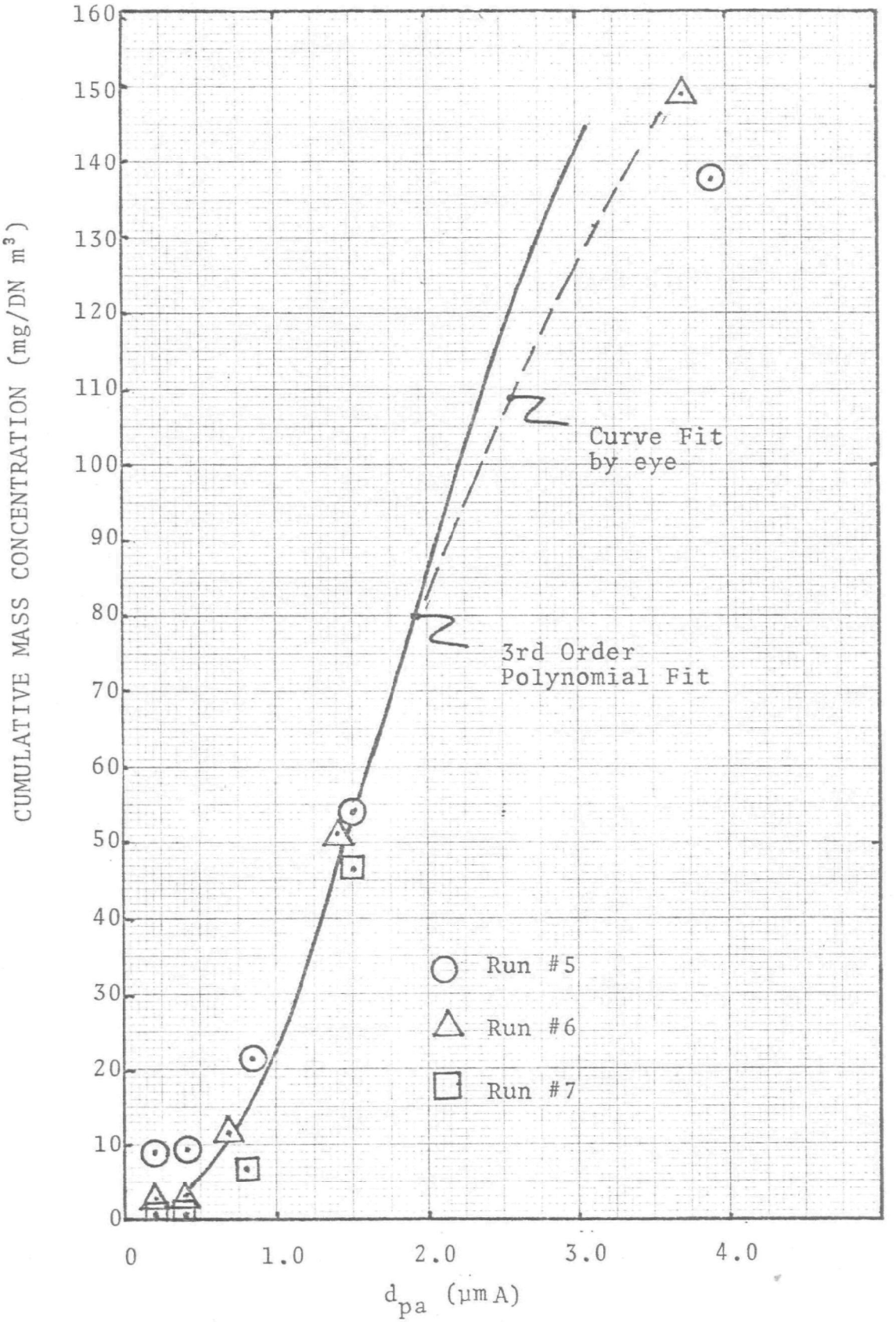

Figure 5-3 - Inlet cumulative mass concentration size distribution.

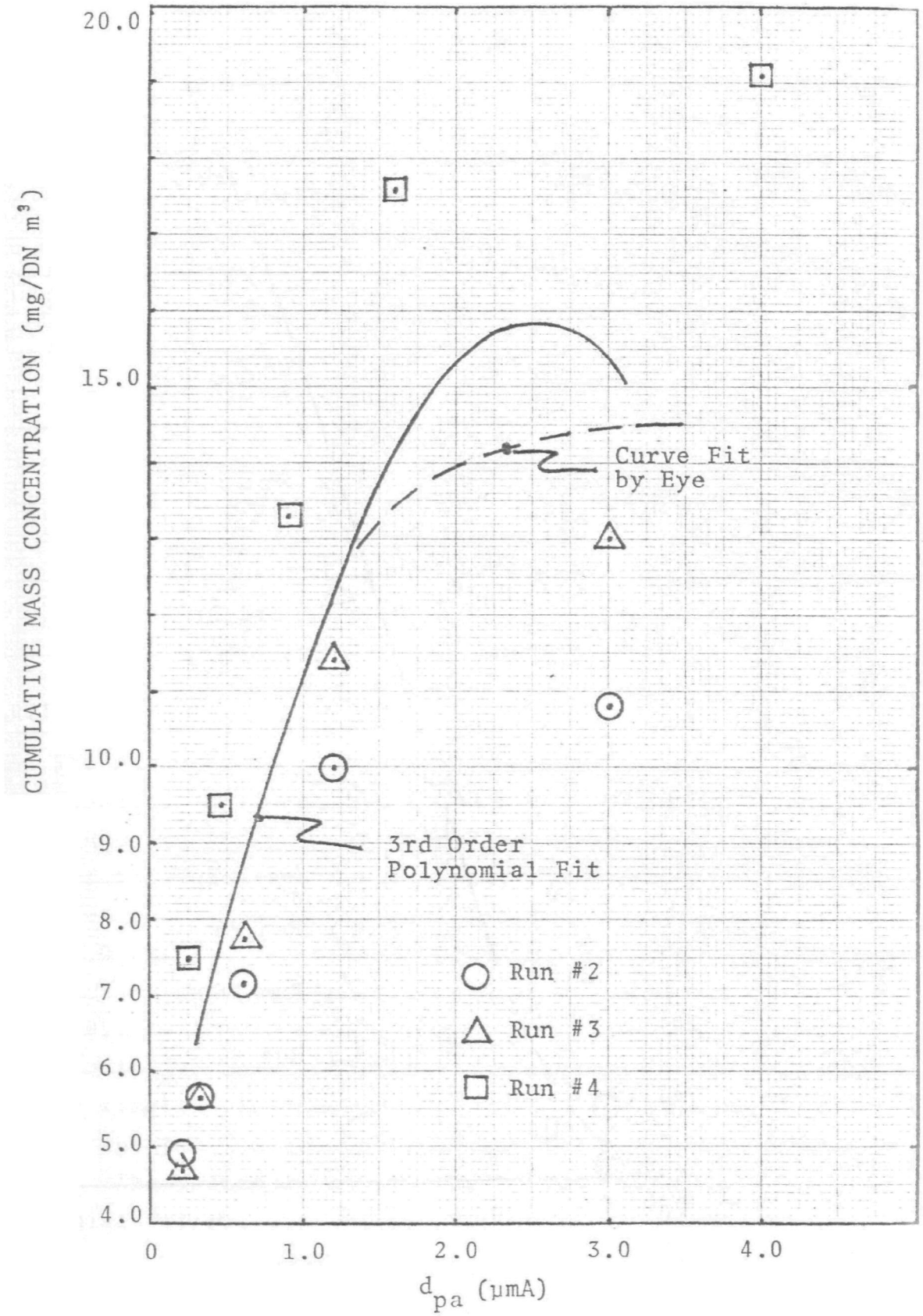

Figure 5-4 - Outlet cumulative mass concentration size distribution.

the points for larger sizes. If the points for larger sizes were included in the least squares regression, however, the fit would be poor at small particle diameters. Since we are most concerned with penetration for fine particles, the option for a better fit at the small end was taken.

Particle Penetration

Particle penetration was computed by the following two methods:

1. The third order polynomials describing the inlet and outlet cumulative concentration distributions were differentiated and the ratio of first derivatives with respect to particle diameter was computed at several values of diameter. The ratio of outlet to inlet derivatives is, as discussed in the section on the computation method, the penetration at that particle diameter.
2. The slopes of the eyeball fit curves in Figures 5-3 and 5-4 were measured by a graphical technique at several values of particle diameter. The ratios of outlet to inlet slopes were computed to yield penetrations at the several diameter values.

Penetrations are computed by the two methods are plotted against particle diameter (aerodynamic) in Figure 5-5. It can be seen that there is a slight discrepancy between the two methods at diameters above 1.0 μmA. As discussed previously, this is an obvious consequence of the curve-fitting computation and can be readily compensated for.

ECONOMICS AND OPERATING PROBLEMS

Points of information on economics and operating problems for the scrubber system are listed below.

1. The approximate installed cost of the scrubber system, for particle removal only, is $3,900,000;

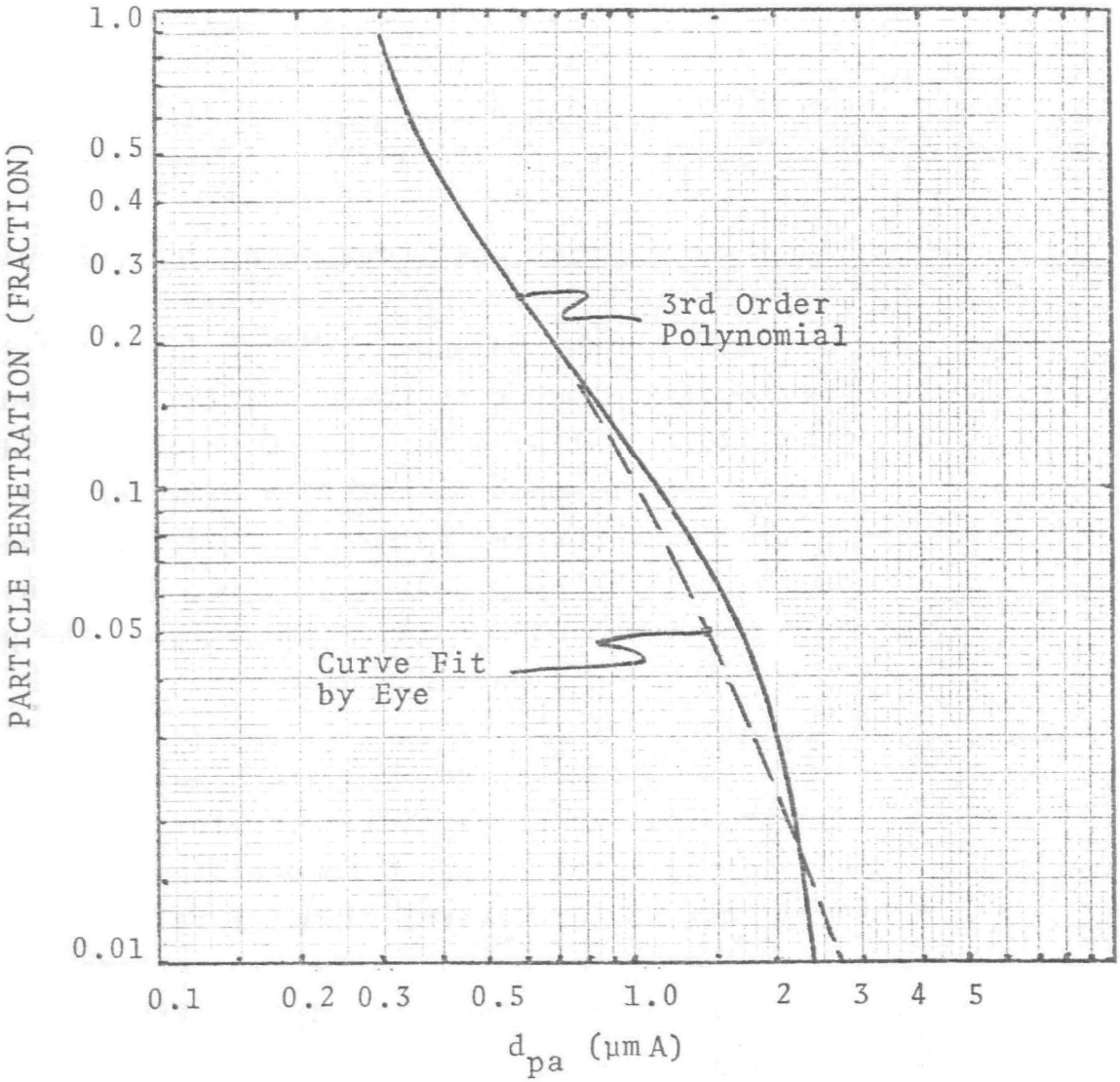

Figure 5-5 - Particle penetration versus aerodynamic particle diameter for T.C.A. scrubber.

or $23.60/KW. It was estimated that the addition of SO_2 control features would cost about $10.00/KW more. The scrubber alone accounts for about 10% of the equipment cost. Power consumption for the scrubber system is about 4% of the gross output of the plant.

2. Scaling has not been much of a problem, due to ash properties.
3. The entrainment separators (mist eliminators) have not been sufficiently effective. Two horizontal layers of zigzag baffles, containing 4 -90° turns in each, were used.
4. Frequent plugging of the reheater has been caused by carry-over from the entrainment separator.
5. Ball wear in the scrubber has been rapid and various materials have been tried.
6. Suitable materials of construction for scrubber internals are 316 L stainless steel or rubber lining. Types 304 and 308 stainless are not satisfactory. Pumps are rubber lined. The stack is acid proof lined and has a double wall for insulation.
7. Dry fans are preferred because of problems with wet fans following inefficient entrainment separators.

MATHEMATICAL MODELS

A major objective of the scrubber performance test program is the validation and/or further development of mathematical models which can be used for the prediction of performance. The data on particle penetration as a function of particle size and scrubber parameters have not been

available prior to this time. Where a design model has been presented before, our first approach is to determine whether the available model(s) fit the data. If this does not prove to be the case, then it will be necessary to develop a model which works properly.

The only model we know of for particle collection in a T.C.A. is the semi-empirical relationship presented by Bechtel Corp. in a June, 1971 report on the Shawnee project for E.P.A. and cited by Calvert et al. (1972)

$$\eta_i = 1 - \exp\left[-2.18\times10^{-18}\left(\frac{L}{\rho_L}\right)^{3.3}\left(\frac{G}{\rho_G}\right)^{0.36} K_i \left(\frac{Z}{D_b}\right)\right] \qquad (5\text{-}1)$$

where, η_i = collection efficiency for particle diameter "d_i"

L = Liquid rate, kg/hr-m^2

ρ_L = Liquid density, kg/ft^3

G = Gas rate, kg/hr-m^2

ρ_G = Gas density, kg/ft^3

K_i = Inertial impaction parameter for "d_i", average gas velocity through bed void space, and ball diameter as the collector diameter.

Z = Static bed depth, cm

D_b = Ball diameter, cm

This correlation is of very dubious value because it is based on the premise that collection efficiency is due to inertial impaction on the balls. We may note that the impaction parameter has a value of about 5×10^{-4} for a gas velocity of 10 ft/sec, ball diameter of 1.5 inches, and aerodynamic particle diameter of 1.0 μmA. The collection efficiency for a sphere is 0% for values of the impaction parameter smaller than about 0.1; consequently it is impossible to attribute high collection efficiency to this mechanism. Collection efficiency due to flow through the curved passages between the balls would be comparably low.

An attempt to explain the observed penetrations by treating the stages of fluidized balls as sieve (or froth) plates was also unsuccessful. In order to have a penetration of 0.1 for three sieve plates in series, the inertial parameter based on perforation diameter would have to be about 0.77 (for foam density = 0.7). If the aerodynamic particle diameter is 1.0 μmA, corresponding to Pt = 0.1, the ratio of velocity through the perforation to perforation diameter would be (for standard air properties):

$$K_p \left[\frac{9\ \mu_g}{d_{pA} \times 10^{-8}} \right] = \frac{u_h}{d_h} = 0.77 \left[\frac{9\ (1.8 \times 10^{-4})}{1 \times 10^{-8}} \right] \simeq 125{,}000\ (\text{sec}^{-1}) \quad (5\text{-}2)$$

Even if the effective perforation diameter, d_h, were 0.5 cm (0.2 in.), which is smaller than seems probable, the gas velocity would have to be about 62,000 cm/sec (2,000 ft/sec), which is not possible.

The attempted rationalization of the observed T.C.A. performance in terms of either a counter-current or co-current gas-atomized spray scrubber was also not fruitful. In both of these cases the cut diameter predicted was much larger than observed.

Observation of a 30 cm (1 ft) diameter mobile bed column in operation revealed that the balls near the column wall move downward. Therefore, there must be channeling in the bed such that the balls in the middle move upward. Based on this clue, computations of collection efficiency for a co-current spray were made for a gas velocity higher than the average superficial velocity in order to allow for gas flow channeling. Assumptions which were explored are as follows:

1. Gas velocity is 2 times the average superficial velocity.

2. Gas velocity is 4 times the average in order to account for bed porosity of about 50% and gas flow channeling.
3. Liquid (drop) flow rate within the bed is that which would cause from 1/3 to 2/3 of the bed pressure drop of about 10 cm W.C. per stage. The remainder of the pressure drop would be due to static head.
4. Drop size is determined by gas atomization of the liquid.
5. Drop shatter within the mobile bed causes drop size to be smaller than that from gas atomization.

None of the above assumptions, alone or in combination, would account for the observed scrubber performance. The predicted penetration of 1.0 μmA diameter particles ranged mainly from 0.85 to 0.9 at 3.0 cm W.C. assumed for liquid acceleration and from about 0.7 to 0.85 at 6 cm W.C. Three stages would result in predicted penetrations ranging from 0.61 to 0.73 for 3.0 cm W.C. and 0.34 to 0.61 for 6.0 cm W.C. The experimentally observed penetration at 1.0 μmA was about 0.1 for three stages, which would require a single stage penetration of 0.46, or less.

If one compares the observed mobile bed performance (i.e., a cut diameter of about 0.4 μmA at 25 cm W.C. pressure drop) with other types, as shown in Figure 4-6, there is an obvious descrepancy. One would expect that a scrubber utilizing inertial impaction only would require 200-400 cm W.C. pressure drop to provide a 0.4 μmA cut diameter.

At least a partial explanation of the high efficiency lies in the fact that SO_2 and some H_2SO_4 were present in the flue gas. Any H_2SO_4 (or SO_3) which adsorbs on the fly ash particles will cause the condensation of water on the particles. This will occur even when the relative humidity

is considerably lower than 100%. The consequent growth of the particles in the saturated scrubber atmosphere will cause them to be collected at higher efficiency than the dry particles. In the absence of any data on particle collection efficiency for non-hygroscopic particles in a mobile bed, we are unable to evaluate the relative importance of condensation and other mechanisms.

Another factor to consider is that the mobile bed follows an electrostatic precipitator and there may be a particle charge effect. However, there is evidence that this is not a significant factor. For one thing, the E.P.A. tests of the mobile bed scrubber at the Shawnee Plant, which does not follow an electrostatic precipitator, show penetrations comparable to those found in the present test. For another thing, Public Service Co. of Colorado has found that there is no difference between mobile bed performances when the units follow cyclones rather than electrostatic precipitators.

CONCLUSIONS

The data obtained for particle penetration as a function of particle size will provide a useful and important basis for the development of a realistic mathematical model and design method. There is scatter in the data and it is obvious that additional data for simultaneous inlet and outlet samples would be very important in providing a more precise basis for design method development. The scrubber reliability has not been good, although the plant personnel felt that continual progress is being made toward its improvement. We strongly recommend that additional performance tests be made on mobile bed scrubbers and that these include further investigations of operating problems and methods of coping with them.

Further work must be done to establish a rational mathematical model for particle collection in a mobile bed. It would be best to start from some reliable data on a system free of condensation effects.

APPENDIX 5-A
PARTICLE AND COAL DATA

Table 5-A-1. COAL ANALYSES

PROXIMATE ANALYSIS

	As Received	Dry Basis
% Moisture	9.51	XXXX
% Ash	8.99	9.93
% Volatile	36.08	39.87
% Fixed Carbon	45.42	50.20
	100.00	100.00
Btu	11028	12187
% Sulfur	0.43	0.48

ULTIMATE ANALYSIS

	As Received	Dry Basis
% Moisture	9.51	XXXX
% Carbon	63.08	69.71
% Hydrogen	4.53	5.01
% Nitrogen	1.38	1.52
% Chlorine	0.00	0.00
% Sulfur	0.43	0.48
% Ash	8.99	9.93
% Oxygen (diff)	12.08	13.35
	100.00	100.00

Table 5-A-2. INLET SAMPLE PARTICLE DATA

U.W. Stage	RUN #5		RUN #6		RUN #7	
	W_{cum}* (mg)	d_{pc}** (μmA)	W_{cum} (mg)	d_{pc} (μmA)	W_{cum} (mg)	d_{pc} (μmA)
1	38.0	18.0	29.7	18.0	35.7	19.0
2	33.3	8.3	27.6	8.0	34.7	8.2
3	31.1	3.9	25.7	3.7	31.7	3.8
4	23.2	1.5	20.1	1.4	21.9	1.5
5	9.0	0.83	6.9	0.7	5.9	0.8
6	3.6	0.42	1.6	0.4	0.9	0.4
7	1.6	0.2	0.3	0.2	0.1	0.2
Filter	1.5		0.3		0.1	
Sample Volume (DN m^3)	0.168		0.135		0.13	

NOTES:

* W_{cum} = Cumulative mass collected on that stage and those below.

** d_{pc} = Cut diameter (aerodynamic) for that stage.

μmA = microns, aerodynamic = $d_p(C'\rho_p)^{1/2}$

Table 5-A-3. OUTLET SAMPLE PARTICLE DATA

U.W. Stage	RUN #2		RUN #3		RUN #4	
	W_{cum} (mg)	d_{pc} (μmA)	W_{cum} (mg)	d_{pc} (μmA)	W_{cum} (mg)	d_{pc} (μmA)
1	30.5	14.0	28.8	14.0	24.2	20.0
2	24.1	6.2	28.2	6.2	23.3	8.6
3	24.1	3.0	28.1	3.0	22.2	4.0
4	24.1	1.2	27.6	1.2	21.2	1.6
5	22.1	0.62	24.2	0.62	19.5	0.9
6	16.0	0.33	16.4	0.33	14.7	0.45
7	12.6	0.2	12.0	0.2	10.5	0.25
Filter	10.9		10.1		8.3	
Sample Volume (DN m^3)	2.23		2.12		1.1	

APPENDIX 5-B
PARTICLE SIZE DISTRIBUTION PLOTS

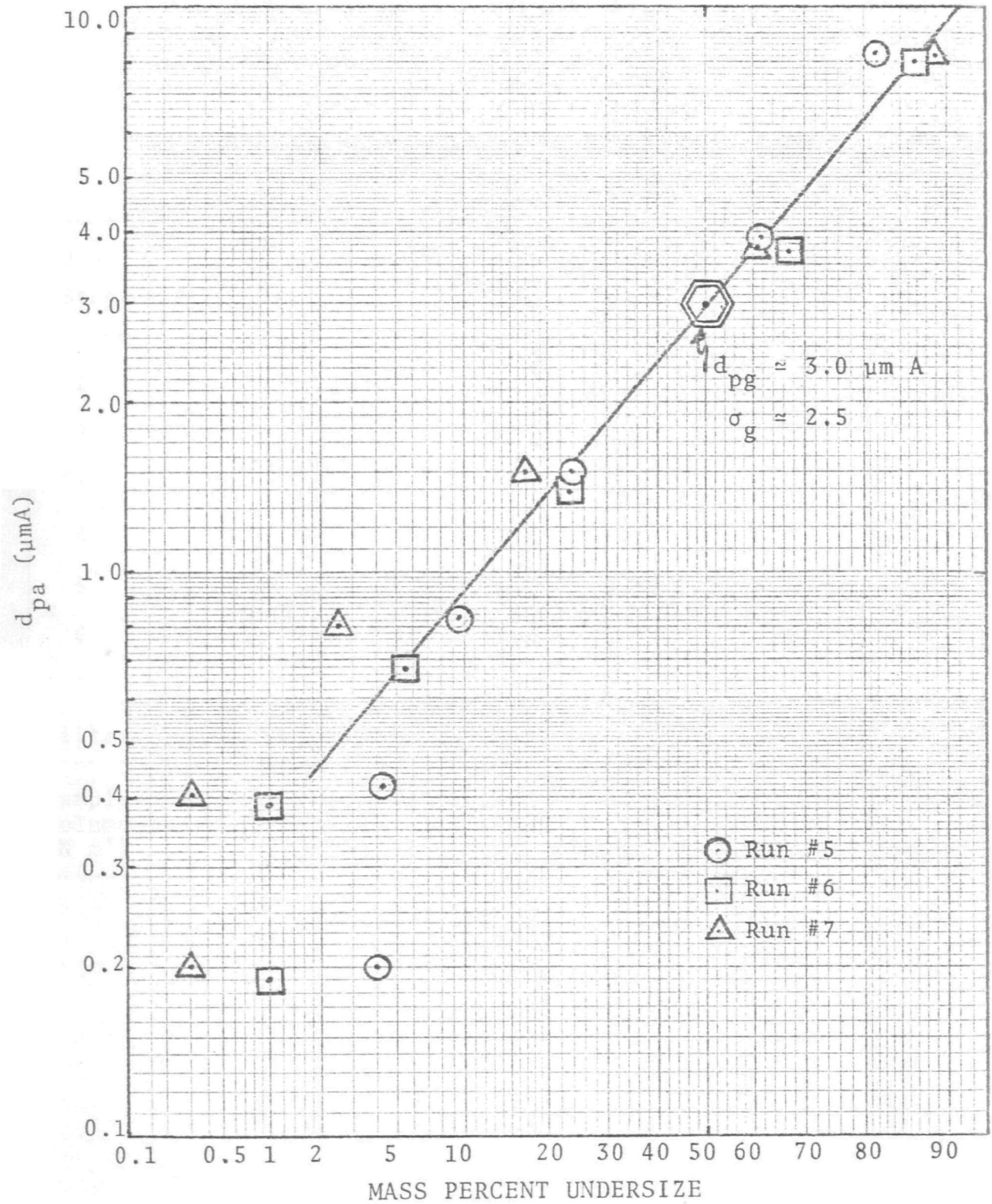

Figure 5-B-1 - Inlet particle size distribution.

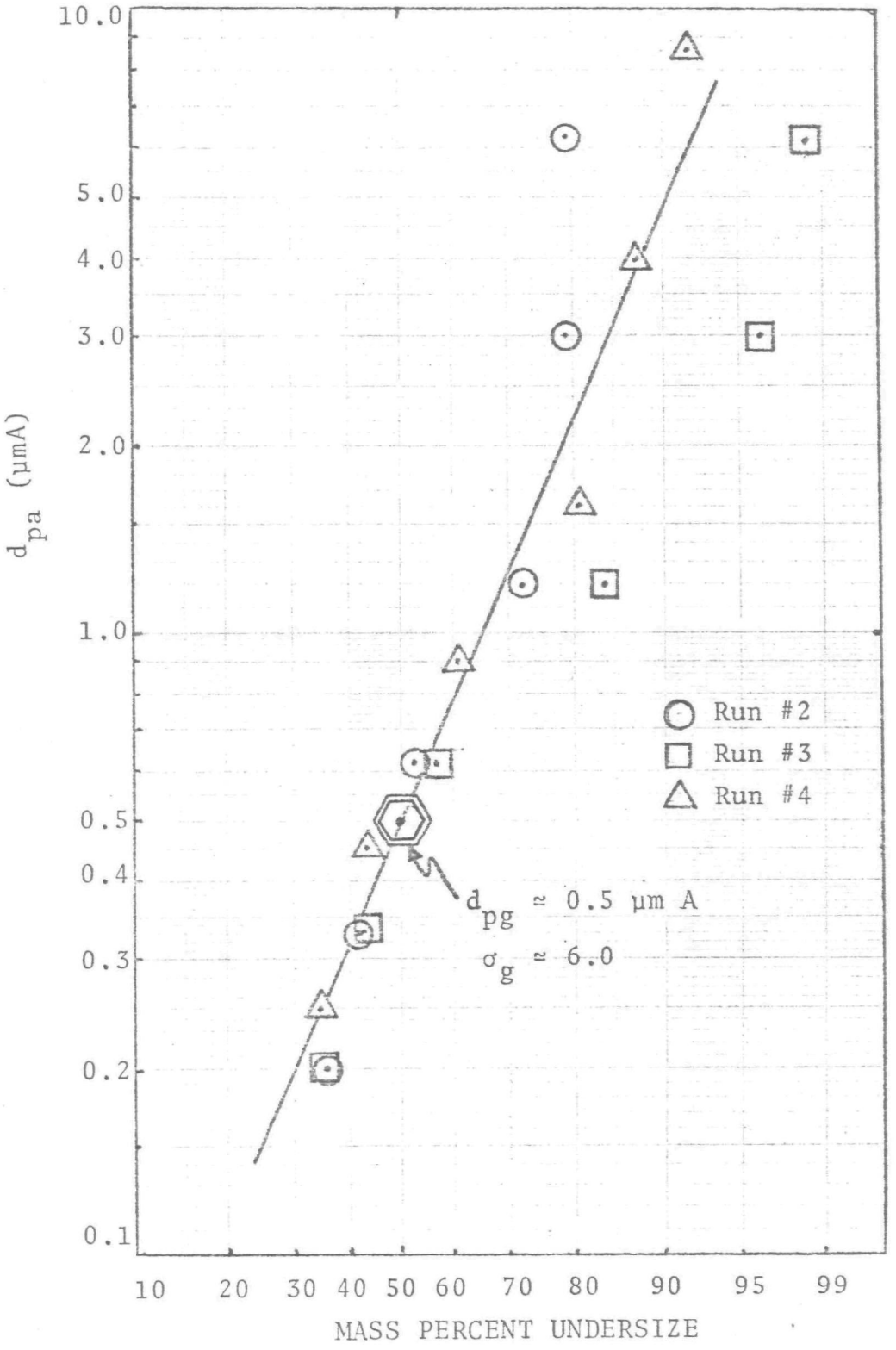

Figure 5-B-2 - Outlet particle size distribution.

VENTURI SCRUBBER ON COAL-FIRED BOILER
(Chemico Venturi)

SOURCE AND SCRUBBER

A Chemico "Venturi" scrubber operating on the flue gas from a coal-fired utility boiler was chosen for test no. 5. The scrubber might more accurately be described as a variable annular orifice type because its throat is formed by a movable "plumb bob" concentrically mounted in a conical "dental bowl", as shown in Figure 6-1.

A chevron type mist eliminator, washed with sprays, is mounted within the scrubber body, as shown in Figure 6-1. Three scrubbers in parallel handle the flue gas from the one boiler. The boiler is a 330 M.W. net, 360 M.W. gross Combustion Engineering unit fired with low sulfur western coal. The coal analysis varied from day-to-day, as shown in Table 6-A-1. Sulfur content varied from 0.34% to 0.75% (as received) during the months of September and October, when our test team was at the plant. While no deliberate effort was made to control SO_2 emissions, the calcium oxide content of the fly ash normally varies from 10% to 26% and there is as much as 40% removal of SO_2 by the scrubber with the pH running around 5.0 to 6.0.

The induced draft fan following the scrubber has a water spray at its inlet to wash off the solids carried over from the mist eliminator. Disengagement of the mist from the fan occurs in the stack, which has an epoxy lining. Reheating is not used after the fan.

Additional information on the scrubber system is as follows:

1. Pressure drop (gas phase) was 25 cm W.C. (10" W.C.) during the test period.

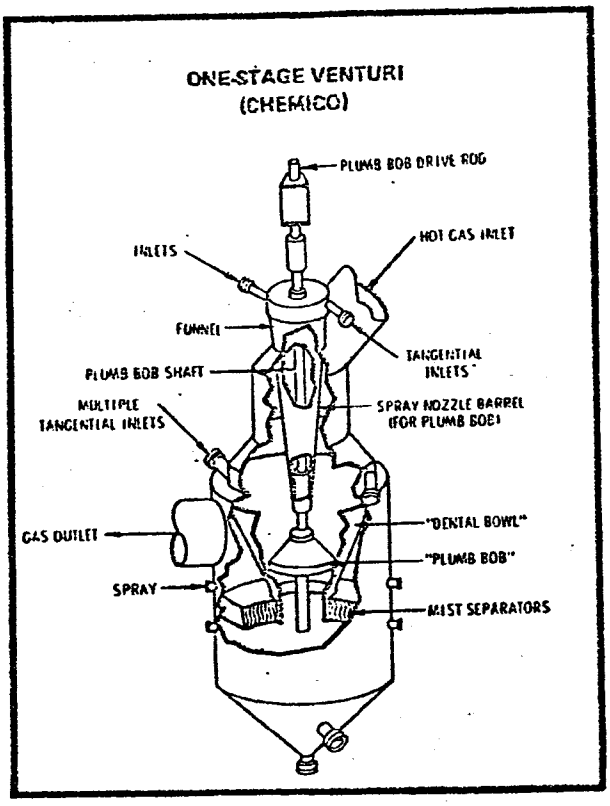

Figure 6-1 - Chemico Venturi

2. Liquid flow rate to the scrubber is 24.6 m^3/min (6,500 G.P.M.), of which about 38% is return from a pond (and treatment with lime) and the remainder is recycled from the scrubber bottom.
3. Makeup water is introduced via the fan sprays.
4. The venturi throat is stainless steel and the vessel is epoxy lined.

There were two interruptions of the testing program. A major disruption occured in September when the boiler was shut down for repairs, due to plugging of the air preheater. This caused a one month postponement and the loss of the data collected during the first period. A minor data loss occured when the boiler had to be operated at reduced load during one test run.

TEST METHOD

Determination of particle size distribution and concentration (loading) in the inlet and outlet of the scrubber provides the basis for computation of performance characteristics. A modified E.P.A. type sampling train equipped with an in-stack University of Washington (Pilat) cascade impactor was used for the inlet and a similar train with an in-stack Brink cascade impactor for the outlet. The U.W. impactor was used on the inlet (at about 1/4 the usual sampling rate) instead of the Brink in order to provide more dust collection capacity for the heavy load of grit which was encountered. Ordinarily the Brink would have been used following a cyclone pre-cutter, but in this case the cyclone had broken during an early test.

Both cascade impactors were allowed to heat up to stack temperature before the sample was taken and the outlet sampler was also heated with an electric resistance wrapping. The filters following the impactors were in-stack and loaded with

Gelman type "E" glass fiber paper. The impactor stages were covered with greased aluminum foils which were treated and weighed in accordance with our usual procedure (as were the filters).

Isokinetic (or near-isokinetic) sampling was used, with the sampler being held at one position in the duct. This is generally an adequate technique for obtaining good samples of particles smaller than a few microns in diameter because they are well distributed across the duct. It does not provide a good sample of the large particles when the nozzle inlet is close to a flow disturbance; as in the case of the inlet sample, which was taken downstream from a butterfly valve. Thus, the total scrubber inlet loading is uncertain because of the one position sample but the inlet fine particle concentration is representative of the entire gas stream.

Gas velocities in the ducts were measured by means of type "S" pitot tube traverses, along with the necessary temperature and pressure measurements. Sample flows were measured with a dry gas meter and an orifice meter.

Several independent inlet and outlet samples were taken by means of both the cascade impactors and a total filter until there was consistency between the two methods of measurement. A series of four simultaneous inlet-outlet tests were then made and one of these was discarded, as discussed previously. The inlet sample was taken in a 3.7 m (12 ft) diameter duct and the outlet sample in a 3.7 m x 4.4 m (12 ft x 14.5 ft) rectangular duct between the scrubber and the I.D. fan.

OPERATING CONDITIONS

The scrubber operating conditions during the test period were as follows:

1. Gas flow rates were as shown in the tabulation below:

Duct	Inlet	Outlet
Temperature	163.0°C(325°F)	54.0°C(130°F)
Pressure during pitot run	60.0 cm Hg	60.0 cm Hg
A m^3/min	13,400	12,700
ACFM	4.75×10^5	4.5×10^5
DN m^3/min	6,300	7,150
DSCFM	2.4×10^5	2.7×10^5
% H_2O vapor (vol.)	6.0%	15.0%

The flow rate measured by the outlet velocity traverse is judged to be more reliable because the velocity distribution was much more regular than at the inlet. Based on 7,120DNm^3/min (2.7×10^5DSCFM), the inlet flow rate would be 15,300Am^3/min (5.4×10^5ACFM), which is 8% higher than the design flow rate of 14,200Am^3/min (5×10^5ACFM).

2. Slurry flow rate to the scrubber was reported by the plant as approximately 24.6 m^3/min (6,500 GPM).
3. Entrainment is known to occur between the scrubber and the fan but was not measured in this test series.

PARTICLE DATA

The particle concentration and size data which were obtained in this performance test are presented in Tables 6-A-2, 6-A-3, and 6-A-4 for the three simultaneous inlet and outlet samples. Figure 6-B-1 shows log-probability plots of inlet and outlet particle size distributions and Figure 6-B-2 is a similar plot for the large diameter end of the inlet distribution. The inlet particles have a mass median diameter, d_{pg},

of about 38.0 μmA and a geometric standard deviation, σ_g, of about 5.0, while the outlet particles have $d_{pg} \simeq 0.15$ μmA and $\sigma_g \simeq 4.6$.

Cumulative mass concentration was plotted against aerodynamic particle size to yield Figure 6-2 and 6-3, for inlet and outlet samples, respectively. The solid lines are for the third degree polynomials which were fit by the least squares method. It is obvious that the inflection of the curves between about 1.5 and 2.5 μmA is not physically realistic and that lines with continuously positive slopes are to be expected. The fits at smaller particle diameters are better, however, and this is the more crucial region in view of our primary interest in fine particles.

Particle Penetration

Particle penetration was computed by the following two methods:

1. The third order polynomials describing the inlet and outlet cumulative concentration distributions were differentiated and the ratio of first derivatives with respect to particle diameter was computed at several values of diameter. The ratio of outlet to inlet derivatives is, as discussed in the section on the computation method, the penetration at that particle diameter.
2. The slopes of eyeball fit curves for the points in Figures 6-2 and 6-3 were measured by a graphical technique at several values of particle diameter. The ratios of outlet to inlet slopes were computed to yield penetrations at the several diameter values.

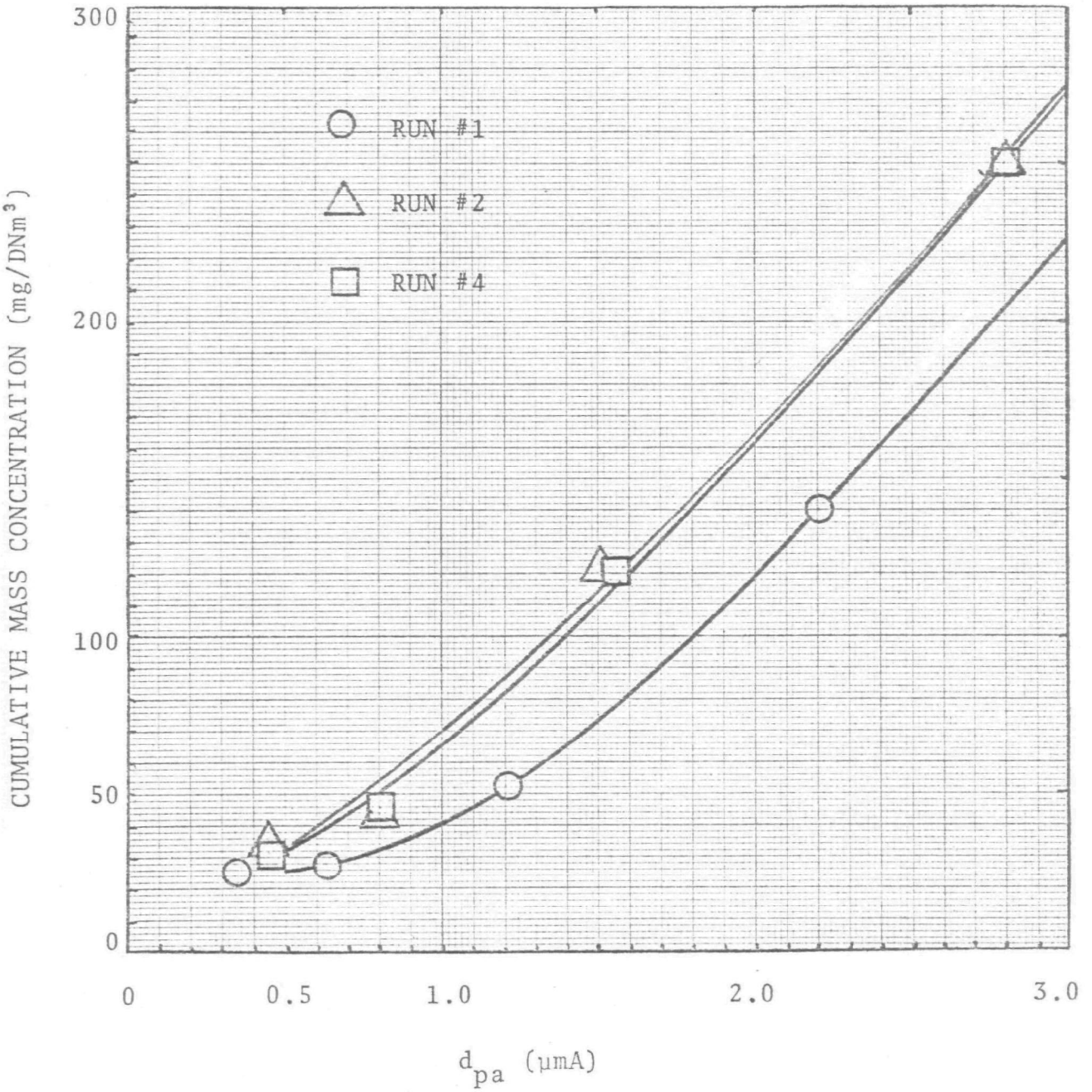

Figure 6-2 - Inlet cumulative mass concentration distribution.

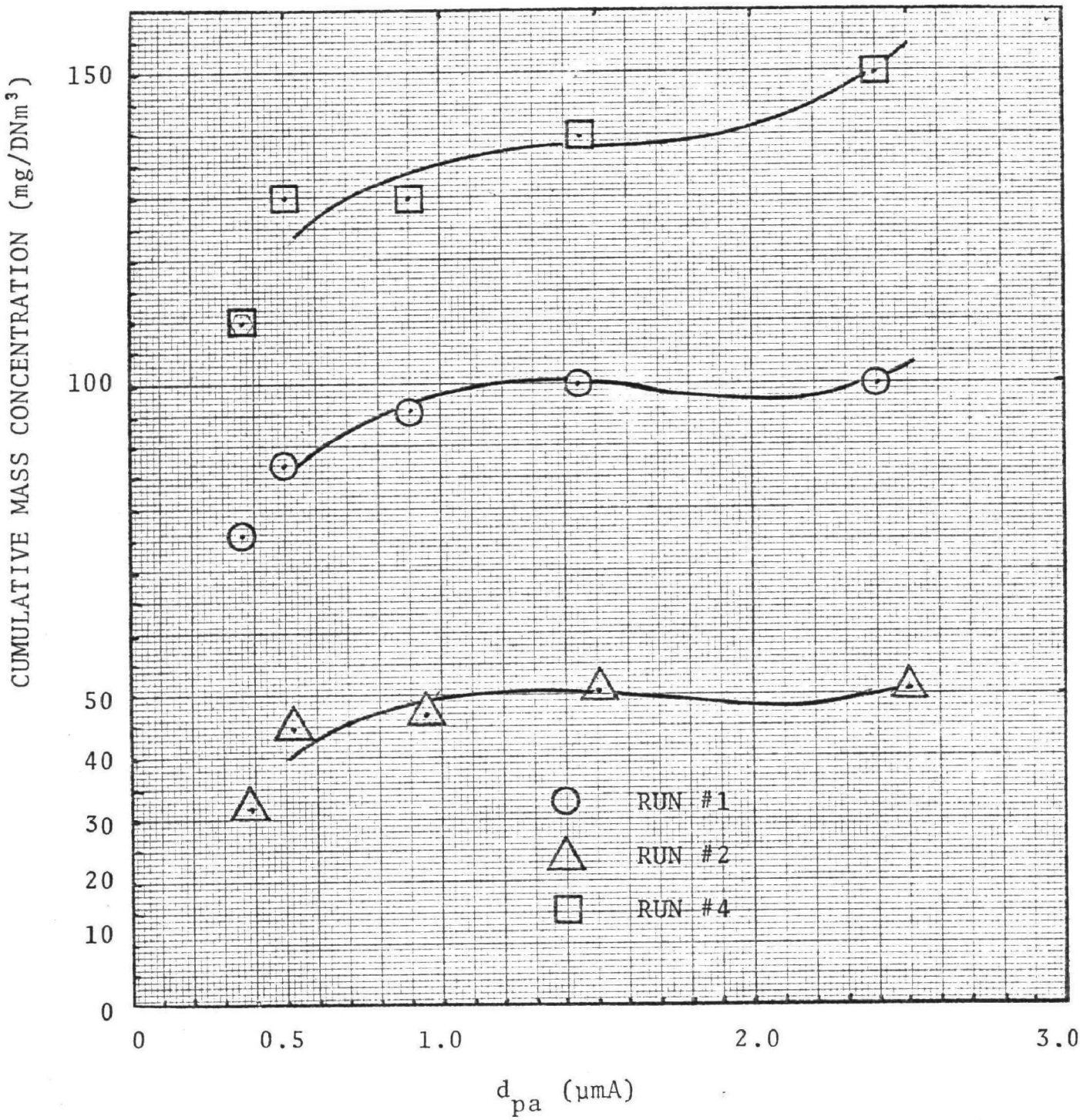

Figure 6-3 - Outlet cumulative mass concentration distribution.

Penetrations computed by the two methods are plotted against particle diameter (aerodynamic) in Figure 6-4. It can be seen that the two methods are in close agreement below about 1.0 μmA particle diameter. We are more inclined to trust the penetrations based on the eyeball fits; especially those for runs #1 and #2. The unbelievably high plateau for the run #4 dashed curve is due to the high concentration at 2.4 μmA, as Figure 6-3 shows.

ECONOMICS AND OPERATING PROBLEMS

Several points relating to the economics and operating problems for the scrubber system are listed below:

1. The initial capital cost of the scrubber system including mechanical equipment, stack and erection costs but excluding ash ponds, development costs since initial operation, environmental monitoring and Owners' cost was $8,247,600. Subsequent development work and modifications have increased this amount significantly.
2. Maintenance labor was estimated to require about four men on three shifts. Operating labor requires less than one man per shift.
3. The boiler had been kept on line in recent months at about 65% load factor and plant personnel were hopeful that this would continue to improve.
4. There have been serious problems due to solids accumulation on the scrubber above the plumb bob, in the scrubber bottom (from material falling from higher points), and on the fans. Deficiencies in the fan wash system during initial stages of operation resulted in fan buildup problems. However the wash system was modified in June 1973 and problems with buildup on the fan since that time have been minimal.

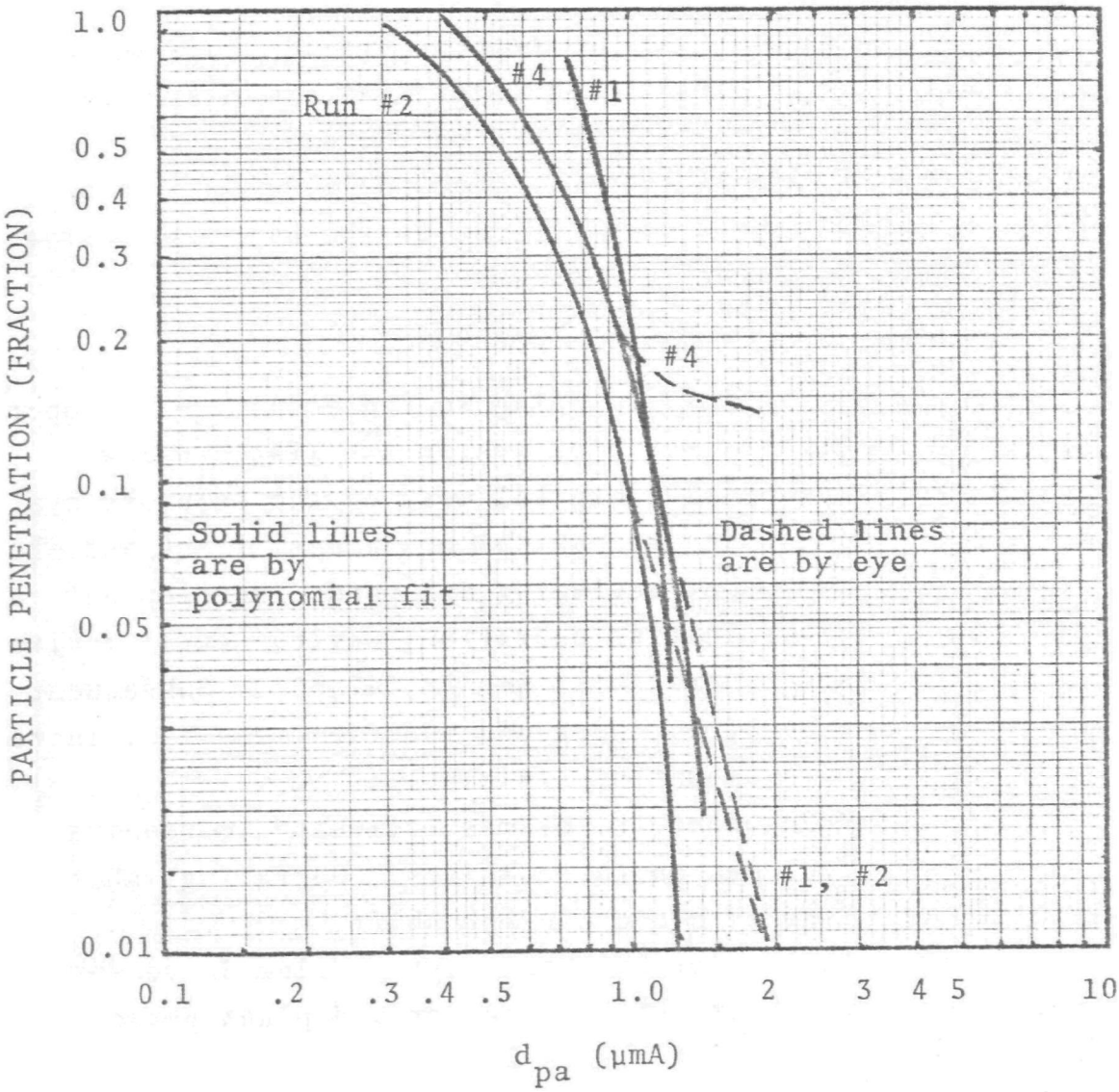

Figure 6-4 - Particle penetration versus aerodynamic diameter.

5. During the period the tests were conducted, lime was added to the pond return at a rate of about 100 lb/hr. However, this proved unsuccessful as a means of reducing scale formation. As a result, lime addition to the pond return was discontinued and lime is now added to each vessel at rates of up to 1000 lb per hour per vessel in an attempt to reduce scaling. Thus far, there has been only limited success in scale reduction through lime injection. The relative benefits of lime addition are still under investigation.
6. Operating experience has indicated that entrainment separation has been satisfactory although dust does collect in the demisters. However, this is attributable to problems with the demister wash system and the scaling tendency of the system; not to poor entrainment separation. The ID fans have to be run with wash water to prevent deposits and unbalancing. The need for wet fans was anticipated and included in the original design. However, entrainment is not necessarily responsible for the dust buildup on the fans. The plant management believe it is likely due to penetration of the scrubber by fine particles and subsequent deposition on the fan due to compression and condensation of the water vapor in the gas stream as it passes through the fan. Problems encountered with buildup on the fan blades during the initial stages of operation (prior to June of 1973) were corrected by modifying the original fan wash system. Experience with the fan wash system has shown that spray nozzles are necessary and are being used to introduce the fan wash water into the fan inlet gases.

7. The slurry pumps last about 1.5 years, pumping 2% solids at about 2 or 3 atm. (30-40 psi) pressure.
8. The scrubber system uses about 1.7% of the gross power (i.e., about 6 M.W.).

VENTURI MODEL

Venturi scrubber performance for the conditions of this test was predicted by means of the method described in the "Scrubber Handbook". Because gas velocity in the throat is not known, it was necessary to compute a throat velocity from the liquid to gas ratio (1.75 ℓ/m^3) and the pressure drop. The use of SHB equation (5.3.6-10) gives a velocity of 38 m/sec (125 ft/sec) but this will be lower than actual because the equation predicts pressure drop about 15% high. Consequently, the throat velocity would probably be around 42 m/sec (138 ft/sec), corresponding to a predicted pressure drop of 30 cm W.C.

The design equation (SHB 5.3.6-5) includes an empirical constant, f, which has a value of about 0.25 for hydrophobic materials and about 0.5 for hydrophyllic. Penetrations were predicted for 1.75 ℓ/m^3, 42 m/sec; with f = 0.25, f = 0.4, f = 0.45 and f = 0.5 and some of the results are tabulated below and plotted on Figure 6-5:

PREDICTED CUT DIAMETER FOR
COMBINATIONS OF "f" AND "ΔP"

	d_{pc} at f =		
	0.25	0.4	0.5
ΔP = 20 cm W.C.	1.5 μmA	1.1 μmA	0.95 μmA
ΔP = 200 cm W.C.	0.52 μmA	0.37 μmA	0.29 μmA

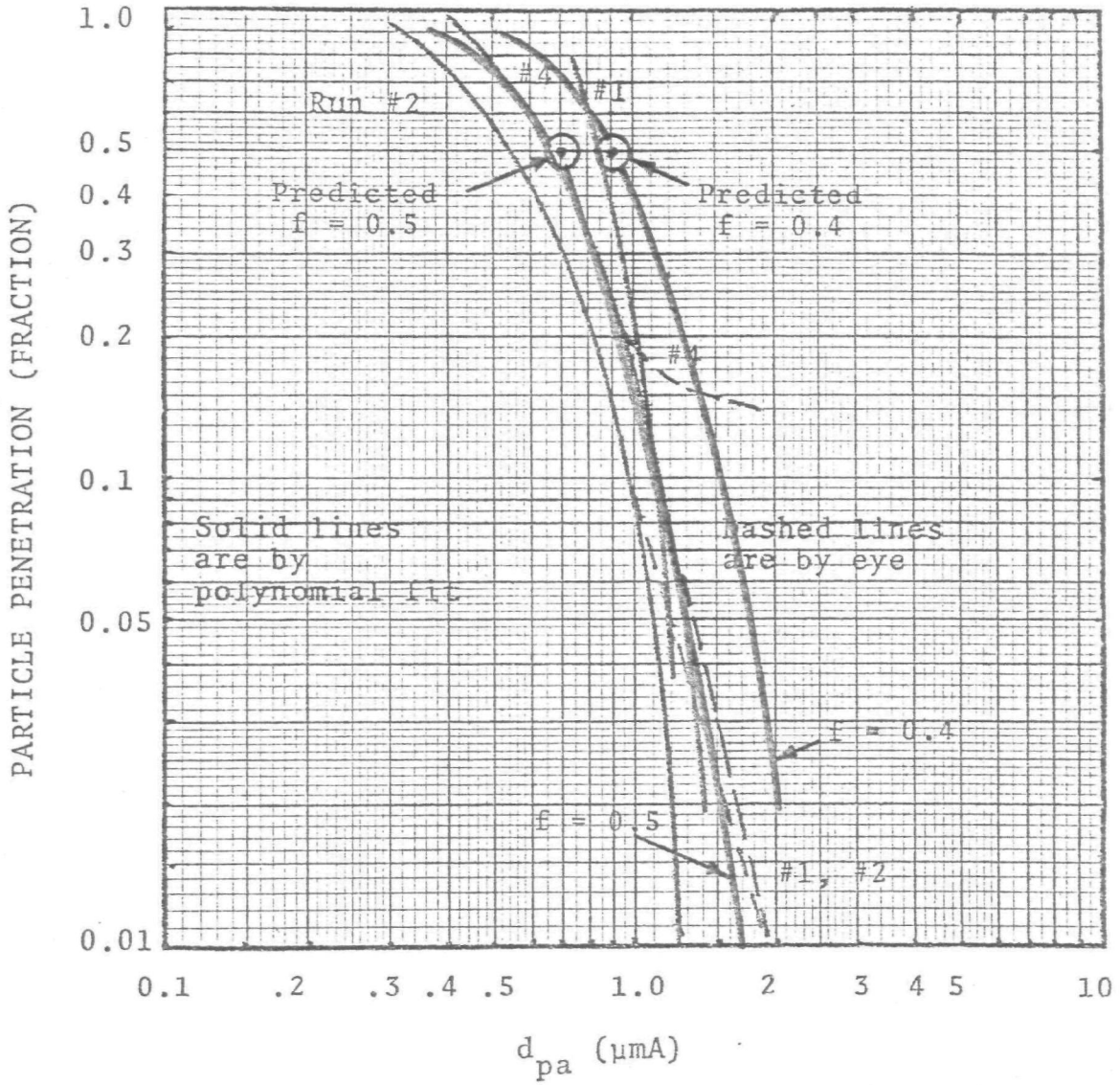

Figure 6-5 - Predicted and experimental penetrations for venturi.

PREDICTED* PENETRATION AT SEVERAL RATIOS OF PARTICLE TO CUT DIAMETER

Pt	0.99	0.95	0.90	0.7	0.5	0.2	0.1	0.05	0.01
d_{pa}/d_{pc}	0.3	0.44	0.54	0.78	1.0	1.4	1.6	1.9	2.4

*for 1.75 ℓ/m^3

Figure 6-5 is an overlay of two prediction lines on Figure 6-4, which presented the experimental data. It can be seen that the prediction for f = 0.4 has a cut diameter of 0.9 μmA and the curve is generally higher than the experimental results. Apparently a value of f = 0.5 is about right for the experimental data because it yields a cut diameter of about 0.7 μmA.

CONCLUSIONS

Particle penetration data based on the measurements made in this test appear to be reliable and the agreement among the three runs is fairly good. The venturi scrubber performance is good while it is running but operating problems have caused the scrubber system to be inoperative about 1/3 of the time. Solids accumulation has been the major cause of unreliability.

Sampling apparatus failures and deficiencies which were experienced in this test have led to our subsequent development of improvements.

Considering all of the uncertainties in the model and the experimental data, the agreement between experiment and prediction is good. It is reasonable that the fly ash acts like a hydrophyllic material because of the presence of sulfur oxides and the consequent high wettability of the particle surface. Because the contact time in the venturi is short and the particles do not have much opportunity for growth before entering the collection zone, one would not expect flux force/condensation effects to be very pronounced.

APPENDIX 6-A
PARTICLE AND COAL DATA

Table 6-A-1. COAL ANALYSIS (AS RECEIVED)

Day	Moisture %	Volatile Matter %	Fixed Carbon %	Ash %	kcal/kg	Sulfur %
15	27.8	34.2	29.2	8.8	4212	.37
16	27.7	31.1	29.3	11.9	4081	.37
17	28.4	31.6	26.5	13.5	4048	.41
18	28.4	31.1	33.5	6.9	4252	
19	27.6	30.5	32.8	9.1	4150	
20	27.6	29.9	31.3	11.2	4116	
21	27.8	29.7	32.1	10.4	4150	
22	29.0	31.2	33.4	6.4	4270	
23	28.2	31.3	32.2	8.3	4664	
24	26.0	33.2	27.6	13.1	4148	
25	34.7	30.1	25.2	10.0	3993	
26	29.6	31.3	30.0	9.1	4200	
27	29.3	31.3	29.3	10.1	4168	
28	28.5	31.8	29.6	10.1	4343	
29	NO SAMPLE					
30	29.0	31.1	30.6	9.3	4304	

Table 6-A-2. INLET AND OUTLET SAMPLE PARTICLE DATA FOR RUN #1

INLET		OUTLET	
W_{cum}* (mg)	d_{pc}** (μmA)	W_{cum} (mg)	d_{pc} (μmA)
562.9	27.0		
348.0	12.0		
148.5	5.7	5.8	2.4
68.9	2.2	5.3	1.45
27.1	1.2	5.1	0.9
10.0	0.63	4.8	0.5
5.1	0.34	4.5	0.36
4.8	Filter	3.9	Filter
Sample Volume (DN m^3)	0.19	0.051	

NOTES:

* W_{cum} = Cumulative mass collected on that stage and those below.

**d_{pc} = Cut diameter (aerodynamic) for that stage.

Table 6-A-3. INLET AND OUTLET SAMPLE PARTICLE DATA FOR RUN #2

INLET		OUTLET	
W_{cum} (mg)	d_{pc} (μmA)	W_{cum} (mg)	d_{pc} (μmA)
421.0	33.0		
240.0	15.0		
103.0	7.0	3.6	2.5
56.9	2.8	3.5	1.5
27.7	1.5	3.5	0.95
13.5	0.8	3.2	0.52
4.9	0.44	3.0	0.38
3.9	Filter	2.0	Filter
Sample Volume (DN m^3)	0.11	0.067	

Table 6-A-4. INLET AND OUTLET SAMPLE PARTICLE DATA FOR RUN #4

INLET		OUTLET	
W_{cum} (mg)	d_{pc} (μmA)	W_{cum} (mg)	d_{pc} (μmA)
548.0	34.0		
226.0	15.0		
108.0	7.0	10.8	2.4
54.8	2.8	10.6	1.5
26.6	1.6	10.1	0.9
12.5	0.8	9.7	0.5
5.0	0.45	9.1	0.36
3.5	Filter	8.2	Filter
Sample Volume (DN m^3)	0.11	0.072	

APPENDIX 6-B
PARTICLE SIZE DISTRIBUTION PLOTS

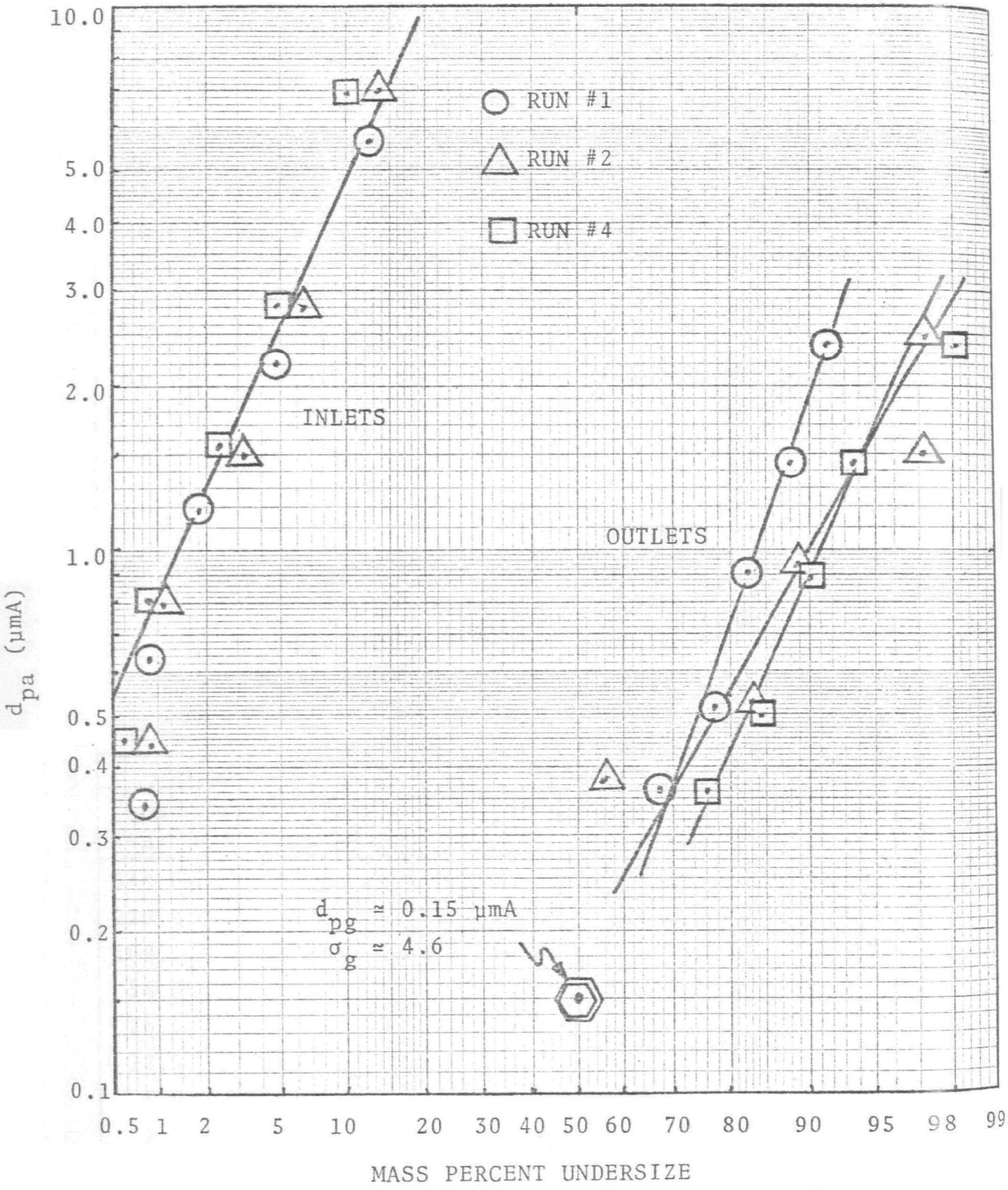

Figure 6-B-1 - Inlet and outlet particle size distributions (log-probability).

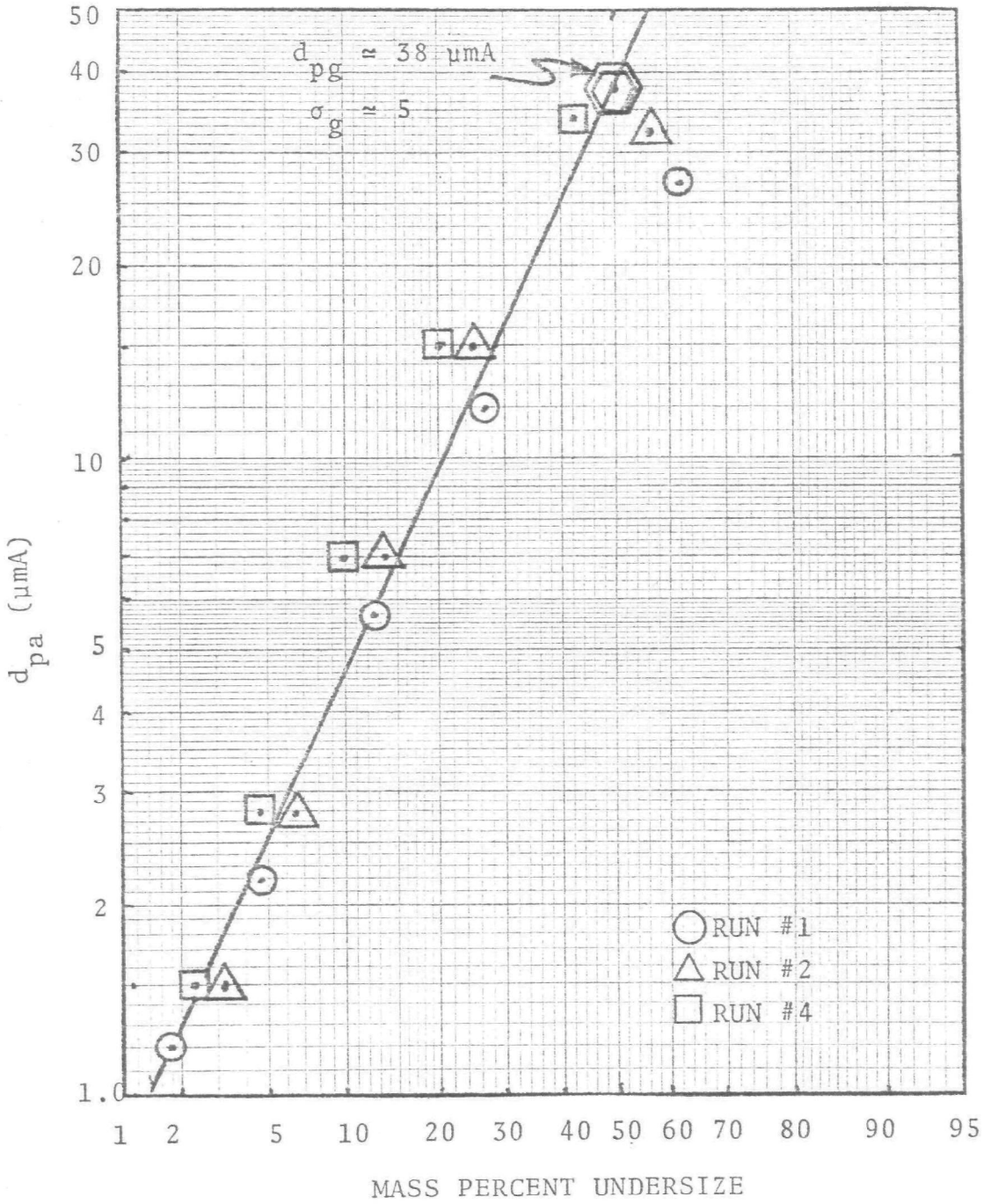

Figure 6-B-2 - Inlet particle size distribution (log-probability)

WETTED FIBROUS FILTER ON SALT DRYER

SOURCE AND SCRUBBER

A 1,700 m^3/min wetted fiber scrubber designed by Encont Corporation was chosen for the sixth scrubber performance test.

The scrubber is installed to clean exhaust gas from two salt dryers, one K.D. Mill and one Vacuum Mill device. The larger size dryer dries 45 tons per hour common salts. This dryer is equipped with one Sturtevant Planovane size 60, 382 m^3/min (13,500 CFM) @ 4.8 cm W.C. and 735 RPM exhauster. The dried salts are supplied to the K.D. Mill system. The smaller salt drier dries 15 TPH salts and is equipped with Sturtevant Planovane size 50, 140 m^3/min (5,000 CFM) @ 5.1 cm W.C., 600 RPM exhauster. The dried salts are supplied to the Vacuum Mill equipment. The exhaust gas from this equipment is collected by means of tunnel collectors and supplied to the scrubber. There is one induce draft fan at the outlet of the scrubber. The fan was made by Buffalo Forge Co. It is model 890H-36 rated at 1,440 m^3/min (51,000 CFM) @ 41 cm W.C., 1,420 RPM with dish control damper.

This scrubber has two filter pads, each containing three layers of plastic filter medium in its inlet duct. Following these is one entrainment separator, which is made from the same type of materials as the inlet filter pad, see Figure 7-1. Originally, this scrubber was equipped with two layers of entrainment separators, but later the scrubber user learned that the efficiency was higher with one pad.

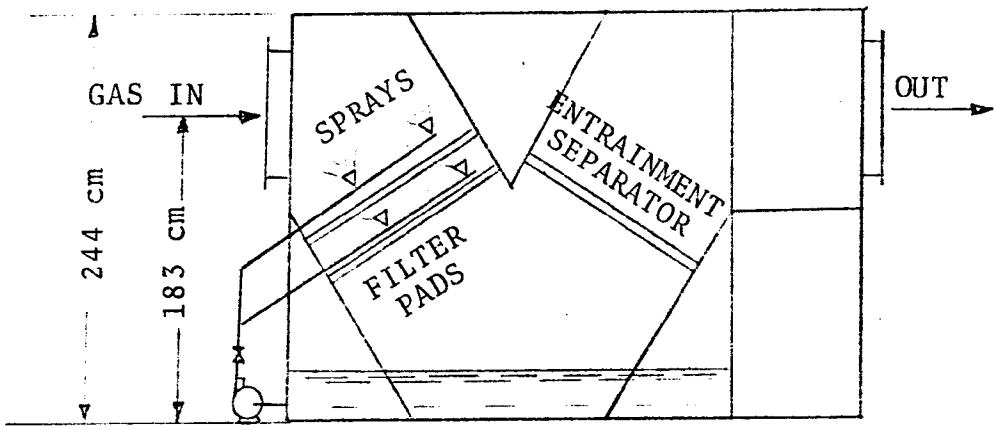

ELEVATION

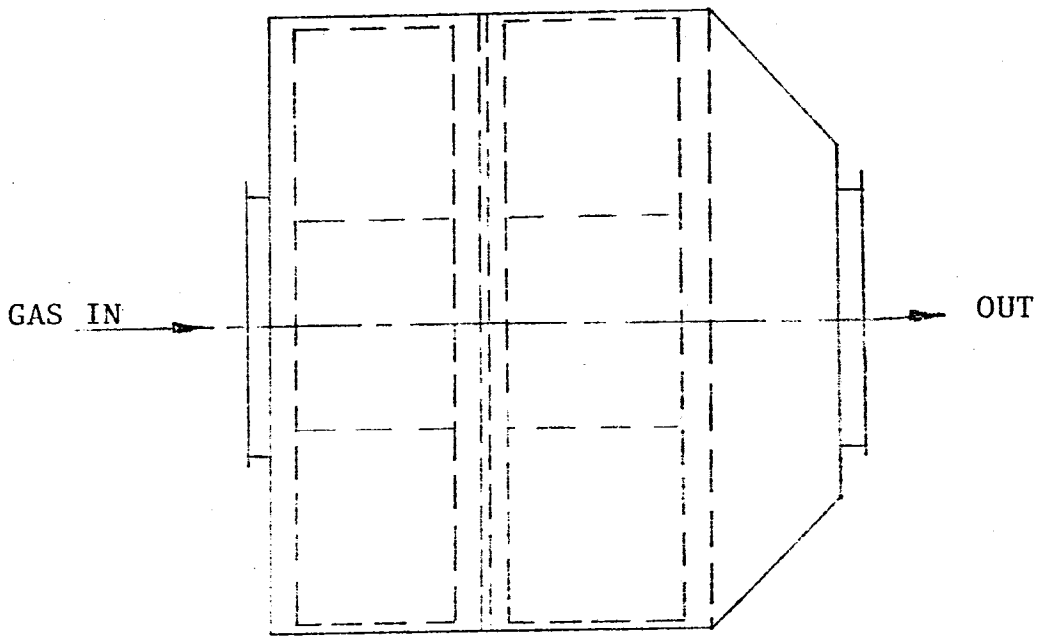

PLAN

Figure 7-1 - Schematic Diagram of Wet Fiber Scrubber

Water is sprayed onto the filter media by means of 18 nozzles. The flow rate of the water is approximately 0.38 m^3/min (100 GPM) under a pressure of 1.76 Kg/cm^2 (25 psi). The sprayed water is collected at the bottom of the scrubber and resupplied to the spray nozzles. Due to entrainment, 0.019 - 0.038 m^3/min (5-10 GPM) of water is added to the scrubber to make up the losses.

TEST METHOD

Determination of particle size distribution and concentration (loading) in the inlet and outlet of the scrubber provides the basis for computation of performance characteristics. A modified EPA sampling train with in-stack University of Washington Mark III cascade impactor was used for particle measurements. Greased aluminum foil substrates were used on each of the collection plates of the impactors. 47 mm Gelman type "A" binderless glass fiber filters were used in the impactor as backup filters.

Substrates for the impactor plates were cut out of thick aluminum foil. A 20% solution of silicone vacuum grease in benzene was prepared. Drops of this solution were placed on the substrates with an eye dropper. It was then evenly spread out on the substrates with a policeman, taking care that it did not spread to the bottom of the substrates. These were then placed in aluminum foil storage cups and heated in an oven for two hours at 200°C. Then they were cooled and stored in a desiccator for about 10 hours. Prior to each run, the substrates and filter were removed from the desiccator, weighed with the storage cups and loaded in the impactors.

Both impactors in the inlet and outlet ducts were kept at one position during the entire sampling period. The location of the impactor was chosen such that the gas velocity at that location is close to the average gas velocity in the duct. The sample flow rate was also fixed during runs.

An in-line precutter was used on the outlet runs to prevent entrained liquid drops from entering the impactor. The impactors were heated above the stack gas temperature with heating tapes. A thermocouple was placed in the inlet sampling probe downstream of the impactor. The impactor heating was controlled with a variac such that the thermocouple reading was about 10°C above the stack gas temperature. Sample flow rates were measured with the usual EPA train instrument so as to obtain isokinetic (or near isokinetic) sampling.

Scrubber inlet and outlet gas duct temperatures were measured by mercury filled glass bulb thermometers. Gas temperature at the sampling location was measured during each test run. The inlet and outlet stack pressures were measured with a U-tube manometer. Barometric pressures were determined before each run from an anaroid barometer. The stack gas humidities were measured by dry and wet bulb thermometers. Gas flow rate was determined by means of a calibrated S-type pitot tube traverse. The inlet gas flow rate was determined from 49 point pitot tube traverses in the 0.8 m x 1.8 m duct. The outlet gas flow rate was determined similarly from 48 point pitot traverses in the 1.1 m x 1.3 m duct.

The scrubber liquid temperature was measured at the recirculating pump with a mercury filled glass bulb thermometer. The inlet liquid line pressure was measured

with a pressure gauge. The flow rate was then determined from the spray nozzle characteristics as reported by the manufacturer.

OPERATING CONDITIONS

The scrubber operating conditions during the test period were as follows:

1. Gas flow rates and conditions were as shown in the tabulation below:

Gas Parameters	Inlet	Outlet
Temperature	38°C (100°F)	32°C (90°F)
Pressure during pitot run	-11 cm WG	-30 cm WG
A m^3/min	1,590	1,630
ACFM	56,300	57,400
DN m^3/min	1,360	1,410
DSCFM	50,190	52,550
% Vol. H_2O vapor	5.8	4.7%

2. Liquid parameters were listed in the following table.

Liquid Parameters	Inlet	Outlet	Makeup
Temperature	32°C	32°C	15°C
Pressure	1.76 Kg/cm^3	—	—
m^3/min	0.38	0.35	0.019 - 0.038
GPM	100	90	10
Suspend Solids	—	—	—
Dissolved Solids	—	—	—
Treatment	None	None	—

3. Entrainment is known to be excessive but was not measured in this test series. Water balance data provided by the plant indicate an entrainment flow rate out of the scrubber of about 0.019 - 0.038 m^3/min (5-10 GPM).

PARTICLE DATA

A total of 10 simultaneous sampling runs were conducted. Runs #1 and #2 were purged due to severe entrainment problems. The remaining 8 runs were grouped into two data sets (Runs #3-5 as set "A" and Runs #6-10 as set "B") corresponding to different impactor locations in duct cross-section.

The particle concentration and size data which were obtained in this performance test are presented in Tables 7-A-1 through 7-A-8. Figures 7-B-1 and 7-B-2 show log-probability plots of inlet and outlet particle size distributions for data sets A and B respectively. There are some variations in particle sizes. This is mainly due to the unsteady nature of the milling and drying processes. The mass median diameter and geometric standard deviation for these sampling runs are listed in the following table.

Run No.	INLET		OUTLET	
	d_{pg}, μmA	σ_g	d_{pg}, μmA	σ_g
3	5.2	3.2	0.23	2.3
4	2.05	2.1	0.31	2.4
5	4.25	2.2	0.34	3.8
6	3.7	2.4	0.46	2.8
7	10	4.8	0.46	2.8
8	10	4.8	0.46	2.8
9	10	4.8	0.96	2.3
10	10	4.8	1.4	1.8

Cumulative mass concentration was plotted against aerodynamic particle size to yield Figures 7-C-1 to 7-C-8.

PARTICLE PENETRATION

The ability of a scrubber to control particulate emissions is interpreted in terms of "grade efficiency" curves, which are plots of particle collection efficiency, or particle penetration versus particle diameter. The eyeball judgement was used here rather than the least squares method because we could not find a simple function that would fit the experimental data. The slopes of the eyeball fit curves in Figures 7-C-1 to 7-C-8 were measured by a graphical technique at several values of particle diameter. The ratios of outlet to inlet slopes were computed to yield penetrations at the several diameter values. The results were plotted in Figures 7-2 and 7-3.

ECONOMICS AND OPERATING PROBLEMS

The approximate installation cost of the scrubber, including the costs of blower and duct work is $60,000. The annual power cost is approximately $13,000 and the annual maintenance cost is estimated at $1,000.

There are no unusual operating problems.

MATHEMATICAL MODEL

A method of performance prediction for a dry filter bed was presented in the "Scrubber Handbook: (Calvert et al 1972). In the following treatment, as recommended in the Handbook, we will assume that collection efficiency for the dry fibers is not affected by the presence of washing water.

The "Scrubber Handbook" (S.H.B.) gave the following equation for the prediction of penetration of a bed of clean fibrous packing on particles of a specified size.

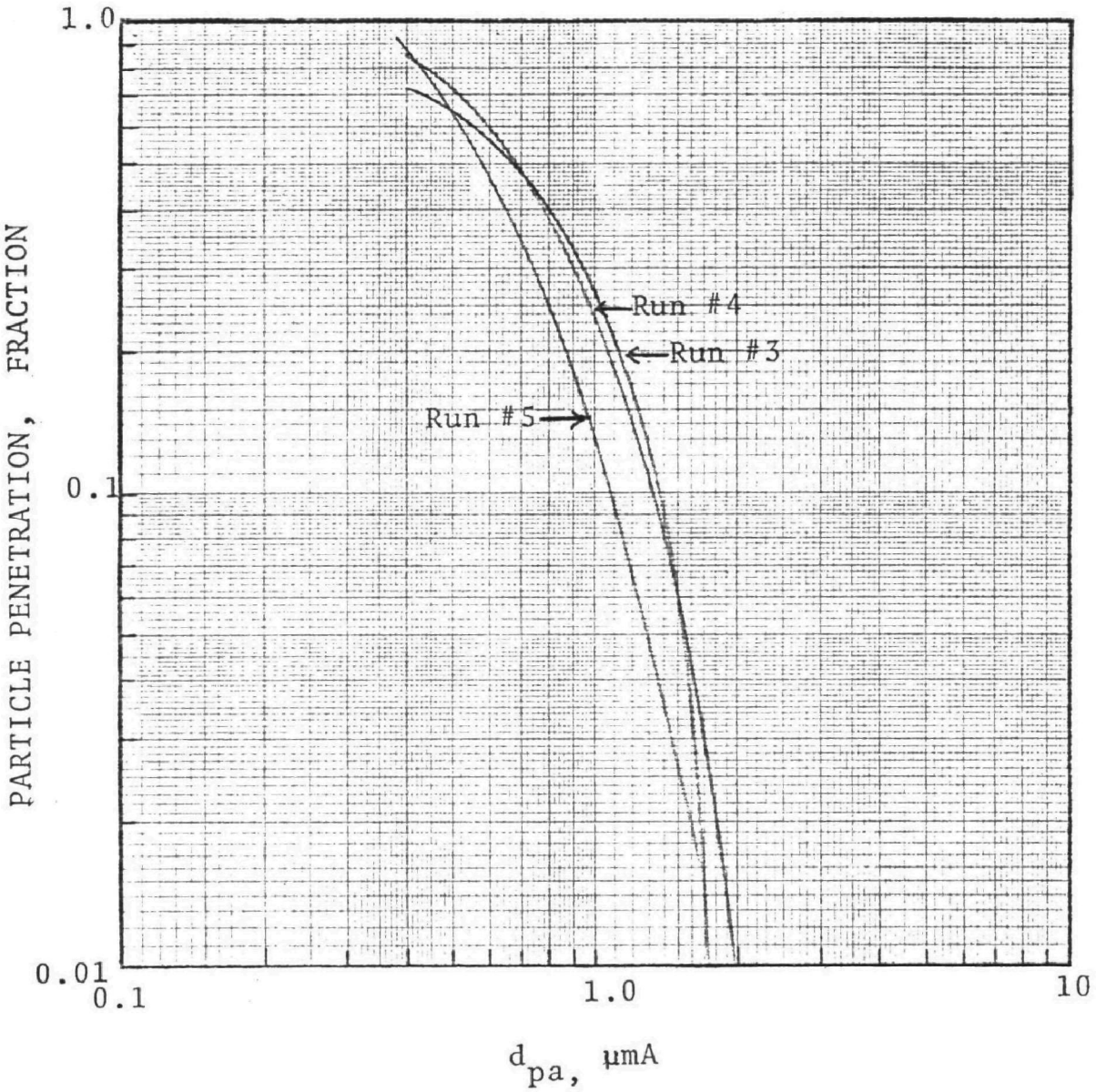

Figure 7-2 - Penetration versus particle diameter (data set "A")

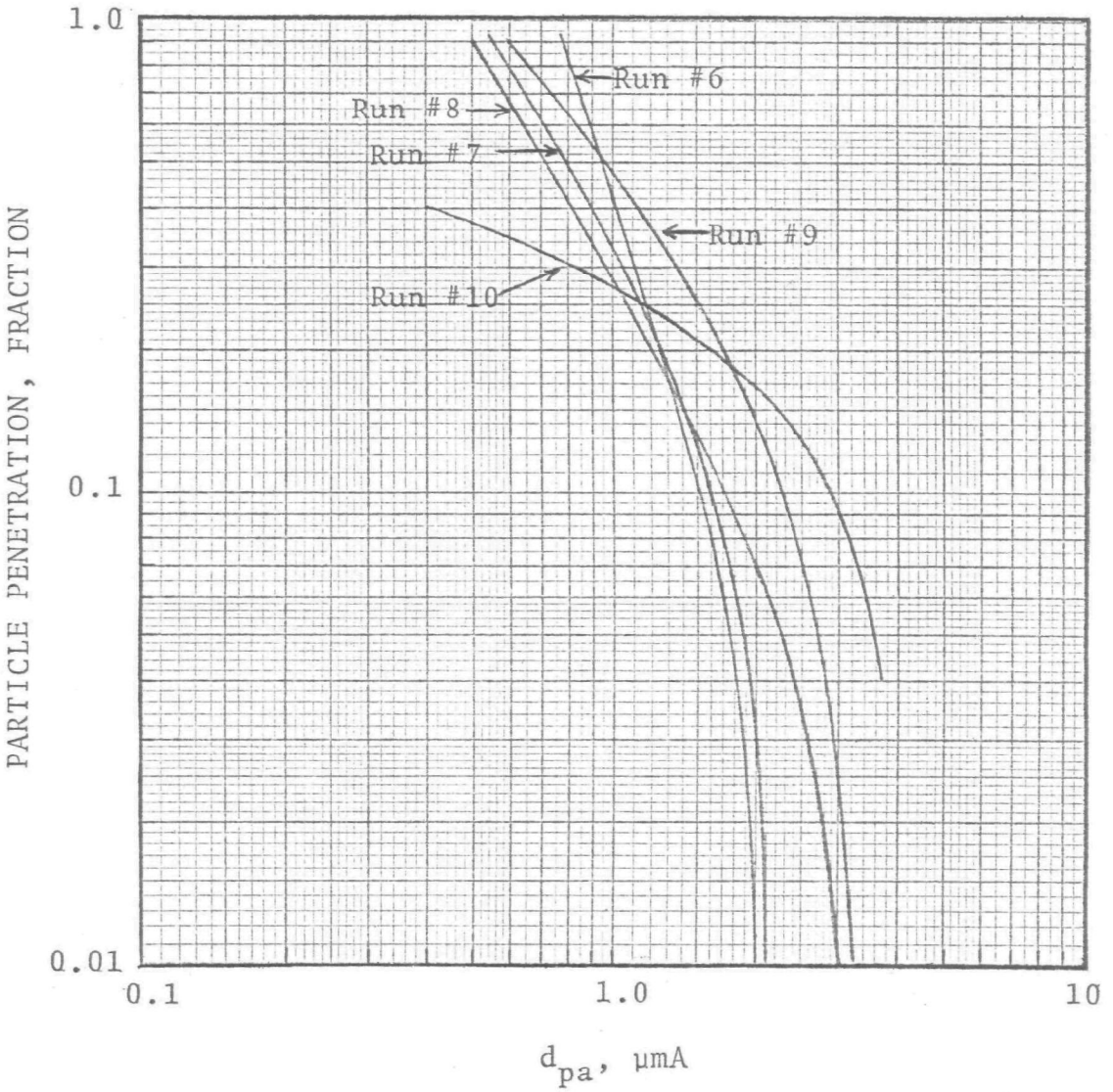

Figure 7-3 - Penetration versus particle diameter (data set "B")

$$Pt = 1 - E = \exp(-\eta_s S) \qquad (7\text{-}1)$$

(S.H.B. Eq. 3.4-1)

where, S is the solidarity factor of the filter bed and

η_s is the effective collection efficiency of a single fiber by all collection mechanisms.

Based on the fiber pad sample obtained from the scrubber user, the filter pad solidarity factor, S, was estimated to be 1. There were six layers of this pad in the inlet filter bed. Therefore, the total solidarity factor for the filter bed was 6.

In this scrubber, impaction was the most important collection mechanism, so that we assumed impaction was the only unit mechanism occuring in the filter bed.

The fibers in the filter pad were ellipsoid in shape with longer axis normal to direction of gas flow. Its collection efficiency should lie somewhere between the collection efficiencies of a ribbon and a cylinder.

Penetration was predicted for ribbon and cylinder with U_o = 1.8 m/sec (undisturbed upstream air velocity) and the results were plotted on Figures 7-4 and 7-5. Experimental results were also plotted on these figures. It can be seen that the penetration for a ribbon fiber has a cut diameter of 1 μmA and is close to the experimental average of around 0.75 μmA. For cylinder fiber, the predicted cut diameter was about 1.5 μmA which was two times larger than the experimental value.

Particle size data presented in Tables 7-A-1 through 7-A-8 were for dry particles because impactors are heated. The theoretical prediction was accordingly based on dry particles. However, in actual scrubber operation, particles were wet and common salt particles were highly hygroscopic. According to Junge (1963), the radius of the particle will increase to about five times that of the dry salt particle at

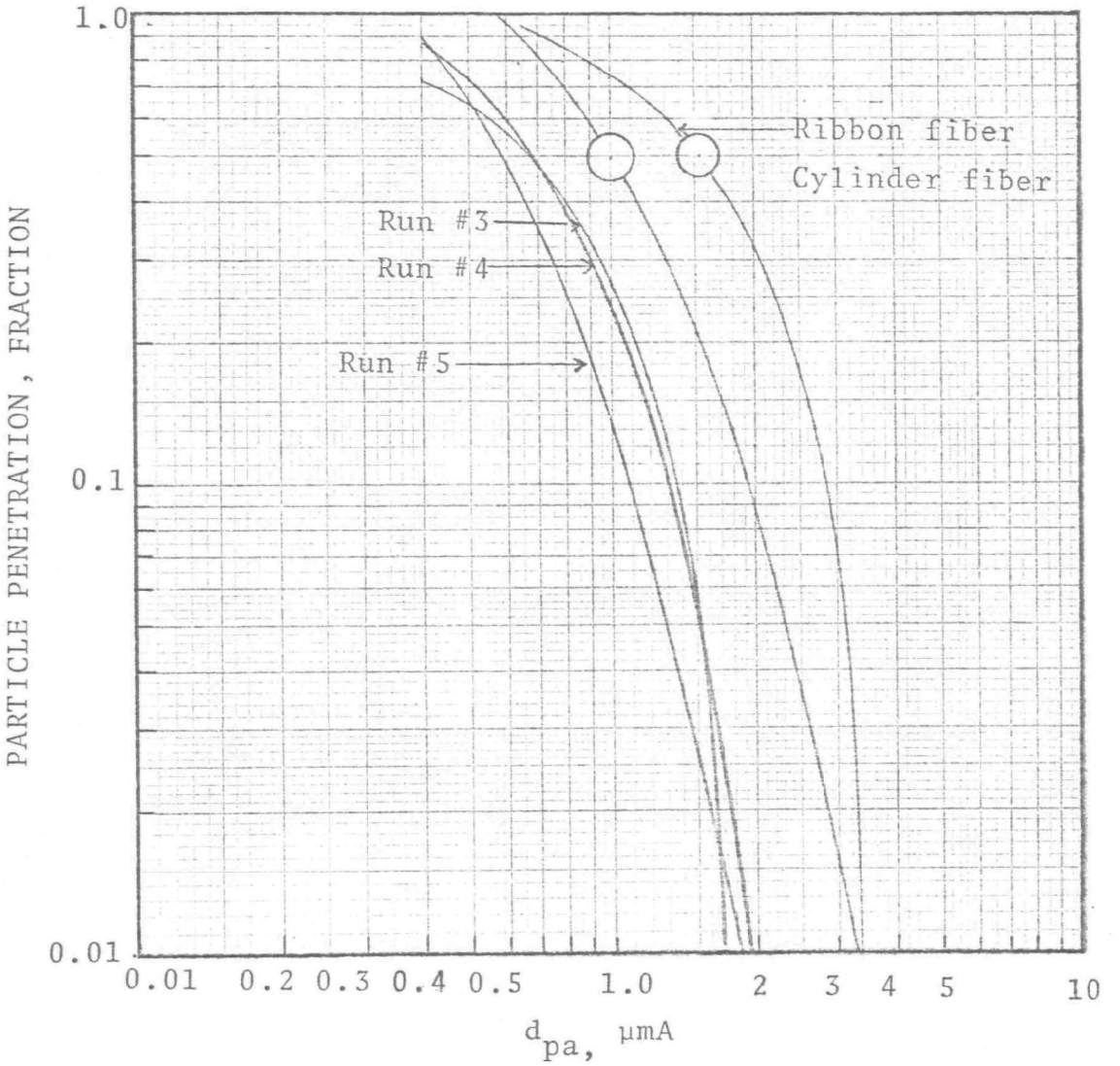

Figure 7-4 - Predicted and experimental penetrations for fiber filter bed (data set "A")

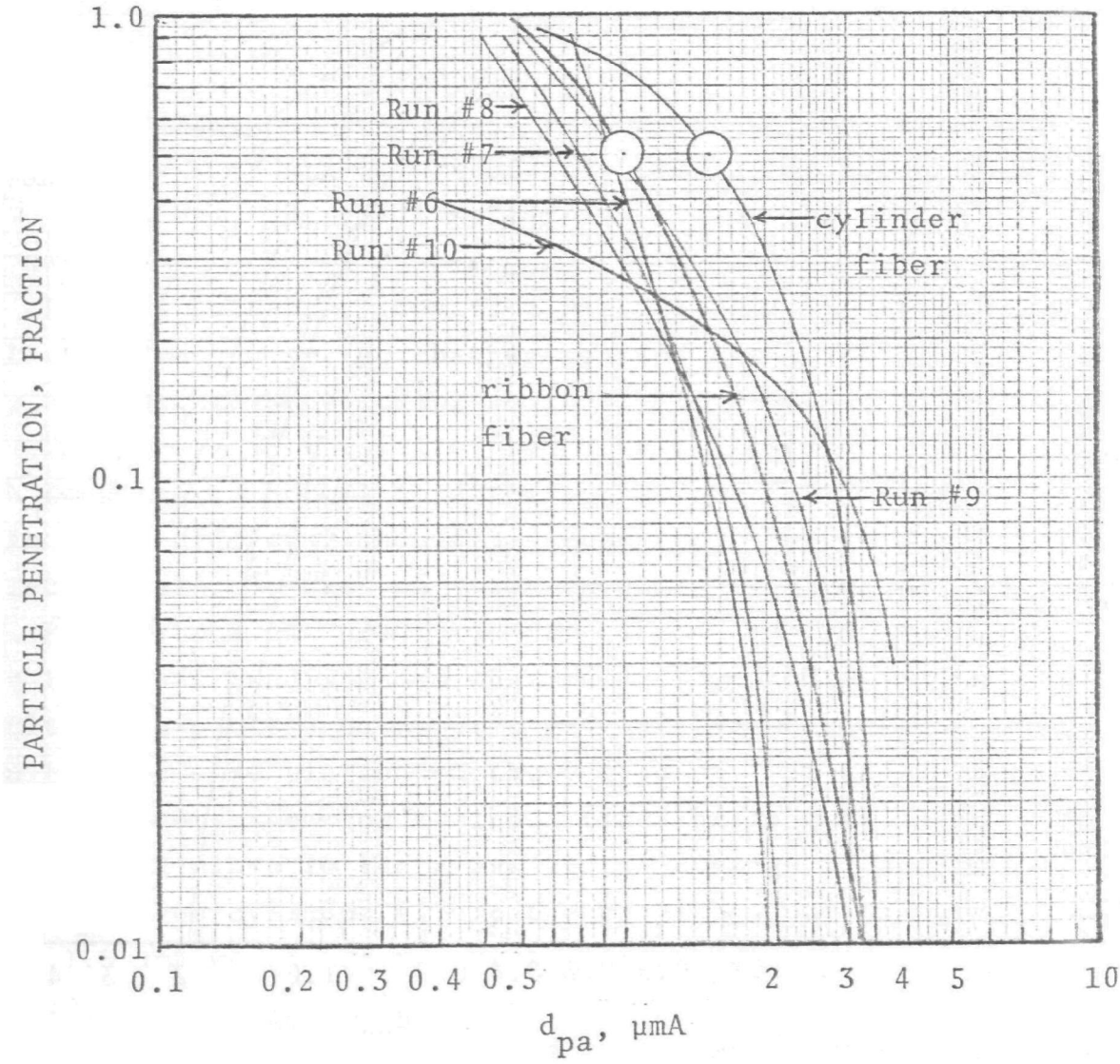

Figure 7-5 - Predicted and experimental penetration for fiber filter bed (data set "B")

high humidity and about double at 75% relative humidity. The predicted cut diameters are about two times higher than the measured ones (for cylinders). This seems consistent with Junge's prediction for NaCl particles.

It is reasonable the predicted cut diameter will have a lower value when we take into account other collection mechanisms. Even if we ignore these mechanisms and based on impaction alone, the agreement between experiment and prediction is good.

CONCLUSIONS

The wetted fiber scrubber performs satisfactorily for this application and presents no substantial operating problems. Particle collection is enhanced by growth due to the condensation of water. Performance prediction by means of the mathematical model for fibrous filters is satisfactory if particle growth is taken into account. Better prediction of penetration would be possible if one could predict particle growth with more accuracy for hygroscopic materials.

APPENDIX 7-A
PARTICLE DATA

TABLE 7-A-1 - INLET AND OUTLET SAMPLE PARTICLE DATA FOR RUN #3

IMPACTOR STAGE NUMBER	INLET		OUTLET	
	W_{cum} (mg)	d_{pc} (μmA)	W_{cum} (mg)	d_{pc} (μmA)
1	19.0	27		
2	14.7	11.8		
3	14.1	5.55		
4	10.6	2.2		
5	1.6	1.22	4.2	1.18
6	1.4	0.64	4.1	0.63
7	0.9	0.36	3.6	0.35
Filter	0.7		3.2	
Sample Volume (DNm^3)	7.889		20.247	

TABLE 7-A-2 - INLET AND OUTLET SAMPLE PARTICLE DATA FOR RUN #4

IMPACTOR STAGE NUMBER	INLET		OUTLET	
	W_{cum} (mg)	d_{pc} (μmA)	W_{cum} (mg)	d_{pc} (μmA)
1	10.8	26.5		
2	10.8	11.5		
3	10.7	5.4		
4	9.9	2.17	5.0	2.35
5	4.4	1.2	4.9	1.3
6	2.2	0.63	4.8	0.7
7	1.1	0.36	4.0	0.39
Filter	0.8		3.3	
Sample Volume (DNm^3)	8.689		20.7	

TABLE 7-A-3 - INLET AND OUTLET SAMPLE PARTICLE DATA FOR RUN #5

IMPACTOR STAGE NUMBER	INLET		OUTLET	
	W_{cum} (mg)	d_{pc} (μmA)	W_{cum} (mg)	d_{pc} (μmA)
1	15.2	26.5		
2	14.6	11.5		
3	13.6	5.6	2.1	5.8
4	9.8	2.2	2.0	2.35
5	2.9	1.2	2.0	1.3
6	0.8	0.64	1.7	0.7
7	0.4	0.35	1.4	0.38
Filter	0.3		1.4	
Sample Volume (DNm^3)	8.76		20.17	

TABLE 7-A-4 - INLET AND OUTLET SAMPLE PARTICLE DATA FOR RUN #6

IMPACTOR STAGE NUMBER	INLET		OUTLET	
	W_{cum} (mg)	d_{pc} (μmA)	W_{cum} (mg)	d_{pc} (μmA)
1	17.2	26.5		
2	16.3	11.8		
3	15.8	5.5		
4	12.5	2.2	2.9	2.25
5	4.2	1.23	2.7	1.25
6	1.3	0.64	2.5	0.66
7	1.1	0.36	1.8	0.37
Filter	1.0		1.5	
Sample Volume (DNm^3)	11.21		21.67	

TABLE 7-A-5 - INLET AND OUTLET SAMPLE PARTICLE DATA FOR RUN #7

IMPACTOR STAGE NUMBER	INLET		OUTLET	
	W_{cum} (mg)	d_{pc} (μmA)	W_{cum} (mg)	d_{pc} (μmA)
1	36.9	26.8		
2	18.5	11.7	5.1	12
3	18.1	5.5	5.0	5.7
4	15.6	2.2	5.0	2.25
5	7.0	1.22	4.9	1.28
6	2.9	0.64	4.4	0.67
7	1.3	0.36	3.0	0.38
Filter	1.0		2.4	
Sample Volume (DNm^3)	10.329		21.32	

TABLE 7-A-6 - INLET AND OUTLET SAMPLE PARTICLE DATA FOR RUN #8

IMPACTOR STAGE NUMBER	INLET		OUTLET	
	W_{cum} (mg)	d_{pc} (μmA)	W_{cum} (mg)	d_{pc} (μmA)
1	40.9	26.5		
2	24.6	11.6		
3	22.4	5.5		
4	17.3	2.18	7.3	2.25
5	6.4	1.22	6.9	1.28
6	2.4	0.64	5.7	0.67
7	0.8	0.36	4.6	0.38
Filter	0.6		3.6	
Sample Volume (DNm^3)	7.781		21.146	

TABLE 7-A-7 - INLET AND OUTLET SAMPLE PARTICLE DATA FOR RUN #9

IMPACTOR STAGE NUMBER	INLET		OUTLET	
	W_{cum} (mg)	d_{pc} (μmA)	W_{cum} (mg)	d_{pc} (μmA)
1	23	26.5		
2	14.7	11.7		
3	13.8	5.45		
4	8.4	2.2	5.7	2.25
5	3.7	1.22	4.9	1.25
6	1.2	0.64	3.1	0.67
7	0.3	0.355	1.9	0.37
Filter	0		0.9	
Sample Volume (DNm^3)	7.824		21.76	

TABLE 7-A-8 - INLET AND OUTLET SAMPLE PARTICLE DATA FOR RUN #10

IMPACTOR STAGE NUMBER	INLET		OUTLET	
	W_{cum} (mg)	d_{pc} (μmA)	W_{cum} (mg)	d_{pc} (μmA)
1	42	26.8		
2	27.3	11.7		
3	24.3	5.5	8.6	5.7
4	16	2.2	8.5	2.25
5	8.9	1.22	6.8	1.28
6	4.2	0.64	3.4	0.67
7	1.2	0.36	0.9	0.38
Filter	0.3		0	
Sample Volume (DNm^3)	7.88		21.40	

APPENDIX 7-B
PARTICLE SIZE DISTRIBUTION PLOTS

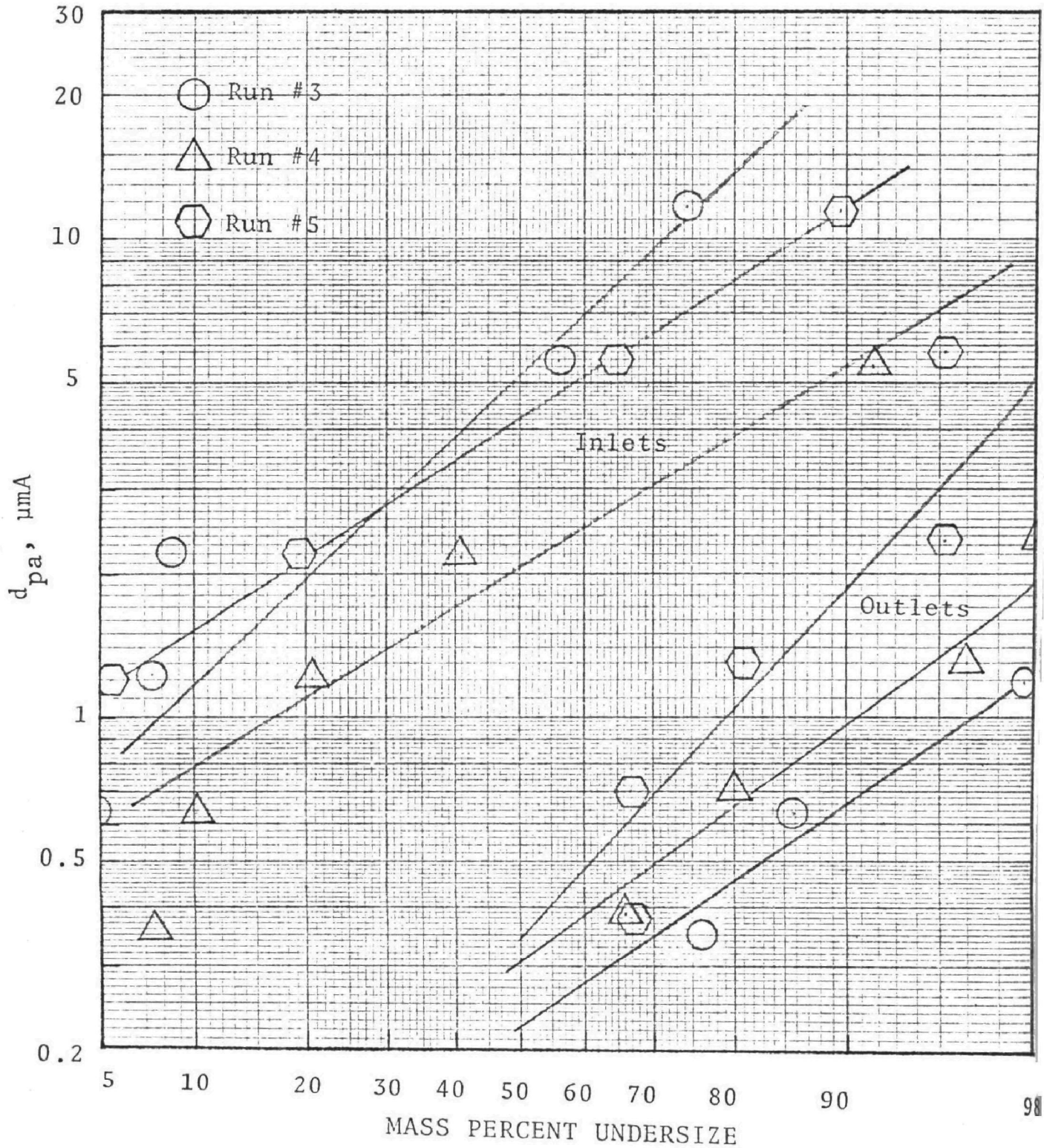

Figure 7-B-1 - Inlet and Outlet particle size distribution (data set "A")

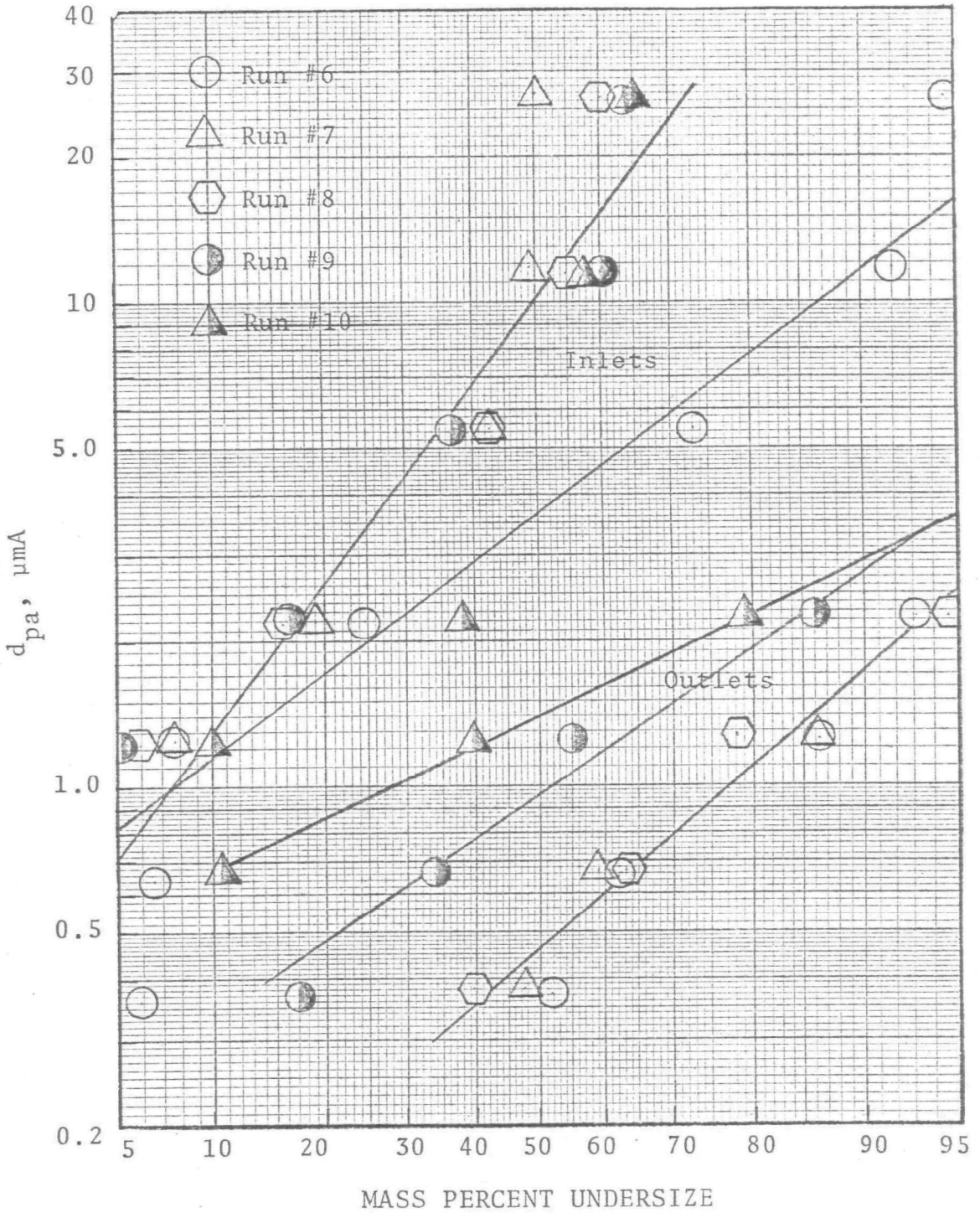

Figure 7-B-2 - Inlet and outlet particle size distribution (data set "B")

APPENDIX 7-C
CUMULATIVE MASS DISTRIBUTIONS

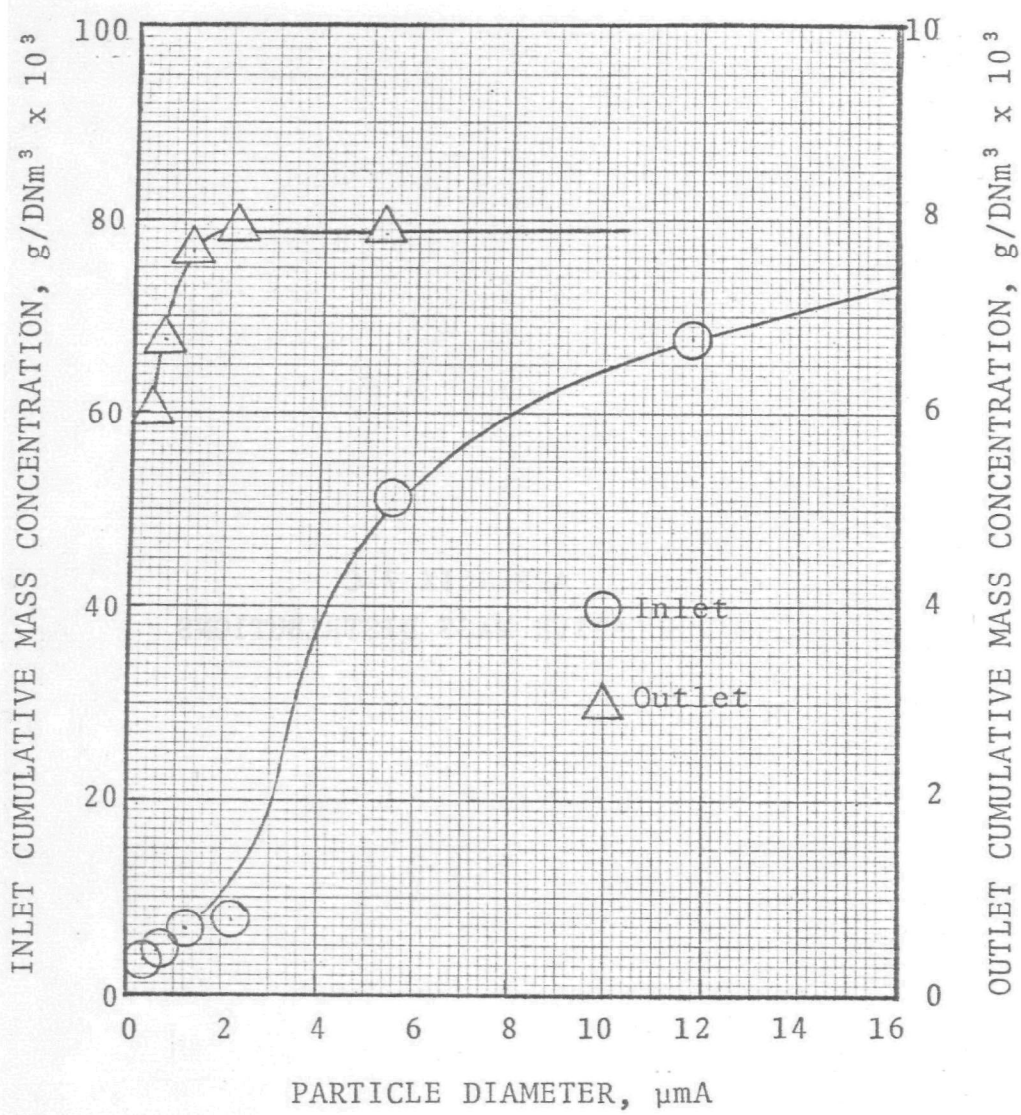

Figure 7-C-1 - Cumulative mass distribution for Run #3

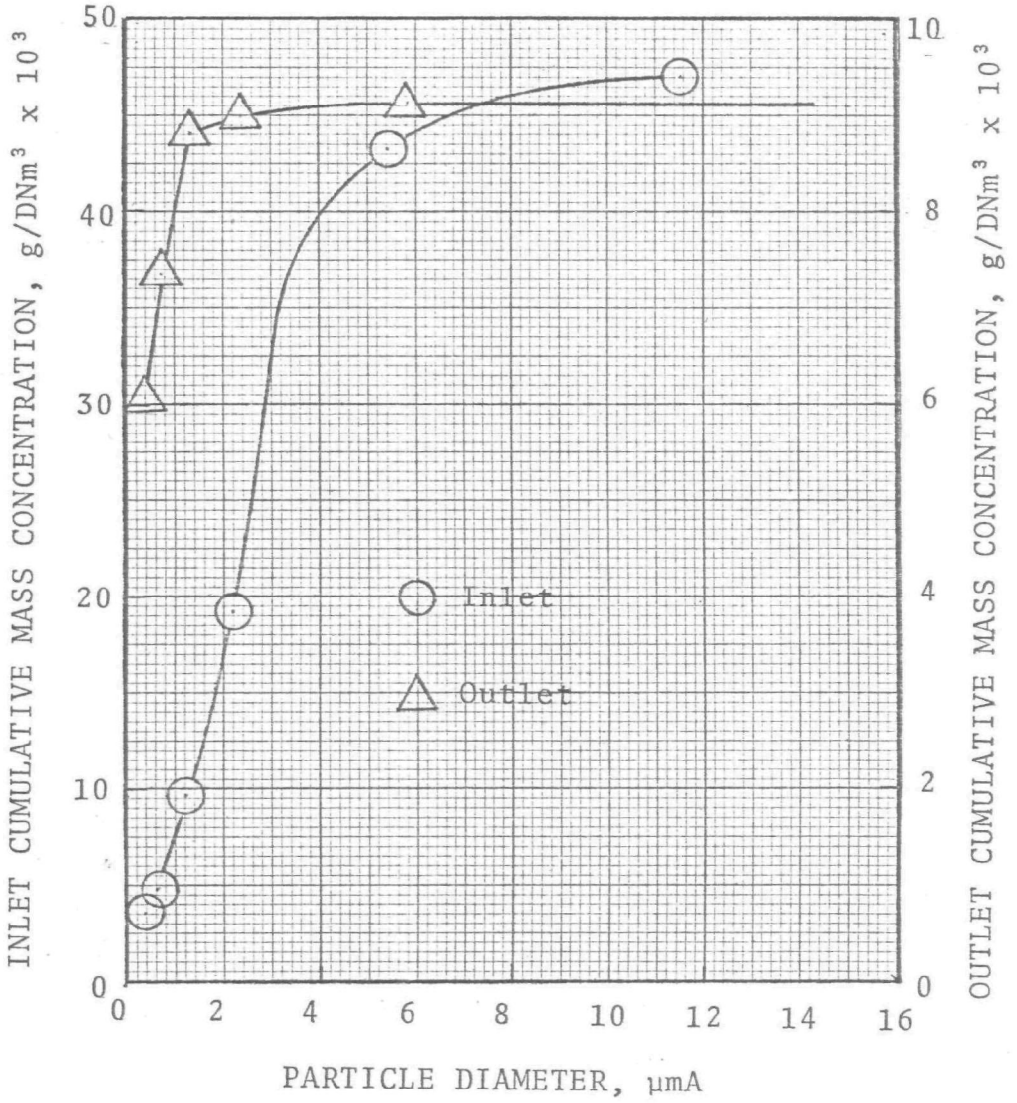

Figure 7-C-2 - Cumulative mass distribution for Run #4

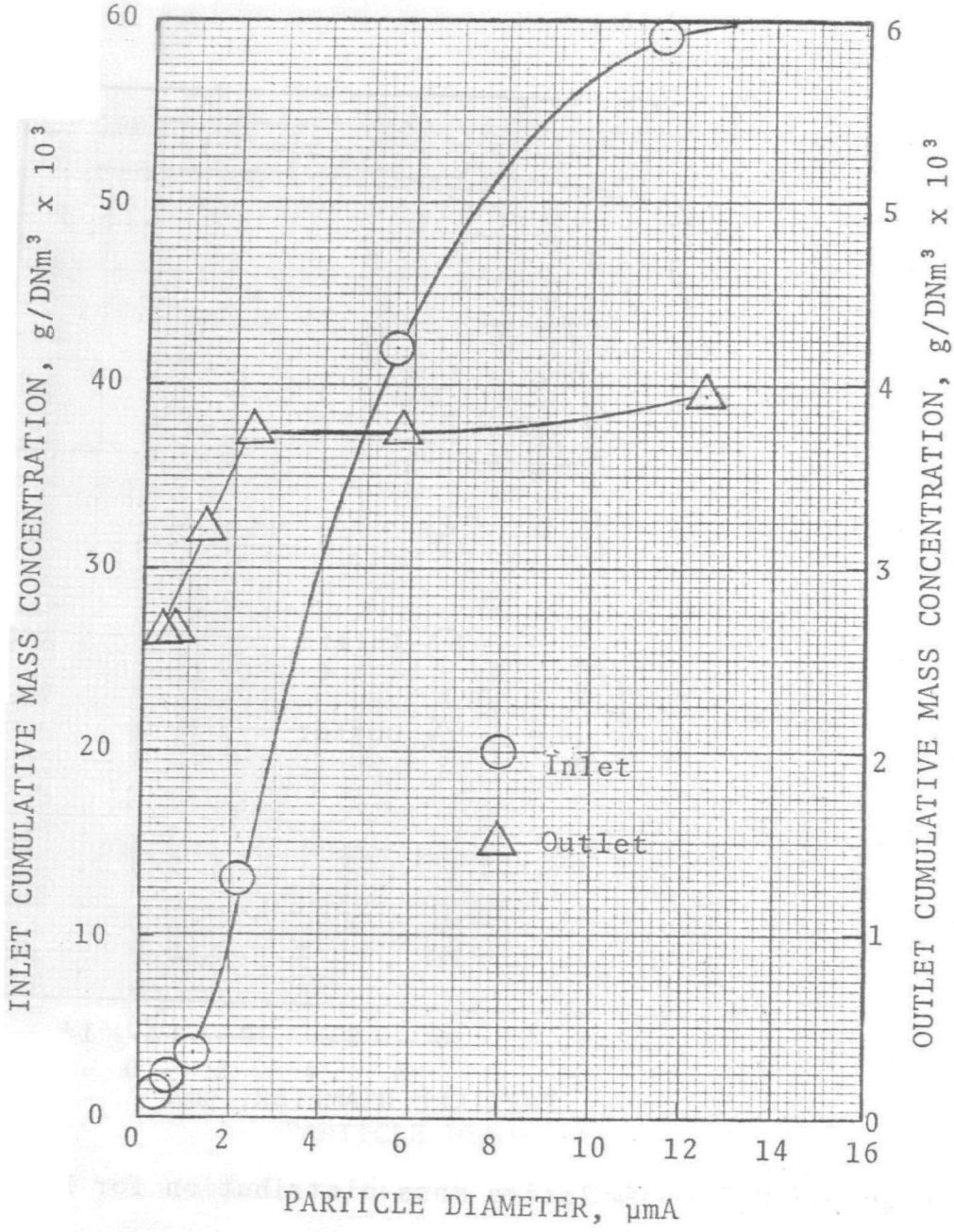

Figure 7-C-3 - Cumulative mass distribution for Run #5

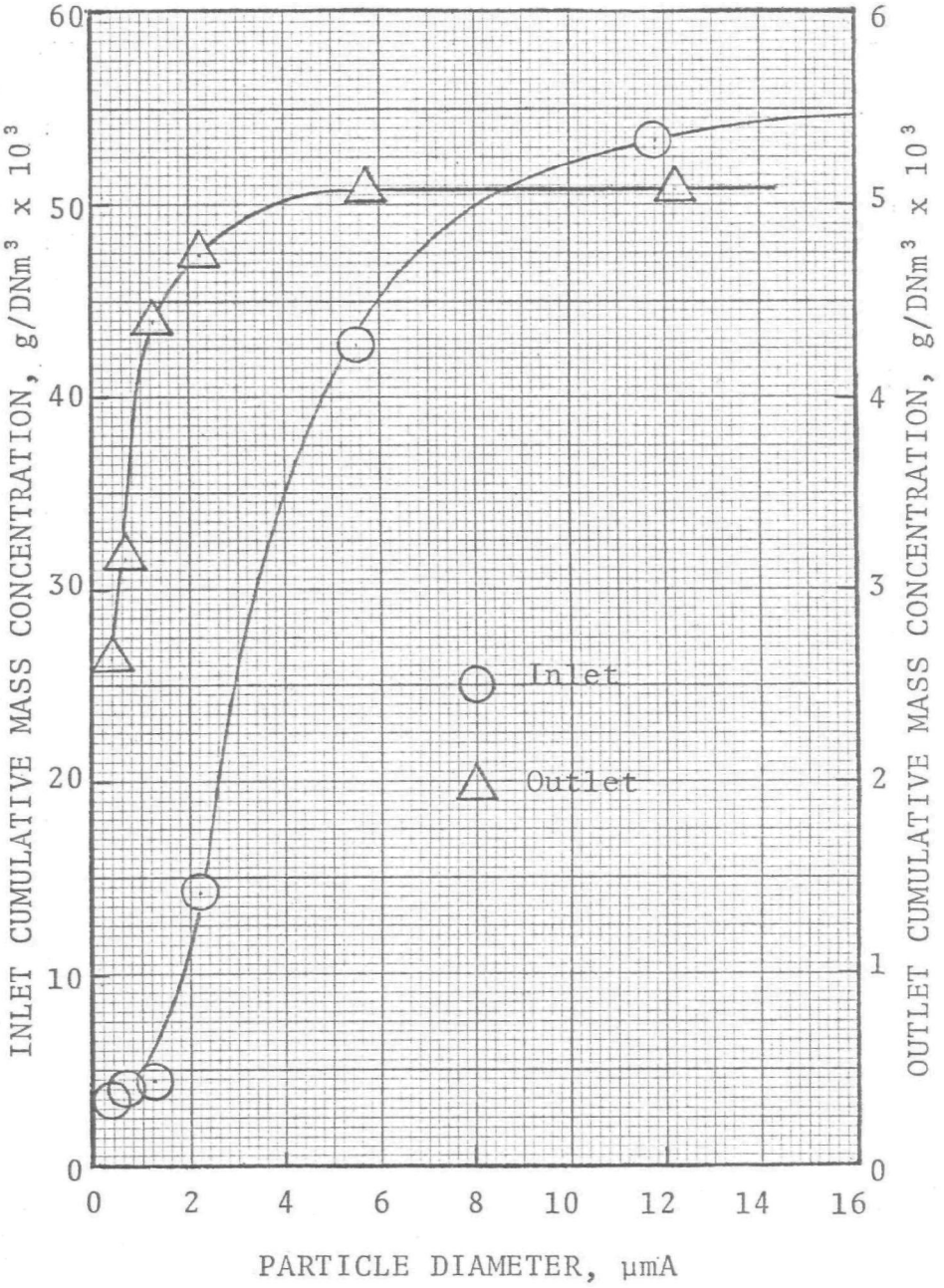

Figure 7-C-4 - Cumulative mass distribution for Run #6

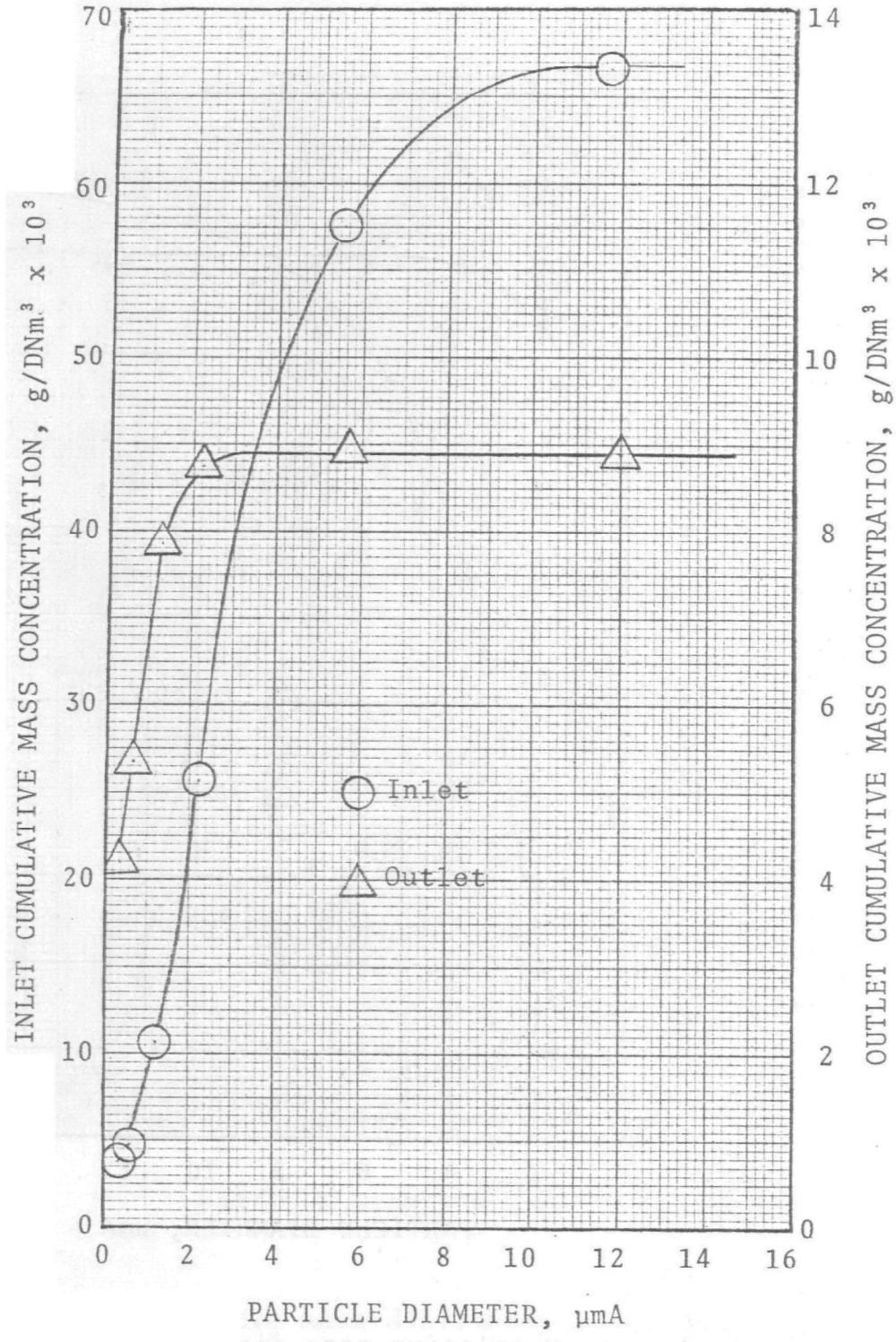

Figure 7-C-5 - Cumulative mass distribution for Run #7

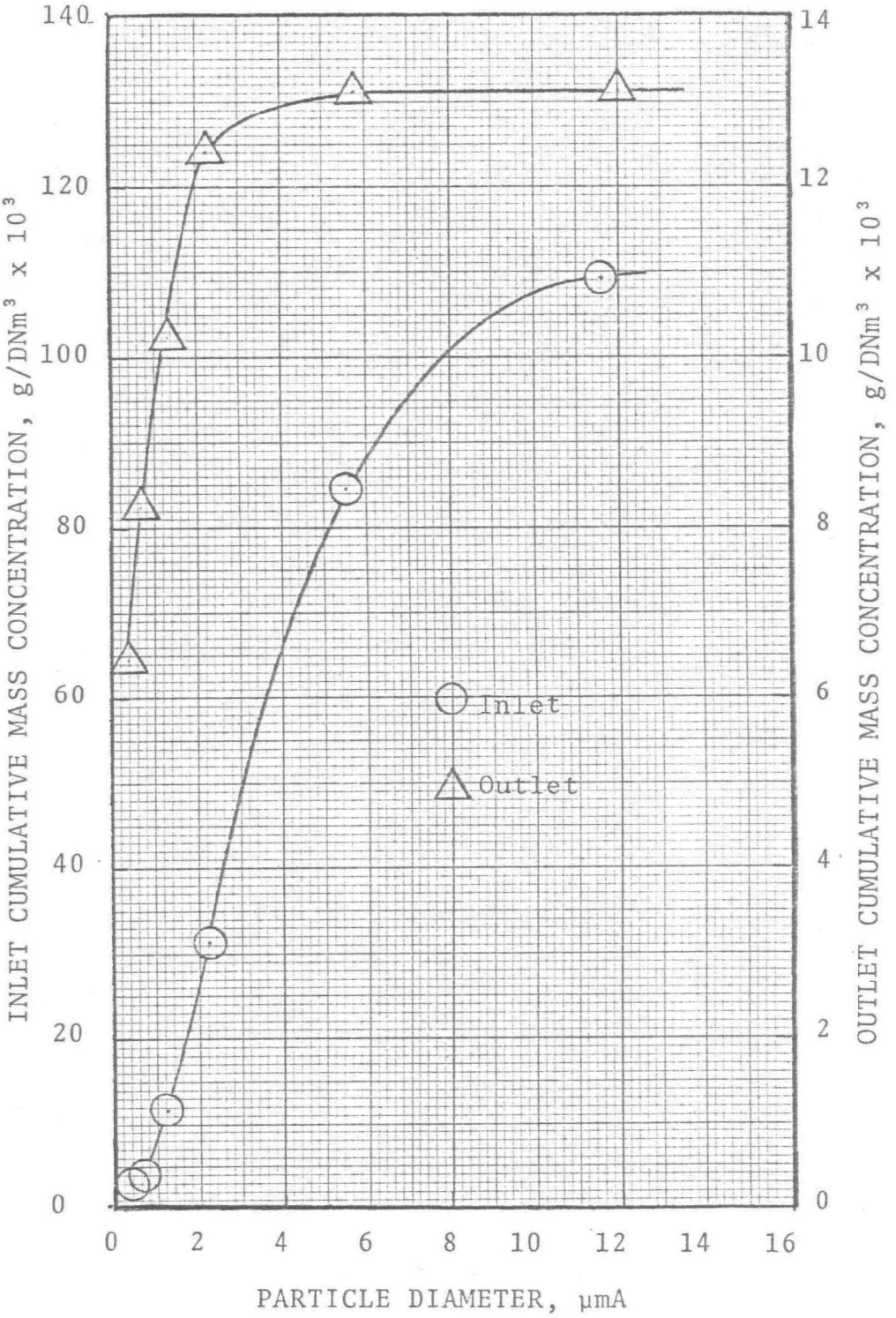

Figure 7-C-6 - Cumulative mass distribution for Run #8

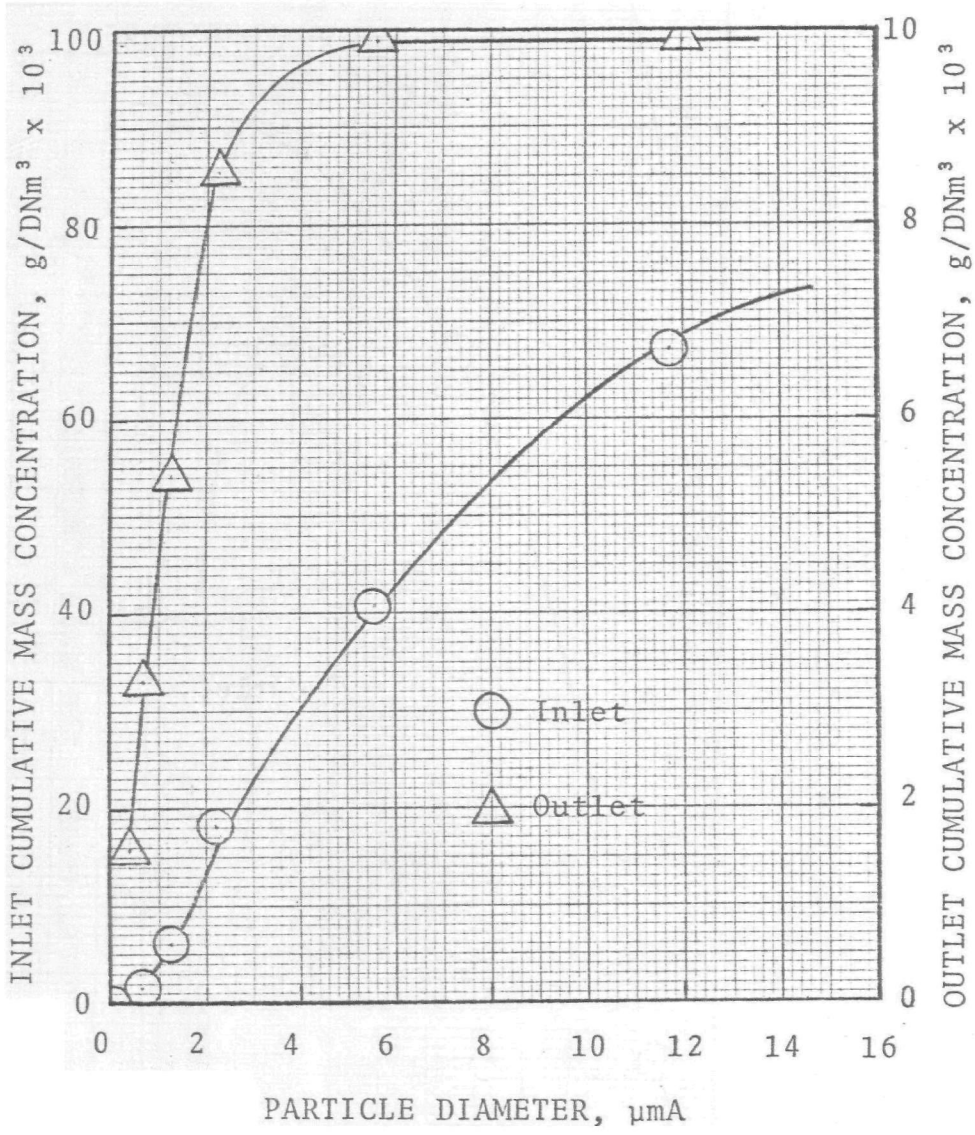

Figure 7-C-7 - Cumulative mass distribution for Run #9

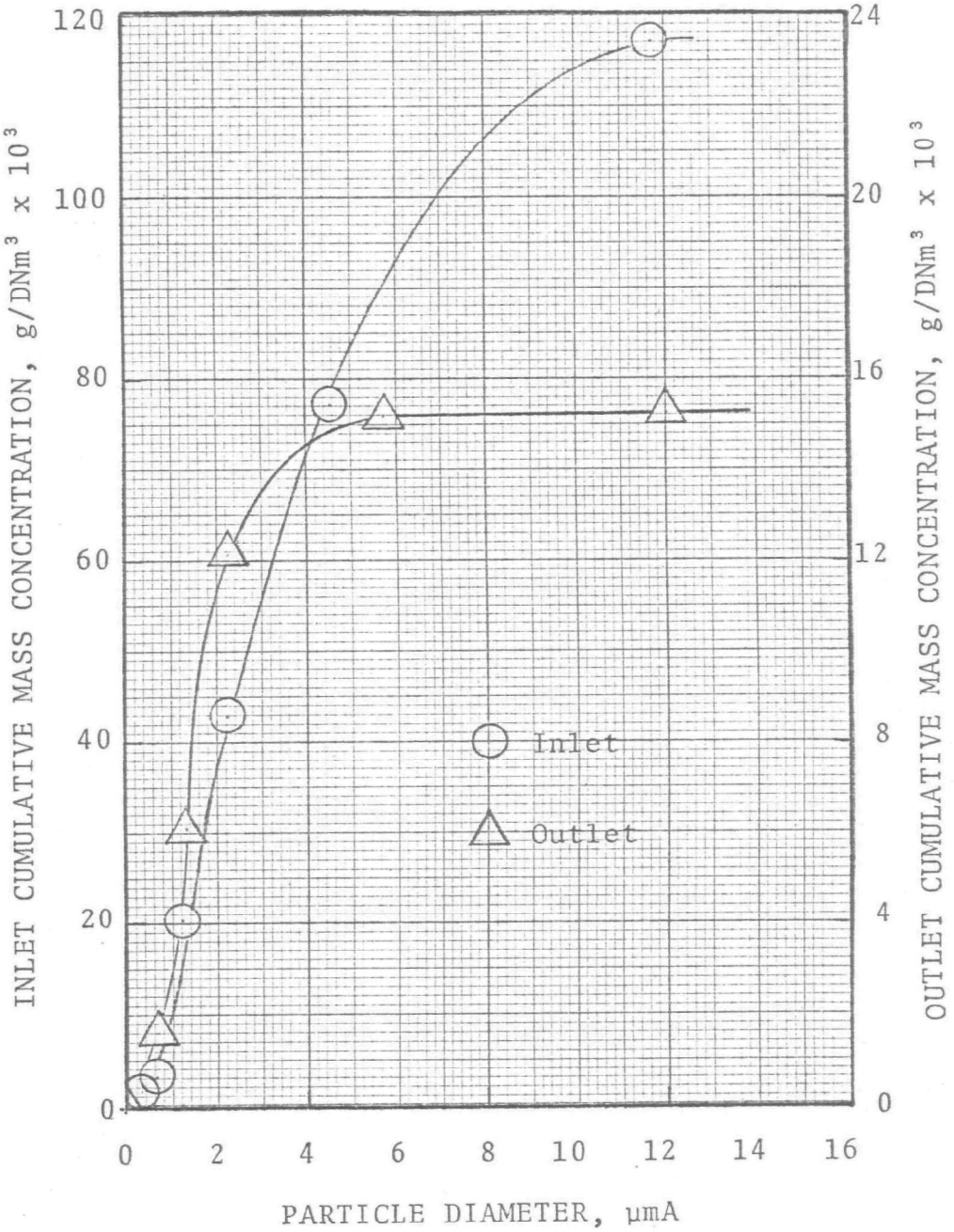

Figure 7-C-8 - Cumulative mass distribution for Run #10

IMPINGEMENT PLATE TEST
(Impinjet)

SOURCE AND SCRUBBER

The impingement plate scrubber selected for the seventh performance test was an Impinjet wet scrubber. This scrubber was installed to control the emission from a gas fired rotary salt dryer. The gas emitted from the dryer contains common salt particulates and combustion by-products (carbon monoxide, methane, etc.).

The scrubber (see Figure 8-1) was designed and manufactured by W. M. Sly Manufacturing Company for a maximum gas capacity of 230 m^3/min (8,100 CFM) at 121°C (250°F). In actual operation, it treats 141 DNm^3/min (5,380 DSCFM) of gas which has particulate loadings about 0.0036 Kg/DNm^3.

Additional information on the scrubber system (see Figure 8-2) is as follows:

1. Gas emitted from the dryer is supplied to the scrubber by means of a 40 HP fan.
2. Water flow rate to the scrubber is 0.035 m^3/min (9 GPM) at 20 psig sprayed onto the bottom of the first impingement stage and 0.038 m^3/min (10 GPM) at free flow to the second stage.
3. Pressure drop (gas phase) was 30 cm W.C. (12"W.C.) during the test period.

TEST METHOD

The performance of the scrubber is determined by analyzing the particle size distribution, mass loading of the inlet and outlet gas sample. Therefore, the most essential part of the performance test was the determination of particle size and mass loading distribution.

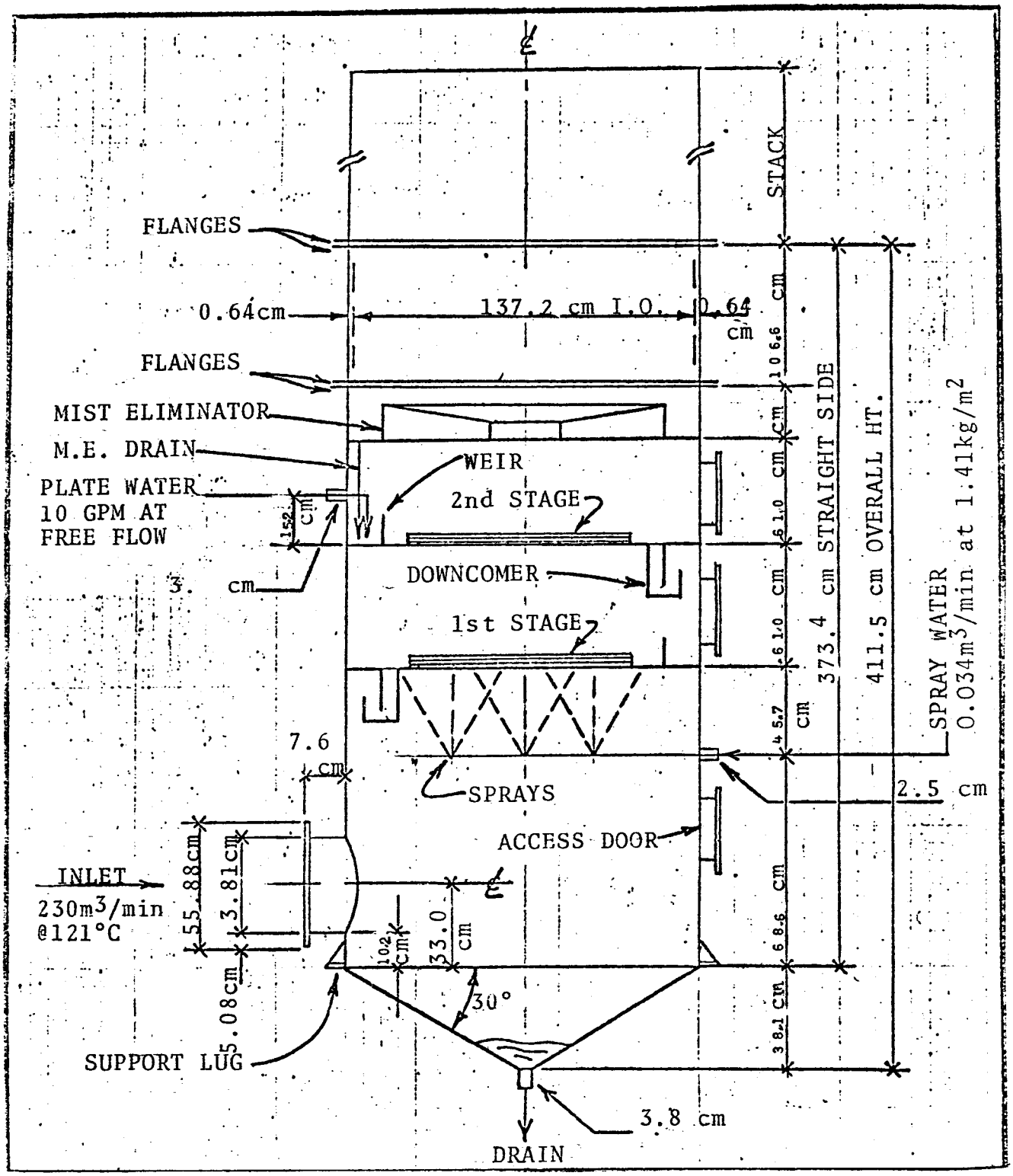

Figure 8-1 - Two stage No. 245 Sly Impingjet Wet Scrubber
Shell - 0.035 cm

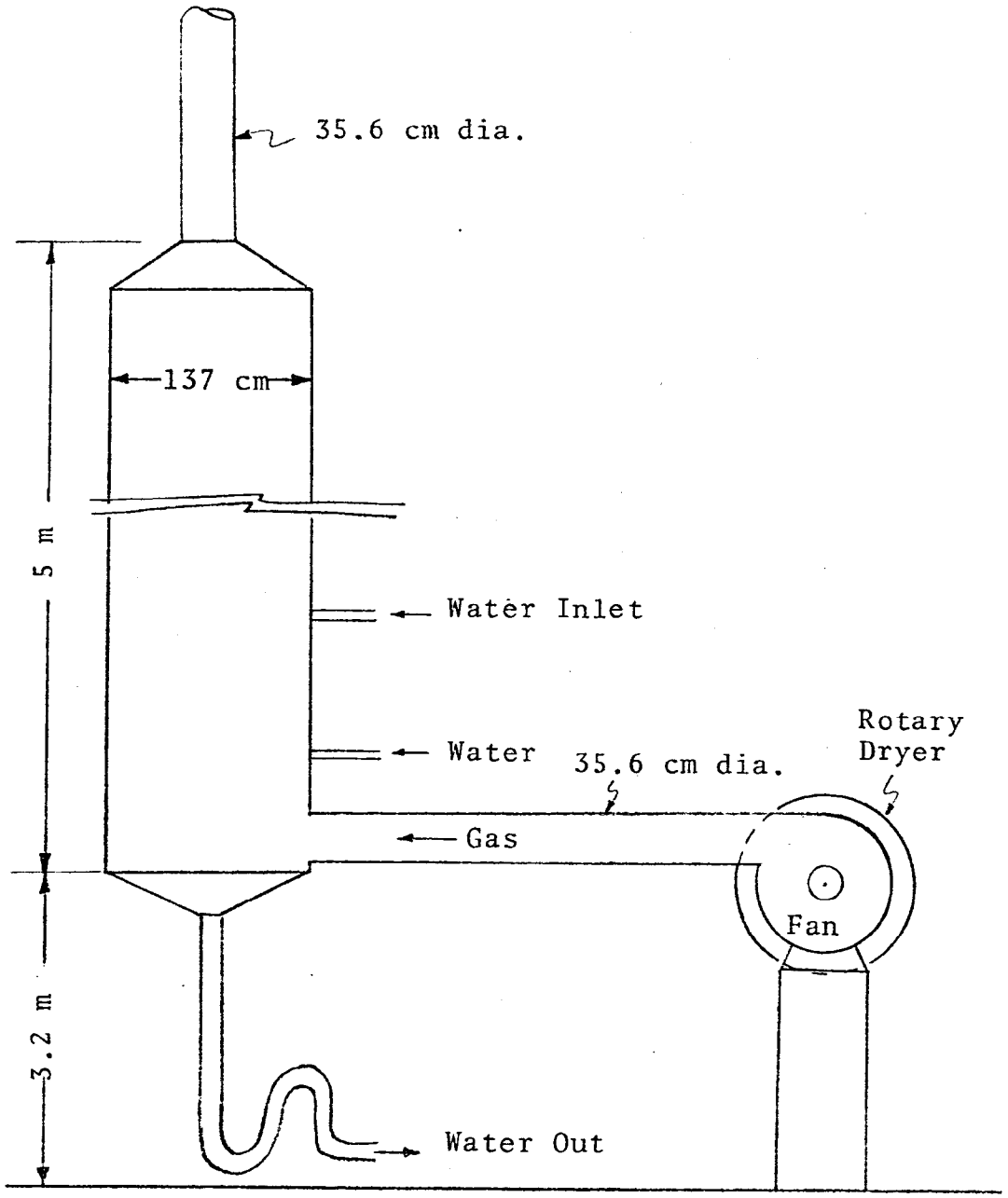

Figure 8-2 - Schematic Diagram of Scrubber System

A modified E.P.A. Method 5 train with an in-stack University of Washington (or Pilat) cascade impactor was used for particle measurements. Gas flow rate was determined by means of type "S" pitot tube traverses along with the necessary temperature and pressure measurements. Sample flows were measured with the usual E.P.A. train instruments so as to obtain isokinetic or near isokinetic sampling.

Both inlet and outlet sampling impactors were kept at one position during the entire sampling period. The inlet impactor was allowed to heat up to stack temperature before the sample was taken and the outlet impactor was electrically heated. The total filter following the impactor were in-stack in the inlet sampling and ex-stack in the outlet sampling. The ex-stack filter was heated with an electric resistance wrapping to prevent condensation. The impactor stages were covered with greased aluminum foils which were treated and weighed in accordance with our usual procedures. The back-up total filter was Gelman type "E" glass fiber paper. Due to liquid entrainment, a pre-cutter was necessary to be used ahead of the impactor in the outlet.

Two independent sampling data sets (several independent simultaneous inlet and outlet sample runs in each set) were obtained. These two sets were taken at different locations across the duct cross-section. Both inlet and outlet ducts were 35.6 cm (14") in diameter.

SCRUBBER OPERATING CONDITIONS

The scrubber operating conditions during the test period were as follows:

1. Gas parameters were as shown in the following tabulation:

Gas Parameters	Inlet	Outlet
Temperature	85°C	38°C
Pressure during pitot run	31.3 cm W.G.	2.2 cm W.G.
A m^3/min	238	263
ACFM	8,400	9,300
DNm^3/min	169	220
DSCFM	6,416	8,377
Vol.% H_2O Vapor	14	7.2

2. Liquid parameters were as shown in the tabulation below:

Liquid Parameters	Inlet		Outlet
	Bottom Plate	Top Plate	
Temperature			
Pressure (Kg/m^2)	14,000	Free Flow	-
m^3/min	0.035	0.038	0.073
GPM	9	10	19
Suspended Solids	-	-	-
Dissolved Solids	-	-	-
Treatment	-	-	-

3. Liquid entrainment was not measured in this test series although it is known to be excessive.

PARTICLE DATA

Sampling data which were obtained in this performance test are presented in Tables 8-A-1 through 8-A-6 for the six simultaneous inlet and outlet samples. Runs 1, 2, 3 and 4

were taken at the same location of the duct cross-section and was designated data set "A". The remaining two runs were sampled at different locations and were grouped into data set "B". Run #6 was purged due to leakage in sampling lines.

Figures 8-B-1 through 8-B-4 shows log-probability plots of inlet and outlet particle size distribution. The mass median diameter and geometric standard deviation are not revealed by these figures because most of the particles are big particles (larger than 20 μmA).

Cumulative mass concentration was plotted against aerodynamic particle size to yield mass loading distribution curves (Figures 8-C-1 through 8-C-6). In some of these figures, the outlet curve crosses the inlet curve. This may be caused by breakdown of large particles. Another possibility is particle growth due to condensation. The gas is cooled from 82°C (180°F) to 38°C (100°F) by water.

PARTICLE PENETRATION

Particle penetration was computed by taking the ratio of the outlet to the inlet cumulative concentration distribution slopes at various particle diameters. The slope can either be obtained by a graphical technique or by fitting the data with a mathematical function and then calculating the slope analytically. The first approach is used here.

Penetrations were computed for each simultaneous run and the results are plotted in Figures 8-3 and 8-4.

ECONOMICS AND OPERATING PROBLEMS

The scrubber's original purchase cost was $6,700 (June, 1969) and the operating costs are estimated at $100 per year. The operating costs consist of power required to pump approximately 0.31 m^3/min (80 GPM) of water and the exhaust

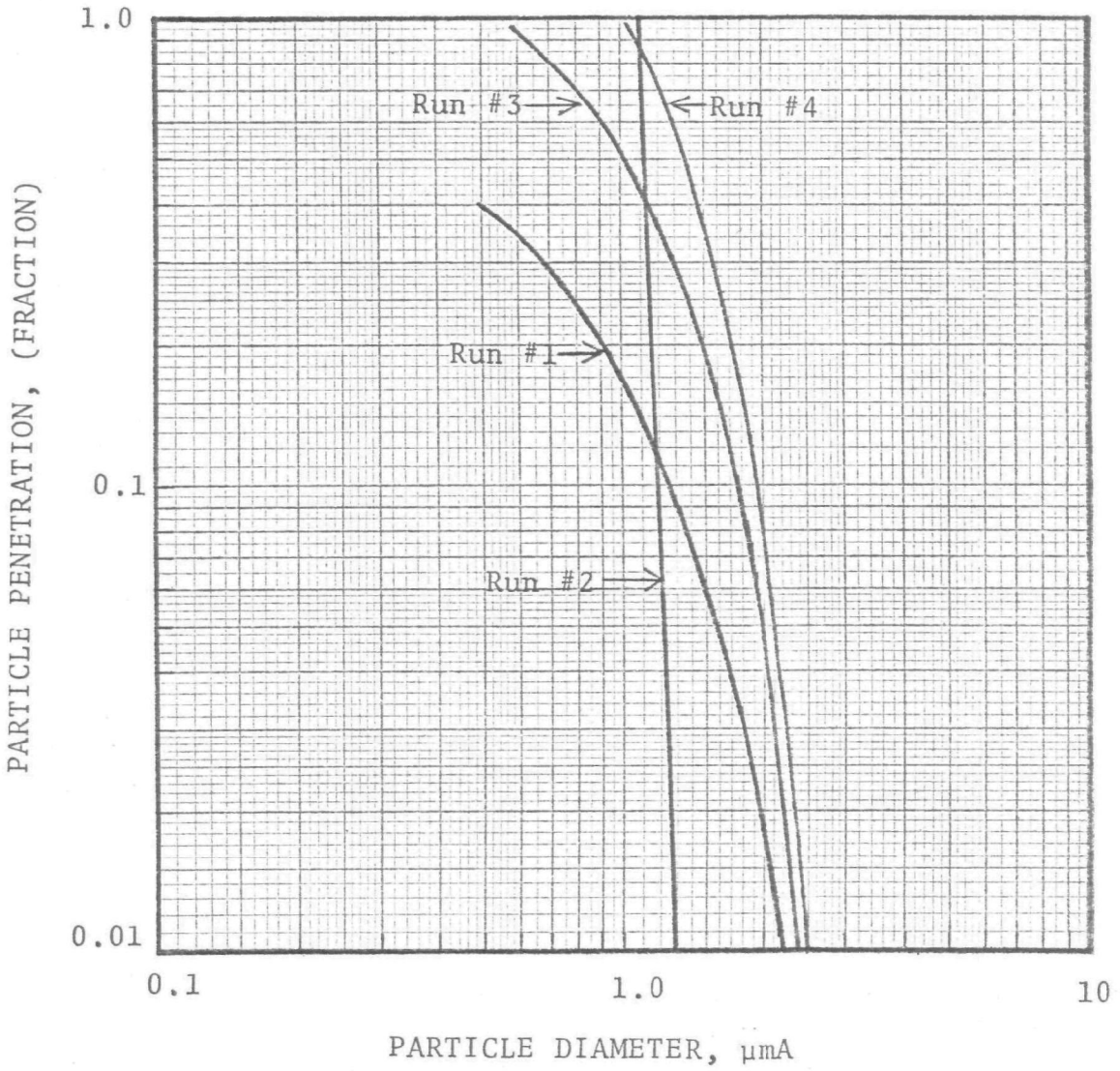

Figure 8-3 - Penetration versus particle diameter (data set "A").

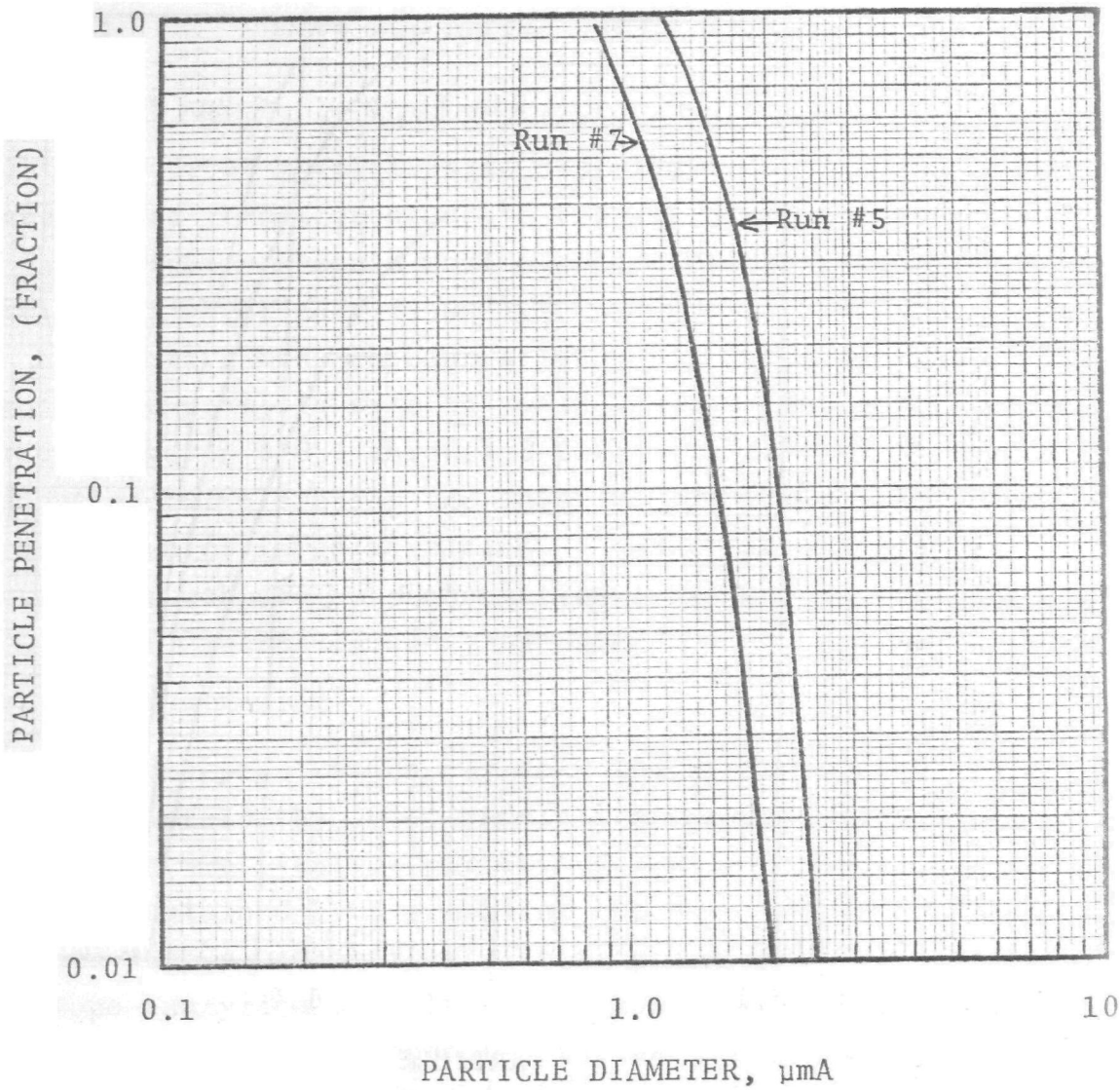

Figure 8-4 - Penetration versus particle diameter.
(data set "B")

blower. Maintenance of the scrubber consists of periodic inspections, clean and occasionally replacement of spray nozzles and piping and its costs are estimated at $300 per year.

There are no unusual operating problems.

MATHEMATICAL MODEL

Section 5.3.2.2 in the "Scrubber Handbook" gave a design equation (Eq. 5.3.2-6) for Impingement type scrubber. This equation uses information on jet hole diameters, number of holes and gas flow rate to predicted d_{pa50}. However, the scrubber user did not have any information on the construction of the jet plate, which makes it impossible to use this equation.

An alternative method to predict scrubber performance is the cut diameter approach as described in Chapter 2. Based on this method, for a pressure drop of 29 cm W.C., the cut diameter for impingement type scrubber is 1.4 μmA. Penetration for other particle diameters is based on the exponential variation of penetration with d^2_{pa}. The predictions so obtained are shown as "prediction 'A'" in Figures 8-5 and 8-6 along with experimental results. It can be seen that the test data indicate a cut diameter of about 1.0 μmA. The density of sodium chloride is about 2.1 g/cm^3 so the diameter of a dry salt particle equivalent to 1.0 μmA is about 0.6 μm. As discussed in the preceeding section on the fibrous filter, the salt particle diameter should increase at least 2 times, and as much as 5 times due to water condensation. A salt solution particle 1.2 μm diameter would have a density of about 1.1 g/cm^3 and an aerodynamic diameter of about 1.3 μmA.

An alternative method was used to predict penetration, assuming that particle growth occurs in the first impingement

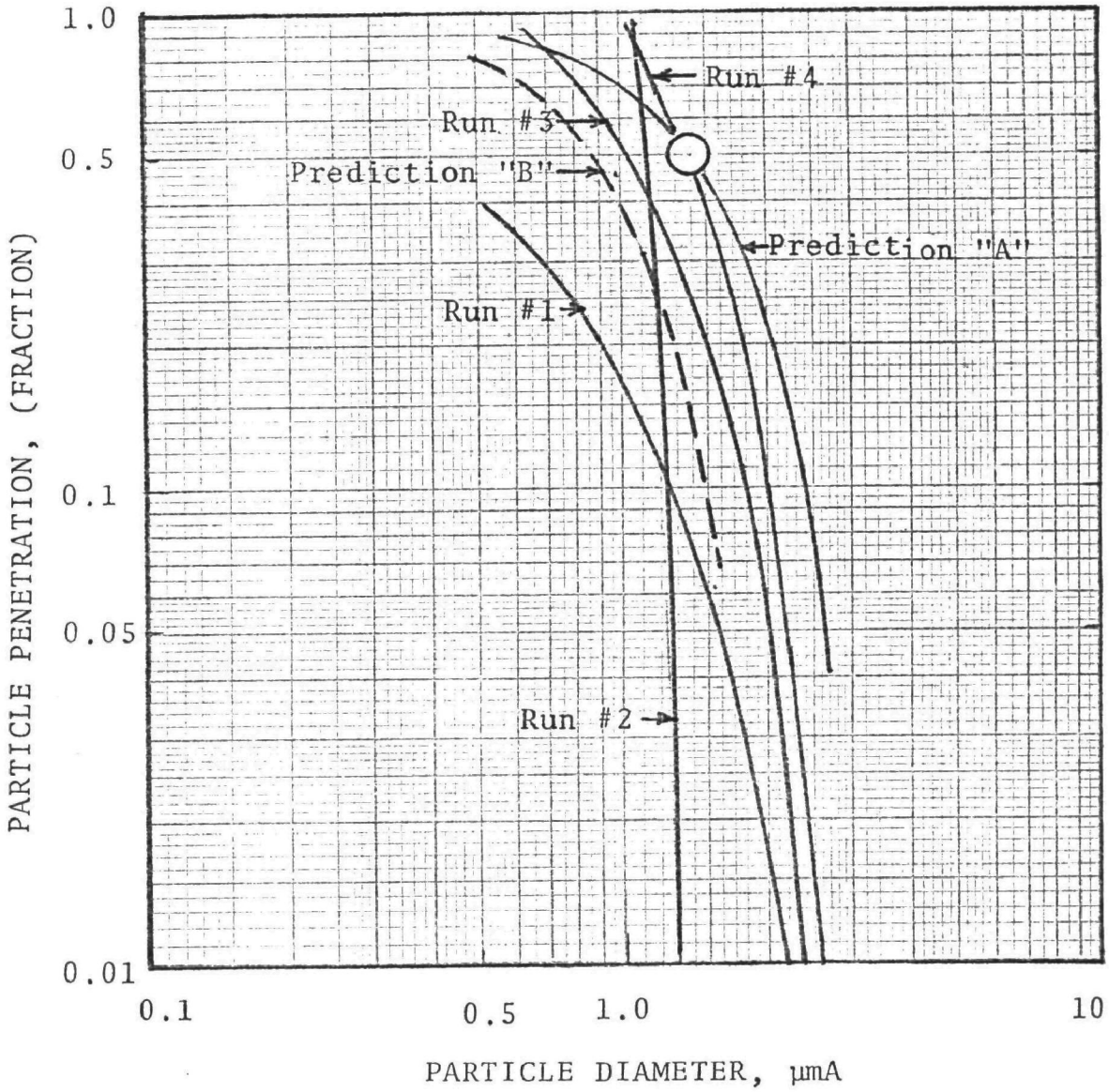

Figure 8-5 - Predicted and experimental penetration. (Data set "A")

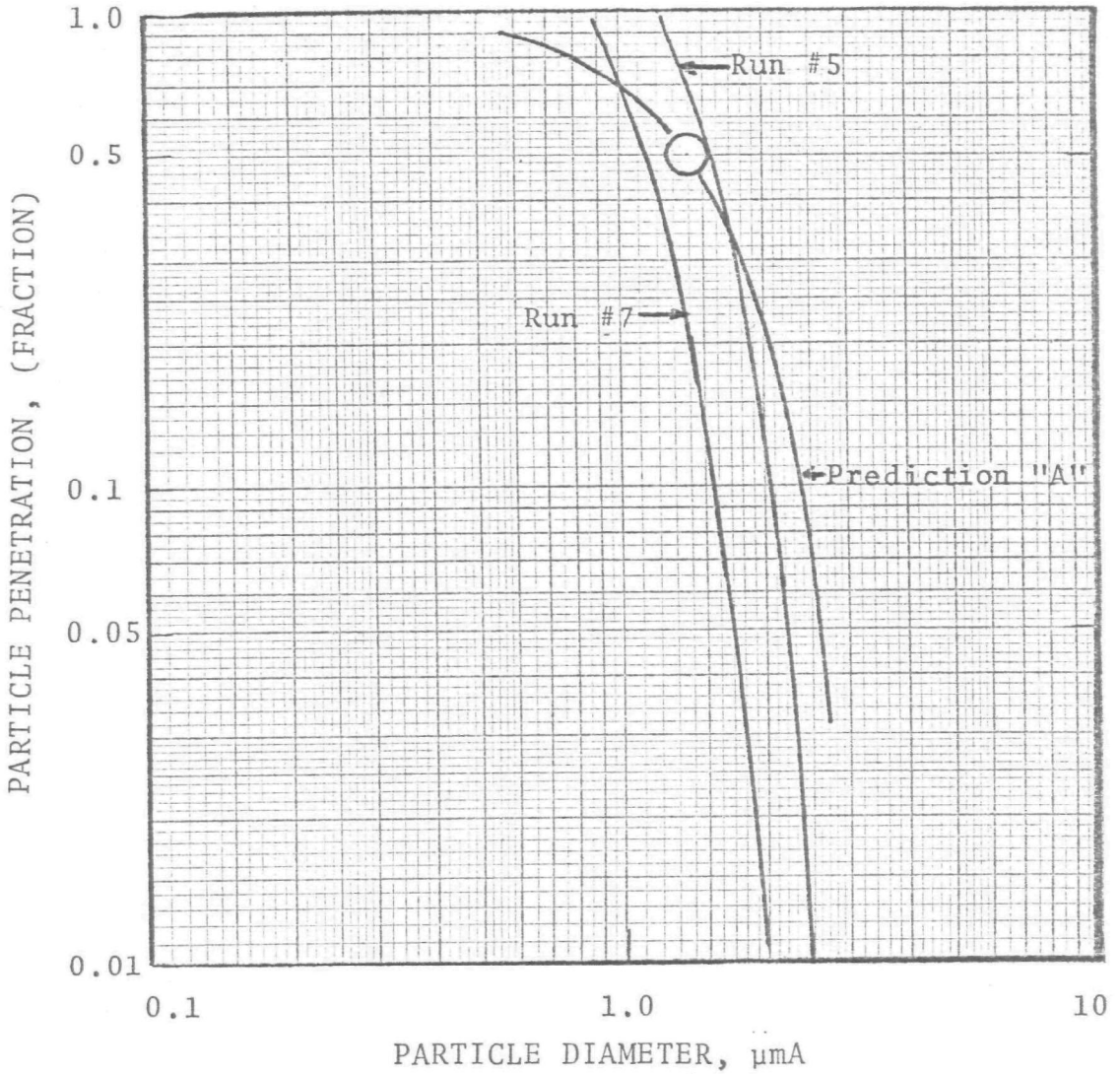

Figure 8-6 - Predicted and experimental penetration (Data set "B").

plate and that penetration based on dry particle size is therefore lower on the second plate. The line labelled "prediction 'B'" on Figure 8-5 is the result of the alternative prediction with the assumed effect of condensation being to double aerodynamic diameter as the particles flow from plate #1 to plate #2. The penetration for each plate was predicted for a pressure drop of 14 cm W.C.. This corresponds to an increase of roughly 3 times in actual diameter. It can be seen in Figure 8-5 that the penetration so predicted is somewhat lower than the experimental results. A particle size increase of about 2 times (actual) would yield a prediction more in accord with the experimental data.

CONCLUSIONS

This scrubber system is generally satisfactory and has presented no significant operating or maintenance problems. Performance appears to be in line with predictions based on the cut diameter-scrubber pressure drop correlation if allowance is made for salt particle growth. The major uncertainty in the prediction method is related to particle growth by condensation in near-saturated gas.

APPENDIX 8-A
PARTICLE DATA

Table 8-A-1. INLET AND OUTLET SAMPLE PARTICLE DATA FOR RUN #1.

IMPACTOR STAGE NUMBER	INLET		OUTLET	
	W_{cum} (mg)	d_{pc} (μmA)	W_{cum} (mg)	d_{pc} (μmA)
1	22.4	23.0		
2	3.2	10.2	8.6	11.2
3	3.2	4.75	8.5	5.25
4	3.2	1.9	8.4	2.10
5	2.7	1.05	8.4	1.18
6	2.2	0.55	8.3	0.615
7	2.0	0.30	8.1	0.34
Filter	1.7		8.1	
Sample Volume (DNm^3)	0.22		0.64	

Table 8-A-2. INLET AND OUTLET SAMPLE PARTICLE DATA FOR RUN #2.

IMPACTOR STAGE NUMBER	INLET		OUTLET	
	W_{cum} (mg)	d_{pc} (μmA)	W_{cum} (mg)	d_{pc} (μmA)
1	17.8	20		
2	5.4	8.7		
3	4.6	4.1		
4	4.3	1.62		
5	4.0	0.9		
6	3.9	0.465	4.5	0.64
7	3.8	0.25	4.2	0.355
Filter	3.7		4.0	
Sample Volume (DNm^3)	0.31		0.42	

Table 8-A-3. INLET AND OUTLET SAMPLE PARTICLE DATA FOR RUN #3.

IMPACTOR STAGE NUMBER	INLET		OUTLET	
	W_{cum} (mg)	d_{pc} (μmA)	W_{cum} (mg)	d_{pc} (μmA)
1	103.2	20		
2	12.4	8.7		
3	4.4	4.1		
4	2.8	1.62		
5	2.6	0.9	35.7	1.28
6	2.2	0.465	35.2	0.62
7	2.0	0.25	34.5	0.34
Filter	2.0		34.2	
Sample Volume (DNm^3)	0.31		1.00	

Table 8-A-4. INLET AND OUTLET SAMPLE PARTICLE DATA FOR RUN #4.

IMPACTOR STAGE NUMBER	INLET		OUTLET	
	W_{cum} (mg)	d_{pc} (μmA)	W_{cum} (mg)	d_{pc} (μmA)
1	66.8	20.5		
2	3.8	9.5	3.6	11.0
3	2.0	4.2	3.5	5.25
4	1.2	1.66	3.5	2.1
5	0.9	0.83	3.4	1.15
6	0.8	0.475	3.2	0.61
7	0.7	0.25	2.3	0.335
Filter	0.7		1.8	
Sample Volume (DNm^3)	0.21		1.03	

Table 8-A-5. INLET AND OUTLET SAMPLE PARTICLE DATA FOR RUN #5.

IMPACTOR STAGE NUMBER	INLET		OUTLET	
	W_{cum} (mg)	d_{pc} (μmA)	W_{cum} (mg)	d_{pc} (μmA)
1	22	21		
2	2.4	9.2		
3	0.6	4.3		
4	0.6	1.7	1.1	2.05
5	0.5	0.97	1.0	1.13
6	0.5	0.5	0.9	0.6
7	0.5	0.265	0.3	0.33
Filter	0.5		0	
Sample Volume (DNm^3)	0.18		1.07	

Table 8-A-6. INLET AND OUTLET SAMPLE PARTICLE DATA FOR RUN #7.

IMPACTOR STAGE NUMBER	INLET		OUTLET	
	W_{cum} (mg)	d_{pc} (μmA)	W_{cum} (mg)	d_{pc} (μmA)
1	179.8	21		
2	6.3	9.2		
3	5.8	4.3		
4	4.0	1.7		
5	3.3	0.97	61.3	1.1
6	2.9	0.5	61.2	0.58
7	2.7	0.265	60.4	0.33
Filter	2.7		48.4	
Sample Volume (DNm^3)	0.39		1.14	

APPENDIX 8-B
PARTICLE SIZE DISTRIBUTION PLOTS

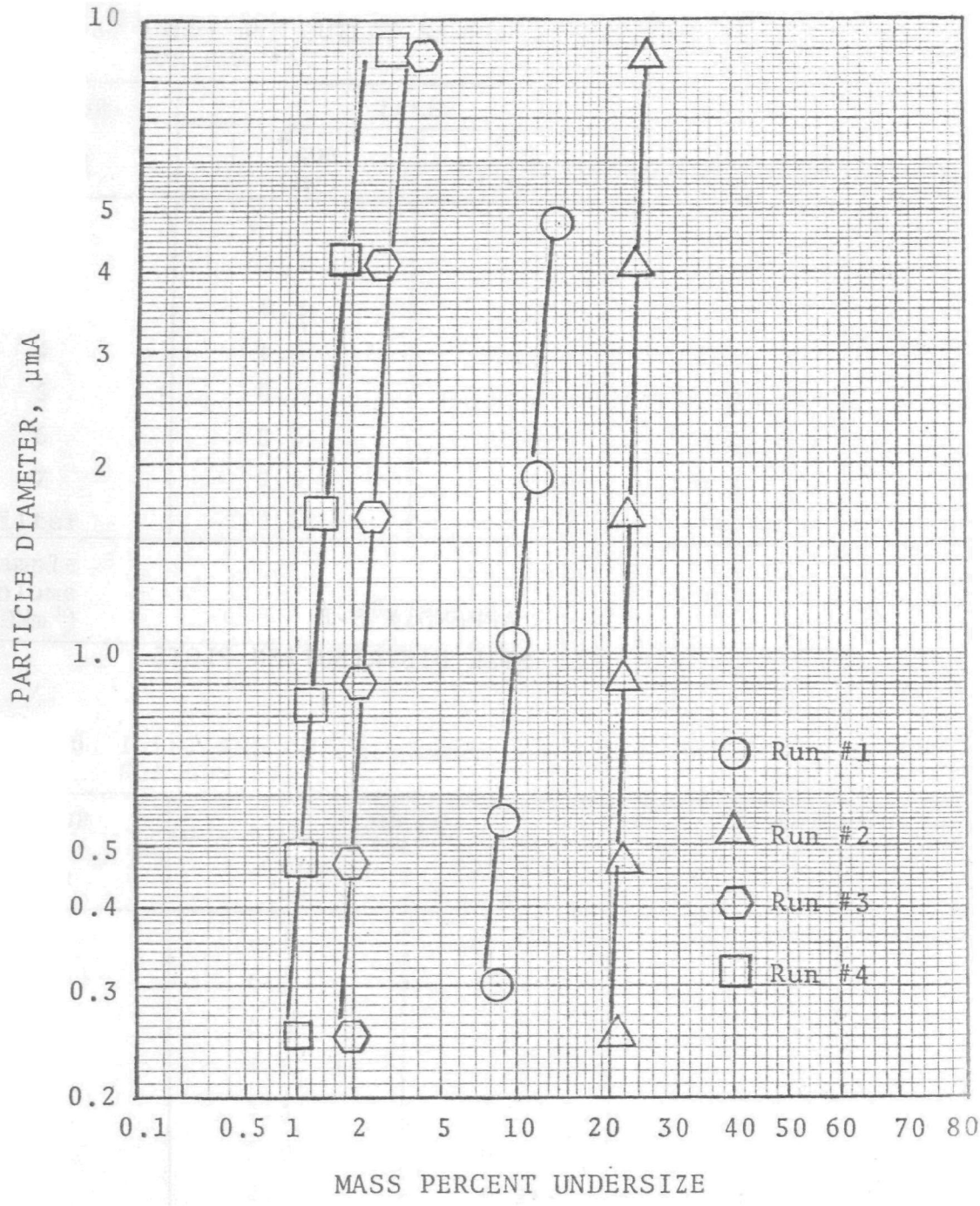

Figure 8-B-1 - Inlet particle size distribution for data set "A".

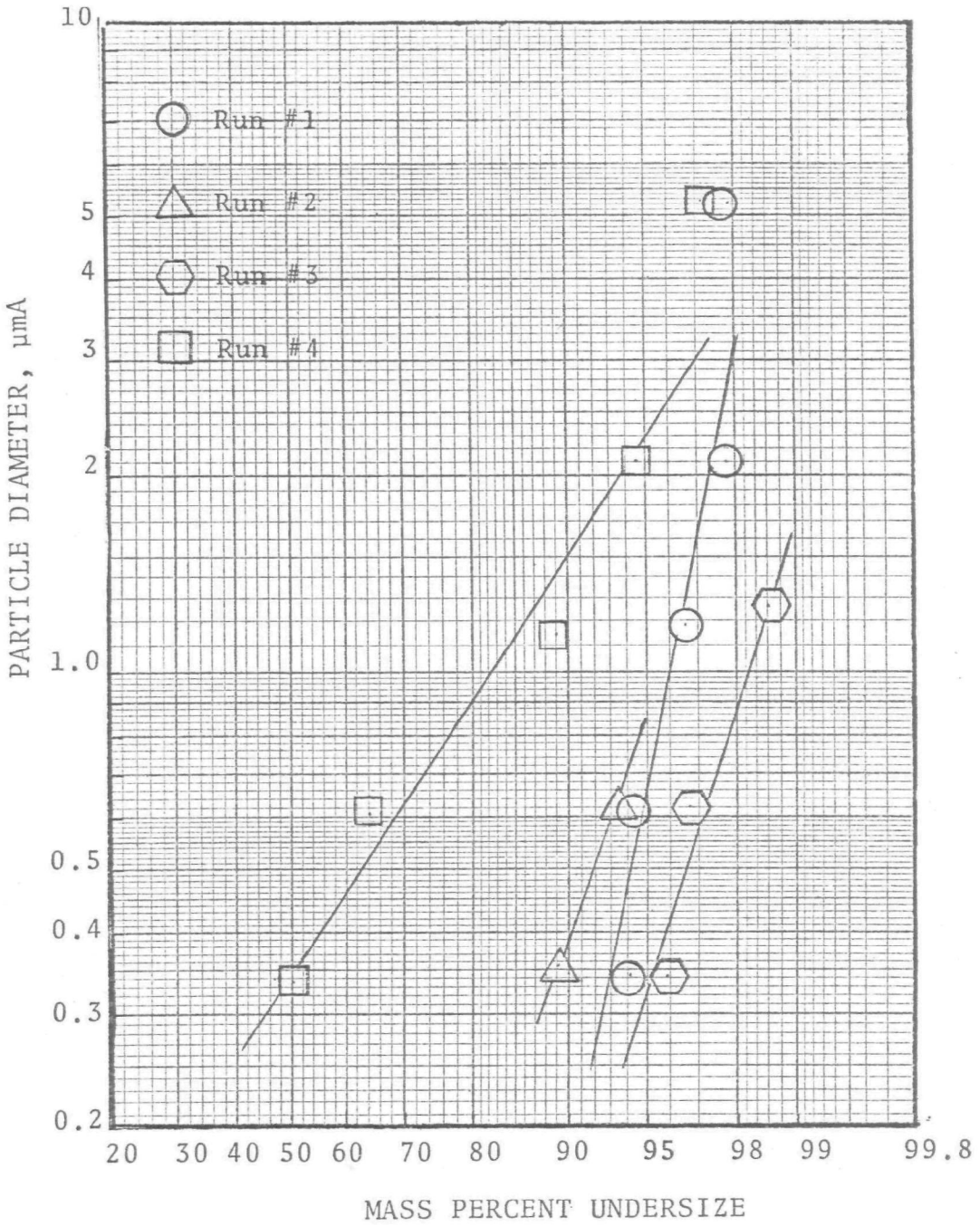

Figure 8-B-2- Outlet particle size distribution for data set "A".

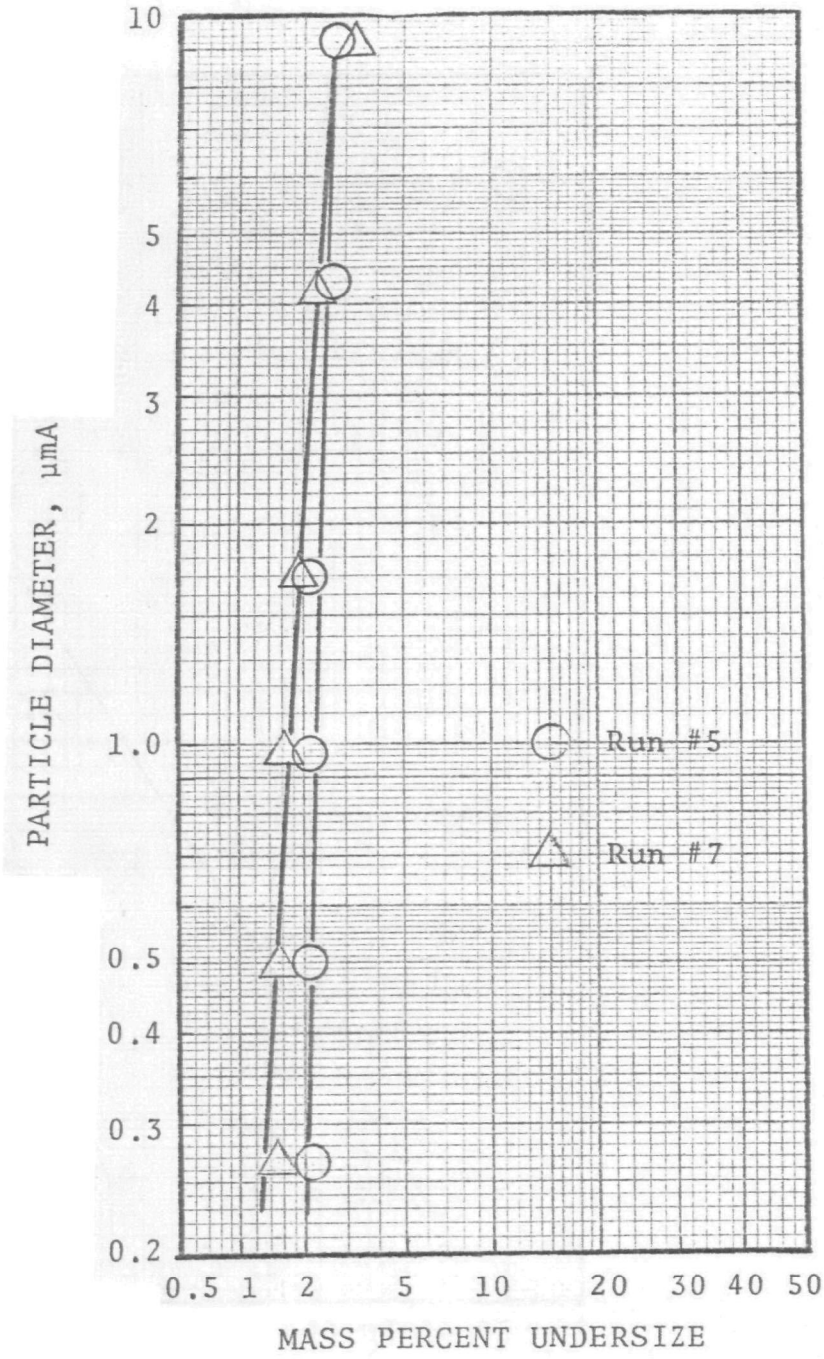

Figure 8-B-3 - Inlet particle size distribution for data set "B".

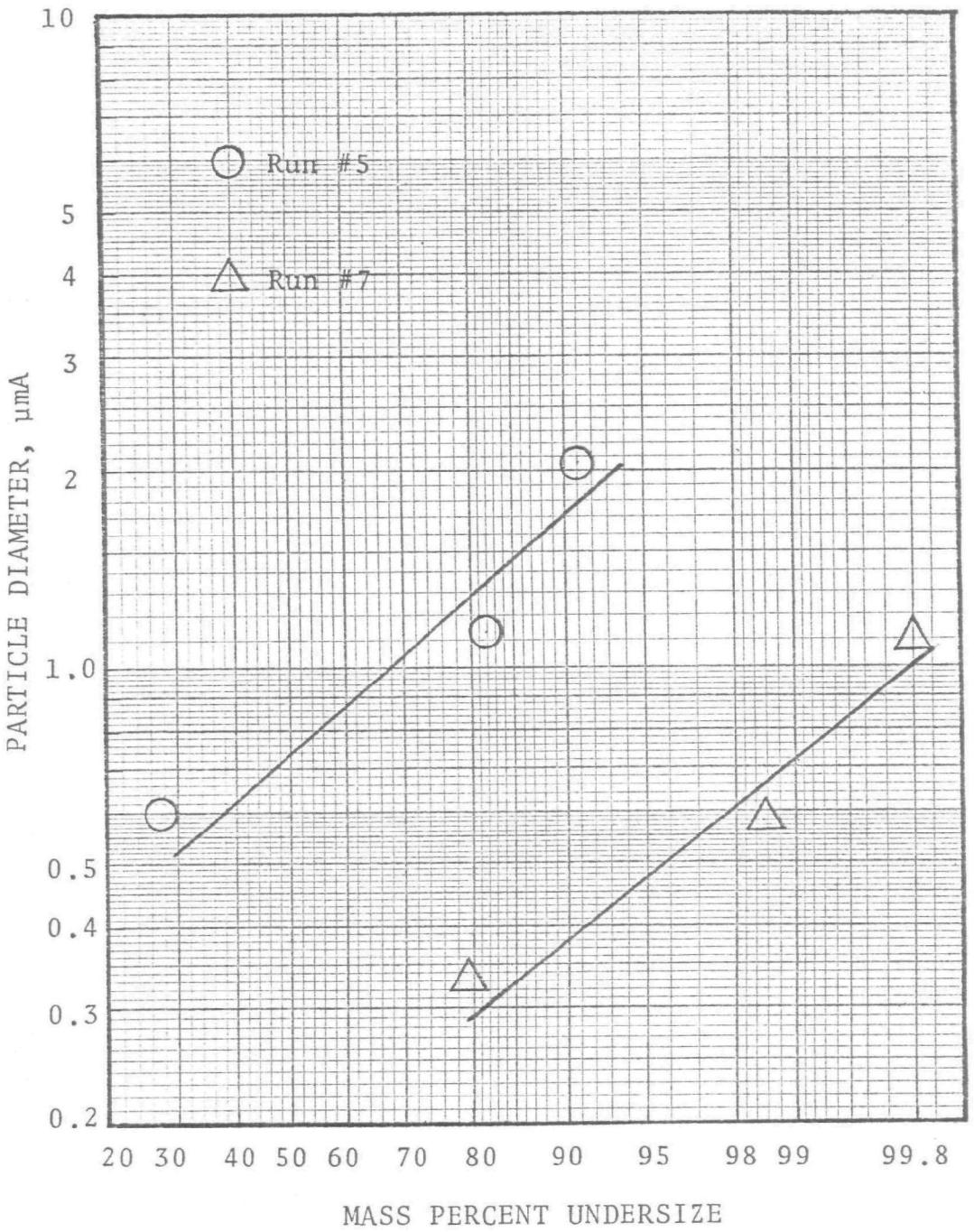

Figure 8-B-4 - Outlet particle size distribution for data set "B".

APPENDIX 8-C
CUMULATIVE MASS DISTRIBUTIONS

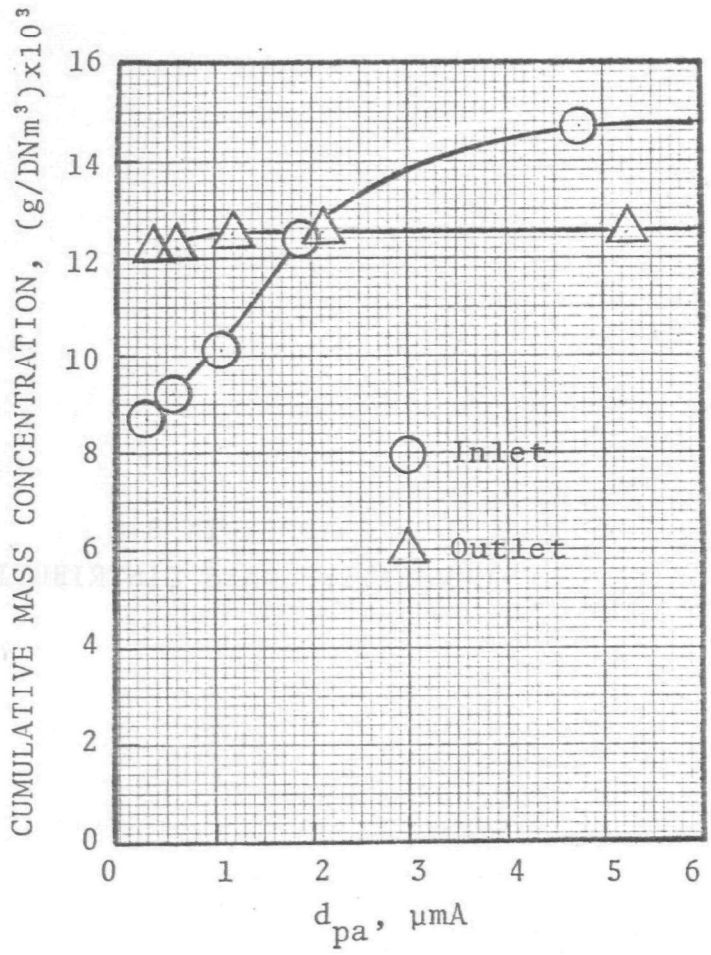

Figure 8-C-1 - Mass concentration distribution for Run #1.

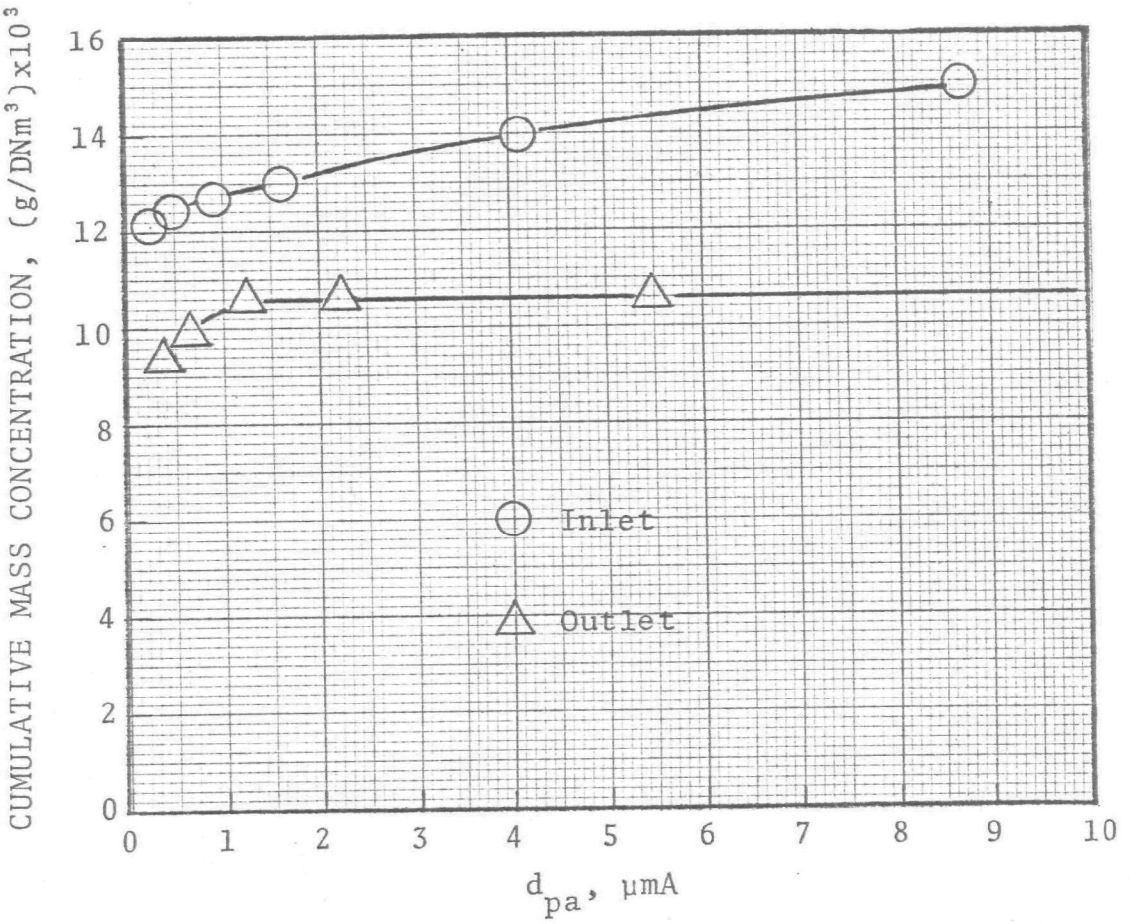

Figure 8-C-2 - Mass concentration distribution for Run #2.

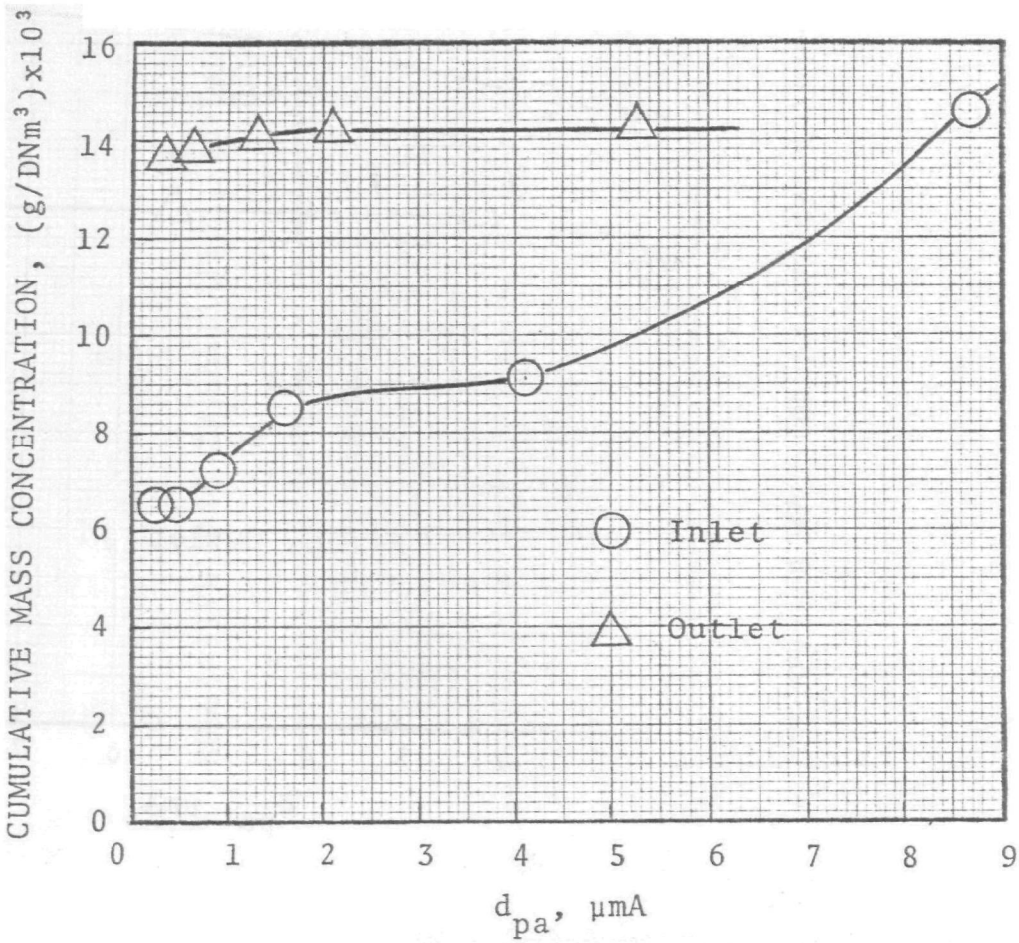

Figure 8-C-3- Mass concentration distribution for Run #3.

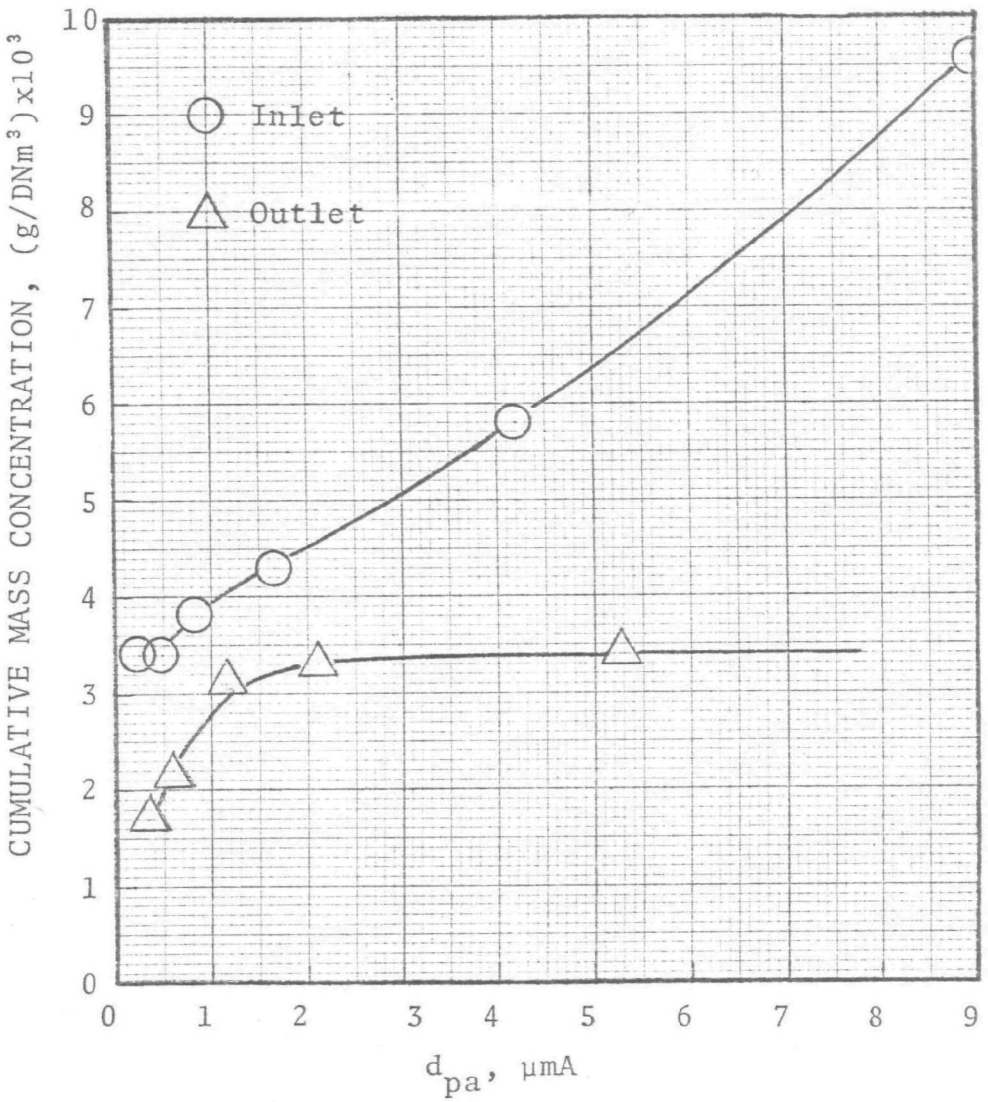

Figure 8-C-4 - Mass concentration distribution for Run #4.

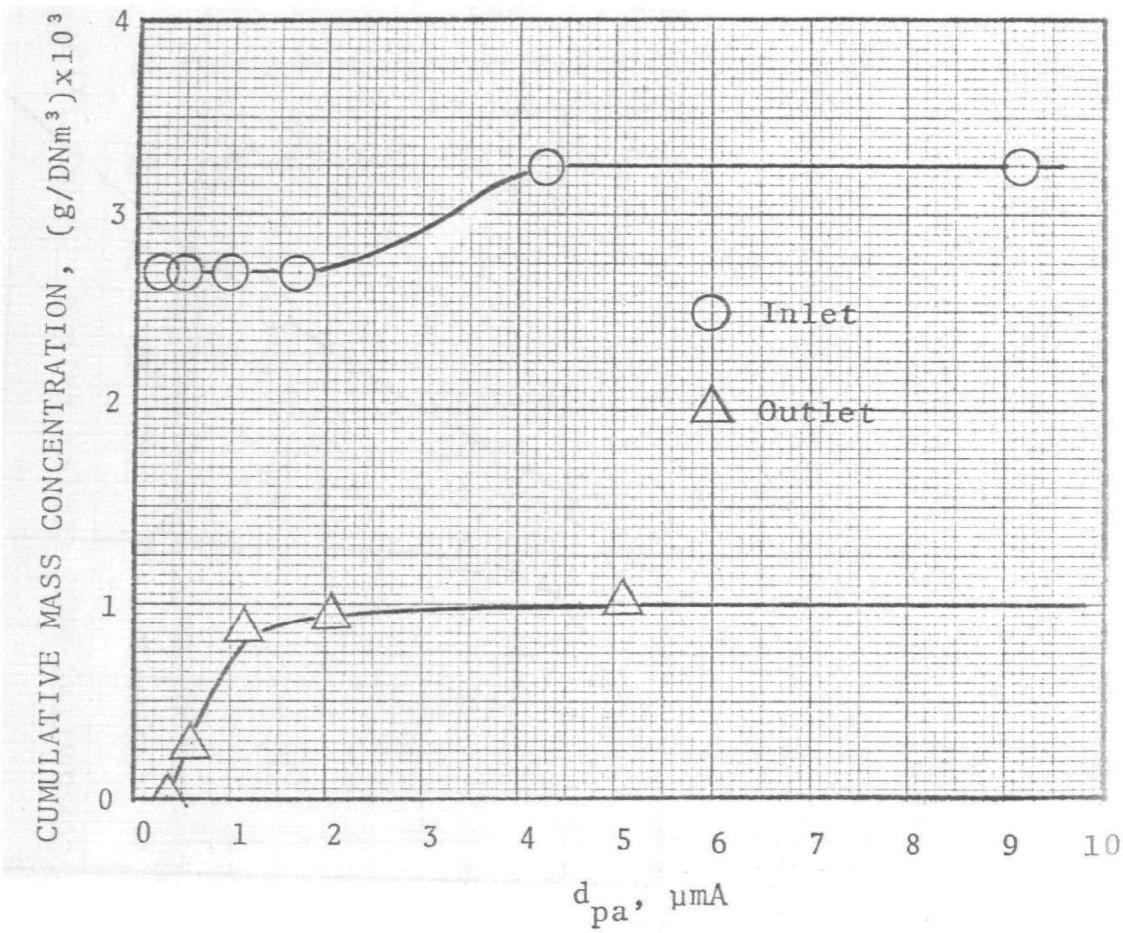

Figure 8-C-5 - Mass concentration distribution for run #5.

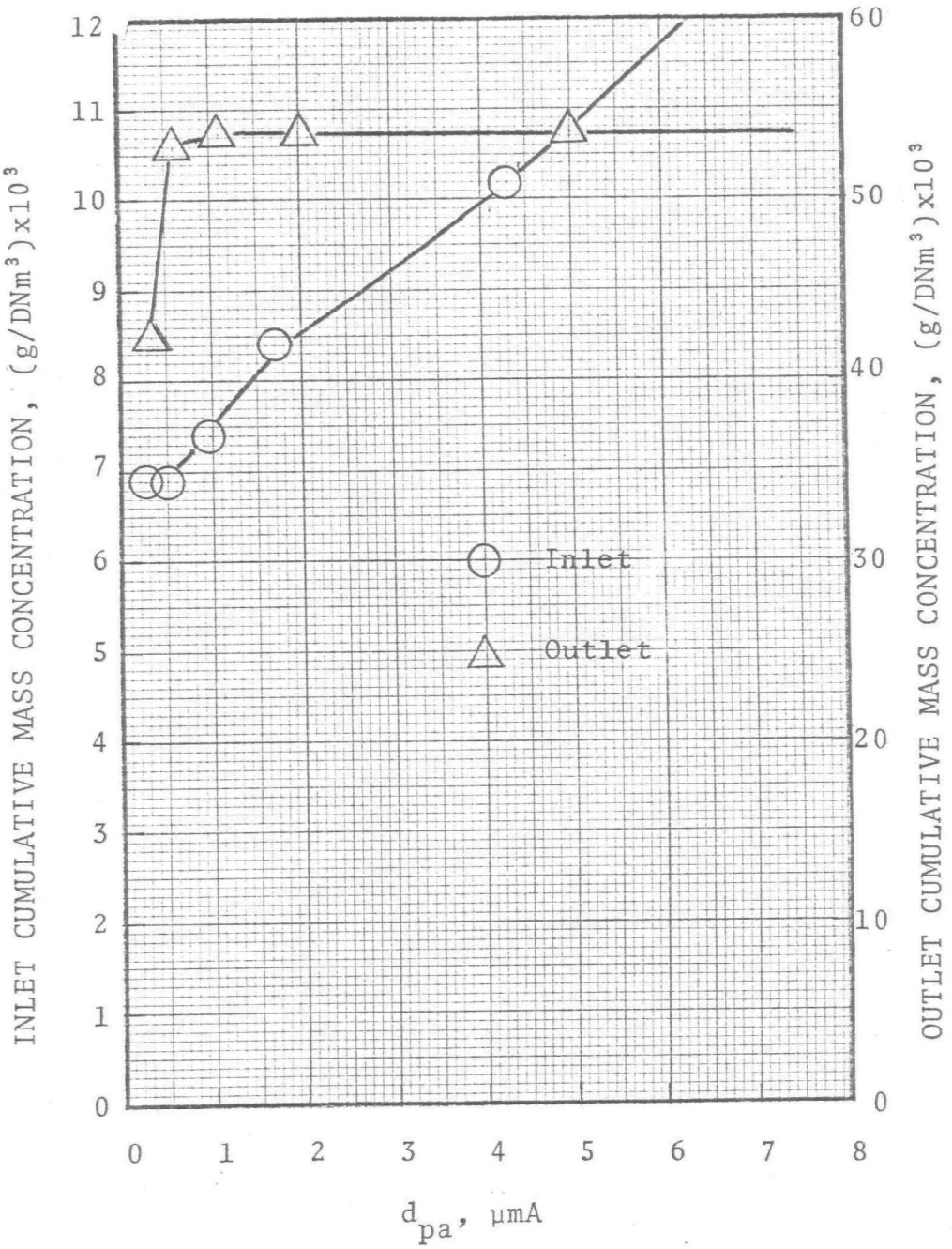

Figure 8-C-6- Mass concentration distribution for Run #7.

VENTURI ROD SCRUBBER ON CUPOLA

SOURCE AND SCRUBBER

An Environeering Venturi-rod scrubber (Model A33 Hydro-Filter) was the subject of performance test no. 8. This device consists primarily of several parallel rods which are positioned in a duct with some space between the rods so that gas can flow between them (see Figures 9-1 and 9-2). Water is introduced upstream from the rod bed and is atomized by the gas stream as it flows between the rods. The basic operating mode (or unit mechanism) of this scrubber is essentially the same as for a venturi scrubber.

The scrubber is installed to control the emissions from an iron melting cupola. The gas from the operating cupola is drawn through the offtake and into the selector box. This gas is pulled into the inlet of an air-to-air heat exchanger, where it is cooled by an air stream on the outside of the exchanger tube. After passing through the heat exchanger the gas enters a quench-dropout box where pre-cleaning and quenching take place. All the large particles drop out in the quench section and they are water washed down the quench-dropout box drain and deposited in one of the sludge tanks.

This scrubbing system consists of:

1. A quench section to reduce temperature of offtake gases prior to their entry into the Hydro-Filter.
2. A venturi-rod section to provide high energy contact of particulate with scrub liquor.
3. A demisting section for removal of scrubbing liquor drops from the cleaned gas stream.

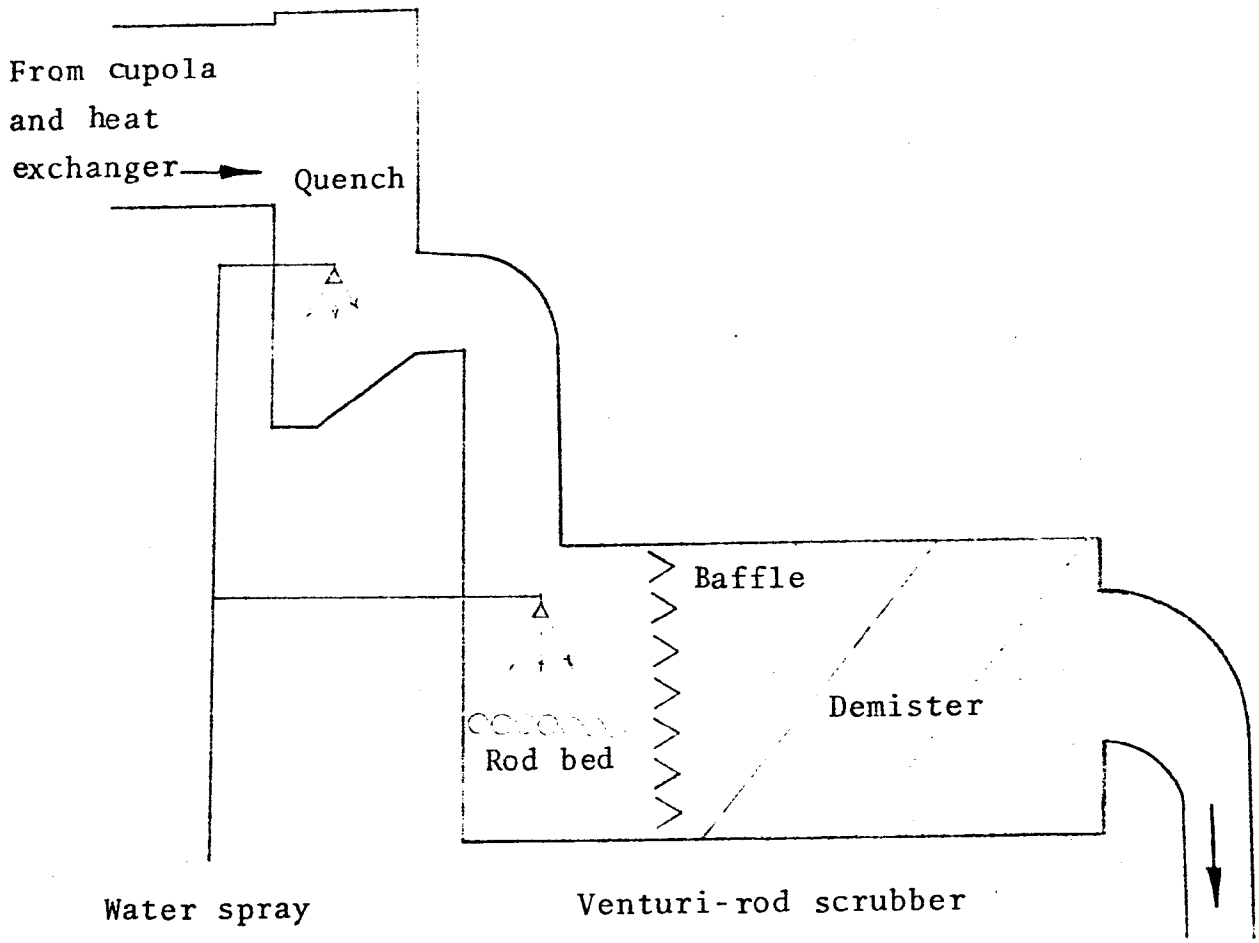

Figure 9-1 - Schematic diagram of scrubber system

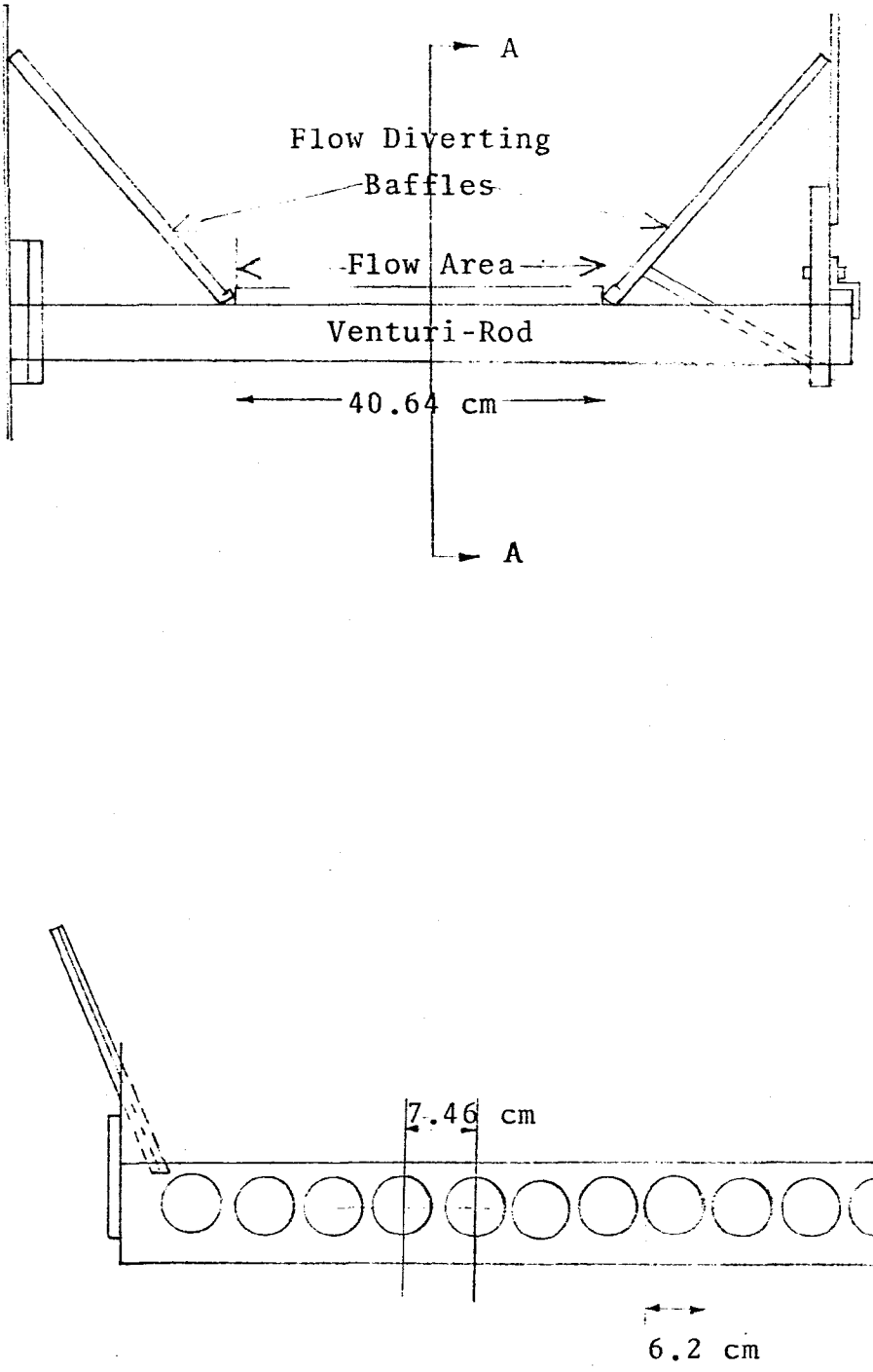

Figure 9-2 - Schematic diagram of venturi-rod bed

The quenched gas is drawn through the venturi-rod where the high energy scrubbing takes place. The particulate laden water is then washed down the Hydro-Filter drain and deposited into the recycle section of one of the sludge tanks.

The scrubbed gas is drawn through the stainless steel demister vanes, where the free water is removed from the gas. The gas is then drawn into the primary and secondary fans and discharged up the stack. In the stack, the scrubbed gas is mixed with the heat exchanger cooling air (at 200°C). This reduces the steam plume and it improves stack appearance.

TEST METHOD

The performance characteristic of the scrubber is determined by analyzing the particle size distribution and mass loading of the scrubber inlet and outlet gas sample.

A modified E.P.A. Method 5 train with an in-stack University of Washington Mark III (or Pilat) cascade impactor was used for particle measurements. The impactors in the inlet and outlet were allowed to heat up to stack temperature before the samples were taken. Gas flow rate was determined by means of type "S" pitot tube traverses along with the necessary temperature and pressure measurements. Sample flow rates were measured with the usual E.P.A. train instruments so as to obtain isokinetic sampling.

The inlet sampling point was located between the quencher and the venturi-rod scrubber. Outlet samples had to be taken after the fan because the negative pressure after the demister was too high (-280 cm W.C.) for the

sampling system to handle. The temperature and pressure of the gas in the duct after the demister were measured.

A total of 13 simultaneous sampling runs were conducted and four of these were discarded due to cupola shutdown during sampling. The remaining 9 runs were grouped into three data sets, namely A, B, C (Run No. 1, 2, 3 as set "A", Run No. 7, 9, 10 as set "B", and Run No. 11, 12, 13 as set "C"), corresponding to different operating conditions, as discussed later. All runs were sampled isokinetically with the sampler being held at one position in the duct.

This is generally an adequate technique for obtaining good samples of particles smaller than a few microns diameter because they are well distributed across the duct. It does not provide a representative sample of the large particles when the nozzle inlet is close to a flow disturbance; as in the case of the outlet sample, which was taken 3 feet downstream of a bend. Thus, the total particulate loading is uncertain because of the one position sample but the fine particle concentration is representative of the entire gas stream.

OPERATING CONDITIONS

The scrubber operating conditions during the test period were as follows:

1. Gas flow rates were as shown in the tabulation below:

DUCT	INLET	OUTLET	
		After demister	After fan
Temperature	(190°F)	(150°F)	(160°F)
Pressure during pitot run	-6.5 cm H_2O	-280 cm H_2O	+13 cm H_2O
A m^3/min	1,274		
ACFM	45,000		
DN m^3/min	780		
DSCFM	29,270		
Vol. % H_2O vapor	19		16

2. Water flow rate to the Hydro-Filter system was reported by the plant as approximately 1.0 m^3/min (265 GPM) sprayed in the quencher and 3.0 m^3/min (800 GPM) sprayed in the venturi-rod bed. Make-up water was estimated at 0.26 m^3/min (70 GPM) which consisted of 0.19 m^3/min (50 GPM) evaporated and 0.076 m^3/min (20 GPM) blow down. The temperature of the spraying water was 24°C (75°F). The temperature of the sludge washed out of the quencher box was 71°C (160°F) and temperature of the venturi-rod bed sludge holding tank was 65°C (150°F).
3. Entrainment is known to be excessive, because it causes fan unbalance, but was not measured in this test series. Scrubber user indicated the slurry blow down was 0.076 m^3/min (20 GPM).

PARTICLE DATA

Three sets of data (3 simultaneous pairs in each set) were obtained. These data sets were obtained at different sampling locations and different plant operating conditions. Particle concentration and size for these runs are presented in Tables 9-A-1 to 9-A-9. Size distributions for these runs are shown in Figures 9-B-1 to 9-B-3. The run numbering system used here is that "a" denotes the inlet sample and "b" is assigned to outlet sample in a simultaneous sampling run (designated by the number).

Data sets "A" and "C" were taken under the same plant operating conditions (melting ductile iron) but at different sampling locations. Data set "B" was obtained when the scrubber user was melting gray iron.

As seen in Figures 9-B-1 to 9-B-3, particles have the following mass median and geometric standard deviation.

DATA SET	INLET		OUTLET	
	d_{pg} (μmA)	σ_g	d_{pg} (μmA)	σ_g
"A" (ductile)	0.92	2.0	0.69	2.1
"B" (gray)	1.15	1.7	0.62	2.0
"C" (ductile)	0.94	2.1	0.62	1.8

A diffusion battery was used to obtain information about the size distribution of particles smaller than 0.3 μmA. This was done by connecting the diffusion battery to the outlet of the U.W. impactor (without backup total filter). The diffusion battery was kept outside the stack and was heated to stack temperature with heating tapes. The arrangement is shown in Figure 9-3. Particle number concentration in the inlet and outlet stream of the diffusion battery was counted by a Gardner condensation nuclei counter. In this performance test, particle number concentration was so high that the condensation nuclei counter was overloaded even with 5 to 1 clean air dilution (5 parts of clean air to 1 part sample gas), and the Gardner CNC was not stable. For these reasons, only one run, namely 4b, was successful. The inlet and outlet number concentration of the diffusional battery for this run were 7×10^3 particles/cm^3 and 3×10^3 particles/cm^3 respectively. This gives a penetration of 0.43. Based on our design of the battery, this corresponds to a 0.05 μm particle diameter cut point, or an aerodynamic diameter cut point of about 0.2 μmA if particle density is about 3 g/cm^3. Unfortunately, the impactor portion of this run was purged due to cupola shutdown during sampling.

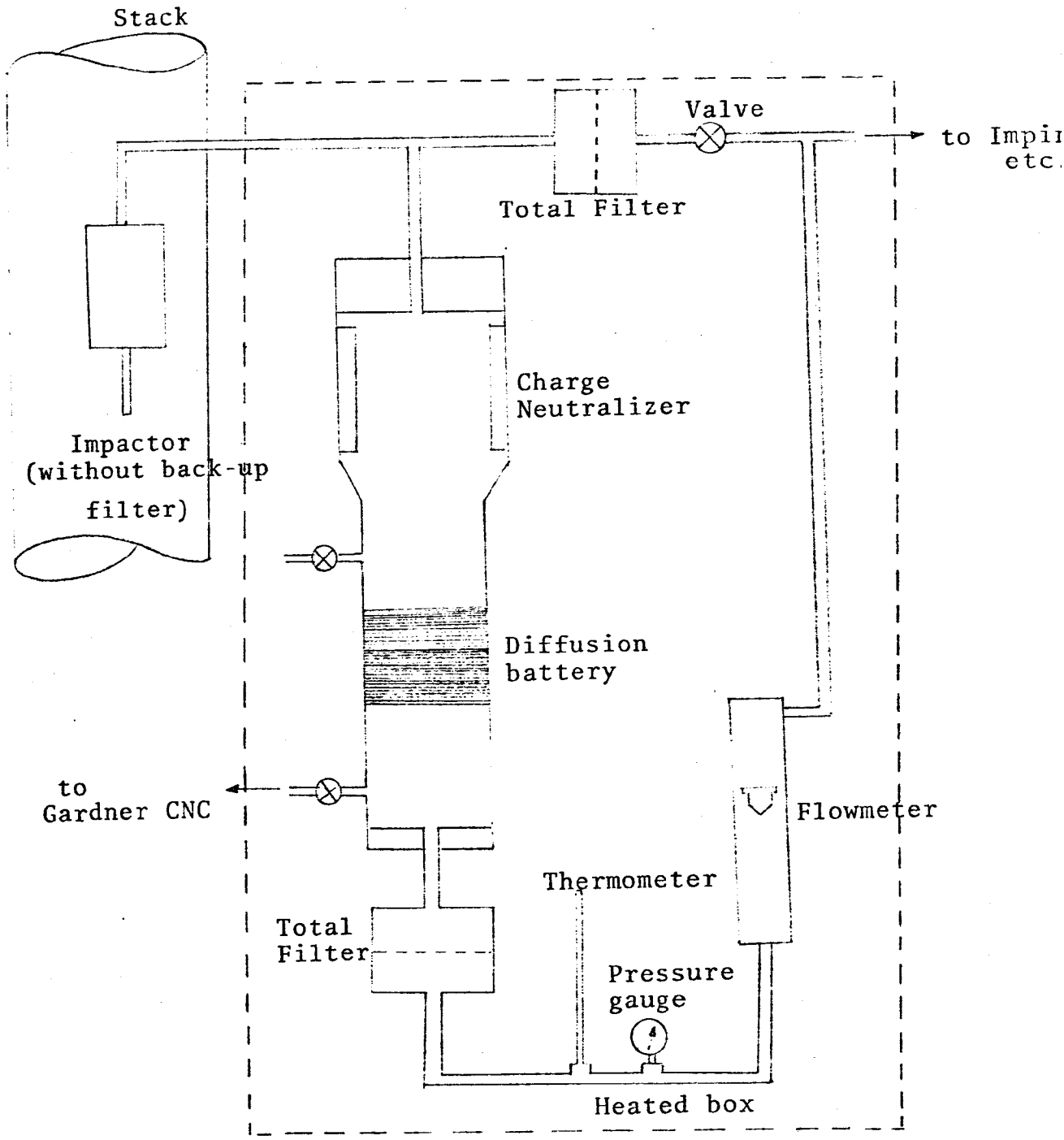

Figure 9-3 - Diffusion battery assembly

Several simultaneous total filter runs were conducted. However, due to the clogging of the filter by water droplets even with a precutter ahead of the filter (the cut diameter of the precutter is 10 μmA), no total particulate loading data were available.

Plume opacity was 15% for runs #1, 2, 3, 11, 12, 13 and 10% for runs #7, 9, 10. All opacity readings were taken by visual observation method by an observer trained in a California Air Resources Board "smoke school".

PARTICLE PENETRATION

Particle penetration was computed and is shown in Figures 9-4 through 9-6. It was calculated by the following method:

Cumulative mass concentration vs. aerodynamic particle diameter data were fitted with a curve by eyeball method. The slopes of these curves (Figs.9-C-1 to 9-C-9) were measured by a graphical technique at several values of particle diameter. The ratios of outlet to inlet slopes were computed to yield penetrations at the several diameter values.

ECONOMICS

The cost of installing and operating air pollution equipment is a function of many direct and indirect cost factors. These factors can be grouped into two cost categories; initial costs and annual costs.

1. Initial costs

   The initial installed costs of the scrubber system (1970) are listed below:

   Scrubber Purchase Cost

a.	F.O.B. Wet Scrubber	$ 14,154
b.	Freight	1,104
	Total	$ 15,258

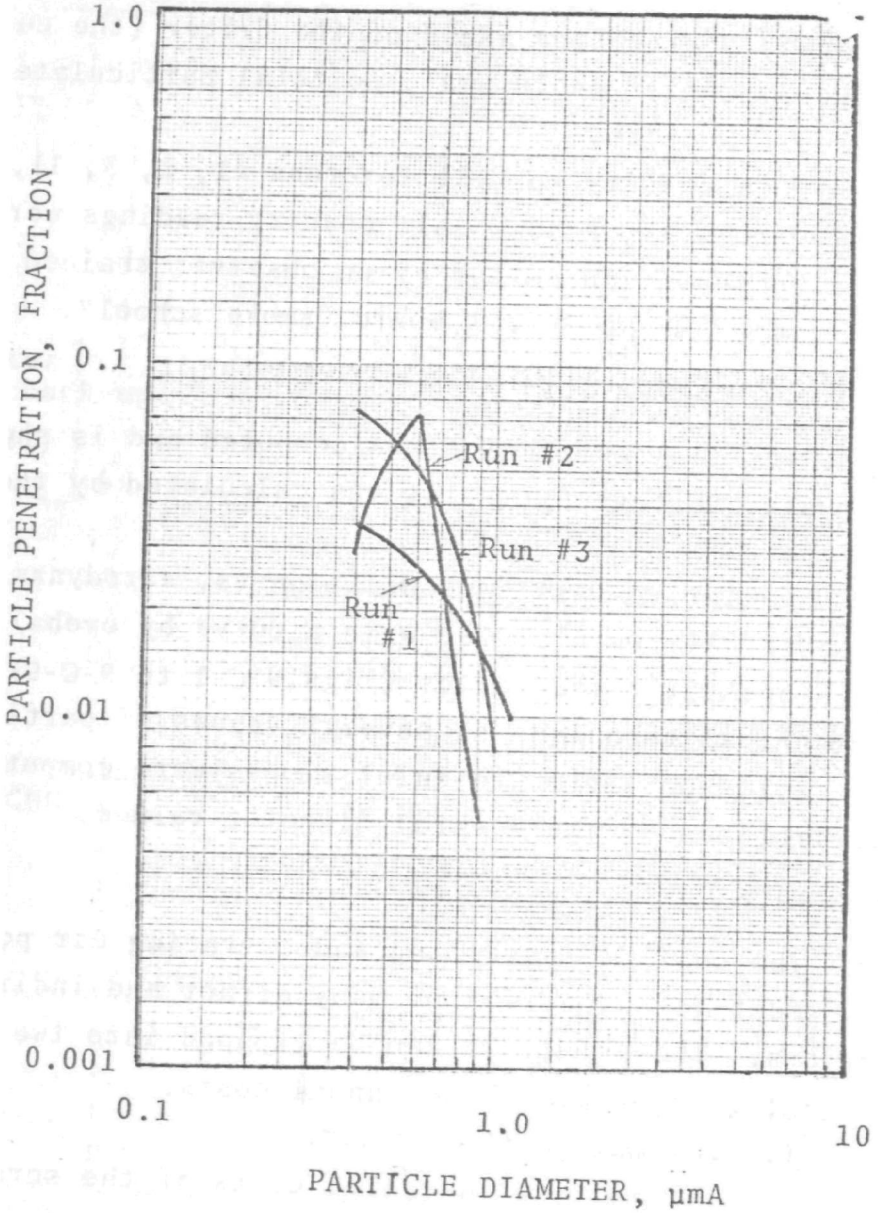

Figure 9-4 - Particle penetration versus diameter for venturi-rod scrubber (data set "A")

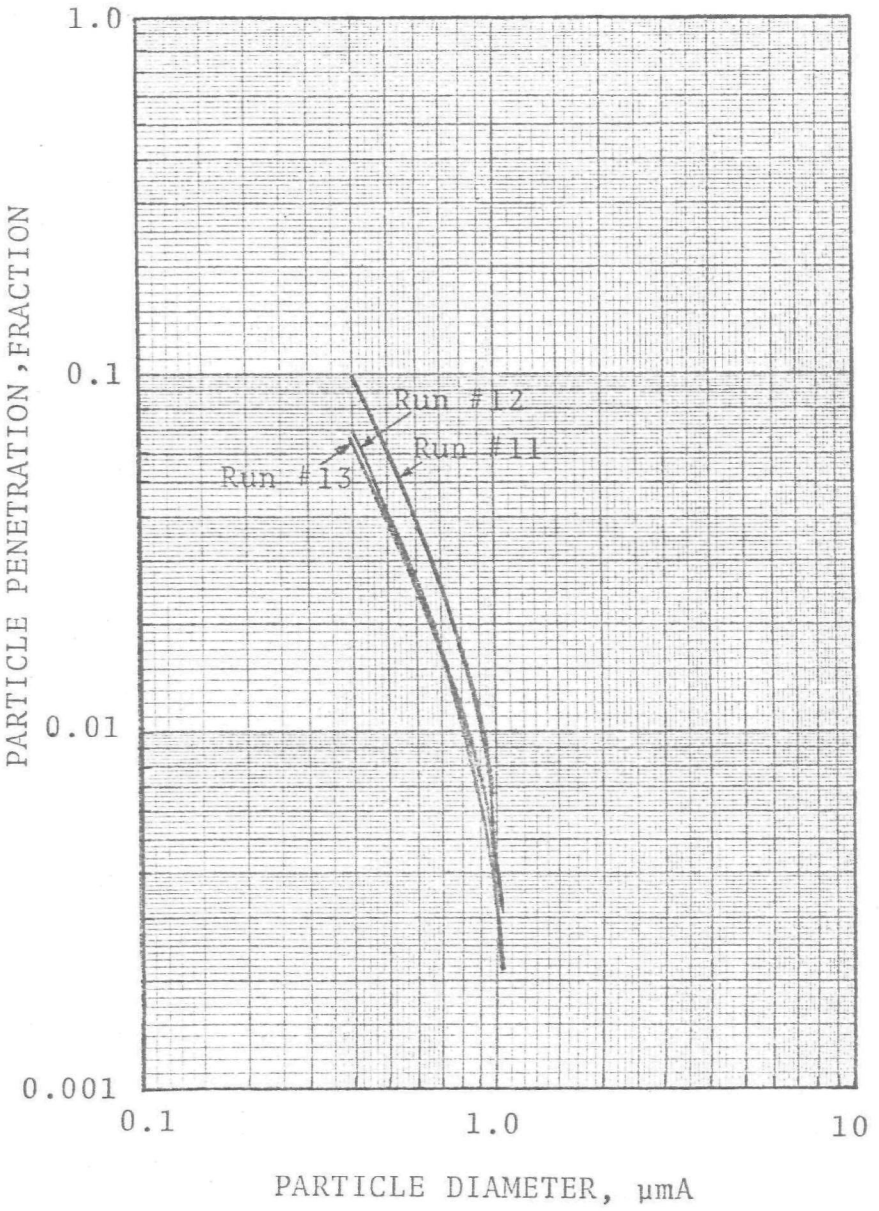

Figure 9-5 - Penetration versus particle diameter for venturi-rod scrubber (data set "C")

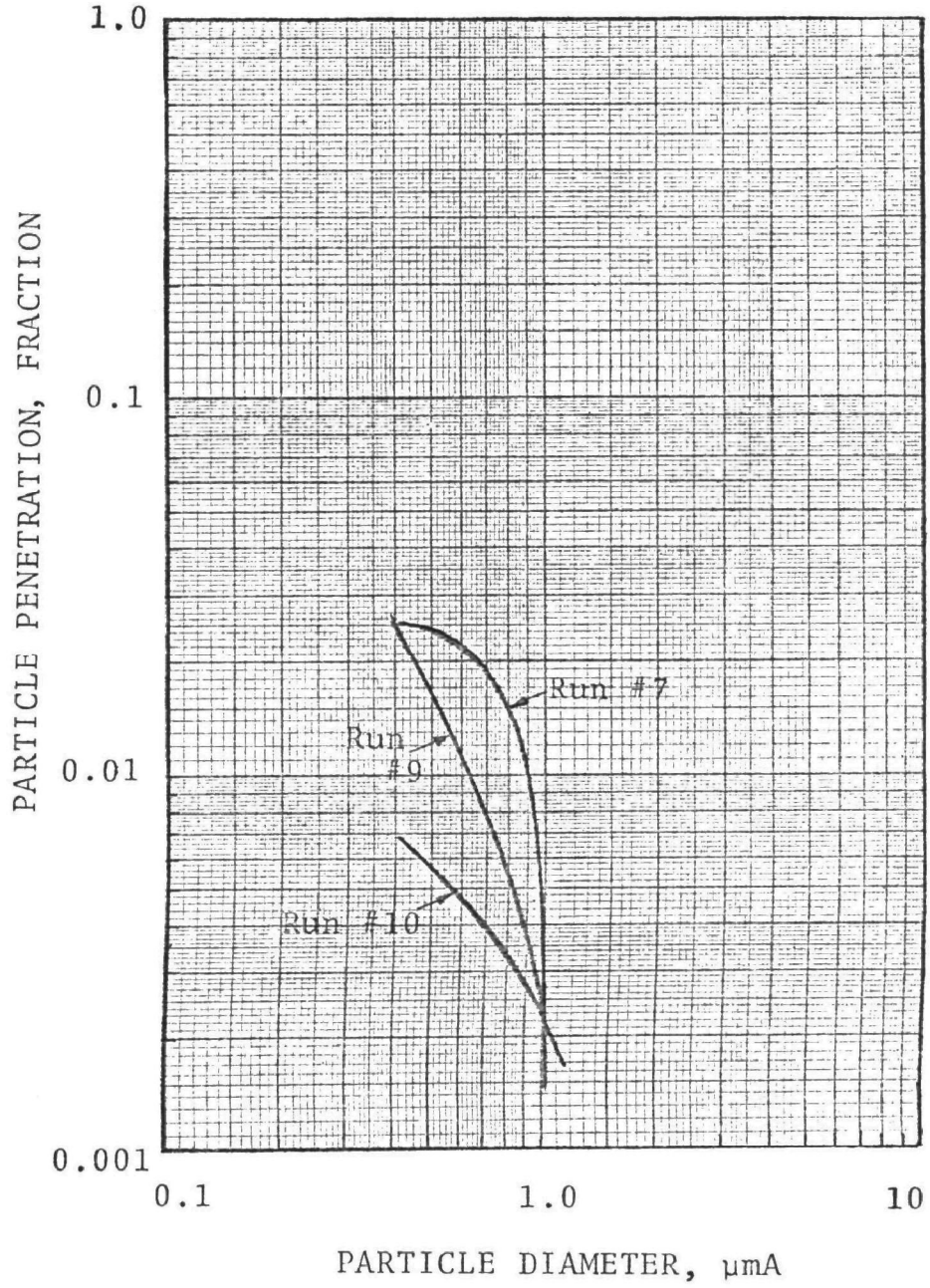

Figure 9-6 - Penetration versus particle diameter for venturi-rod scrubber (data set "B")

Scrubber Auxiliaries

a.	Fans, motors and motor starters	$119,046
b.	Ducting	78,086
c.	Liquid and solid handling and treatment	38,090
d.	Instrumentation	6,750
e.	Electrical material	10,694
	Total	$252,666

Scrubber Installation Cost

a.	Site preparation, including foundations and supports	$ 16,465
b.	Modifications in existing processes	88,764
c.	Installation	75,147
d.	Start-up and modification	72,951
e.	Engineering	36,000
	Total	$289,327

Total Initial Cost (1970 prices) $557,251

2. Annual Costs

Annual Costs include the following factors

Operating Costs

a.	Utilities	$ 80,000
b.	Labor	20,000
c.	Supplies and Materials	9,000
d.	Treatment and Disposal	4,000
	Total	$113,000

Maintenance Costs

a.	Labor	$ 44,000
b.	Materials	6,000
	Total	$ 50,000

Plant overhead, space, heat, light, insurance, etc.	$ 7,000
Total Annual Costs	$170,000

OPERATING PROBLEMS

Several points relating to operating problems for the scrubber system are listed below:

1. Entrainment separation has not been satisfactory with the result that it causes fan unbalancing even with chemical spray to minimize deposits on fan blades.
2. Scrubbing water is recycled to reduce its consumption. However, the sludge holding tank is too small to allow solids to settle and clarify the scrubbing water. Therefore, some solids are recycled to the scrubber and eventually cause the nozzle plug-up problem.
3. The pressure drop across the venturi-rod bed is about 260 cm W.C. (100"W.C.) and the throat velocity is very high. This induces erosion problems, especially on tube supports, scrubber bottom and back plates.
4. Some quencher liquids are washed down to the venturi-rod scrubber. The liquor contains large amounts of solids which settle in the scrubber.

MATHEMATIC MODEL

A major objective of the scrubber performance test is to compare the measured particle collection with that predicted by mathematical models and/or further improvement of the models which can be used for prediction of performance.

The venturi-rod scrubber is essentially several venturis or orifices connected in a parallel arrangement. A method for prediction of performance for gas atomized scrubbers was presented in "Scrubber Handbook" and a further development is described in Chapter 2.

The operating conditions of the venturi-rod scrubber were

1. Total gas flow rate is 21 m^3/sec which gives a throat velocity of 196 m/sec (643 ft/sec)
2. The liquid flow rate is 50 ℓ/sec, corresponding to Q_L/Q_G = 2.4 ℓ/m^3
3. Pressure drop across the rod-bed is 275 cm W.G.

The "Scrubber Handbook" presented an equation (Eq. 5.3.6-10) for estimating the pressure drop through a venturi scrubber by assuming that all energy is used to accelerate the liquid to the throat velocity of the gas. Based on this equation, we calculated the pressure drop across the rod-bed would be 916 cm W.G. However, measurements showed the drop was only 275 cm W.G. This is an indication that the liquid droplets are only accelerated to about half the gas throat velocity. This is probably due to the short exposure time of the droplets in the "throat" between the pipes. At a velocity of 197 m/sec (647 ft/sec) the gas moves a distance of 1 pipe diameter (6.2 cm) in about 0.0003 sec.

Because the mathematical model given in the "Scrubber Handbook" was based on the assumption that the liquid is accelerated to the throat velocity, it seemed less appropriate than the cut diameter - pressure drop correlation. The latter relationship should account for the opposing

effects of higher relative velocity and shorter exposure time in the venturi rod than in the venturi scrubber. Consequently, cut diameters were predicted by means of Figure 9-7 for a pressure drop of 275 cm W.C. and values of f = 0.25, 0.4, and 0.5; corresponding to the particles being more wettable as "f" increases.

Penetration for other particle diameters is based on the exponential variation of penetration with d_{pa}^2. The predictions so obtained are shown in Figures 9-8 through 9-10 along with experimental curves. It can be seen that the data are fairly well represented by predictions for "f" between 0.4 and 0.5 in the size range of 1.0 μmA. Smaller particles have lower penetration than predicted, based on inertial impaction, and this can be explained in part by diffusional collection.

As an estimate, we can assume that Brownian diffusion in the venturi rod scrubber, entrainment separator, and two blowers would account for the same efficiency as in a 3 sieve plate column. The predictions for 3 sieve plates (S. Calvert, 1974) are converted to aerodynamic size (assuming $\rho_p = 3.0$), as tabulated below, and plotted on Figure 9-11. The dashed line on Figure 9-11 is the estimated combined effect of inertial impaction and Brownian diffusion on particle penetration.

d_p, μm	0.015	0.032	0.053	0.11
d_p, μmA	0.1	0.15	0.2	0.3
Pt	0.22	0.5	0.65	0.8

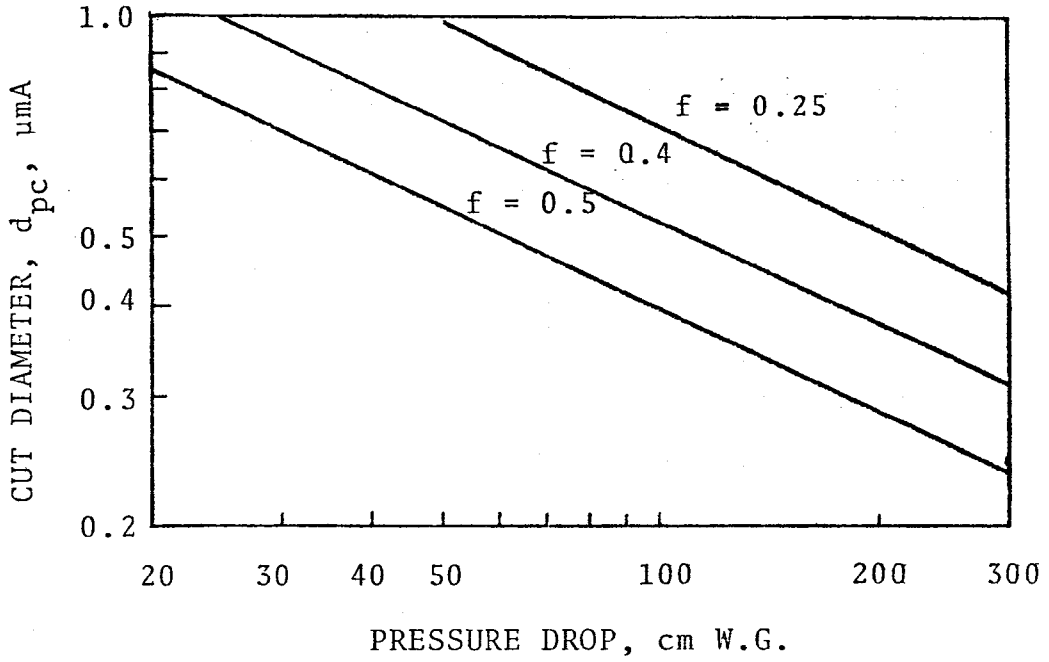

Figure 9-7 - Predicted particle cut diameter versus pressure drop for venturi scrubber.

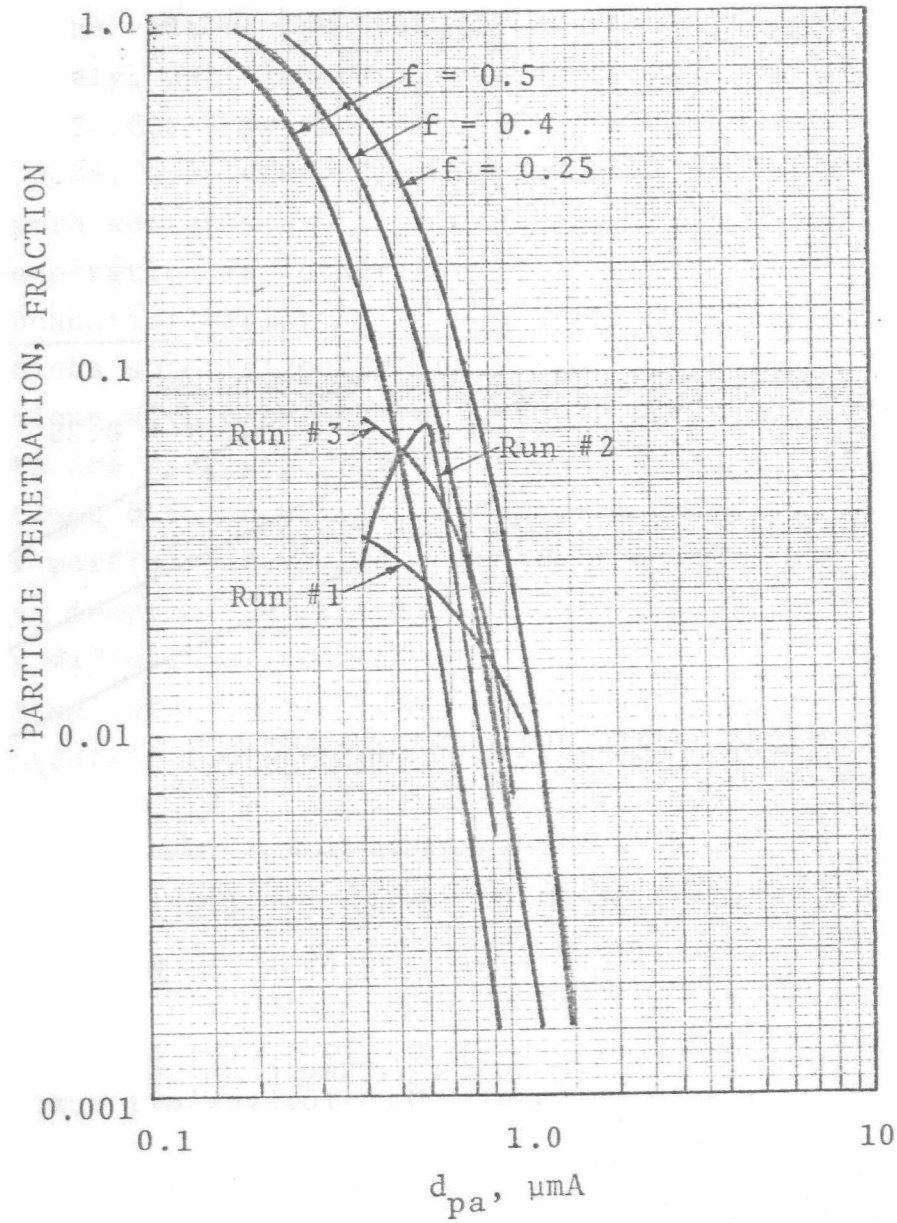

Figure 9-8 - Predicted and experimental penetration for venturi-rod scrubber (data set "A" — Ductile).

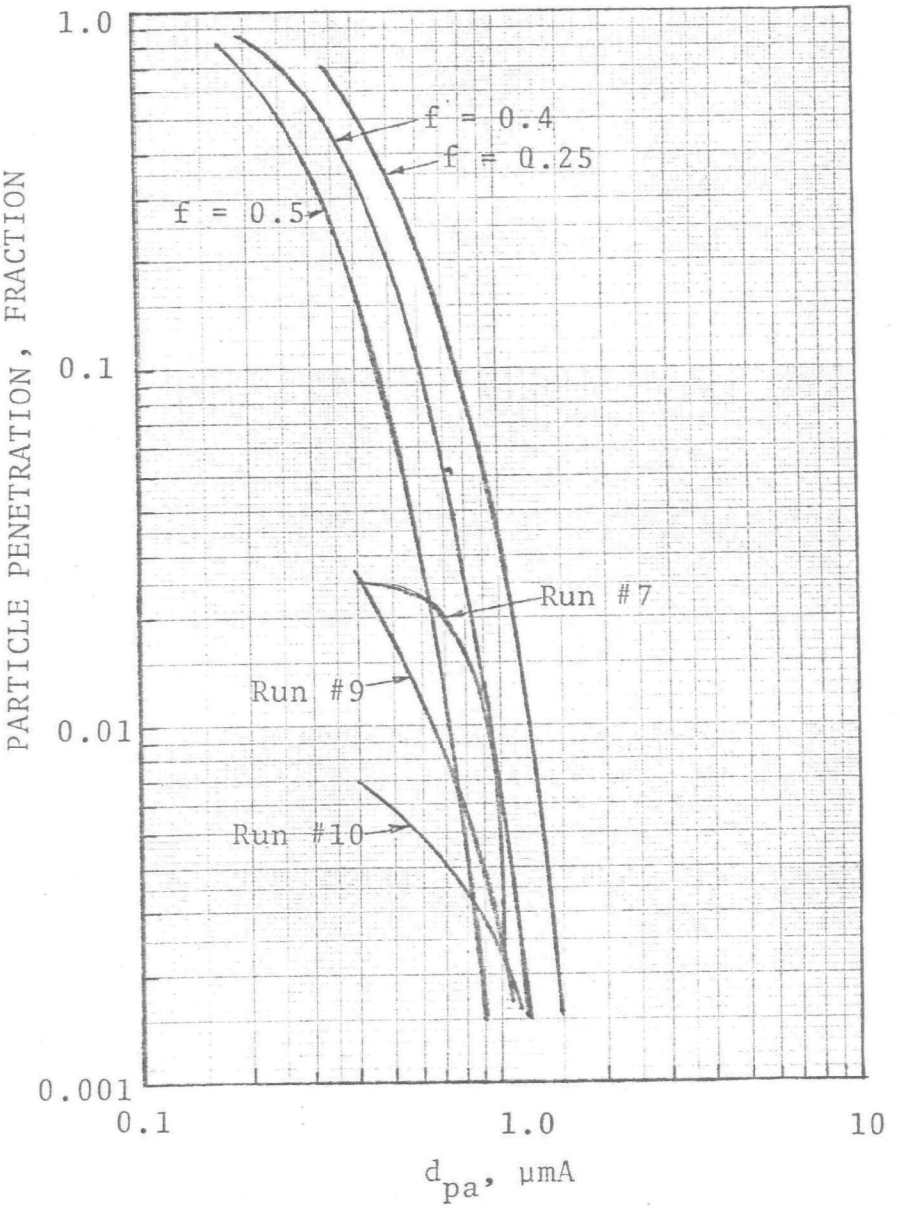

Figure 9-9 - Predicted and experimental penetration for venturi-rod scrubber (data set "B" - gray iron).

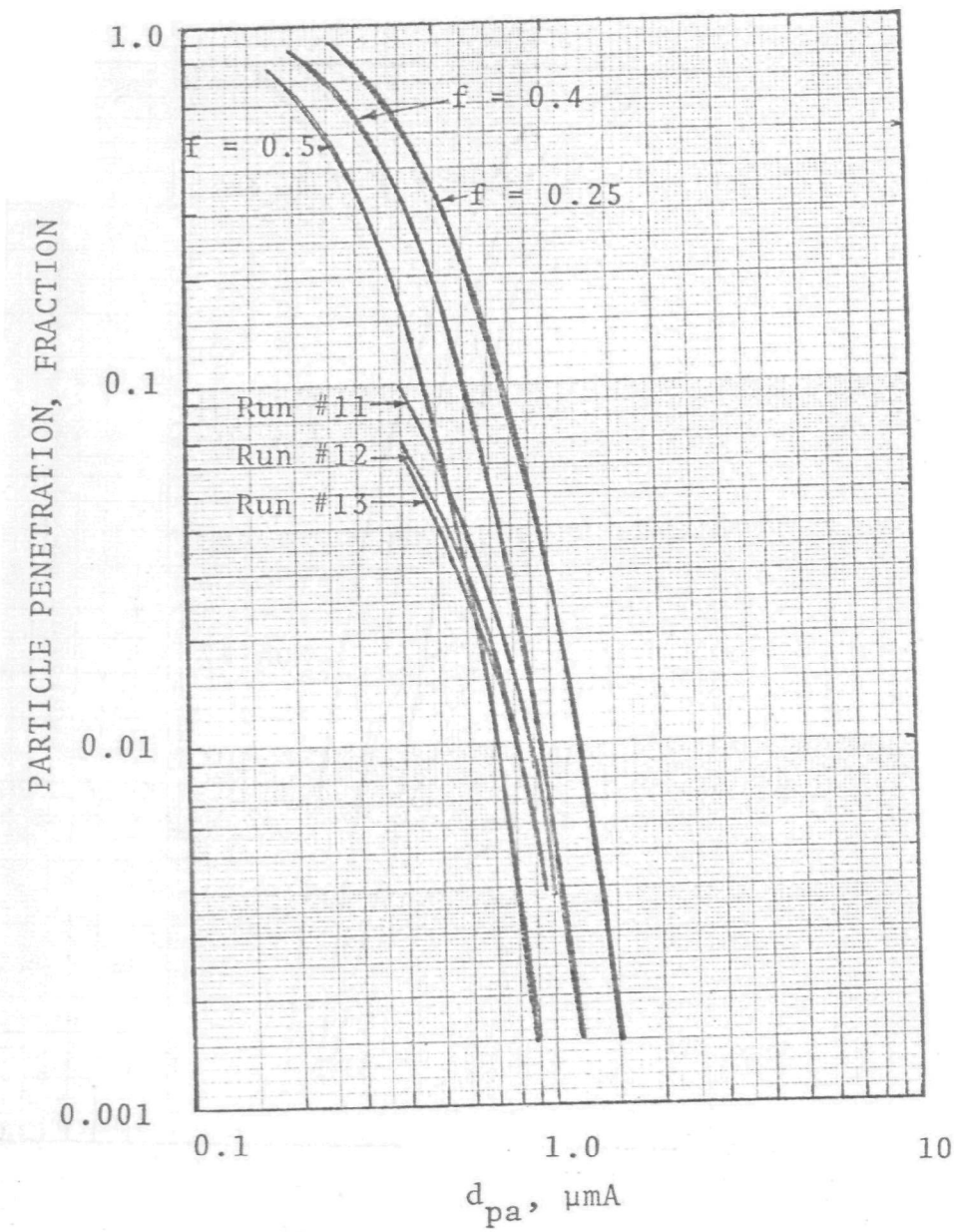

Figure 9-10 - Predicted and experimental penetration for venturi-rod scrubber (data set "C" - Ductile).

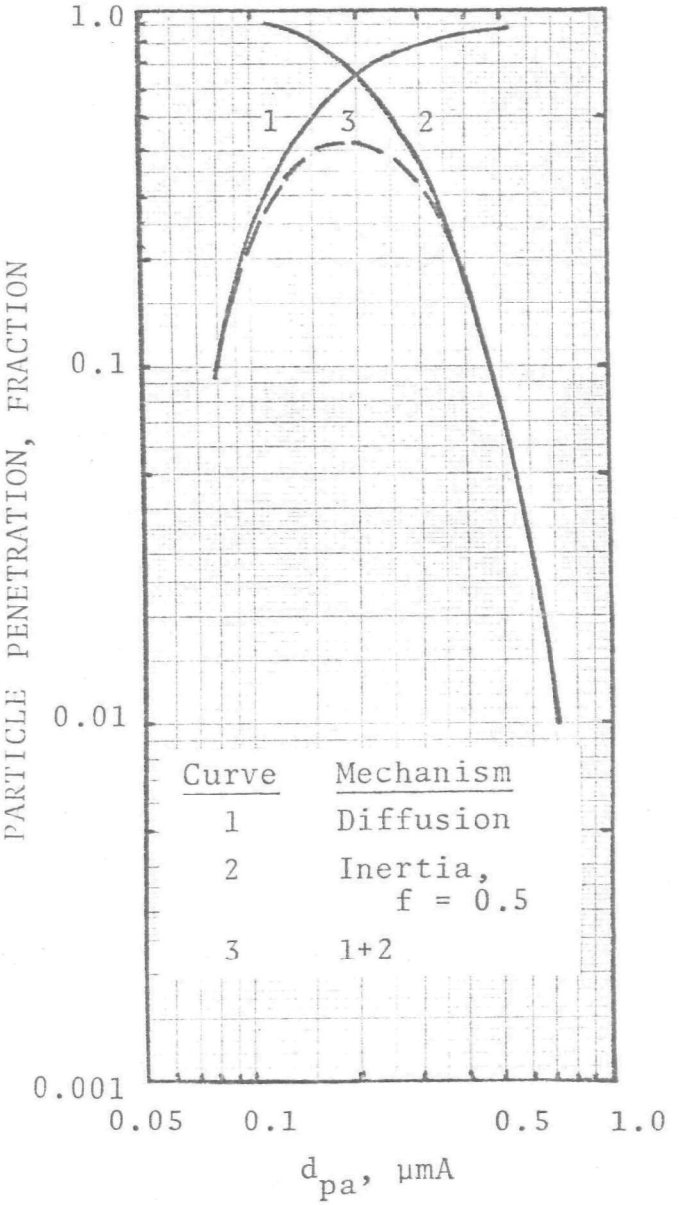

Figure 9-11 - Predicted penetration by Brownian Diffusion and Inertial Impaction

As Figure 9-11 shows, Brownian diffusion can have a very significant effect on particle penetration for sizes smaller than a few tenths micron (aerodynamic). However, the predicted penetration at about 0.4 μmA is still higher than computed from experimental data. Additional points to consider are as follows:

1. Flux force effects are unlikely to be significant because the scrubber water is recycled and little heat transfer can be obtained in the system.
2. The high velocity and extreme turbulence in the two blowers in series may be quite effective in causing particle collection; especially in the presence of the entrained liquid which reaches the blowers.
3. Particle size determination and the efficiency computation at the 0.4 μmA diameter region are dependent on the last impactor stage measurements and are subject to error. The one diffusion battery data point indicates a penetration of 43% by number for particles smaller than about 0.05 μm, corresponding to about 0.2 μmA. Because the penetration drops off so rapidly for smaller diameters, one would expect the penetration based on particle mass to be of about the same magnitude, although smaller than the number penetration.

CONCLUSIONS

Particle penetration data based on the measurements made in this test agrees with prediction in the size range of 1.0 μmA. Smaller particles have lower penetration than predicted based on inertia impaction. Improvement

of the model is needed for this type of scrubber and probably has to account for the wet fans in series with the scrubber.

The venturi-rod scrubber performance is good while it is running but numerous operating problems forced the system to be shut-down about half of the time.

High particle concentration and the stability problem of the CNC have interfered with most of the diffusion battery measurements. An efficient diluter and a more stable CNC are necessary for future work.

APPENDIX 9-A
PARTICLE DATA

Table 9-A-1. INLET AND OUTLET SAMPLE PARTICLE DATA FOR RUN #1

IMPACTOR STAGE NUMBER	INLET		OUTLET	
	M_{cum}* (g/DNm³)	d_{pc}** (μmA)	M_{cum} (g/DNm³)	d_{pc} (μmA)
1	2.336	28	0.0487	23
2	2.280	12.3	0.0487	10
3	2.275	5.7	0.0487	4.7
4	2.219	2.25	0.0484	1.85
5	2.122	1.31	0.0447	1.03
6	1.491	0.68	0.0210	0.54
7	0.804	0.375	0.0210	0.295
Filter	0.219		0.0036	
Sample Volume, DNm³	0.060		0.27	

* M_{cum} = Cumulative mass collected on that stage and those below

** d_{pc} = Cut diameter (aerodynamic) for that stage

μmA = Microns, aerodynamic = $d_p(c'\rho_p)^{1/2}$

Table 9-A-2. INLET AND OUTLET SAMPLE PARTICLE DATA FOR RUN #2

IMPACTOR STAGE NUMBER	INLET		OUTLET	
	M_{cum}* (g/DNm^3)	d_{pc}** (μmA)	M_{cum} (g/DNm^3)	d_{pc} (μmA)
1	2.280	28	0.0437	23
2	2.231	12.3	0.0437	10
3	2.209	5.7	0.0437	4.7
4	2.157	2.25	0.0426	1.85
5	2.068	1.31	0.0404	1.03
6	1.767	0.68	0.0374	0.54
7	0.722	0.375	0.0174	0.295
Filter	0.308		0.0067	
Sample Volume, DNm^3	0.041		0.27	

Table 9-A-3. INLET AND OUTLET SAMPLE PARTICLE DATA FOR RUN #3

IMPACTOR STAGE NUMBER	INLET		OUTLET	
	M_{cum}* (g/DNm^3)	d_{pc}** (μmA)	M_{cum} (g/DNm^3)	d_{pc} (μmA)
1	1.644	28	0.0515	23
2	1.622	12.3	0.0515	10
3	1.605	5.7	0.0508	4.7
4	1.563	2.25	0.0493	1.85
5	1.489	1.31	0.0457	1.03
6	1.252	0.68	0.0393	0.54
7	0.461	0.375	0.0202	0.3
Filter	0.221		0.0065	
Sample Volume, DNm^3	0.041		0.28	

Table 9-A-4. INLET AND OUTLET SAMPLE PARTICLE DATA FOR RUN #7

IMPACTOR STAGE NUMBER	INLET		OUTLET	
	M_{cum}* (g/DNm³)	d_{pc}** (μmA)	M_{cum} (g/DNm³)	d_{pc} (μmA)
1	3.522	23.5	0.0213	27.5
2	3.508	11	0.0213	10.8
3	3.505	5.15	0.0208	5.05
4	3.481	2.04	0.0208	2.0
5	3.377	1.16	0.0202	1.15
6	2.936	0.6	0.0197	0.58
7	0.532	0.33	0.0115	0.32
Filter	0.124		0.0038	
Sample Volume, DNm³	0.041		0.18	

Table 9-A-5. INLET AND OUTLET SAMPLE PARTICLE DATA FOR RUN #9

IMPACTOR STAGE NUMBER	INLET		OUTLET	
	M_{cum}* (g/DNm³)	d_{pc}** (μmA)	M_{cum} (g/DNm³)	d_{pc} (μmA)
1	3.019	26.5	0.0119	24.2
2	3.005	11.7	0.0119	10.8
3	2.995	5.4	0.0119	5.0
4	2.963	2.3	0.0119	1.97
5	2.623	1.24	0.0119	1.13
6	2.004	0.64	0.0103	0.58
7	0.218	0.36	0.0060	0.32
Filter	0.014		0.0027	
Sample Volume, DNm³				

Table 9-A-6. INLET AND OUTLET SAMPLE PARTICLE DATA FOR RUN #10

IMPACTOR STAGE NUMBER	INLET		OUTLET	
	M_{cum}* (g/DNm³)	d_{pc}** (μmA)	M_{cum} (g/DNm³)	d_{pc} (μmA)
1	2.532	26	0.0096	
2	2.467	11.6	0.0096	
3	2.460	5.3	0.0096	5.15
4	2.418	2.1	0.0096	2.04
5	2.122	1.22	0.0091	1.16
6	1.526	0.63	0.0059	0.6
7	0.225	0.35	0.0021	0.33
Filter	0.029		0.0011	
Sample Volume, DNm³	0.14		0.19	

Table 9-A-7. INLET AND OUTLET SAMPLE PARTICLE DATA FOR RUN #11

IMPACTOR STAGE NUMBER	INLET		OUTLET	
	M_{cum}* (g/DNm³)	d_{pc}** (μmA)	M_{cum} (g/DNm³)	d_{pc} (μmA)
1	2.837	26.5	0.0387	24.5
2	2.837	11.7	0.0387	]0.8
3	2.798	5.4	0.0387	5.1
4	2.793	2.3	0.0387	2.6
5	2.726	1.24	0.0381	1.14
6	2.507	0.64	0.0327	0.58
7	0.791	0.36	0.0174	0.32
Filter	0.577		0.0054	
Sample Volume, DNm³	0.02		0.18	

Table 9-A-8. INLET AND OUTLET SAMPLE PARTICLE DATA FOR RUN #12

IMPACTOR STAGE NUMBER	INLET		OUTLET	
	M_{cum}* (g/DNm³)	d_{pc}** (μmA)	M_{cum} (g/DNm³)	d_{pc} (μmA)
1	3.535	27		
2	3.483	11.8		
3	3.471	5.5		5.1
4	3.414	2.4	0.0302	2.03
5	3.214	1.27	0.0296	1.15
6	2.354	0.65	0.0279	0.595
7	0.473	0.36	0.0156	0.325
Filter	0.155		0.0034	
Sample Volume, DNm³	0.019		0.18	

Table 9-A-9. INLET AND OUTLET SAMPLE PARTICLE DATA FOR RUN #13

IMPACTOR STAGE NUMBER	INLET		OUTLET	
	M_{cum}* (g/DNm³)	d_{pc}** (μmA)	M_{cum} (g/DNm³)	d_{pc} (μmA)
1	2.522	26.5		
2	2.443	11.7		
3	2.438	5.4		
4	2.374	2.3	0.0205	2.05
5	2.201	1.24	0.0188	1.16
6	1.859	0.64	0.0172	0.6
7	0.661	0.36	0.0100	0.33
Filter	0.493		0.0039	
Sample Volume, DNm³	0.042		0.18	

APPENDIX 9-B
PARTICLE SIZE DISTRIBUTION PLOTS

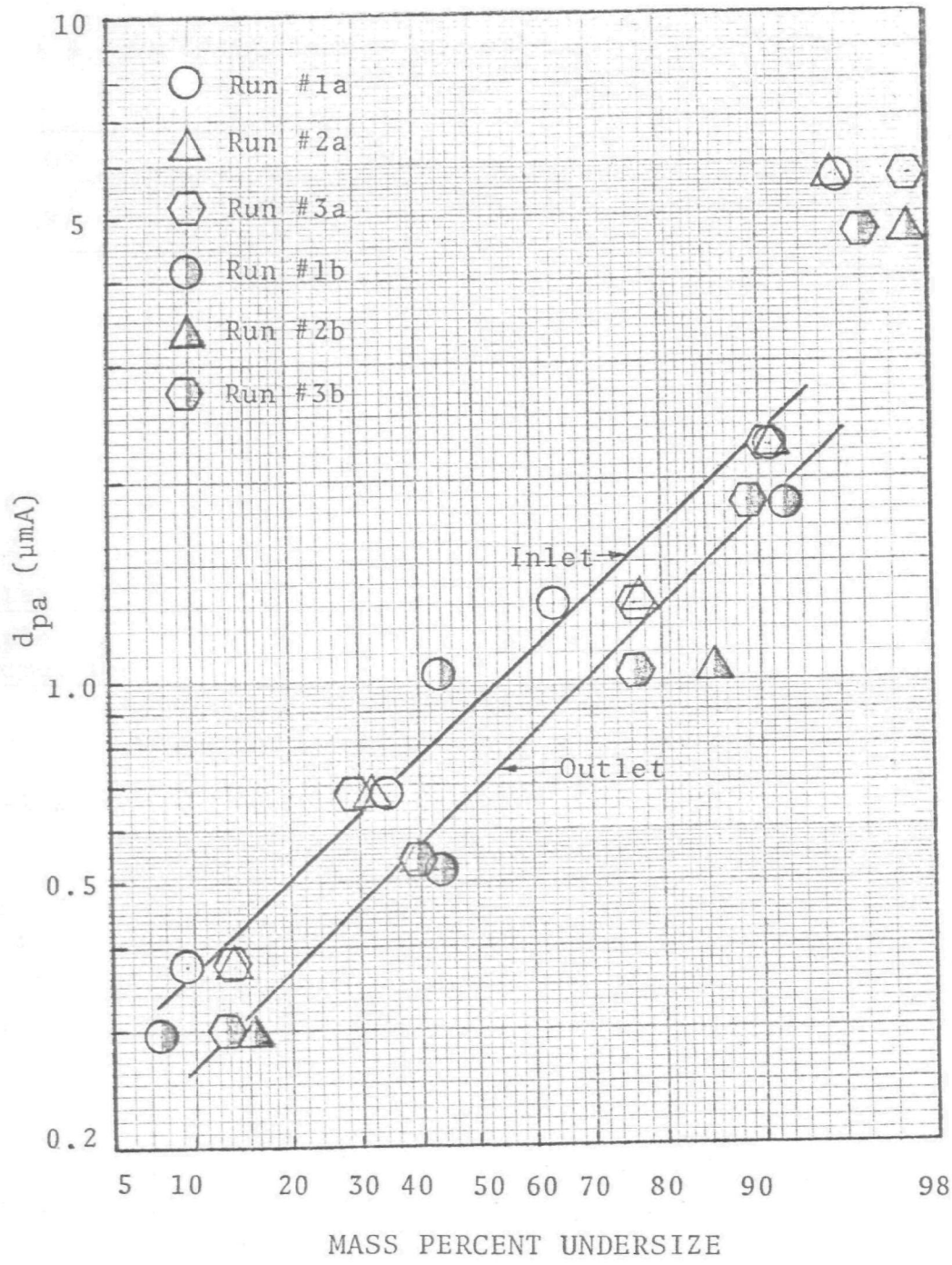

Figure 9-B-1 -Inlet and outlet size distribution (set "A")

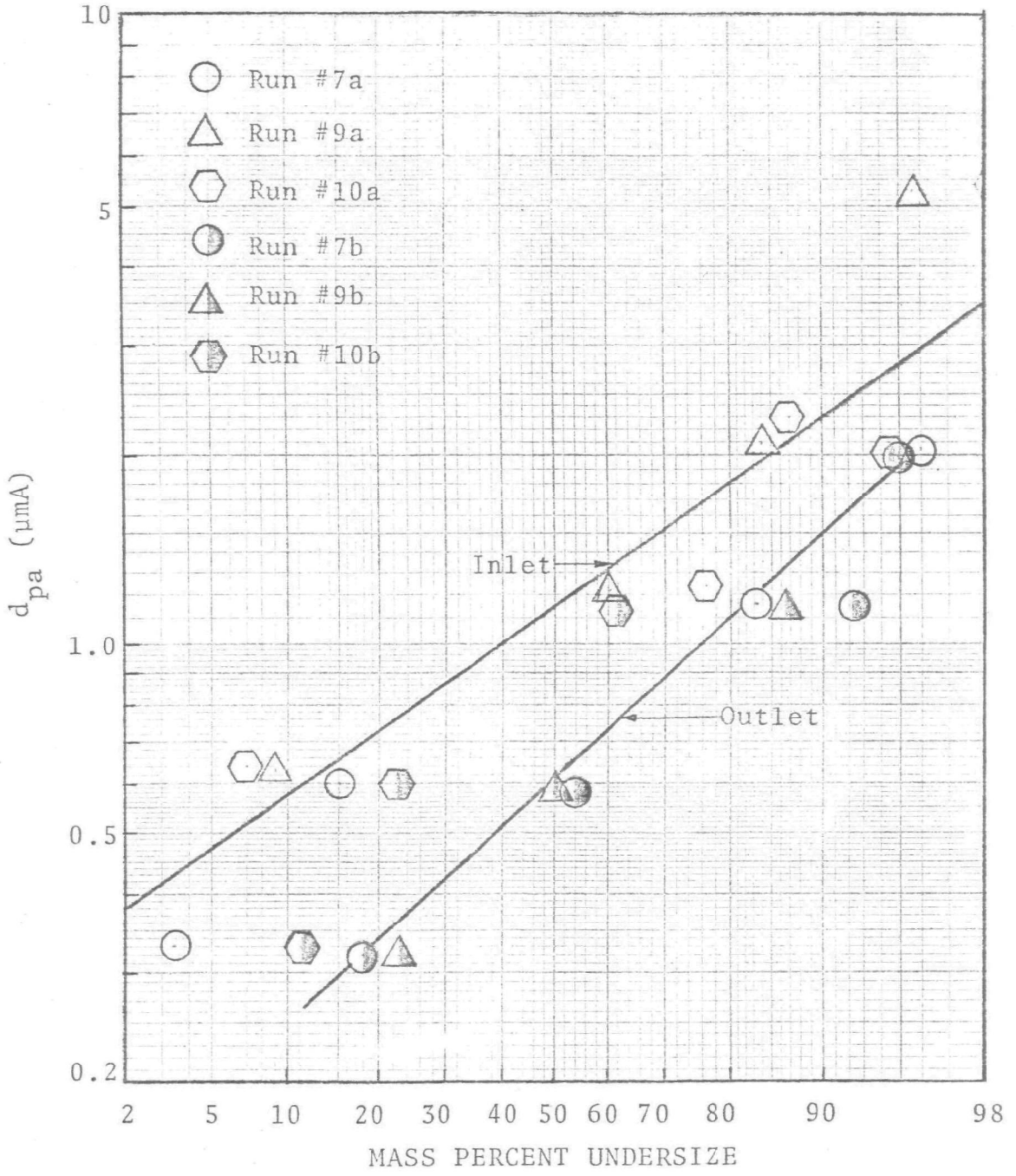

Figure 9-B-2 - Inlet and outlet size distribution (set "B")

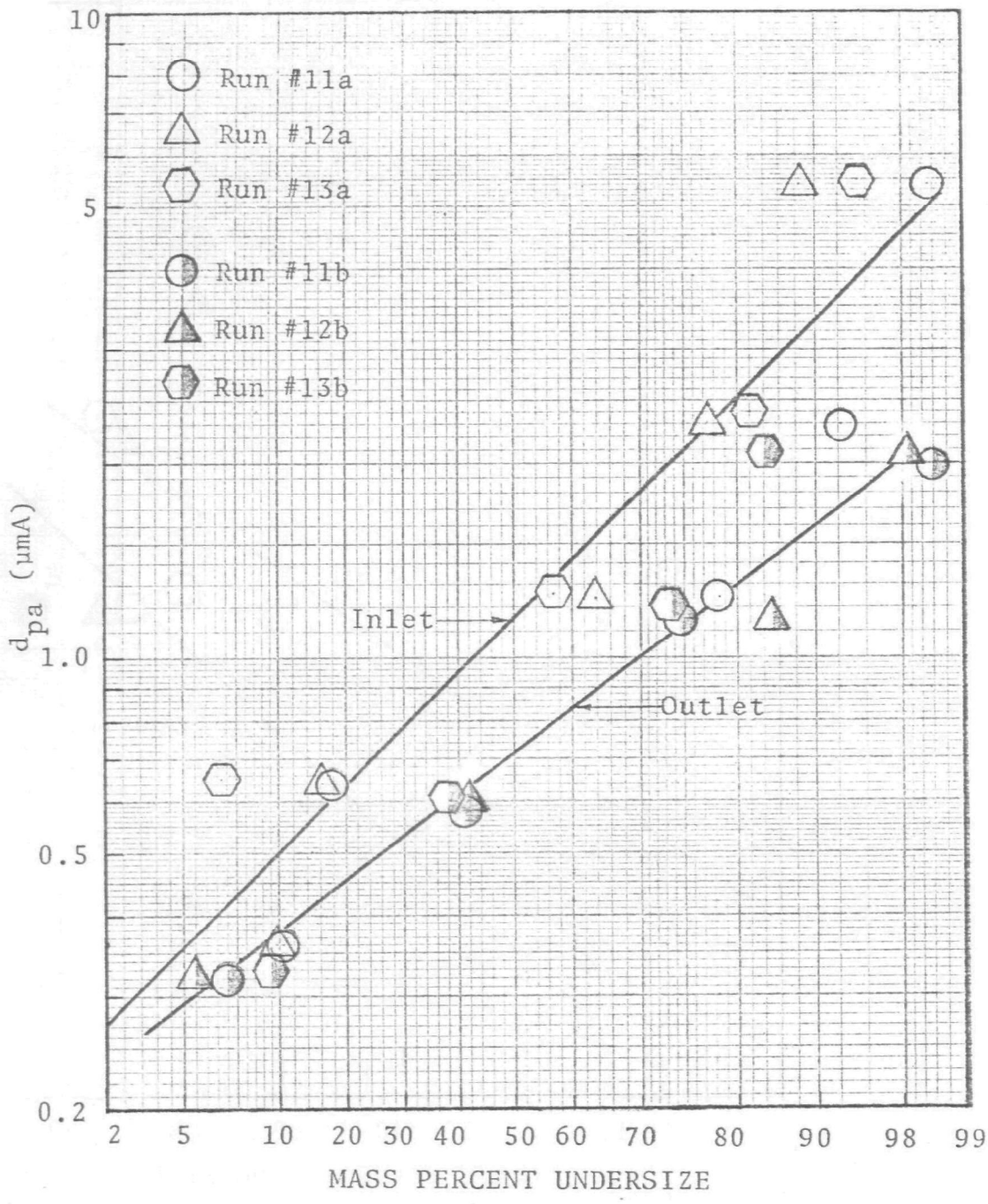

Figure 9-B-3- Inlet and outlet size distribution (set "C")

APPENDIX 9-C
CUMULATIVE MASS DISTRIBUTIONS

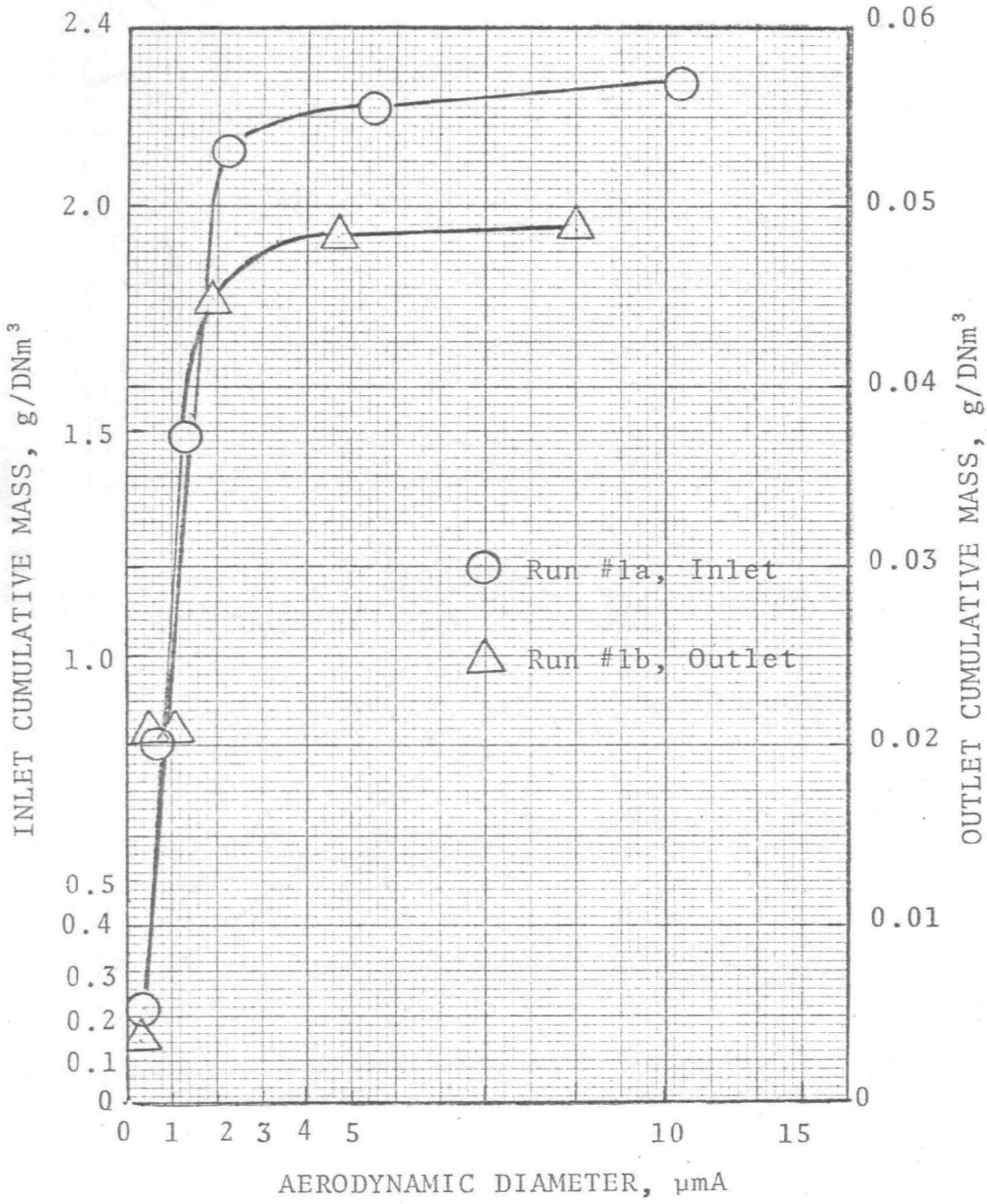

Figure 9-C-1 - Cumulative mass concentration for Run #1

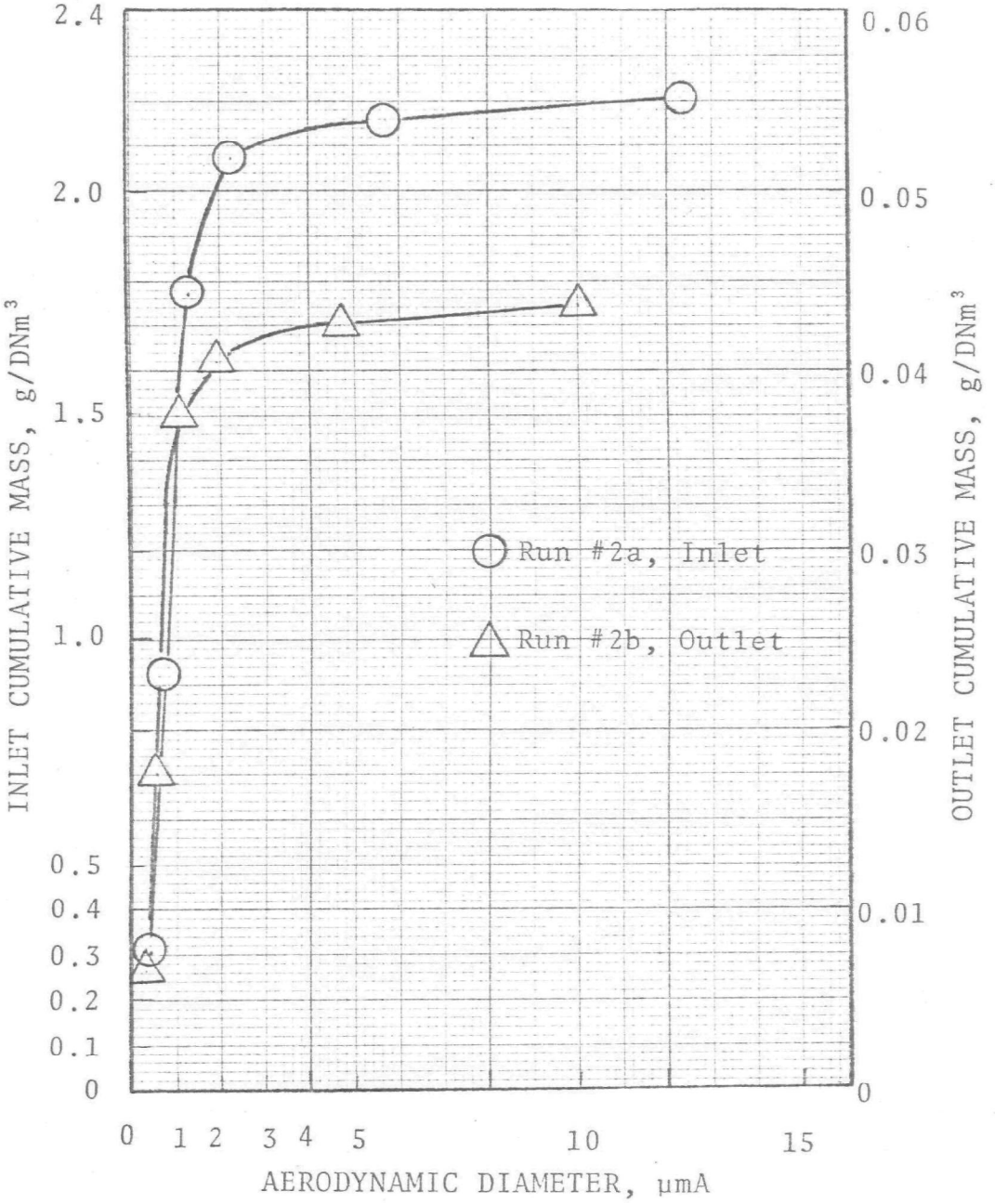

Figure 9-C-2-Cumulative mass concentration for Run #2

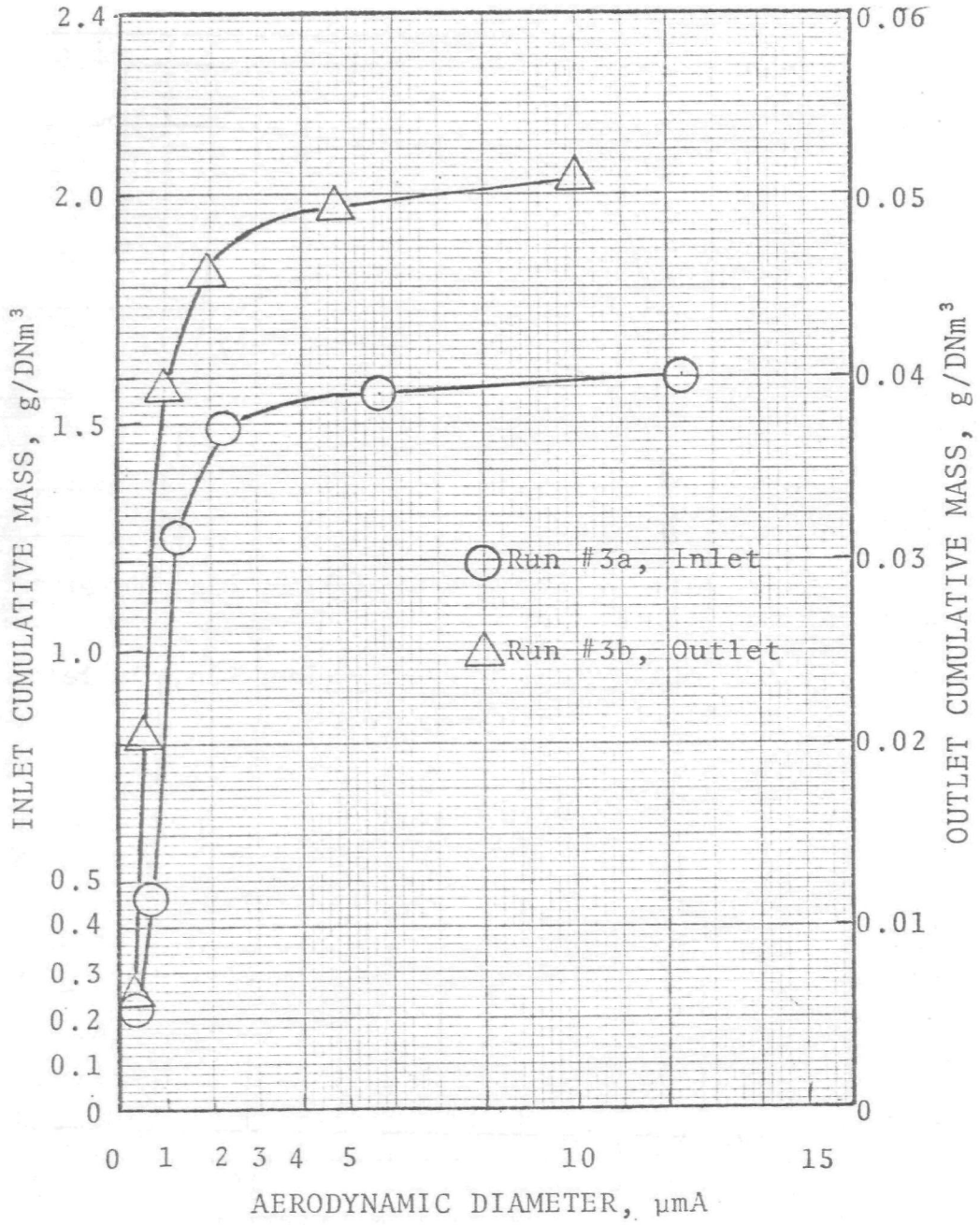

Figure 9-C-3- Cumulative mass concentration for Run #3

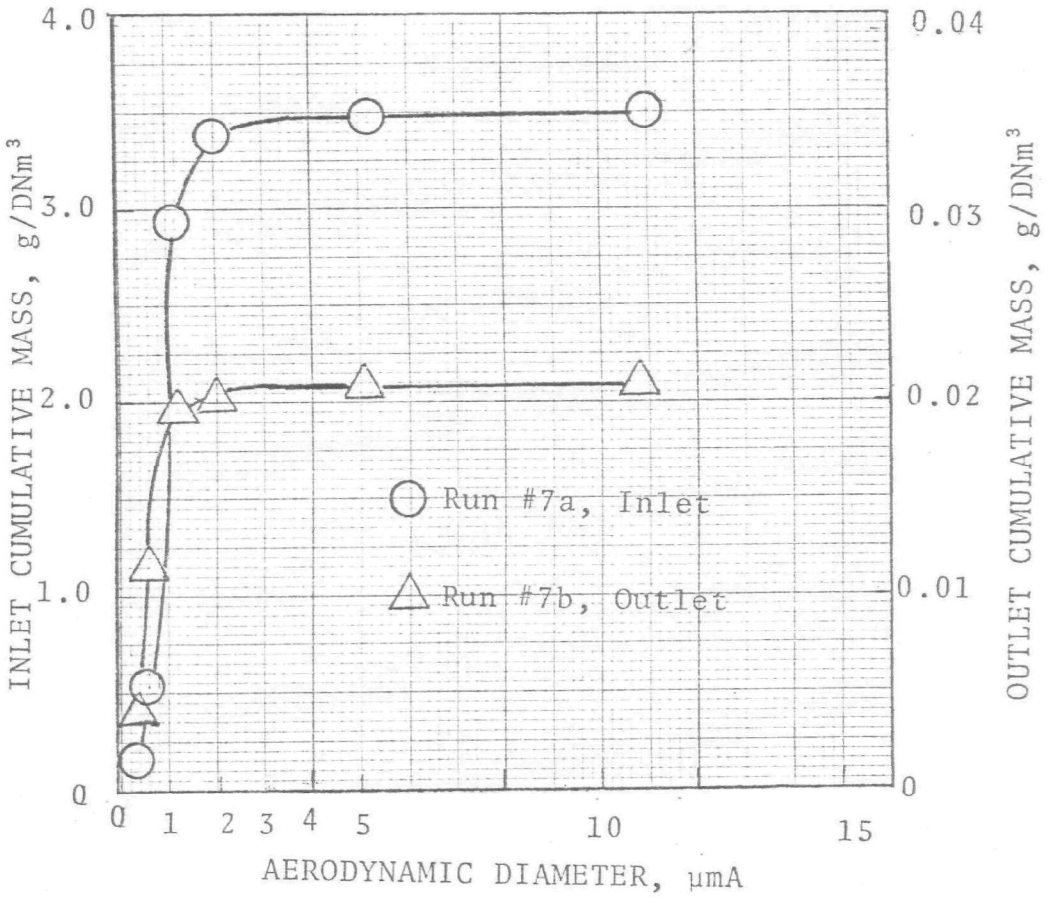

Figure 9-C-4 - Cumulative mass concentration for Run #7

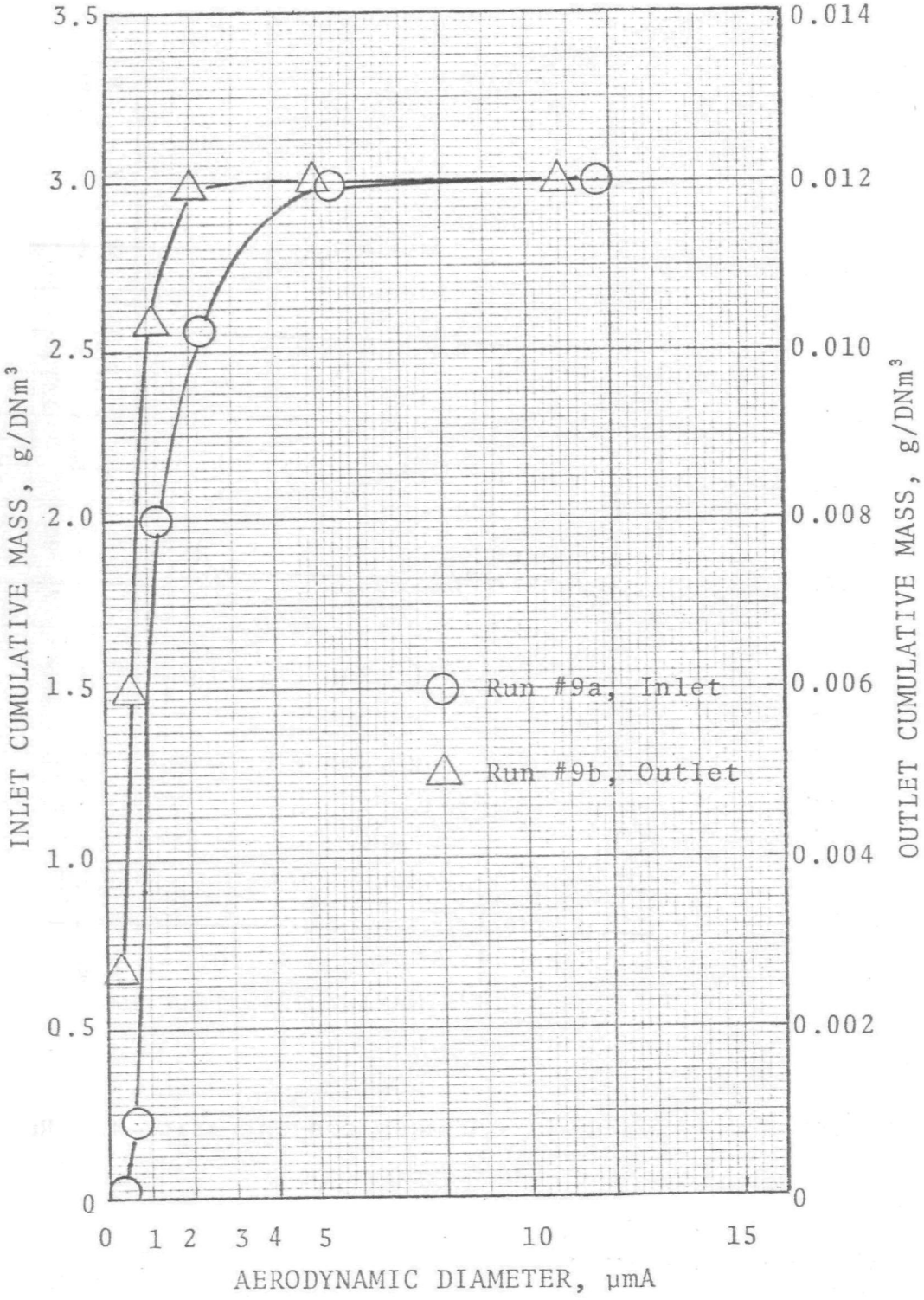

Figure 9-C-5 - Cumulative mass concentration for Run #9

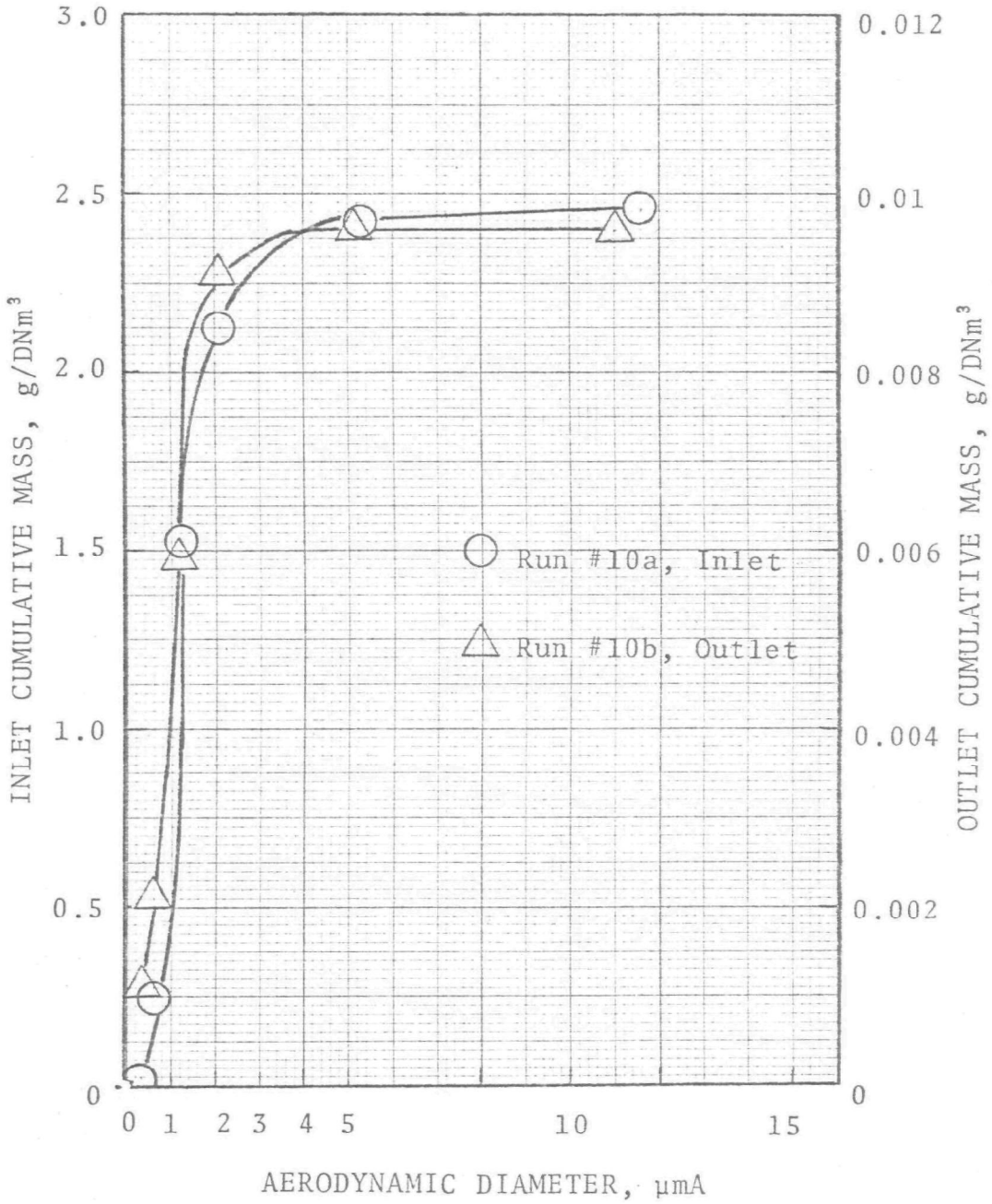

Figure 9-C-6 - Cumulative mass concentration for Run #10

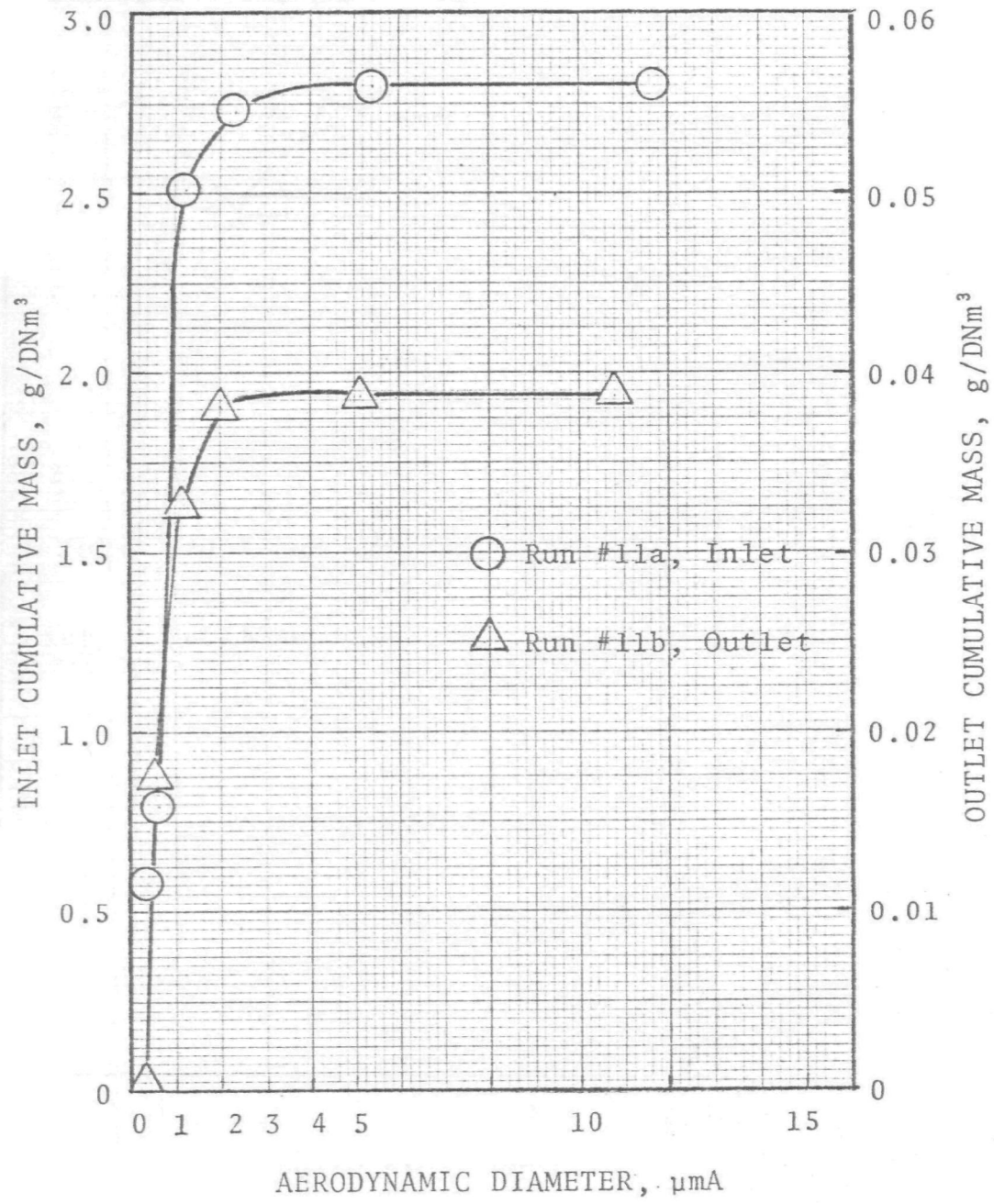

Figure 9-C-7 - Cumulative mass concentration for Run #11

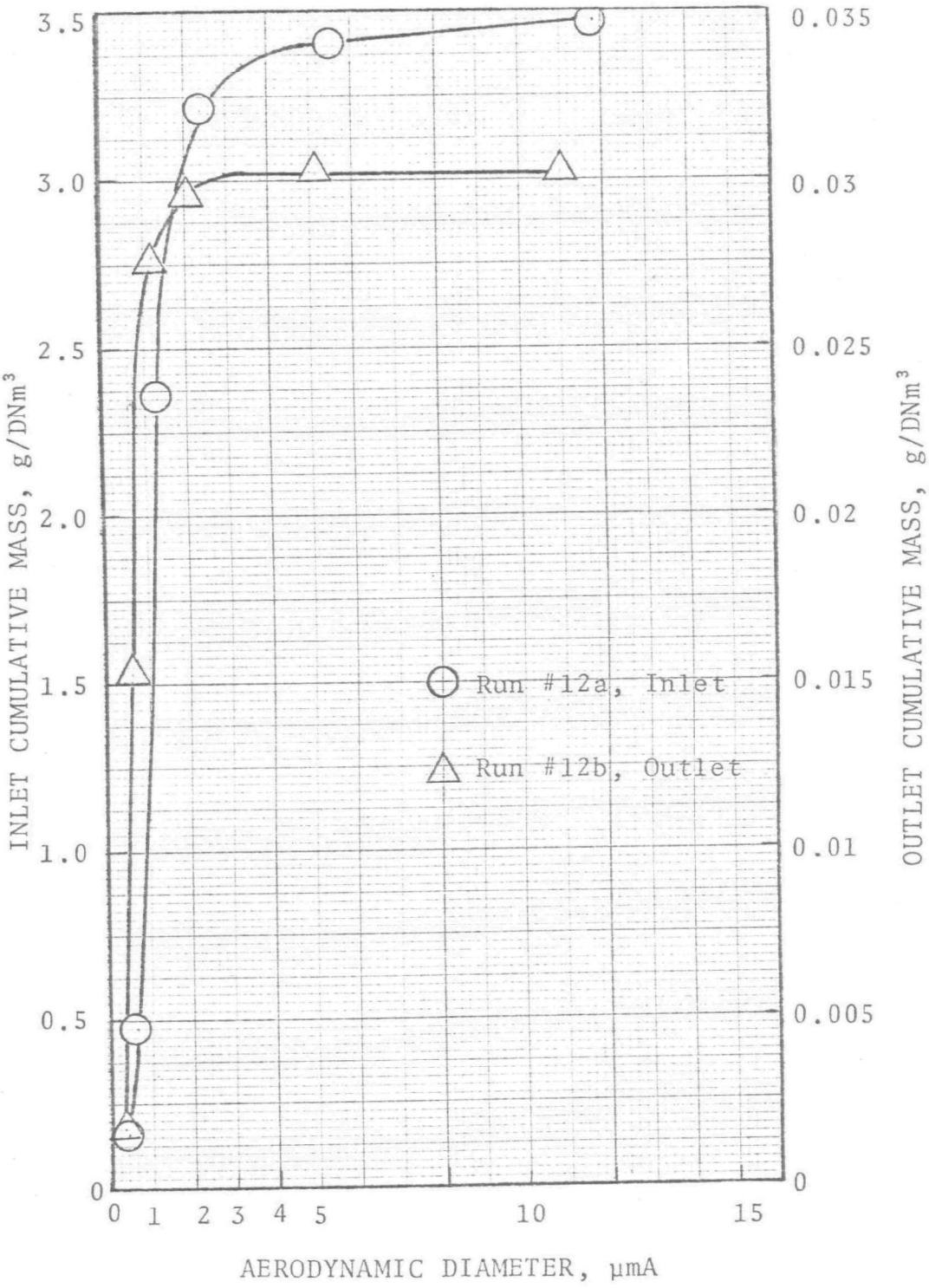

Figure 9-C-8 - Cumulative mass concentration for Run #12

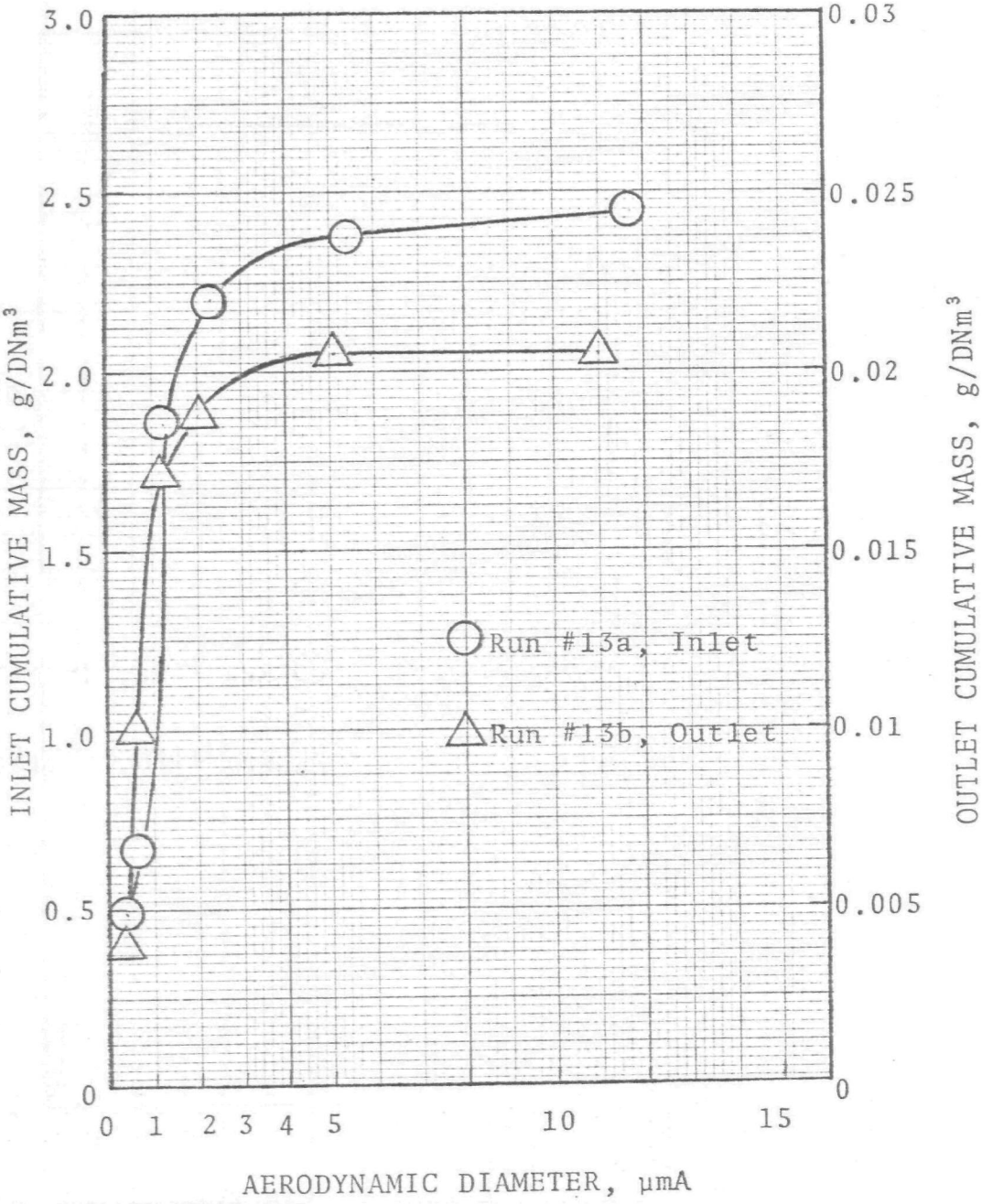

Figure 9-C-9 - Cumulative mass concentration for Run #13

REFERENCES

S. Calvert, J. Goldshmid, D. Leith, and D. Mehta. "Scrubber Handbook", A.P.T., Inc. Riverside, California. EPA Contract No. CPA-70-95. August 1972. PB-213-016.

S. Calvert, J. Goldshmid, and D. Leith, "Scrubber Performance for Particle Collection", A.I.Ch.E. Symposium Series 70 (137):357(1974).

C. E. Junge. "Air Chemistry and Radioactivity". Academic Press. 1963.

C. W. Lapple, and H. J. Kamack. "Performance of Wet Dust Scrubbers". Chem. Eng. Prog. 51(3):110-121, March 1955.

K. T. Semerau. J. Air Pollution Control Assoc. 10, 200 (1960).

M. Taheri, and S. Calvert. "Removal of Small Particles From Air by Foam in a Sieve Plate Column". J. Air Pollution Control Association. 18:240-245, 1968.

NOMENCLATURE

A = a constant in eq. (2-4) and (2-5)

A_a = Constant

A_d = total outside surface area of drops in scrubber, cm^2

B = constant defined by equation (2-5)

C' = Cunningham correction factor, dimensionless

d = diameter, m or cm

d_b = bubble diameter, cm

d_c = packing diameter (nominal), cm

d_d = drop diameter, cm

d_h = sieve plate hole diameter, cm

d_p = geometric mean particle diameter, μm

d_{pa} = aerodynamic particle diameter, μmA $\equiv d_p (C' \rho_p)^{1/2}$

d_{pi} = particle diameter, μm

d_{pg} = geometric mean particle diameter, μm

d_{p50} = diameter of particle collected with 50% efficiency, μm

d_{PC} = performance cut diameter (aerodynamic), μmA

d_{RC} = required cut diameter, μmA

d_w = differential mass, g

D = diffusivity, cm^2/sec

D_b = ball diameter, cm

D_p = particle diffusivity, cm^2/sec

DNm^3 = dry standard cubic meter, at 0°C and 760 mm Hg

E = efficiency, fraction or %

E_p = particle collection efficiency

f = ratio of drop velocity relative to gas velocity, empirical constant

F = froth density, g/cm^3

G = gas rate $lb/hr\text{-}ft^2$ or $kg/hr\text{-}m^2$

h = height of scrubber, cm

h_i = inertial impaction parameter

i = Van't Hoff factor

K_i = inertial impaction parameter for "d_i"

K_p = particle inertial impaction parameter

$$= \frac{d_{pa}^2 \, v_h \times 10^{-8}}{9 \, \mu_G \, d_h}$$

L = liquid rate, $Kg/hr\text{-}m^2$ or $lb/hr\text{-}ft^2$

m = mass, kg or g

mg = milligram

M_{cum} = cumulative mass collected on that stage and those below, g

Pt = penetration (one minus efficiency), fraction or percent

$\overline{Pt}$ = overall penetration

ΔP = pressure drop, cm W.C. or atm.

Q = heat transferred per unit cross-section area of column, cal/cm^2

Q_G = gas volumetric flow rate, m^3/sec

Q_L = liquid volumetric flow rate, m^3/sec or ℓ/sec

S = solidarity factor

u_{BD} = particle deposition velocity for Brownian diffusion

u_G = gas velocity relative to duct, cm/sec

u_h = gas velocity through sieve plate hole, cm/sec

u_o = gas velocity, cm/sec

u_{PD} = deposition velocity, cm/sec

U_o = undisturbed upstream air velocity, m/sec

U_h = hole velocity, cm/sec

W = cumulative mass, g

W_t = total collected mass, g

Z = static bed depth, m or cm

Greek

Σ = summation

η = efficiency due to unit mechanism, fraction or percent

η_i = collection fficiency for particle diameter "d_i"

η_s = effective collection efficiency of a single fiber by all collection mechanisms

θ = penetration time, sec

σ_g = geometric standard deviation of particle size distribution

μ = viscosity, g/cm-sec

μ_G = gas viscosity, centipoise

μm = micron (micrometer)

μmA = aerodynamic diameter $\equiv d_p(C' \rho_p)^{1/2}$, $\mu m\ (g/cm^3)^{1/2}$

ρ = density, kg/m^3 or g/cm^3

ρ_G = gas density, g/cm^3

ρ_L = liquid density, $lb/hr\text{-}ft^3$; g/cm^3

ρ_p = particle density, g/cm^3

TECHNICAL REPORT DATA
(Please read Instructions on the reverse before completing)

1. REPORT NO.	2.	3. RECIPIENT'S ACCESSION NO.
EPA-650/2-74-093		

4. TITLE AND SUBTITLE	5. REPORT DATE
Fine Particle Scrubber Performance Tests	October 1974
	6. PERFORMING ORGANIZATION CODE

7. AUTHOR(S)	8. PERFORMING ORGANIZATION REPORT NO.
Seymour Calvert, Nikhil C. Jhaveri, and Shuichow Yung	

9. PERFORMING ORGANIZATION NAME AND ADDRESS	10. PROGRAM ELEMENT NO.
A. P. T., Inc. P. O. Box 71 Riverside, California 92502	1AB012; ROAP 21ADJ-037
	11. CONTRACT/GRANT NO.
	68-02-0285

12. SPONSORING AGENCY NAME AND ADDRESS	13. TYPE OF REPORT AND PERIOD COVERED
EPA, Office of Research and Development NERC-RTP, Control Systems Laboratory Research Triangle Park, NC 27711	Final
	14. SPONSORING AGENCY CODE

15. SUPPLEMENTARY NOTES

16. ABSTRACT The report gives results of fine particle scrubber performance tests on industrial installations and the comparisons of experimental data with mathematical models. Particle size and concentration in the inlet and outlet scrubber gas streams were measured by means of cascade impactors and other apparatus. Tests were completed for a valve-type tray on a urea prilling tower, vaned centrifugal on a potash dryer, mobile bed on a coal-fired boiler, venturi on a coal-fired boiler, wetted fibrous filter on a salt dryer, impingement plate on a salt dryer, and venturi rod on a cupola. Performance is reported as particle penetration as a function of particle diameter. Mathematical models are satisfactory for all the scrubbers tested except the mobile bed. Information on costs, operating problems, maintenance, and other system characteristics are reported.

17. KEY WORDS AND DOCUMENT ANALYSIS

a. DESCRIPTORS	b. IDENTIFIERS/OPEN ENDED TERMS	c. COSATI Field/Group
Air Pollution Scrubbers Performance Tests Mathematical Models Measurement Particle Size Distribution Operating Costs	Air Pollution Control Stationary Sources Fine Particulate	13B, 14A 07A 14B 12A

18. DISTRIBUTION STATEMENT	19. SECURITY CLASS *(This Report)*	21. NO. OF PAGES
Unlimited	Unclassified	271
	20. SECURITY CLASS *(This page)*	22. PRICE
	Unclassified	

EPA Form 2220-1 (9-73)